COMPRES

Understanding the Building Blocks of Our Planet: The Materials Science of Earth Processes

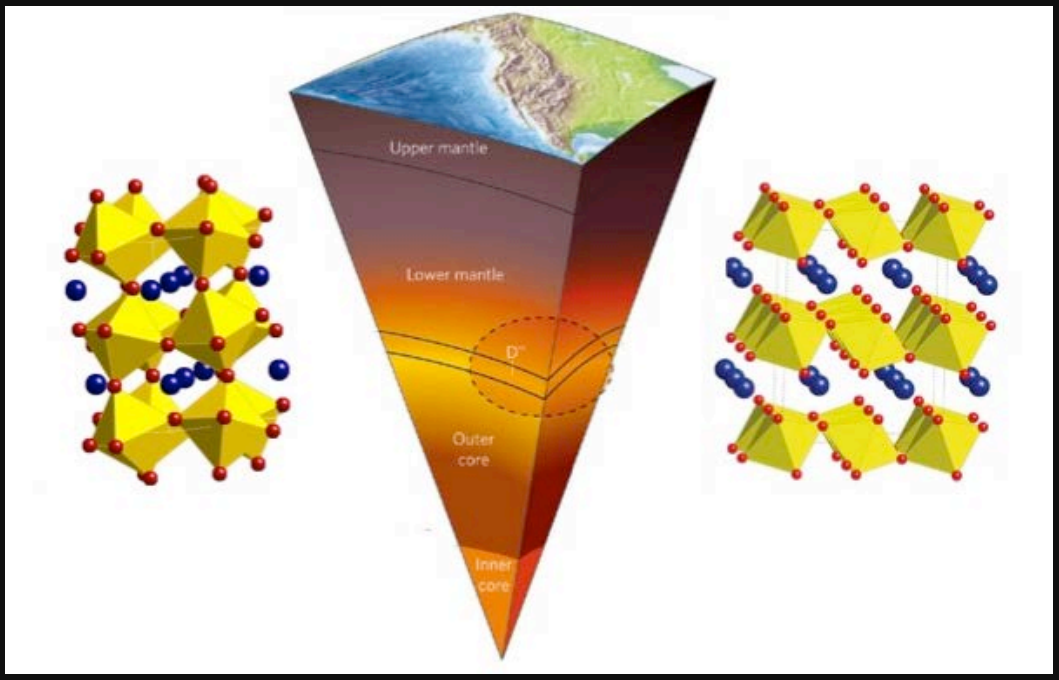

COMPRES:
The Consortium For Materials Properties Research in Earth Sciences

National Facilities and Infrastructure Development for High-Pressure Geosciences Research

Proposal to NSF 2012-2017 **Volume II: Accomplishments**

COMPRES Proposal Volume II: Accomplishments

Introduction

Through its support of community facilities and infrastructure development projects, COMPRES has enabled major advances in experimental studies of the physical and chemical properties of Earth and other materials over the past five years. Scientists at many member institutions, both large and small, in the U.S. and around the world have benefitted from access to COMPRES facilities and infrastructure. To illustrate the vitality and excitement of COMPRES science, approximately 180 community-submitted "one-pagers" are collected here and organized into eleven categories:

- Rheology of the Upper Mantle
- Elastic and Anelastic Properties of Mantle Minerals: Keys to the Structure and Composition of the Upper Mantle
- Earth's Deep Water and Carbon Cycles
- New Insights into the Deep Mantle
- Iron, Iron Alloys and Earth's Core
- New Techniques Enabled by COMPRES
- Anvils and More: Essential Materials for High-Pressure Research
- Planets and Planetary Materials
- Mineralogy, Crystal Chemistry, and Phase Transitions
- Equations of State and Elastic Properties
- Physics and Chemistry of Materials

We begin this volume with short summaries of the scientific achievements in six of the focus areas to highlight the role played by COMPRES and the importance of our science to forefront geophysical questions. The collection of one pagers follows after this summary.

Rheology of the upper mantle

Understanding the dynamics of the solid Earth is one of the forefront unsolved problems in the Earth sciences. The tectonic activity at Earth's surface that can so profoundly affect humanity has its ultimate source in the dynamic processes of the Earth's interior. Understanding large-scale geological processes such as mantle convection and plate tectonics require knowledge of the rheological properties of minerals and rocks. Rheological behavior also exerts control over the long-term thermal and chemical evolution of the Earth, and holds the key to interpreting the wide variety of planetary styles observed across our solar system. Quantitative experimental studies of plastic deformation under conditions of the lithosphere and mantle are, however, very challenging technically. Until very recently, such studies could not be conducted at the relevant pressure and temperature conditions. This was a major limitation as many rheological properties are highly sensitive to pressure. The development of new experimental apparatus combined with advances in synchrotron X-ray diffraction facilities supported by COMPRES has enabled major breakthroughs in this area in the last decade. The techniques pioneered at COMPES have since been adopted at other facilities worldwide.

Study of plastic deformation of minerals poses a number of important challenges. Plastic deformation can occur by various mechanisms involving motions of point defects, dislocations, and grain boundaries. As a thermally activated process, it is highly sensitive to temperature, pressure, and chemical environment. In the past, studies of rheological properties and microstructural development have been based on devices such as the gas apparatus that can reach up to ~0.5 GPa and ~1600 K or the Griggs rig which reaches to ~3 GPa and ~1600 K. Extending the capabilities of experimental studies of plastic deformation beyond depths of ~100 km is critical to understanding the large-scale rheological properties and deep mantle dynamics. Major advances in this area have resulted from technical developments in two areas. First, new apparatuses have been designed to extend high-temperature deformation studies to pressures of the deep upper mantle and the transition zone. Such devices include the deformation DIA (D-DIA) and rotational Drickamer apparatus (RDA) which are modules incorporated into a large-volume, multi-anvil press. In the D-DIA device, deformation experiments are carried out by moving two sets of anvils independently. The RDA is based on a Drickamer apparatus which has two anvils, one of which can be rotated to enable torsion experiments at high P-T conditions

Developments at the large-volume press beamline (X17B2) of the NSLS have also been critical to this effort by enabling stress and strain measurements under *in situ* mantle conditions. The intense x-ray beam is able to penetrate the surrounding material to probe the sample directly at high pressure and temperature conditions. An image of the sample is recorded by x-ray absorption and this image provides a measure of total (elastic + plastic) strain, giving a direct measurement of the deformation geometry. Diffraction measurements are also recorded and these provide a measure of change in lattice plane spacing. In combination with the elastic constants, the measured elastic distortion allows determination of the stress. Development of a high-resolution slit system has enabled diffraction to be recorded at various angles relative to the

loading direction, allowing the differential stress to be constrained (Weidner et al. II-118). It has been discovered that plastic deformation also plays an important role in controlling the stress distribution, and so these techniques also offer promise for constraining plastic anisotropy (Karato, II-38).

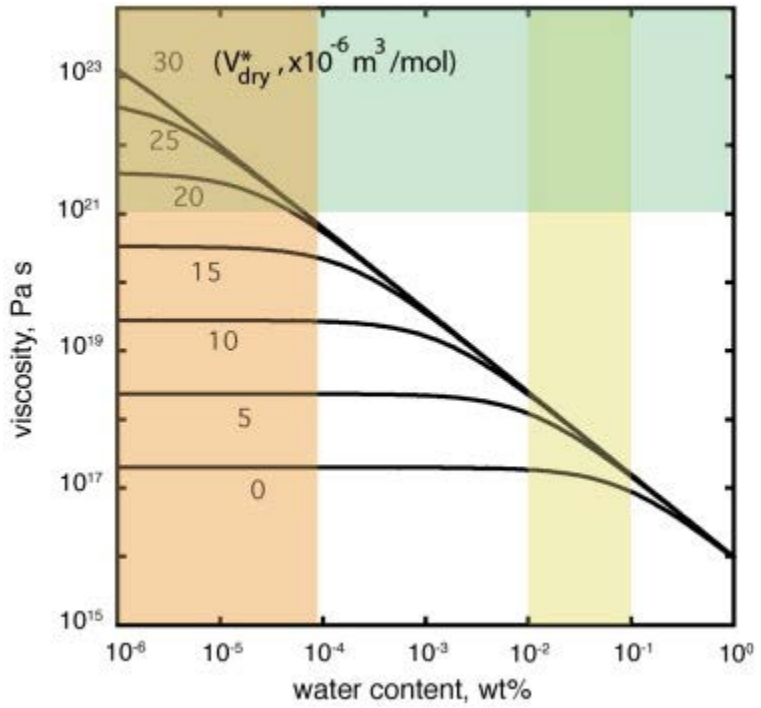

Fig. II-1. The viscosity contrast corresponding to the change in water content and activation volume for deformation estimated from new data on the influence of pressure on deformation of olivine (from Karato (2010)).

Over the last five years, a number of studies have been carried out at COMPRES beamline X17B2 using the D-DIA and RDA to conditions as high as 20 GPa and 2000 K and strain rates of 10^{-7} – 10^{-5} s^{-1}. Many major mantle minerals have been studied: MgO, olivine, garnet, diopside, serpentine, wadsleyite, and ringwoodite. A team led by Shun Karato of Yale has measured the creep strength of anhydrous olivine, wadsleyite, and ringwoodite to >20 GPa (II-25, II-30, II-31). These results help understand the stability of deep continental roots, and energy dissipation from deep slab deformation (II-37). The relative strengths of olivine and its high pressure polymorphs has been compared quantitatively for the first time.

Measurements of the activation volume of olivine up to 10 GPa indicate there is a substantial pressure effect, with one study finding a pressure-induced viscosity increase of nearly 7 orders of magnitude from the base of the lithosphere to the bottom of the upper mantle (Dixon et al., II-26). Experiments on olivine at lower temperatures have been carried out by Mei et al. (II-28) and Long et al. (II-29) resulting in a better understanding of slip systems and deformation behavior under lithospheric conditions. New methods for deformation studies on single crystals at high pressures and temperatures have been employed to understand the effect of water on

olivine deformation (Girard et al, II-27). The presence of water is shown to have an important effect on the pressure of transitions from one slip system to another and therefore may explain the regional variation of seismic anisotropy in the upper mantle

Experimental techniques have and no doubt will continue to play a central role in understanding the rheological properties of the Earth. COMPRES synchrotron facilities have been the world-leader in extending the capabilities of quantitative measurements to over 20 GPa and ~2000 K (at strain-rates of $\sim 10^{-5}$ s^{-1}). As illustrated by the above examples, these advances have already been used to study a range of important mantle minerals under new P-T conditions for the first time. Results so far are very promising and we expect that the influence of a broad range of physical and chemical conditions on the plastic properties of mantle minerals will be explored comprehensively in the coming years.

Elastic and Anelastic Properties of Minerals: Keys to the Structure and Composition of the Upper Mantle

Understanding the structure, composition, and evolution of Earth's mantle is a central goal of geophysical research. The most direct information about the interior structure of the Earth comes from seismic wave velocities. Radial variations in seismic velocity point to phase transitions, melting, and general pressure increase. Seismic tomographic images provide insights into lateral variability and the underlying dynamics. Interpretation of both one-dimensional and three-dimensional seismic properties of the mantle requires a detailed understanding of how sound velocities and elastic properties of minerals vary with pressure, temperature, crystal structure, and composition as well as the potential role of phenomena such as anelasticity and melting. Two specific challenges that can be highlighted include: the interpretation of seismic anisotropy throughout the planet, from uppermost mantle to inner core conditions; and understanding lateral variations of compressional and shear wave velocities (∂Vp and ∂Vs) in terms of composition and/or temperature variations. These goals require the mineral physics community to provide complete characterization of elastic anisotropy, as well as aggregate acoustic velocities, in minerals, and also the variation of these properties with pressure, temperature, and composition.

As the resolution of seismological studies continues to improve, the need for more and better elasticity data, under simultaneous high pressures and high temperatures, increases. COMPRES facilities and infrastructure projects have enabled major advances in the study of elastic and anelastic properties of Earth materials. Developments in ultrasonic interferometry in the large-volume press have been pioneered at X17B2 of NSLS (B. Li and R. Liebermann, II-46) and provide the only means to measure elastic properties directly at the pressure and temperature conditions of the upper mantle and transition zone. COMPRES support for the development of a Brillouin spectroscopy system at the Advanced Photon Source (GSECARS sector) has opened up capabilities to combine X-ray diffraction measurements with Brillouin spectroscopic determination of the complete elastic tensor. The COMPRES partnership with Sector 3 at the

APS has led to novel studies of elastic properties at extreme pressures (and temperatures) using emerging techniques such as nuclear resonant inelastic scattering (NRIXS) and phonon inelastic x-ray scattering (IXS) (e.g. B. Chen et al. II-86; J. Wicks et al., II-88). As a testament to the pioneering success of COMPRES in initiating major advances in our ability to characterize elastic properties, we note that other facilities around the world have adopted the COMPRES lead and are adapting Brillouin systems for synchrotron facilities (SPring-8, Petra-III) and the development of ultrasonic elasticity in combination with large-volume press facilities (SPring-8, DESY).

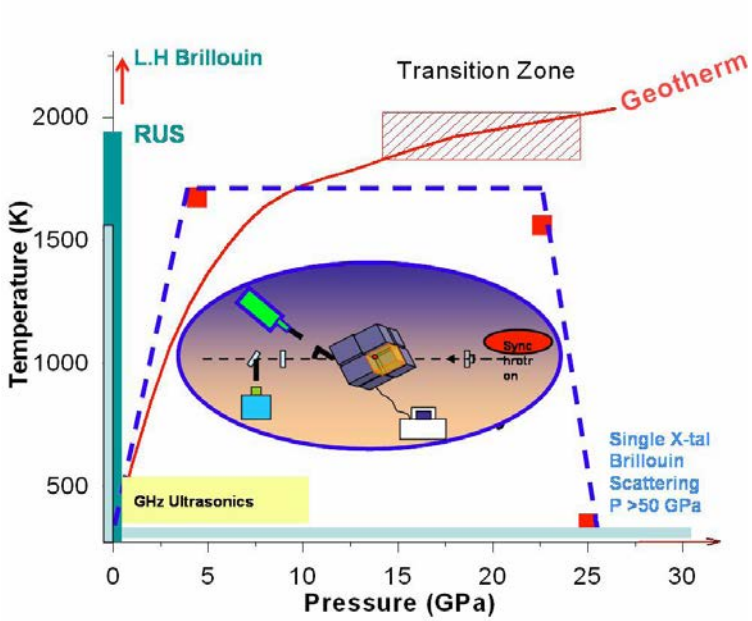

Fig.II-2. Current experimental pressure and temperature conditions accessible in laboratory acoustic velocity measurements using various techniques and the mantle conditions shown with a representative geotherm.

Compilations of mineral elastic properties and their pressure and temperature derivatives are widely used in geophysical studies involving petrological, seismic, geodynamic, and other types of data to address questions about the nature of Earth's crust and mantle. Such databases suffer from major limitations due to unknown values for pressure- and temperature derivatives of many important phases. Ultrasonic interferometry and Brillouin spectroscopy have been used to provide new constraints on high-pressure or high P-T elastic behavior of important mantle minerals including diopside (Li and Neuville, II-52; Sang et al, II-53), pyrope-majorite garnets (Gwanmesia et al, II-50), and wadsleyite, β-$(Mg,Fe)_2SiO_4$, the olivine polymorph stable between 410- and 520-km depth in the mantle (Isaak et al, II-47, II-48 ; Liu et al.,II-49). A number of studies have addressed how elastic properties are altered either across or near phase transitions for orthoenstatite (Kung et al., II-54; Zhang et al., II-55), fayalite (Armentrout and Kavner, II-56; Liu et al., II-57), and stishovite, the six-coordinated high-pressure phase of silica (Jiang et al, II-51). Grain size and grain shape parameters have a great influence on the physical properties of minerals as well as on geophysical processes. Grain-size reduction can occur as a consequence of

phase transitions or in regions of localized deformation. X-ray diffraction measurements of the compressibility of nanocrystalline forsterite show a reduction in bulk modulus due to the influence of grain boundaries and triple junctions (Couvy et al., II-59), and a much larger effect in MgO (Gleason et al., 2011).

Anelastic effects at seismic frequencies must also be accounted for in modeling seismic wave velocities. For example, phase transition results in significant anelastic relaxation, which leads to large energy dissipation and concurrent softening of elastic modulus. When pressure promotes a material going through a phase transition, it gives rise to extra volume change of the system in addition to the elastic volume strain. Synchrotron based experiments by Weidner and Li (II-62) at X17B2, NSLS demonstrate softening of the bulk modulus within the two-phase loop of olivine-ringwoodite at a time scale of 100 seconds. Scaling the amplitude of the pressure perturbation and grain size to those expected in the Earth, the P wave velocities within the discontinuities at 410, 520, and possibly 660 km may be reduced by as much as 10% over a narrow depth range (Weidner and Li, II-63). Li (II-64) has shown that bulk attenuation calculated for a pyrolite model using mineral physics data is consistent with the inverted bulk attenuation of the upper mantle from seismic observations.

Earth's Deep Water and Carbon Cycles

Water, stored in minerals as OH defects or molecular H_2O, can have a dramatic effect on their physical properties, including density, seismic velocities, anisotropy, strength, and viscosity. The ability of some nominally anhydrous mantle materials to incorporate appreciable amounts of water at high pressures has lead to a greater awareness of the potential role of water in shaping physical and geochemical evolution of the Earth. Water, among other volatiles such as CO_2 may control melting in the mantle, weakening of the lithosphere, and thus plate tectonics itself allowing our habitable planet to develop. The study of Earth's deep water cycle has become a central topic in solid-Earth geophysics and is recognized as a frontier area of research.

Infrared spectroscopy provides a key and often unique experimental tool with exceptional sensitivity to O-H bonds. The NSLS-U2A beamline was the first synchrotron facility dedicated to high-pressure infrared micro-spectroscopy and micro-Raman spectroscopy and remains unique in the world in its capabilities. Both by itself, and in combination with X-ray studies at X17, NSLS-U2A provides the COMPRES community with an invaluable tool for evaluating the behavior of hydrous and nominally anhydrous minerals under conditions of Earth's deep interior. Major applications of the facility include determination of water solubility in mantle minerals, characterization of vibrational properties and the corresponding thermodynamic characterization, and uncovering the crystal chemistry of hydrogen storage in minerals.

The mantle X-discontinuity, usually assigned to seismic reflectors in the 260~330 km depth range, has proved difficult to explain in terms of a single mineralogical phase transformation in part because of its depth variability. The coesite to stishovite transition of SiO_2 matches deeper X-discontinuity depths but requires 5~10% free silica in the mantle to match the observed

impedance contrast. The orthoenstatite (OEn) to high-pressure clinoenstatite (HPCen) transformation of $MgSiO_3$ also broadly coincides with depths of the X-discontinuity but requires chemically depleted and orthoenstatite-rich lithology at a depth near 300 km in order to match observed seismic impedance contrast. On the basis of high-pressure synchrotron infrared spectroscopy, X-ray diffraction, and Raman spectroscopy, Steve Jacobsen and colleagues (II-66) show that just 1300 ppm variation of H_2O content in $MgSiO_3$ can displace the transition of low-pressure clinoenstatite (LPCen) to HPCen by up to 2 GPa, similar to previous quench experiments on the OEn to HPCen phase transition, where about 30–45 km (1.0–1.5GPa) of deflection could occur per 0.1 wt% H_2O. If the mantle X-discontinuity results from pyroxene transitions in a depleted harzburgite layer, the depth of the mantle X-discontinuity could serve as a potentially sensitive indicator of water content in the upper mantle due to the strong influence of minor amounts of water on the transformation boundary. This study also demonstrates that synchrotron-based IR at the NSLS-U2A is highly suitable for studying the behavior of mantle silicates containing relatively low concentrations of water (10's to 100's of ppm by weight). Further synchrotron-IR studies can be carried out on other OH-bearing mantle phases to study hydrogen bonding at pressure and applied to interpretation of mantle velocity structure in potentially hydrous regions of the mantle.

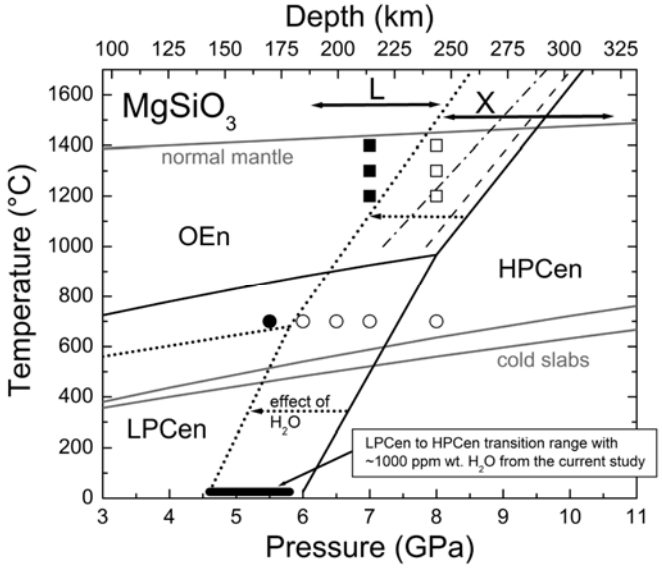

Figure II-3. The effect of water on LPCen-HPCen transitions in this study (dark solid bar) are compared with quench experiments for OEn-HPCen (squares and circles). The overall influence of ~0.1wt% H_2O is shown by the dashed line, and may explain depth variability in the seismic Lehman (L) or X-discontinuities.

The high-pressure stability of hydrated metamorphic phases and their importance in transporting water into Earth's deep interior is well appreciated. Yet, the manner in which hydrogen is retained within these phases is a topic of considerable uncertainty. In particular, the role of hydrogen bonding (and its pressure dependence) in stabilizing these metamorphic phases at high pressure remains unclear. Among metamorphic phases stable to high pressures, talc

($Mg_3Si_4O_{10}(OH)_2$) and lawsonite ($CaAl_2Si_2O_7(OH)_2 \cdot H_2O$) represent two different means of sequestering hydrogen. Talc is a chemically simple layer silicate, with the hydroxyl unit oriented nearly perpendicular to the layers and weak hydrogen bonding. In contrast, lawsonite contains both hydroxyl units and water molecules; it has both weak and intermediate strength hydrogen bonding. High-pressure infrared spectroscopy by Scott et al. (II-79) to 25-30 GPa span the mid- and far-infrared ranges. Together with complementary Raman data, the evolution of the vibrational component to the thermodynamic properties is characterized. There is a gradual modification of spectral features for both phases to the highest attained pressures without evidence for breakdown of their overall framework. These observations indicate that at low temperature and with only modest pressure-induced changes, the basic structural frameworks of both talc and lawsonite could metastably transport water well beyond the known thermodynamic decomposition conditions of these phases.

Dense hydrous magnesium silicates (so-called alphabet phases) are a class of hydrous silicates that form under high-pressure-temperature conditions in the MgO-SiO_2-H_2O system. These silicates are also potentially important components of the deep Earth water cycle especially in cold slab environments. In particular, phase E is likely to be an important water carrier near the base of the upper mantle and the transition). Phase D may be the major H_2O-bearing phase at the top of the lower mantle in low-temperature slab environments for peridotite compositions. Using synchrotron infrared (IR) spectroscopy, Shieh et al. (II-74) measured the infrared spectra of polycrystalline samples of phases D and E to 42 and 41 GPa, respectively. For both phases, at least three broad OH stretch vibrations were observed at elevated pressures indicating that each phase has multiple hydrogen positions that exhibit disorder. No structural phase transition or amorphization was observed for either phase over the measured pressure range. These high-pressure infrared spectra for phase D do not support the occurrence of hydrogen bond symmetrization as predicted by first-principles calculations.

In addition the above examples, COMPRES-based research has contributed to a wide range of science involving hydrous and nominally anhydrous minerals. Combined studies involving X-ray diffraction and Brillouin scattering have enabled characterization of the single-crystal elastic properties of zoisite (a member of the epidote family) (II-76), diaspore ($AlOOH$) (II-75), and hydrous olivine (II-67), wadsleyite (II-68), and ringwoodite (II-69, II-70). Such data contribute important pieces to understanding the variation in seismic wave speeds above subduction zones and in other potentially hydrous regions of the mantle. Understanding how hydrogen is stored in minerals and the evolution of the structure and bonding in hydrous minerals has also been the subject of COMPRES research studies involving amphiboles (II-164) and hydroxides (II-77, II-78), for example. It should also be emphasized that infrared spectroscopic studies play an essential role enabling the determination of water contents for a wide range of fundamental studies of elasticity, rheology, and crystal chemistry of nominally anhydrous olivine polymorphs and other minerals.

New Insights into the Deep Mantle

Advances in experimental methods and probes at synchrotron radiation facilities including those facilitated by COMPRES have expanded the *P-T* range accessible to direct measurements to conditions of Earth's core-mantle boundary and beyond, while at the same time leading to improved resolution that has resulted in dramatically better ability to constrain physical and crystallographic properties. In combination with new geophysical observations of the deep Earth, we can now better address such fundamental questions as the origin of seismic discontinuities, chemical heterogeneity in the deep mantle, and the nature of the core-mantle boundary region.

Sound velocity and density measurements of lower mantle minerals are essential to interpreting the seismic complexities observed in the lower mantle. A variety of COMPRES facilities and infrastructure projects have opened up new opportunities for exploring these properties in ferropericlase, perovskite, and post-perovskite phases. X-ray diffraction measurements at 12.2.2 ALS carried out by Speziale et al (II-85) on $(Mg_{0.8}Fe_{0.2})O$ at lower mantle pressures revealed a discontinuous pressure dependence of the bulk modulus that is related to a spin pairing transition of Fe^{2+}. Deformation behavior of ferropericlase across this spin transition has been studied by Lin et al (II-96) at X17, NSLS, constraining the change in strength and deformation across the transition. Sound velocities have also been measured on (Mg,Fe)O compositions up to 140 GPa using NRIXS at Sector 3, APS (Chen et al., II-86). In a very Fe-rich composition $(Mg_{0.16},Fe_{0.84})O$, a recent NRIXS study by Wicks et al. (II-88) reveal unexpectedly low sound velocities at pressures up to 120 GPa and suggest this may provide an explanation for ultra-low velocity zones of the deep mantle. These findings have been used as the basis for new geodynamical models that account from the effect of the spin transition in ferropericlase on the style and vigor of mantle convection (II-89, II-90).

The *D″* region lies just above the core mantle boundary (CMB) and is one of the most poorly understood regions of the planet. In contrast to the bulk of the lower mantle, this enigmatic ~200-km-thick layer exhibits a seismic discontinuity with large topographic variations, pronounced lateral heterogeneity, increased seismic anisotropy, and ultra-low velocity zones. The CMB is of great geophysical interest as a boundary layer between the core and mantle which is expected to play an active role in controlling mantle dynamics, heat flow and thermal structure, and the long-term evolution of the Earth. The discovery of a phase transition in $MgSiO_3$ from a perovskite (Pv) to a post-perovskite (pPv) structure at conditions closely corresponding to those of the CMB provide a new model for interpreting the *D″* layer. The study of (Mg,Fe)(Al,Si)O3 perovskite and post-perovskite is complicated by the variable crystallopgraphic sites, spin states, and valences that iron can adopt under the P-T conditions of the deep mantle. Using the nuclear forward scattering capabilities of sector 3, APS, several groups are exploring the behavior of Fe in a range of mantle-relevant perovskite and post-perovskite compositions. In a series of studies on Fe-bearing magnesium silicate perovskite and post-perovskite (Shim, II-92, II-94, and II-95), it was discovered that Fe^{2+} in perovskite remains

high spin to at least 70 GPa whereas Fe^{3+} in the octahedral site undergoes a gradual transition to a low spin configuration, resulting in a stiffening of the perovskite. In post-perovskite, it was found that Fe^{3+} in the Mg site (8 fold) remains high spin, while Fe^{3+} in the octahedral site becomes low spin, and this results in a density increase implying that mantle heterogeneities containing elevated Fe^{3+} may have detectable seismically due to distinctive elastic properties and density.

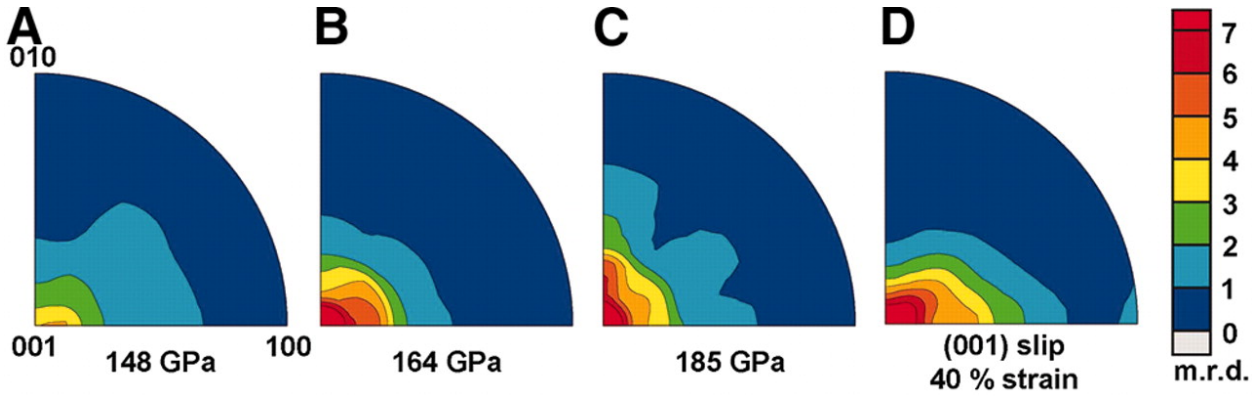

Fig. II-4. Inverse pole figures of MgSiO3 pPv at 148 GPa (A) just after transformation and at two pressure steps up to 185 GPa (C) (Miyagi et al., 2010) (II-98).

One of the most intriguing properties of the core-mantle boundary region is its relatively strong (and variable) seismic anisotropy. Seismic anisotropy holds the key to uncovering the nature dynamic flow at the base of the mantle. However, interpretation of anisotropy in the deep Earth is challenging as it requires an understanding of mineral deformation mechanisms and preferred orientation development, the anisotropic elastic properties of the relevant phases, and mantle deformation history. Previous work on deformation behavior of analog and silicate post-perovskites has been ambiguous with studies reporting texture development consistent with slip on a variety of different planes. To resolve this, Miyagi et al. (II-98) carried out new deformation experiments on $MgSiO_3$ post-perovskite at the COMPRES beamline 12.2.2 at the Berkeley Advanced Light Source. In the new experiments, it was observed that a texture consistent with (001) slip develops under compression. Previously observed (100) textures are now understood as a result of a phase transformation under stress rather than a deformation texture. When the new results are used to model deformation and anisotropy development in the D" region, the predicted shear-wave splitting (characterized by fast horizontally polarized shear waves) is in agreement with seismic observations.

Anvils and More: Essential Materials for High-Pressure Research

Synchrotron-based techniques play a large role in experimental studies of geological materials at high pressures and temperatures. Over last decade, development of new synchrotron methods augmented by improvements in x-ray optics and detectors has led to many technical advances. The new synchrotron-based capabilities have also spurred or benefitted from the development and improvement of high-pressure techniques. Differential stress in the sample, for example, rather than being a hindrance, is now being exploited for new experimental measurements. Established techniques such as x-ray diffraction are being used at higher pressures and temperatures with increased precision and accuracy of measurement. New methods in x-ray spectroscopy and scattering have greatly advanced capabilities for studying thermodynamic, elastic, and electronic properties. Development of new materials and better characterization of existing materials for high-pressure experimentation is an essential component for continued advances. Over the last five years, COMPRES-sponsored projects have contributed to a number of important high-pressure materials developments.

Diamond anvil cell technology has undergone continual refinement since its inception. Materials required for high-pressure diamond cell research fall into a number of categories including anvil materials, pressure transmitters, pressure calibrants, gaskets, stress sensors, and insulating materials. As one illustrative example, it is often desired that experiments be conducted under hydrostatic stress conditions. The uniaxial load in a diamond anvil cell can be transformed to a hydrostatic pressure by surrounding the sample with a fluid pressure medium. However, at room temperature, all known pressure media freeze in excess of 10 GPa, resulting in the development of variable degrees of non-hydrostatic stresses. By surrounding the sample with a soft solid, "quasi-hydrostatic" conditions can be achieved. Alkali halides (NaCl) and rare gas solids (He, Ar, Ne) are especially useful as quasi-hydrostatic media due to their low strength and simple structures. To determine their performance, it is necessary to characterize pressure-dependent shear strength of such materials. Examples of such efforts include the characterization of the strength of NaCl as it crosses the B1-B2 phase boundary (Mi et al., II-135). The development of the GSECARS/COMPRES gas loading system at the APS has now made rare gas pressure media available to the entire community rather than just a few specialized labs. The question of how "good" such media remain as pressure increases has been addressed in recent experimental work on the strength of argon and neon to megabar pressures (Dorfman et al., II-139). In a brief period of time, the COMPRES/GSECARS gas loading system has raised the bar for diamond cell research, making near-hydrostatic conditions in rare-gas pressure media like Ne the norm, whereas previously it was the exception. For studies of phase transitions, in particular, this advance is crucial in terms of the accuracy of results.

Pressure measurement in the diamond anvil cell relies on the use of calibrated standards. One common method involves measurements of the R_1 fluorescence wavelength of small ruby crystals placed in the sample chamber that are excited with visible laser irradiation. The ruby fluorescence pressure scale has been calibrated against room-temperature isotherms derived from

shock Hugoniot data. For synchrotron-based diffraction studies in both the DAC and multi-anvil apparatus, the use of internal x-ray standards is common. The development of improved high P-T pressure standards is recognized as an important research need. It has long been known that combined measurements of density and elastic properties would enable development of pressure scales independent of any calibrant. The COMPRES-sponsored development of a Brillouin spectroscopy system at the GSECARS sector of APS makes this a practical reality for the first time. Initial experiments on widely used pressure standards such as MgO, NaCl, Ar, and cubic boron nitride (cBN) have now been carried out both at ambient and high temperatures (II-131, II-132, II-133, II-134). New work on the strength and elastic properties of metallic standards such as Pt and Mo has been reported from diffraction and ultrasonic interferometry experiments (Dorfman et al., II-139; Liu et al., II-140). Characterization of materials that have potential to develop into new standards, such as LiF (Kantor et al., II-138), has also been reported.

Finally, research into diamond and other superhard solids have the enormous potential to advance the capabilities for high-pressure research using both diamond anvil and large-volume devices. New efforts to grow and characterize transparent nano-crystalline diamonds, large CVD-grown single-crystal diamond, and diamond/tungsten composites have been ongoing at COMPRES facilities (II-143, II-144, II-145). For large-volume devices, the COMPRES infrastructure development project on multi-anvil cell development has been a major success as described elsewhere in this proposal. The continued need for improved accuracy and precision on more complex samples to ever-higher pressures and temperatures will continue to drive fundamental research efforts on those materials upon which we rely for the success of our high-pressure geoscience research. COMPRES facilities and development projects will continue to play a leading role in such work.

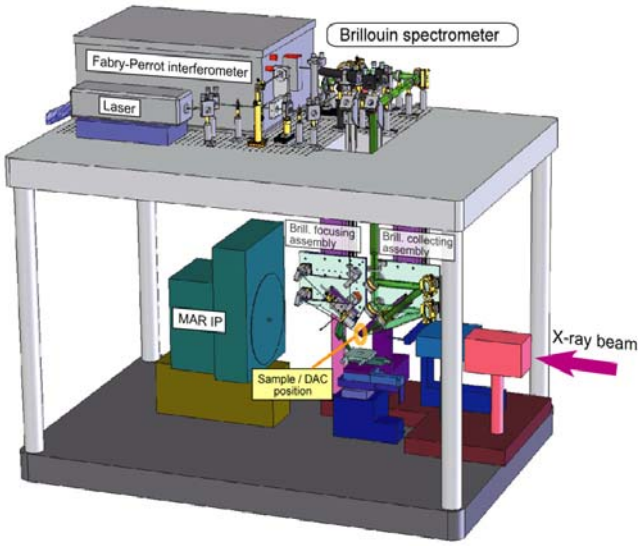

Figure II-5. Schematic illustration of the COMPRES/GSECARS Brillouin scattering system at Sector 13 of the APS.

Table of Contents – One Pagers

Rheology of the Upper Mantle

Shear deformation of dry polycrystalline olivine under deep upper mantle conditions using a rotational Drickamer apparatus (RDA)

Kawazoe, T.[1], S. Karato[2], K. Otsuka[2], Z. Jing[3], M. Mookherjee[4]

[1] Ehime University, Matsuyama, Japan
[2] Yale University, New Haven, CT 06520, USA
[3] University of Chicago, Argonne, IL, USA
[4] Bayerisches Geoinstitut, Universität Bayreuth, Bayreuth, Germany

Shear deformation experiments on dry hot-pressed polycrystalline San Carlos olivine have been conducted at 4.9–9.6 GPa, 1300–1870 K and strain rates of 0.6–7.4 x10^{-5} s^{-1} using a rotational Drickamer apparatus (RDA) at a synchrotron facility. The stress was measured from the orientational dependence of lattice spacing for the (1 3 0), (1 3 1), (1 1 2), (1 2 2), (1 4 0) and (2 4 1) planes, as well as from the dislocation densities. Based on the mechanical and microstructural observations, we infer that deformation occurs by power-law creep involving dislocation glide and climb under high temperature conditions, whereas deformation is due to exponential creep through the Peierls mechanism at relatively low temperatures. In both regimes the strength of olivine at steady-state deformation at these pressures is much larger than those at lower pressures. The activation volumes V^* is estimated to be ~15–20 x10^{-6} m^3/mol for the power-law creep. Combined with the previous results under wet conditions,we present the recommended values of flow law parameters on olivine for power-law creep constrained by high-pressure deformation experiments.

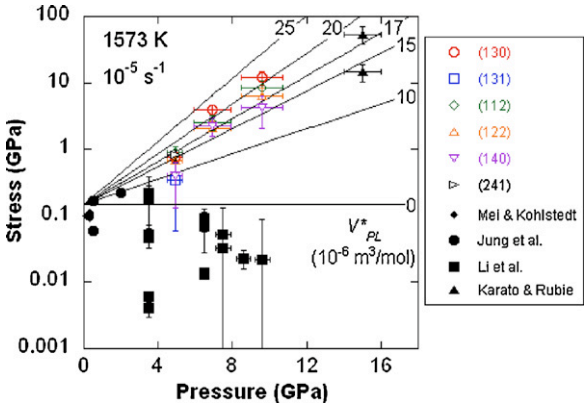

Creep strength of olivine as a function of pressure

Kawazoe, T., et al., 2009. Shear deformation of dry polycrystalline olivine under deep upper mantle conditions using a rotational Drickamer apparatus (RDA). Physics of the Earth and Planetary Interiors. 174, 128-137.

This work was conducted using X17B2 at NSLS (Brookhaven) supported by COMPRES and NSF-EAR-0652960.

Measurement of activation volume for creep of dry olivine at upper mantle pressure

Nathanial A. Dixon, William B. Durham, Massachusetts Institute of Technology
Shenghua Mei, David L. Kohlstedt, Ayako Suzuki, University of Minnesota
Liping Wang, Stony Brook University (now at University of Nevada Las Vegas)
Justin Hustoft, Brown University

Olivine, $(Mg,Fe)_2SiO_4$, is the volumetrically dominant mineral in Earth's upper mantle, so the dynamic behavior of olivine, in particular its creep response to deviatoric stress, probably controls convective flow in the mantle. Although this fact has been recognized for decades, defining the creep properties of olivine through laboratory experiment has remained elusive because of the poorly understood influence of hydrostatic pressure (P) on creep. P reaches nearly 15 GPa in the upper mantle (corresponding to a depth of approximately 400 km), and very special techniques are required to do well-resolved creep experiments at P > 2 GPa. Using a deformation DIA (D-DIA) at beam line X17B2 at the NSLS we use synchrotron x-ray Bragg diffraction to measure lattice spacing—and thus deviatoric as well as hydrostatic stress—in polycrystalline materials during creep experiments to 10 GPa pressure. We have refined techniques to reach a stress resolution of ±0.01 GPa (figure below, left). For dry San Carlos olivine we have measured an average activation volume of about 17 cm^3/mol between 2 and 9 GPa. This is a substantial pressure effect, representing a pressure-induced viscosity increase of nearly 7 orders of magnitude from the base of the lithosphere to the bottom of the upper mantle.

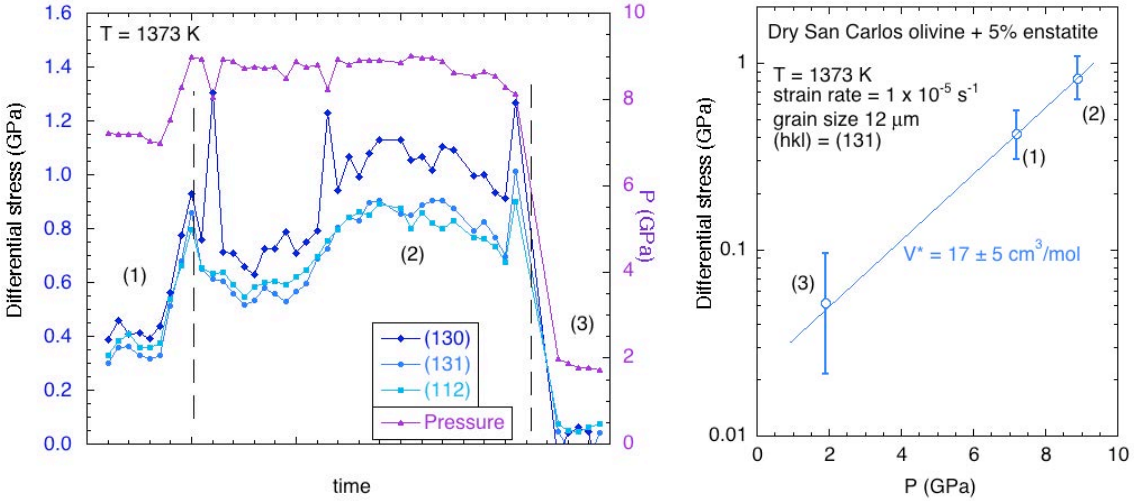

An example of synchrotron x-ray-based measurements of creep behavior to 9 GPa in the D-DIA. At the left are stress vs. time curves for a polycrystalline sample tested over the course of approximately 9 hours and 18% total shortening at T = 1373 K. Different stress-time curves at different Bragg (hkl) conditions (left) result from plastic anisotropy of the olivine lattice. Three different pressures were probed in this run, in steps labeled (1), (2), and (3). If pressure at fixed other conditions changes stress as exp(PV*/RT), where R is the gas constant, then the activation volume V* defined by this run alone is 17 ± 5 cm^3/mol (right). Error bars combine stress resolution of ±0.01 GPa plus the effect of a ±25-K relative T uncertainty.

This research was supported by US Department of Energy Office of Basic Energy Sciences under contract DE-FG02-04ER15500 (UMN) and DE-FG02-07ER15839 (MIT), and by the National Science Foundation under award EAR-0968863 (MIT). Experiments were carried out at the X17B2 beamline of the National Synchrotron Light Source, which is supported by the US Department of Energy, Division of Materials Sciences and Division of Chemical Sciences under Contract No. DE-AC02-76CH00016 and by COMPRES, the Consortium for Materials Properties Research in Earth Sciences under NSF Cooperative Agreement EAR 01-35554.

Determination of water effect on deformation of olivine single crystal at high pressure and high temperature

Jennifer Girard[1], Jiuhua Chen[1], Paul Raterron[2], Caleb W. Holyoke III[3]

CeSMEC, Florida International University, Miami, FL 33199

[2] UMET, CNRS 8207, Bât C6, Université Lille 1, F-59655 Villeneuve d'Ascq, France

[3] Texas A&M University, Dept. of Geology and Geophysics, College Station, TX 77843- 3115, United States

The main goal of this study is to test the water effect on the activation of the [100] slip and [001] slip at high pressure (between 4 and 8GPa) and high temperature around 1200 Celsius degrees with a water content between 300-600ppmH/Si. To be able to activate these slip systems, we deformed olivine single crystal, oriented along [110]c and [011]c in order to activate [100](010) and [001](010) slip systems respectively and along and [101]c in order to active [100](001) and [001](100) slip systems simultaneously. The deformations were carried out in a modified multi anvils press, D-DIA. Stress and strain rate in situ measurements during the deformation will be conducted using synchrotron x-ray beam at X17B2 beamline of National Synchrotron Light Source (NSLS). 2 single crystals, with different orientation, were deformed simultaneously, to compare their relative deformation. This study was done on both fosterite and San Carlos olivine at different pressure to take in account the eventual effect of pressure on the slip systems activities. The results show a change in the slip system activity, with a slip system transition between [100](010) and [001](010) occurring around 5-6GPa. This confirms the results obtained in previous studies carried out in dry condition. (Raterron et al.,(2007), and (2008)). However in dry condition, this same transition was observed at higher pressure (8GPa). These results revealed that the presence of water in the assembly during the deformation has the tendency to lower down the transition pressure. Part of the work has been published in the Journal of Physics and Chemistry of Solid (vol 71, 2010, 1053-1058), and is supported by NSF (EAR-0711321 and EAR-1015509).

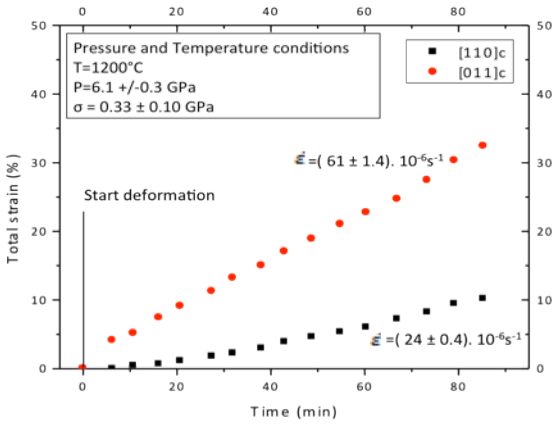

Figure 1: Total strain versus time for two single crystals ([110]c and [011]c orientation) deformed simultaneously at 6GPa

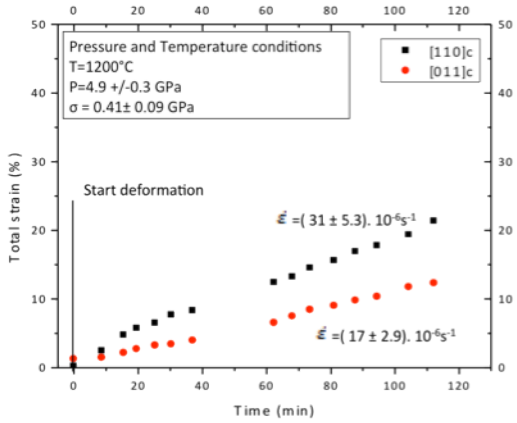

Figure 2: Total strain versus time for two single crystals ([110]c and [011]c orientation) deformed simultaneously at 5GPa.

References

- Raterron, P., J. Chen, L. Li, D. Weidner et P Cordier, 2007, Pressure induced slip-system transition in forsterite: Single crystal rheological properties at mantle pressure and temperature, American Mineralogist, 92 1436-1445
- Raterron, P., 2008, Experimental deformation of olivine single crystals at mantle pressures and temperatures, Physics of the Earth and Planetary Interior

Experimental Constraints on the Strength of the Lithospheric Mantle

S. Mei, A. M. Suzuki, and D. L. Kohlstedt, *University of Minnesota, 310 Pillsbury Dr. SE, Minneapolis, MN 55455*
N. A. Dixon and W. B. Durham, *MIT, 77 Massachusetts Ave., Cambridge, MA 02139*

To provide a better understanding of rheological properties of mantle rocks under lithospheric conditions, we carried out a series of experiments on the creep behavior of polycrystalline olivine at high pressures (~4 to 9 GPa), relatively low temperatures ($673 \leq T \leq 1273$ K), and anhydrous conditions using a deformation-DIA (D-DIA). Differential stress and sample displacement were monitored *in-situ* using synchrotron x-ray diffraction and radiography, respectively. Flow behavior of olivine under lithospheric *P-T* conditions was well quantified with a Peierls stress of $\sigma_P = 5.9 \pm 0.2$ GPa. Compared with published results for high-temperature creep of olivine, a transition from low-temperature plasticity to high-temperature creep occurs at ~1300 K for a strain rate of $\sim 10^{-5}$ s^{-1}. The low-temperature, high-stress flow law for olivine from this study provides a solid basis for modeling tectonic processes occurring within Earth's lithosphere; an example on estimating the strength of oceanic lithosphere is illustrated in Figure 1 as follow.

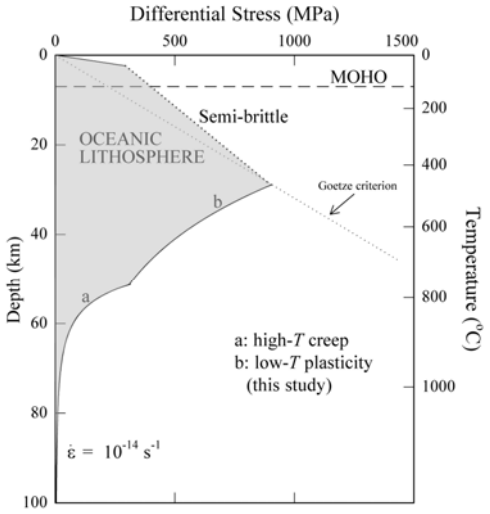

Figure 1. Strength as a function of depth for the oceanic lithosphere deforming at 10^{-14} s^{-1}; modified from *Kohlstedt and Mackwell* [2009]. The oceanic geotherm used in this plot is from *Turcotte and Schubert* [2002, p. 184] with *T*surface = 273 K. Labels a and b illustrate extrapolations of high-*T* flow law from *Chopra and Paterson* [1984] and low-*T* plasticity flow laws from this study, respectively.

References: Mei, S., A. Suzuki, D. L. Kohlstedt, N. A. Dixon, and W. B. Durham (2010), Experimental constraints on the strength of the lithospheric mantle, *J. Geophys. Res.-Solid Earth*. doi:10.1029/2009JB006873.

This research was supported by US Department of Energy Office of Basic Energy Sciences under contract DE-FG02-04ER15500 (UMN) and DE-FG02-07ER15839 (MIT). Experiments were carried out at the X17B2 beamline of the National Synchrotron Light Source, which is supported by the US Department of Energy, Division of Materials Sciences and Division of Chemical Sciences under Contract No. DE-AC02-76CH00016 and by COMPRES, the Consortium for Materials Properties Research in Earth Sciences under NSF Cooperative Agreement EAR 01-35554.

Deformation of Olivine at Subduction Zone Conditions Determined from *In situ* Measurements with Synchrotron Radiation

Hongbo Long[1], Donald J. Weidner[1], Li Li[1], Jiuhua Chen[1,2], Liping Wang[1]

[1] Mineral Physics Institute, Stony Brook University, Stony Brook, NY 11794
[2] Center for the Study of Matters at Extreme Conditions, Florida International University, Miami, FL 33199

We report measurements of the deformation stress for San Carlos olivine at pressures of 3-5 GPa, temperatures of 25 - 1150°C, and strain rates of 10^{-7}-$10^{-5}s^{-1}$. We determine a deformation stress of approximately 2.5 GPa that is relatively temperature and strain rate independent in the temperature range of 400-900°C. The deformation experiments have been carried out on a deformation DIA apparatus, Sam85, at X17B2, NSLS. Water content is confirmed by IR spectra (at U2A, NSLS) of the recovered samples.

In the regime of 25-400°C, there is a small decrease of stress at steady state as temperature increases; in the regime of 400°C to the 'transition temperature', the differential stress at steady state (~2.5 GPa) is relatively insensitive to the changes of temperature and strain rate; however, it drastically decreases to about 1 GPa and becomes temperature-dependent above the transition temperature and thereafter. The transition temperature is near 900°C. Above the transition temperature, the flow agrees with power law creep measurements of previous investigations. The anisotropy of differential stress in individual planes indicates that the deformation of olivine at low temperature is dominated by [001](100). Accounting to a slower strain rate in the natural system, the transition temperature for the olivine in the slab is most likely in the range of 570-660°C.

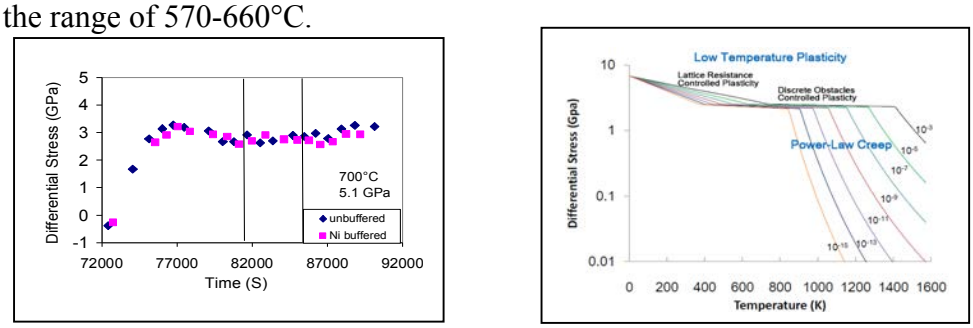

Figure Left: Stress vs. time diagram at 700°C. Right: The deformation map of olivine.

Reference: **Long, HB.,** Weidner, D., Li, L., Chen, JH, Wang, LP. (in press). Deformation of Olivine at Subduction Zone Conditions Determined from *In situ* Measurements with Synchrotron Radiation. ***Physics of the Earth and Planetary Interiors.*** doi:10.1016/j.pepi.2011.02.006.

This research was by NSF under grant EAR0711365. X17B2 and U2A are supported by COMPRES, the Consortium for Materials Properties Research in Earth Sciences under NSF Cooperative Agreement EAR 06-49658 and.

Plastic deformation of wadsleyite and olivine at high-pressure and high-temperature using a rotational Drickamer apparatus (RDA)

Nishihara, Y[1], D. Tinker[2], T. Kawazoe[1], Y. Xu[2], Z. Jing[3], K.N. Matsukage[1], S. Karato[2],

[1] Ehime University, Matsuyama, Japan
[2] Yale University, New Haven, CT 06520, USA
[3] University of Chicago, Argonne, IL, USA

Drickamer apparatus (RDA) up to pressure and temperature conditions corresponding to the Earth's mantle transition zone. Sintered ring-shaped $(Mg,Fe)_2SiO_4$ wadsleyite and olivine samples were deformed at P~16 GPa and T = 1600 and 1800 K, and P~11 GPa and T = 1800K, respectively, with equivalent strain rate of $\dot{\varepsilon} \sim 6 \times 10^{-5}$ s^{-1}. In situ observations of deforming samples were carried out using the synchrotron radiation facility at Brookhaven National Laboratory, NSLS, X17B2. Stress was measured by X-ray diffraction at six different angles with respect to the compression axis. The stress estimated by X-ray diffraction was in good agreement with the stress estimated from dislocation density (for olivine). Strain was determined using X-ray radiographs of a strain marker (Re or Mo foil). Deformation of samples with a RDA involves both uniaxial compression and simple shear. A new formulation is developed to analyze both components to determine the rheological properties of a sample. Stress–strain curves show strain-hardening up to the equivalent strain of ε ~0.2 followed by the quasi-steady state deformation. Wadsleyite is found to be stronger than olivine compared at similar conditions and the creep strength of olivine at P~11 GPa is much higher than those at lower pressures.

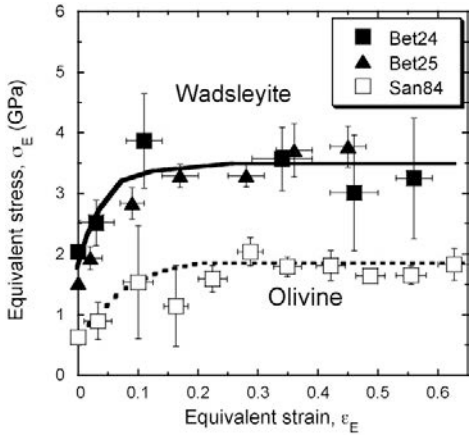

Stress-strain curves of olivine and wadsleyite

Nishihara, Y., et al., 2008. Plastic deformation of wadsleyite and olivine at high-pressures and high-temperatures using a rotational Drickamer apparatus (RDA). Physics of the Earth and Planetary Interiors. 170, 156-169.

This work was conducted using X17B2 at NSLS (Brookhaven) supported by COMPRES and NSF-EAR-0510682.

Shear deformation of polycrystalline wadsleyite

Kawazoe, T.[1], S. Karato[2], J. Ando[3], Z. Jing[4], K. Otsuka[2], and J. Hustoft[5]

[1] Ehime University, Matsuyama, Japan
[2] Yale University, New Haven, CT 06520, USA
[3] Hiroshima University, Higashi-Hiroshima, Hiroshima, Japan
[4] University of Chicago, Argonne, IL, USA
[5] Brown University, Providence, RI, USA

Shear deformation experiments on polycrystalline wadsleyite (water content, ~200–2200 H/10^6 Si) have been conducted at 14.4–17.0 GPa, 1690–2100 K, and strain rates of 2.6–16 °— 10^{-5} s^{-1} using a rotational Drickamer apparatus (RDA) at a synchrotron facility. The stress was measured from the orientation dependence of lattice spacing for the (013), (211), (141), (240) and (244) planes. On the basis of the mechanical and microstructural observations, we infer that deformation occurs by exponential creep through the Peierls mechanism at relatively low temperatures of 1690–2030 K. However, a sample deformed at the temperature of 2100 K showed significant grain-size reduction, and most of small grains are dislocation-free, although sub-boundaries were observed in some grains in the sample. We interpret these observations as evidence for dynamic recrystallization and that diffusion creep (and grain boundary sliding) plays an important role after dynamic recrystallization caused by power law creep. Consequently, the strength observed in the high-temperature conditions determined by the present study provides an important constraint on strength of diffusion creep and a lower limit for that of the power law dislocation creep. We conclude that the strength of wadsleyite in the power law dislocation creep is higher than or comparable to that of olivine and the strength of wadsleyite in the Peierls regime is similar to that of olivine.

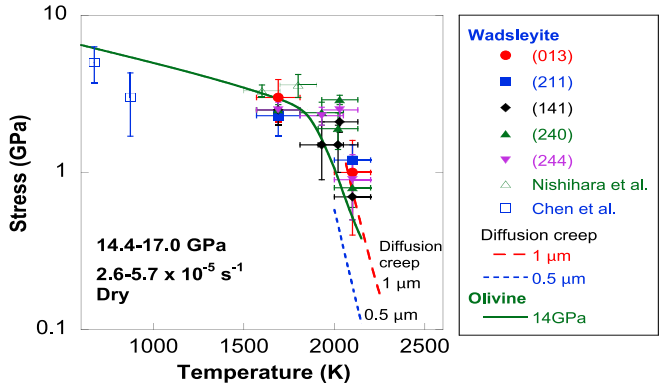

Creep strength of wadsleyite as a function of temperature

Kawazoe, T., S. Karato, J. Ando, Z. Jing, K. Otsuka, and J. Hustoft (2010), Shear deformation of polycrystalline wadsleyite up to 2100 K at 14-17 GPa using a rotational Drickamer apparatus (RDA), *J. Geophys. Res*, *115*, B08208.

This work was conducted using X17B2 at NSLS (Brookhaven) supported by COMPRES and NSF-EAR-0510682.

Rheology of Clinopyroxenes in the Earth's Mantle

P. Raterron, UMET (CNRS 8702), Université Lille 1, France

Clinopyroxenes (cpx) are major constituents of eclogites, and present in excess of 10 vol.% at all depths in the pyrolitic upper mantle. Among mantle minerals, they also exhibit the strongest anisotropy for seismic wave propagation. Cpx plastic properties may thus significantly affect both mantle rheology and seismic properties. Yet, very little is known about their plastic properties at high-pressure (P > 3 GPa), whereas P reaches 14 GPa at the transition zone boundary.

A series of experiments have been carried out on diopside ($CaMgSi_2O_6$) single crystals in the Deformation-DIA apparatus (D-DIA) at the X17B2 beamline (NSLS), at mantle pressure and temperature (T) in the range 5–9 GPa and 1100°–1400°C, respectively. Run products deformation microstructures were investigated in transmission electron microscopy (TEM) (Amiguet et al., 2009 and 2010). Oriented crystals allow activating specific dislocation slip systems during deformation which activities can be quantified, i.e. studying the mechanisms responsible for plasticity in the dislocation creep regime, as well as the effect of pressure on these mechanisms. A strong inhibiting effect of pressure on ½<110> dislocation glide - diopside dominant slips at low P - was evidenced (Figure). This translates in a large activation volume V*~17 cm^3/mol in classical creep power laws. Since P does not affect as much [001] slip activity, ½<110> and [100] dislocation slips show comparable activities at mantle P and T. Three important geological implications result from these observations: i) cpx are likely much stronger in the deep upper mantle - by several orders of magnitude in terms of strain rate - than one can expect from low-P rheological laws. ii) ½<110> and [001] slip comparable activity at mantle P and T explains the lattice preferred orientation (LPO) often observed in naturally deformed eclogites, while low-P data obtained on single crystals could not account for these observations. iii) cpx LPO should not significantly contribute to the seismic anisotropy of mantle peridotites. This study, the first investigation of cpx rheology at asthenospheric pressures, provides an explanation for observation in naturally deformed rocks and constrains quantitatively the contribution of cpx deformation to upper-mantle plasticity and seismic anisotropy.

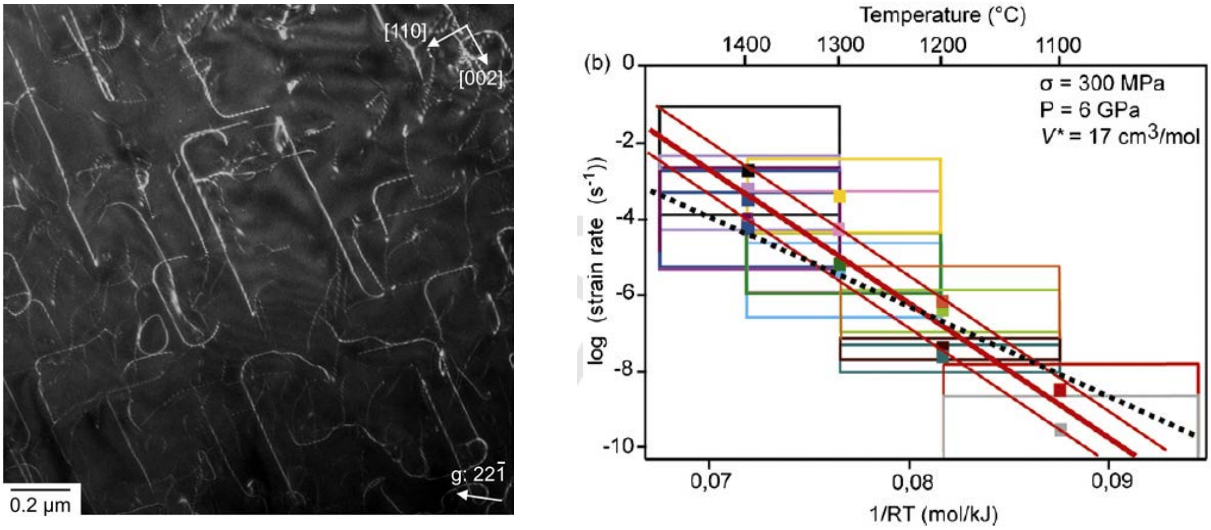

Figure, from *Amiguet et al.* (2009) and (2010): (left) Weak-beam dark-field TEM micrograph of ½<110> dislocations segments in glide configuration at mantle pressure (P ~7 GPa). (right) Rheological data obtained while activating ½<110>{110} slip systems: the error rectangles show all sources of uncertainties; the dashed line fits the data using the activation energy E* ~ 442 kJ/mol reported at low P; the red lines obtained with the high-P data alone suggest a higher E*~ 702 kJ/mol, which may characterize ½<110> dislocation glide at high P.

Cited references:

Amiguet, E., Raterron, P., Cordier, P., Couvy, H., Chen, J. (2009) Deformation of diopside single crystal at mantle pressure, 1, Mechanical data, Physics of the Earth and Planetary Interiors, 177, 122–129.

Amiguet, E., Cordier, P., Raterron, P. (2010) Deformation of diopside single crystals at mantle pressure, TEM characterization of dislocation microstructures, European Journal of Mineralogy, 22, 181-187.

Experimental investigation of the creep behavior of garnet at high temperatures and pressures

S. Mei, A. M. Suzuki, and D. L. Kohlstedt, *University of Minnesota, 310 Pillsbury Dr. SE, Minneapolis, MN 55455*
L. Xu, *Institute of Geophysics and Geomatics, Chinese University of Geosciences, China* (now at University of Minnesota)

The creep behavior of garnet has been investigated at high pressures and temperatures using a deformation-DIA. Samples were cold-pressed from a garnet powder and deformed at constant displacement rates ranging from 1.1 to 2.6 × 10^{-5} s^{-1} at high temperatures (1273 -1473 K) and high pressures (2.4 - 4.1 GPa). Differential stress and pressure were measured using x-ray diffraction techniques based on the elastic strain of various lattice planes as a function of orientation with respect to the applied stress field. The plastic strain of a deforming sample was monitored *in-situ* through a series of radiographs. Our results provide a measure of the dependence of creep rate of garnet on the temperature with an activation energy of ~280 kJ/mol and on pressure with an activation volume of ~10 × 10^{-6} m^3/mol. Results of stress vs. strain rate are illustrated in Figure 1. The flow behavior of garnet quantified by this study provides the basis for modeling geodynamic processes occurring within subducted lithosphere.

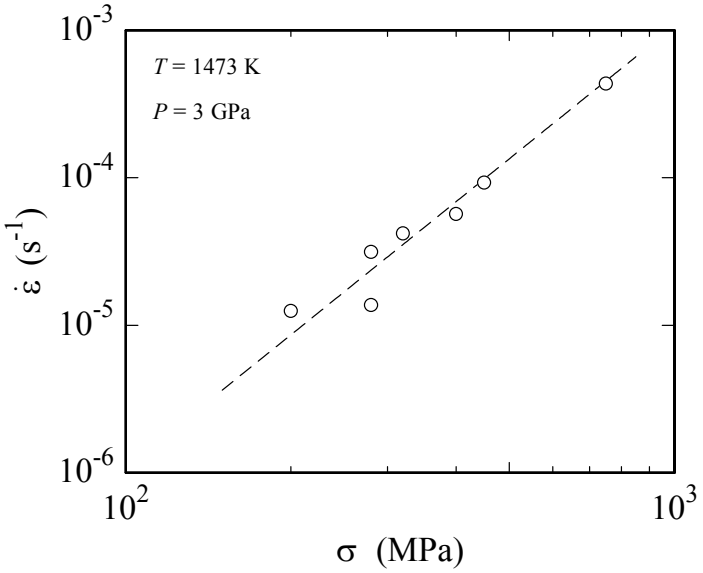

Figure 1. A log-log plot of strain rate versus stress for the creep of garnet. Data from samples deformed at different temperatures and pressures are normalized to a temperature of 1473 K and pressure of 3 GPa. The flow law obtained from this study for the creep of garnet is plotted as a dashed line.

References: Mei, S., A. Suzuki, D. L. Kohlstedt, and L., Xu (2010), Experimental investigation of the creep behavior of garnet at high temperatures and pressures, *J. Earth Sci.,* doi:10.1007/s12583-010-0127-8.

This research was supported by US Department of Energy Office of Basic Energy Sciences under contract DE-FG02-04ER15500 (UMN) and National Science Foundation (No. NSF-EAR-0652852). Experiments were carried out at the X17B2 beamline of the National Synchrotron Light Source, which is supported by the US Department of Energy, Division of Materials Sciences and Division of Chemical Sciences under Contract No. DE-AC02-76CH00016 and by COMPRES, the Consortium for Materials Properties Research in Earth Sciences under NSF Cooperative Agreement EAR 01-35554.

Relative strength of the pyrope-majorite solid solution and the flow-law of majorite containing garnets.

Hunt, S. A.[1], D. P. Dobson[1], L. Li[2], D. J. Weidner[2], and J. P. Brodholt[1]

1. University College London, UK. 2. SUNY at Stony Brook

The garnet phase is the second most abundant mineral component of the upper mantle and transition zone, after olivine and its high pressure polymorphs. In undifferentiated pyrolite mantle, the modal amount of garnet is about 15% at depths of 100–300km increasing to around 40% between 500 and 600 km. In subducting slabs the percentage garnet in the MORB component of the slab can be as high as 90% between depths of 450 and 550 km. There is potential, therefore, for the garnet phase to have a significant influence on mantle dynamics. However, despite this there have been, to date, relatively few studies measuring the rheology of even pure pyrope, let alone other garnet compositions relevant to the mantle. The increasing amount of garnet with depth in the subducting slab and mantle is the result of the increased solubility of pyroxene (generically $AB(Si_2O_6)$, where A and B are the two cations) in garnet as the pressure and temperature increase. This changes the composition of the pyrope ($Mg_3Al2Si_3O_{12}$)-rich garnet to give an increasing majorite (Mg_4Si_4O12) content, by substituting Mg^{2+} and Si^{4+} onto the octahedral site, which is occupied by Al^{3+} in pyrope.
We have performed measurements to determine the relative strength of paired samples of garnets in the $Mg_{3+x}Al_{2-2x}Si_{3+x}O_{12}$ solid solution. The relative-strength experiments reported here were performed on beamline X17B2 at the NSLS using both the Deformation-DIA and T-Cup multi-anvil press modules in a 200 tonne load frame in order to cover the pressure range required for study of the pyrope-majorite system.
The activation energy for dislocation creep in pure majorite is ~175 J/mol higher than in pure pyrope. This might be because the incorporation of Si^{4+} on the octahedral site increases the activation enthalpy of migration on this site, making the rate-limiting step of creep (diffusion of atoms to/from the climbing dislocation) more slow.

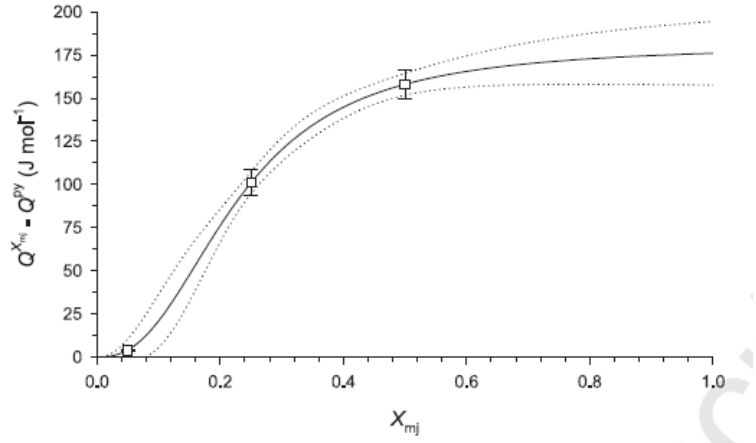

Figure 1. Change in activation energy of dislocation creep in the pyrope-majorite solid solution as a function of majorite content. The data have been fitted to an asymmetric sigmoidal function (solid line).

This work was supported by NSF. NSLS X17b is supported by COMPRES through NSF EAR 06-49658.

Garnet yield strength at high pressures and implications for upper mantle and transition zone rheology

Abby Kavner Earth & Space Science Department, University of California, Los Angeles 90095
(Work performed at NSLS X17C)

Garnet helps control the mechanical behavior of the Earth's crust, mantle, and transition zone. Here, measurements are presented suggesting that garnet, long considered to be a high-viscosity phase, is actually weaker than the other dominant components in the transition zone. The mechanical behavior of garnet at high pressures was examined using radial diffraction techniques in the diamond anvil cell. The yield strength of grossular garnet was inferred from synchrotron X-ray measurements of differential lattice strains. The differential stress was found to increase from 1.3 (±0.6) GPa at a hydrostatic pressure 5.8 (±1.1) GPa to 4.1 (±0.4) GPa at 15.7 (±1.0) GPa, where it was level to 19 GPa. The strength results are consistent with inferred strength values for majorite garnet from measurements in the diamond cell normal geometry, bolstering the idea that garnet- structured materials may have similar strengths. In this low-temperature, high differential stress regime, garnet is shown to be significantly weaker than anhydrous ringwoodite and to have a strength similar to hydrous ringwoodite. This result suggests that the presence of water in the transition zone may not be required to explain a weak rheology, and therefore models of transition zone behavior built assuming that garnet is the high-strength phase may need to be revised.

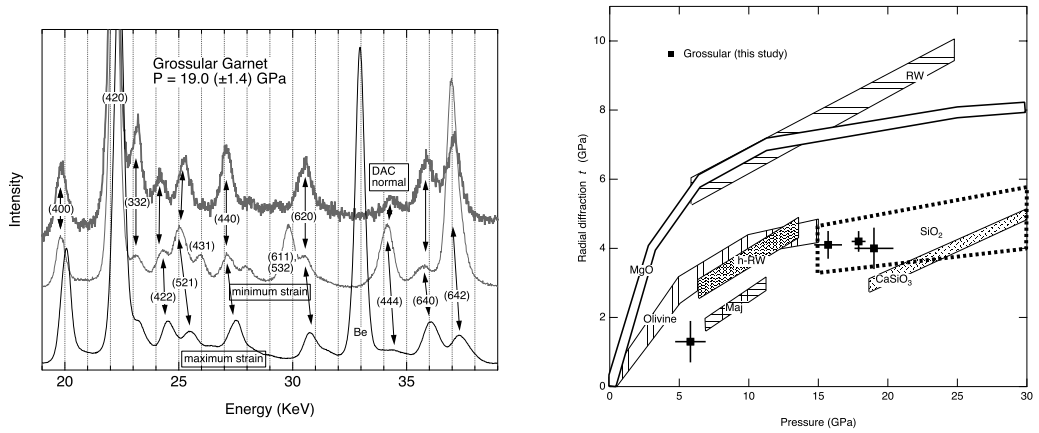

Figure 1 (left). Representative energy-dispersive X-ray diffrac- tion patterns for grossular garnet, at highest compression. Data collected from diamond anvil cell (DAC) normal direction (gray line at top), minimum strain direction (gray line in middle), and maximum strain direction (black line at bottom) are shown. Indexed diffraction peaks are shown with arrows to indicate peak shifts in different patterns. The large peak at 32.0 keV is due to the Be gasket. Patterns are all normalized to the intensity of the (420) peak; 2q = 12.44° for all patterns. Figure 2 (right) A summary of radial diffraction measurements of differential stress inferred from lattice strain for grossular garnet and other mantle materials. Abbreviations and references are as follows: RW, ringwoodite [Kavner and Duffy, 2001]; h-RW, hydrous ringwoodite [Kavner, 2003]; MgO [Duffy et al., 1995]; SiO2, stishovite [Shieh et al., 2002]; Maj, majorite [Kavner et al., 2000]; olivine [Uchida et al., 1995]; CaSiO3 [Shieh et al., 2004]

A. Kavner (2007) Garnet yield strength at high pressures and implications for upper mantle and transition zone rheology *J. Geophys. Res. Solid Earth*, vol. 112, B12207, doi:10.1029/2007JB004931.

Experimental investigation of the creep behavior of MgO at high pressures

S. Mei and D. L. Kohlstedt, *University of Minnesota, 310 Pillsbury Dr. SE, Minneapolis, MN 55455*
W. B. Durham, *MIT, 77 Massachusetts Ave., Cambridge, MA 02139*
L. Wang, Stony Brook University (now at University of Nevada Las Vegas)

The high-temperature rheological behavior of polycrystalline periclase, MgO, has been investigated using the deformation-DIA on a synchrotron beamline at pressures up to 10 GPa. Although temperature and stress sensitivities are not well constrained, there is a clear dependence of creep rate on pressure. Based on our results, the creep rate of MgO depends on confining pressure with an activation volume of $V^* \approx 2.4 \times 10^{-6}$ m^3/mol (see Figure 1). The grain-scale view of deformation processes reveals, as other D-DIA studies have, that subpopulations of grains, grouped by orientation, obey slightly different flow laws. The measurements also reveal that stress heterogeneity in the sample, whether caused by external conditions or processes internal to the sample itself, contribute a significant portion of the overall uncertainty in stress measurement.

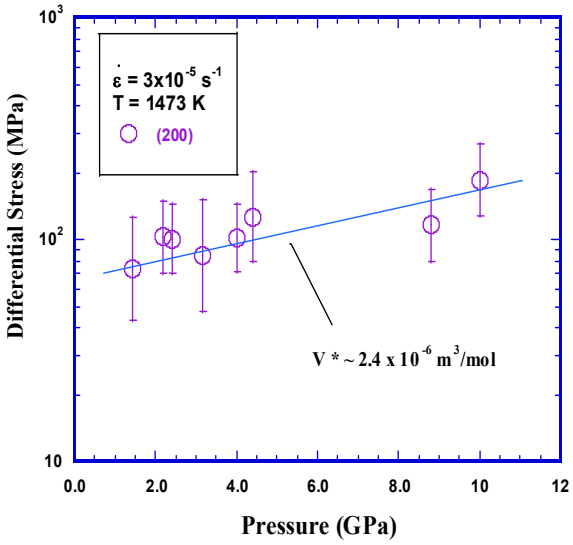

Figure 1. Semi-log plot of differential stress vs. confining pressure based on measurements made with (200) reflection. Stresses from those experiments conducted at different temperatures and strain rates were normalized to 1473 K and 3 × 10^{-5} s^{-1}, respectively. The straight line is the least-squares best fit to the (200) data with stress exponent $n = 3$.

References: Mei, S., D. L. Kohlstedt, W. B. Durham, and L. Wang (2008), Experimental investigation of the creep behavior of MgO at high pressures, *Phy. Earth Plan. Int.*, doi:10.1016/j.pepi.2008.06.030

This research was supported by US Department of Energy Office of Basic Energy Sciences under contract DE-FG02-04ER15500 (UMN) and DE-FG02-07ER15839 (MIT). Experiments were carried out at the X17B2 beamline of the National Synchrotron Light Source, which is supported by the US Department of Energy, Division of Materials Sciences and Division of Chemical Sciences under Contract No. DE-AC02-76CH00016 and by COMPRES, the Consortium for Materials Properties Research in Earth Sciences under NSF Cooperative Agreement EAR 01-35554.

Rheology of the deep upper mantle and its implications for the preservation of the continental roots: A review

Shun-ichiro Karato
Yale University, Department of Geology and Geophysics

The rheological structure of the deep continent was investigated based on the latest experimental study on the influence of pressure and water on the rheological properties of olivine. The influence of pressure (at a fixed water content) on rheological properties is difficult to determine and there were variations in the inferred viscosity of the deep upper mantle up to ~10 orders of magnitude. We have conducted an experimental study of plastic deformation of olivine using the rotational Drickamer apparatus at the NSLS synchrotron radiation facility (supported by COMPRES) to ~10 GPa and ~2000 K. The pressure dependence of olivine creep strength (viscosity) was determined to the conditions equivalent to the deep continental roots (~300 km depth). The results show a large effects of pressure to increase viscosity that will stabilize the deep continental roots after the removal of water by deep upper mantle melting by which the deep continental roots were formed.

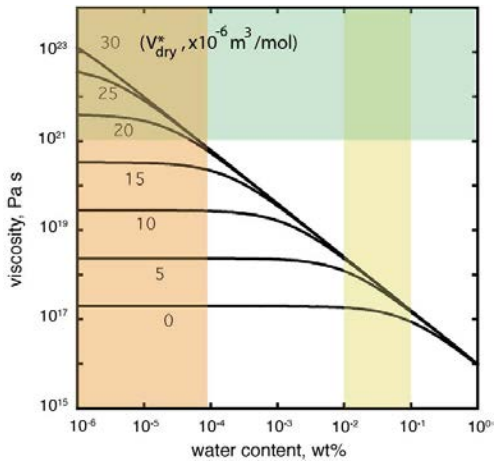

The viscosity contrast corresponding to the change in water content and the activation volume for deformation (V^*_{dry}) estimated from the new data on the influence of pressure on deformation of olivine.

Karato, S., 2010. Rheology of the deep upper mantle and its implications for the preservation of the continental roots: A review. Tectonophysics. 481, 82-98.

This work was conducted using X17B2 at NSLS (Brookhaven) supported by COMPRES and NSF-EAR-0652960.

Theory of lattice strain in a material undergoing plastic deformation: Basic formulation and applications to a cubic crystal

Shun-ichiro Karato
Yale University, Department of Geology and Geophysics

Theory of lattice strain in a polycrystalline aggregate under deviatoric stress is extended to include the influence of ongoing plastic deformation. When deviatoric stress is applied to a polycrystalline material at high temperatures (or above the yield stress), applied macroscopic stress is redistributed to individual grains by plastic deformation according to their orientations with respect to the macroscopic stress and plastic anisotropy of a given crystal. This microstress causes elastic deformation of individual grains that can be measured by x-ray diffraction. Consequently, the observed lattice strain depends on two material properties, viscosity (plasticity) and elastic compliance as well as the applied macroscopic stress and the stress-strain distribution among various grains. The influence of plastic deformation on lattice strain is analyzed using an anisotropic and nonlinear power-law constitutive relationship. In this model, the dependence of inferred macroscopic stress on the crystallographic orientation of diffraction plane (*hkl*) comes from elastic and plastic anisotropy of a crystal. In many materials, plastic anisotropy dominates over elastic anisotropy. This explains the observed large dependence of inferred stress on the diffraction plane and means that the determination of elastic anisotropy is difficult when plastic deformation occurs with anisotropic plasticity. When elastic anisotropy is known, plastic anisotropy of single crystal and/or stress-strain distribution in a deformed polycrystal can be determined from radial x-ray diffraction using the present model. Some examples are presented using the data on MgO.

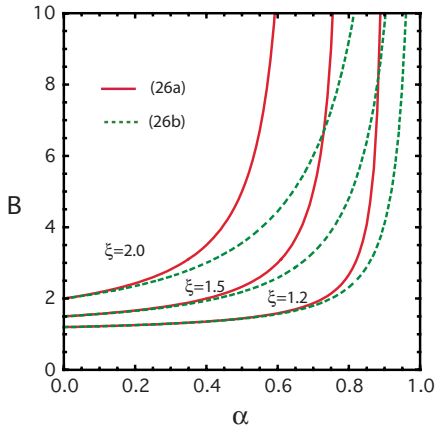

The relation between a parameter characterizing stress-strain distribution α and plastic anisotropy *B* for various values of ξ (strength ratio for the (111) and (200) slip) and the relation for microscopic and macroscopic viscosity

Karato, S., 2009. Theory of lattice strain in a material undergoing plastic deformation: Basic formulation and applications to a cubic crystal. Physical Review. B79, 10.1103/PhysRevB.79.214106.

This work was conducted using X17B2 at NSLS (Brookhaven) supported by COMPRES and NSF-EAR-0652960.

Constraining Earth's Upper-mantle Plasticity

P. Raterron, UMET (CNRS 8702), Université Lille 1, France

Earth's plate tectonics generates major hazards for human societies. In the upper mantle (top 410 km) it is constrained by the plastic properties of aggregates composed mainly of $(Mg,Fe)_2SiO_4$ olivine, mixed with pyroxenes and other minor phases. Upper-mantle dynamics is not well understood because: i) pressure (P) reaches 14 GPa in the upper mantle and until recent years deformation experiments were limited to low P<3 GPa. ii) Recent high-P reports show an unexpected effect of P on olivine rheology. iii) Data refinement and extrapolation to natural (low) stress requires an approach coupling experimental data with aggregate mean-field homogenization modeling.

In order to better constrain Earth's mantle plasticity, a series of experiments have been carried out on single crystals in the Deformation-DIA apparatus (D-DIA) at the X17B2 beamline (NSLS), at mantle pressure and temperature (typically up to 12 GPa and 1400°C, respectively). Oriented single crystals allow activating specific dislocation slip systems during deformation, which activities can then be isolated and quantified. Single crystals of olivine (Fo100 and Fe-bearing olivine) were deformed to investigate the dominant mechanisms responsible for the deformation of this material in the dislocation creep regime, as well as the effect of pressure on these mechanisms. A dislocation slip transition with increasing P has been observed - from a dominant [100] dislocation slip to a dominant [001] slip (Raterron et al., 2009). This transition, which occurs in experiments at 7-8 GPa and may occur in nature at lower P, may be responsible for the seismic velocity anisotropy attenuation observed in the Earth's mantle from 200-km depth. From these rheological data coupled with *ab initio* computational results and a viscoplastic self-consistent (VPSC) approach, a first multi-scale modeling of olivine aggregate rheology in a corner flow geometry (a classic geological context) was recently obtained (Castelnau et al., 2010). This study opens the way to a thorough understanding of mantle plasticity, and more generally of aggregate plasticity, taking into account all available information on crystal plasticity integrated at all scales in a global modeling (Figure).

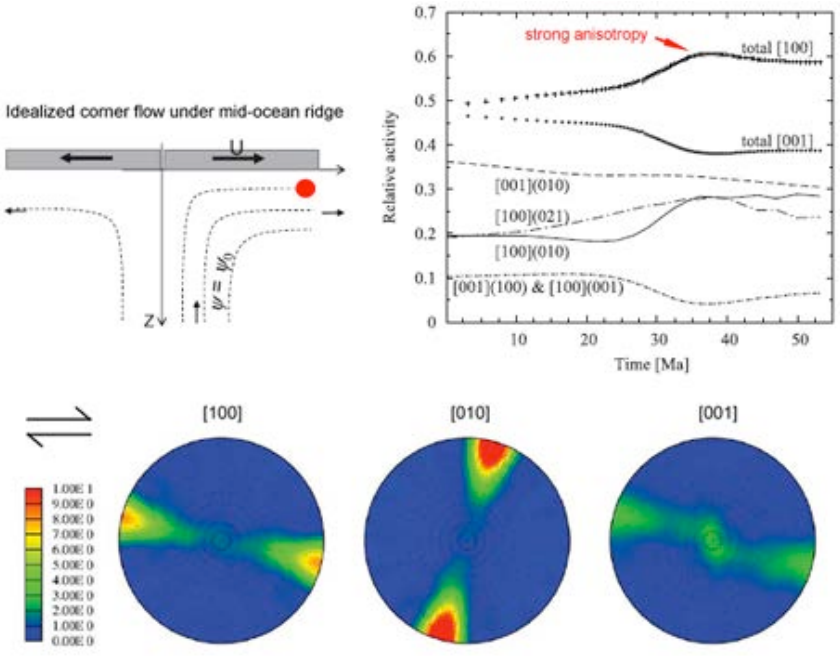

Figure, adapted from *Castelnau et al.* (2010): schematic drawing of a typical flow beneath an idealized ocean ridge, and predicted activities of olivine dislocations slip systems in an aggregate along the streamline. The pole figure represents the LPO in the aggregate after 52 Ma (red circle, depth 67 km, strain 2.1), starting at 410 km depth with a randomly oriented aggregate. The model reproduces the strong olivine LPO (dominant [100](010) system) observed at shallow depths in the mantle. It also shows that most of the LPO is acquired within the corner of the "corner flow".

Cited references:

Castelnau, O., Cordier, P., Lebensohn, R. A., Merkel, S., Raterron, P. (2010) Microstructures and rheology of the Earth upper mantle inferred from a multiscale approach, Comptes Rendus de l'Accadémie des Sciences (Physique), *11*, 304-315.

Raterron, P., Amiguet, E., Chen, J., Li, L., Cordier, P. (2009) Experimental deformation of olivine single crystals at mantle pressures and temperatures, Physics of the Earth and Planetary Interiors, *172,* 74-83.

Interpreting in-situ x-ray diffraction data from high pressure deformation experiments using elastic-plastic self-consistent models: an example using quartz

P C Burnley[1,2] and D Zhang[1]

The high pressure rheology of Earth materials governs many aspects of Earth's behavior from mountain building to the mixing of geochemical reservoirs in the mantle. In the last decade, technical advances have allowed for a significant expansion of the pressure range over which quantitative high temperature deformation studies can be conducted. These new high pressure deformation experiments rely on in-situ diffraction to monitor the state of stress in the sample. Differential strains of individual lattice planes have been used to calculate the stress supported by the sample using a method pioneered by Singh *et al* (1998). However, stresses calculated from multiple sets of lattice planes in a single experiment have been shown by a number of investigators to produce widely differing estimates of the sample strength. As seen in Figure 1, the same effect is evident in quartz. This discrepancy arises because diffraction is generated by individual grains in the polycrystal and therefore reflects grain-scale phenomena rather than macroscopic properties. As an alternative to Singh's method, we have used elastic plastic self-consistent (EPSC) modeling to derive the macroscopic stress supported by the sample from the stresses measured in the grains. We find that elastic strain of the (100), (101) and (112) lattice reflections from polycrystalline quartz deformed at 2 GPa and 800 °C can be modeled using an EPSC model (Figure 2). We are able to match the measured differential elastic lattice strains with a model in which basal and prism <a> slips are activated.

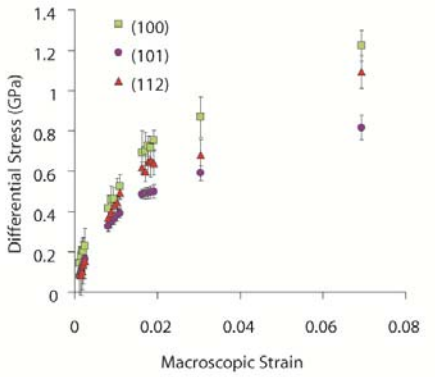

Figure 1 Stresses calculated using Singh et al. (1998) diffraction elastic constants from a SiO_2 (α -quartz) polycrystal deformed at 800 C, 2 GPa , 2 x 10^{-5} /sec.

An interesting outcome of the EPSC model is the prediction that the macroscopic stress experienced by the sample should be greater than the stress calculated from any of the reflections that we observed (Figure 3). This observation serves as a caution against using reflection stresses as a proxy for the macroscopic stress in in-situ deformation experiments.

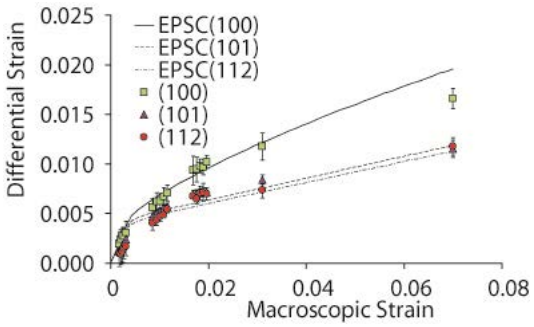

Figure 2 EPSC model of deforming polycrystalline quartz. CRSS for Prismatic <a> slip 0.15 GPa and 0.16 GPa for Basal slip. A hardening parameter of 1.8 GPa was used for basal slip.

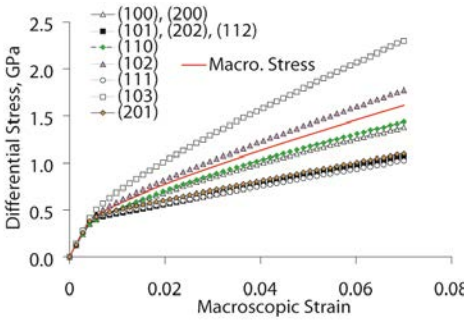

Figure 3 Stresses for 10 lattice planes calculated from the model in Figure 2.

This research was partially supported by NSF grant EAR 01-36107 and partially supported by COMPRES, the Consortium for Materials Properties Research in Earth Sciences under NSF Cooperative Agreement EAR 10-43050. Use of the National Synchrotron Light Source, Brookhaven National Laboratory, was supported by the US Department of Energy, Office of Science, Office of Basic Energy Sciences, under contract Co. DE-AC02-98CH10886.

[1] Department of Geoscience, Georgia State University, Atlanta, GA 30303

[2] Department of Geoscience and High Pressure Science and Engineering Center, University of Nevada, Las Vegas, NV 89154-4010

Li, L., A. Addad, D. Weidner, H. Long, and J. Chen (2007), High pressure deformation in two-phase aggregates, *Tectonophysics*, *439*(1-4), 107-117.

We investigate the rheological behavior of multi-phase aggregates at high pressure and high temperature. Using synchrotron X-ray radiation as the probing tool, we are able to quantify the stress state of individual phases within the aggregates. This method provides fundamental information in interpreting the behavior of two phase/multi-phase mixtures, which contribute to our understanding of the deformation process at deep earth conditions. We choose $MgAl_2O_4$ spinel and MgO periclase as our model materials. Mixtures of various volume proportions were deformed in a multi-anvil high pressure deformation apparatus at pressure of 5 GPa and elevated temperatures. Stress is determined from X-ray diffraction, providing a measure of stress in each individual phase of the mixture *in situ* during the deformation. Macroscopic strain is determined from x-ray imaging. We compare the steady state strength of various mixtures at 1000 °C and 800 °C and at the strain rate in the range of 1.8 to 8.8 x 10^{-5} s^{-1}. Our data indicate that the weak phase (*MgO*) is responsible for most of the accumulated strains while the strong phase (spinel) is supporting most of the stress when the volume proportion is 75% spinel and 25% MgO. The intermediate compositions (40/60) are much weaker than either of the end members, while the grain sizes for the intermediate compositions (sub-microns) are much smaller than the end members (5-10 microns). We conclude that a change in flow mechanism resulting from these smaller grains is responsible for the low strength of the intermediate composition mixtures. This study demonstrates an approach of using synchrotron X-rays to study the deformation behaviors of multi-phase aggregates at high pressure and high temperature.

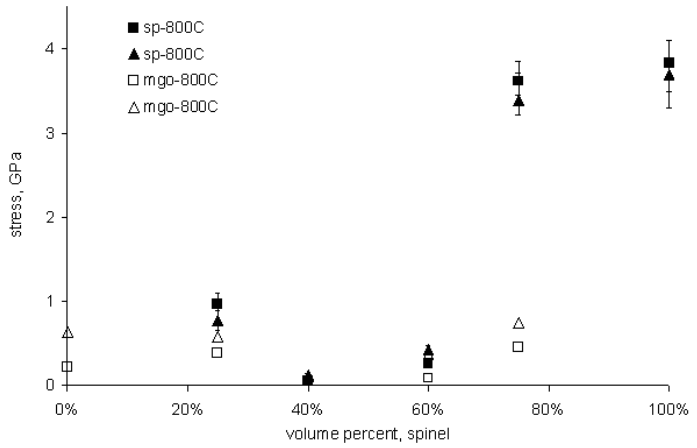

Stress vs. spinel volume percent at 700°C and 5 GPa. Solide triangle represnets spinel sample in the mixture and the pure spinel (100%). Open triangle represents MgO sample in the mixure and pure MgO (100%). Square symbols are likewise but at a different strain rates.

Thermal diffusivity of MORB-composition rocks to 15 GPa: Implications for triggering of deep seismicity

Dobson, D[1]., S. Hunt[1], R. McCormack[1], O. Lord[2], D. Weidner[3], L. Li[3], and A. Walker[1]

1.University College London, UK. 2. Bristol University, UK. 3. SUNY at Stony Brook

Conductive heat transport through mantle materials plays a fundamental role in mantle convection and hence the secular cooling of the Earth. It is the main mechanism for thermally equilibrating subducting oceanic lithosphere with the surrounding mantle which, in turn, determines the depth of the equilibrium (and metastable) phase transitions and buoyancy forces in subducting slabs. However, despite their importance for mantle dynamics, the thermal conductivity, κ, and diffusivity, D, of mantle minerals at high pressure are very poorly constrained. For example, there are no measurements for perovskite above 1 atmosphere and 340 K (Osako and Ito, 1991) and only one set of thermal diffusivity measurements of the high-pressure polymorphs of Mg_2SiO_4, wadsleyite and ringwoodite.

We have measured the thermal diffusivity of eclogite and majorite with a model MORB composition at pressures of 3 and 15 GPa respectively (figure 1), using our new radiographic technique on X17b2 of the NSLS. Both phase assemblages show inverse dependences of their thermal diffusivities on temperature: $D_{eclogite}=9(10)\times10^{-10}+ 7(1)\times10^{-4}/T(K)$ m^2/s and $D_{majorite}=6.2(5)\times10^{-7}+ 3.0(5)\times10^{-4}/T(K)$ m^2/s. The values for majorite are in good agreement with previous measurements for other garnets and are considerably lower than thermal diffusivities of wadsleyite and ringwoodite which are the main components of the mantle transition zone.

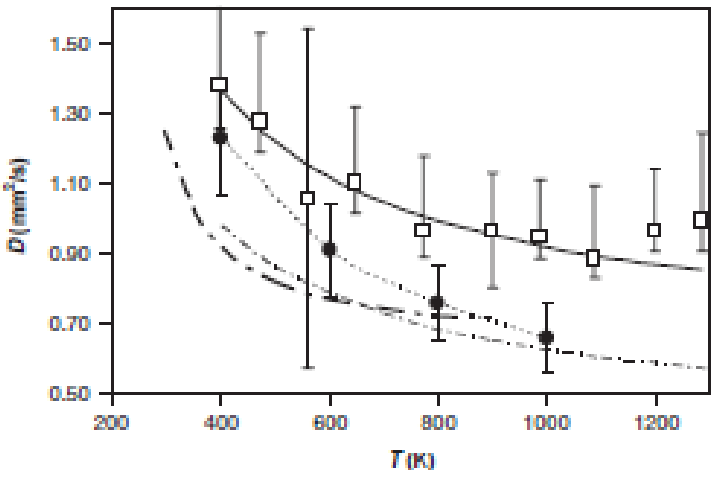

Figure 1. Variation of garnet thermal diffusivity with temperature. Open squares: this study, majorite at 15 GPa. Solid circles: Osako et al., 2004, almandine-pyrope at 8 GPa. Dotted, dot-dashed lines: 'pyrope' garnets at 1 atmosphere from Oasko 1997 and Hoffmeister, 2006.

These results suggest that, at pressures of majorite stability, silica-rich regions of the mantle will have lower thermal conductivity than silica-poor regions. This could be significant for the dynamics of subducting slabs where silica is concentrated into the crustal component in the upper 7-10 km of the slab. In particular, thermal feedback mechanisms of deep seismicity should be more effective in the crus al component of slabs in the deep transition zone. This might explain the apparent migration of earthquake hypocentres into the upper portions of the slab in the mid- to lower- transition zone.

This work was supported by NSF. NSLS X17b is supported by COMPRES through NSF EAR 06-49658.

Radial diffraction strength and elastic behavior of CaF_2 in low- and high-pressure phases

Abby Kavner Earth & Space Science Department, University of California, Los Angeles 90095

(Work performed at X17C)

Halides are an important class of materials for high pressure research because they serve as a testbed for predictions of elastic and phase behavior of minerals at high-pressures. The radial diffraction lattice behavior of CaF_2 was analyzed in its low pressure (fluorite) and high pressure phase up to 11.5 GPa using radial X-ray diffraction techniques in the diamond anvil cell. Between 3.5 and 7.1 GPa, fluorite develops a radial diffraction strength of ~0.8 GPa. The corresponding lattice anisotropy of the fluorite phase was measured to be equal to 0.73, in good agreement with previous Brillouin spectroscopy measurements. By 8.8 GPa, CaF_2 has undergone a phase transformation to its high pressure (orthorhombic) phase, with a corresponding volume decrease of 10.4%. By 11.5 GPa, the volume drop between the low pressure and high pressure phase has increased to 11.5%. In addition, the high pressure phase is found to withstand a significantly larger differential stress than the low pressure fluorite phase, with a large degree of lattice anisotropy. In the maximum stress direction at 8.8 GPa, we observe a time-dependent evolution of the lattice parameters of CaF_2, indicating that the high pressure structure is still undergoing deformation on timescales of hours after the phase boundary has been crossed.

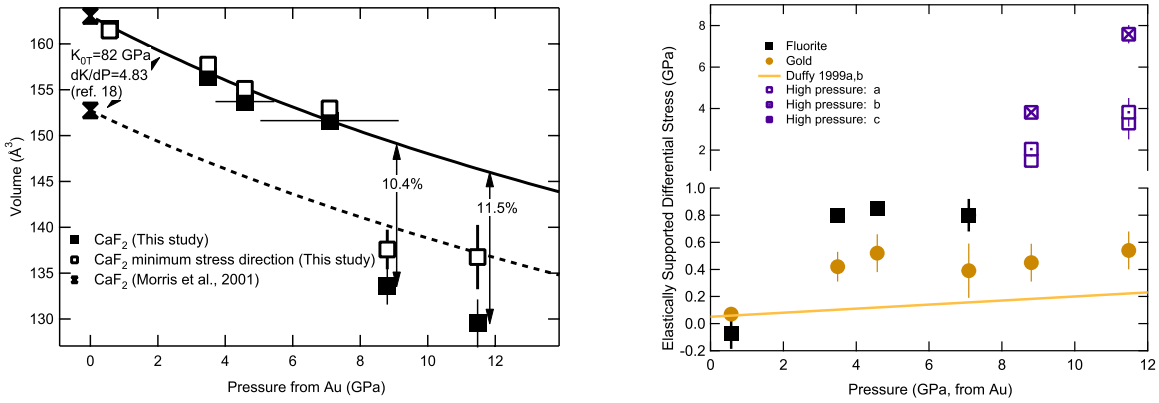

Figure 1 (left). Measured unit cell volumes as a function of pressure for CaF_2. Solid squares are volumes at the hydrostatic conditions. Open squares are volumes inferred from strains in the minimum stress direction. Pressure is determined by using the lattice parameters of Au, added as a pressure calibrant in the diamond anvil cell. The measured $\Delta V=(V_2-V_1)/V_1$ for the transition between the high pressure phase and low pressure phase are shown at the two highest pressure steps. Figure 2 (right) Differential stress as a function of pressure for CaF_2 and Au. The high pressure phase of CaF_2 appears to be much stronger than the fluorite phase.

Kavner, A. (2008) Radial diffraction strength and elastic behavior of CaF_2 in low- and high-pressure phases, *Phys Rev. B*, 77, 224102

Understanding depth variation of deep seismicity from in situ measurements of mineral strengths at high pressures

Jiuhua Chen, *Florida International University*

When materials are subject to differential stress, most of them undergo elastic, anelastic deformation, and plastic change after yielding. Strength of minerals plays a dominant role in governing Earth's mantle dynamics such as convection and earthquakes. Here we report systematic analysis of high pressure strength characteristics of major mantle minerals measured using *in situ* synchrotron X-ray diffraction and peak broadening deconvolution. The result supplies important information for understanding the cause of depth variation of deep seismicity.

Experiments were carried out on major minerals of Earth's mantle at high pressures and high temperatures. Analysis of the diffraction peak widths is used to derive the yield strengths. Systematic analysis of the experimental result for olivine, wadsleyite, ringwoodite and perovskite indicates that minerals in the upper mantle, the transition zone and the lower mantle have very distinct strength character. Increasing temperature weakens the upper mantle mineral, olivine, significantly. At high temperature and high pressure, the transition zone minerals, wadsleyite and ringwoodite, have higher strengths than the upper mantle mineral. Among all the minerals studied, the lower mantle mineral, perovskite, has the highest strength. While both the upper mantle and the transition zone minerals show a notable strength drop, the strength of the lower mantle mineral shows just an increase of relaxation rate (no strength drop) when the temperature is increased stepwise by 200 K. The strength characteristics of these major mantle minerals at high pressures and temperatures indicate that yield strength and its temperature dependence may play a crucial role in defining the profile of deep earthquake occurrence with depth.

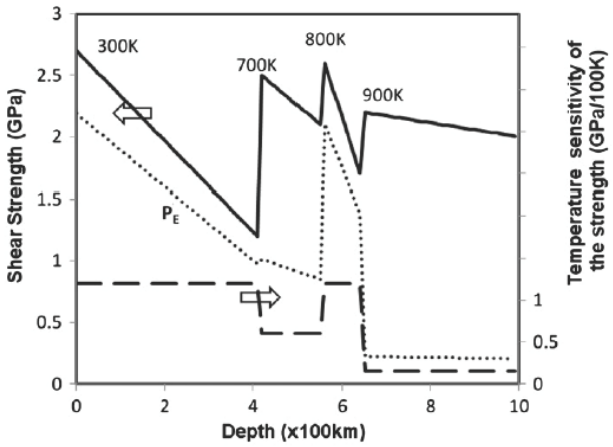

Figure on the left summarizes the Stress capacity of a subducting slab represented by the shear strength of dominant minerals (solid line) along a geotherm of cold center of the slab. Influence of pressure variation on the strength is not taken into account (the experimental pressure of strength measurement is 10 GPa for olivine and wadsleyite and 20 GPa for ringwoodite and perovskite). The broken line represents the temperature sensitivity of the strength. The dotted line represents the possibility for earthquakes to happen $P_E = P_G \bullet P_A \bullet P_I$, ($P_G$ is the availability of stress generation assumed to be 1, P_A capability of stress accumulation, *i.e.* strength and P_I possibility of plastic instability, *i.e.* temperature sensitivity of the strength). P_E presented here matches well the profile of the accumulated number of earthquakes as a function of depth (occurred beneath Tonga Island).

Reference: Jiuhua Chen, Understanding depth variation of deep seismicity from in situ measurements of mineral strengths at high pressures, *Journal of Physics and Chemistry of Solids* 71 (2010) 1032–1037.

Research is supported by NSF (EAR-0711321 and EAR-1015509). Use of high pressure beamline X17B of NSLS is supported by COMPRES, the Consortium for Materials Properties Research in Earth Sciences under NSF Cooperative Agreement EAR 10-43050

Elastic and Anelastic Properties of Mantle Minerals: Keys to the Structure and Composition of the Upper Mantle

Indoor Seismology: Probing the Earth's Interior using Sound Velocity Measurements at High Pressures and Temperatures in the Laboratory

Baosheng Li and Robert C. Liebermann, Mineral Physics Institute and Department of Geosciences, Stony Brook University

The adiabatic bulk (K_S) and shear (G) moduli of mantle materials at high pressure and temperature can be obtained directly by measuring compressional (V_P) and shear (V_S) wave velocities in the laboratory using experimental techniques based on physical acoustics. We present the application of the current state-of-the-art experimental techniques using ultrasonic interferometry in conjunction with synchrotron X-radiation to study the elasticity of olivine and pyroxenes and their high-pressure phases. Using these updated thermoelasticity data for these phases, velocity and density profiles for a pyrolite model are constructed and compared with radial seismic models. We conclude that pyrolite provides an adequate explanation of the major seismic discontinuities at 410 and 660-km depths, the gradient in the transition zone, as well as the velocities in the lower mantle if the uncertainties in the modeling as well as the variations in different seismic models are considered. The characteristics of the seismic scaling factors in response to thermal anomalies suggest that anticorrelations between bulk sound and shear wave velocities, as well as the large positive density anomalies observed in the lower mantle cannot be fully explained without invoking chemical variations.

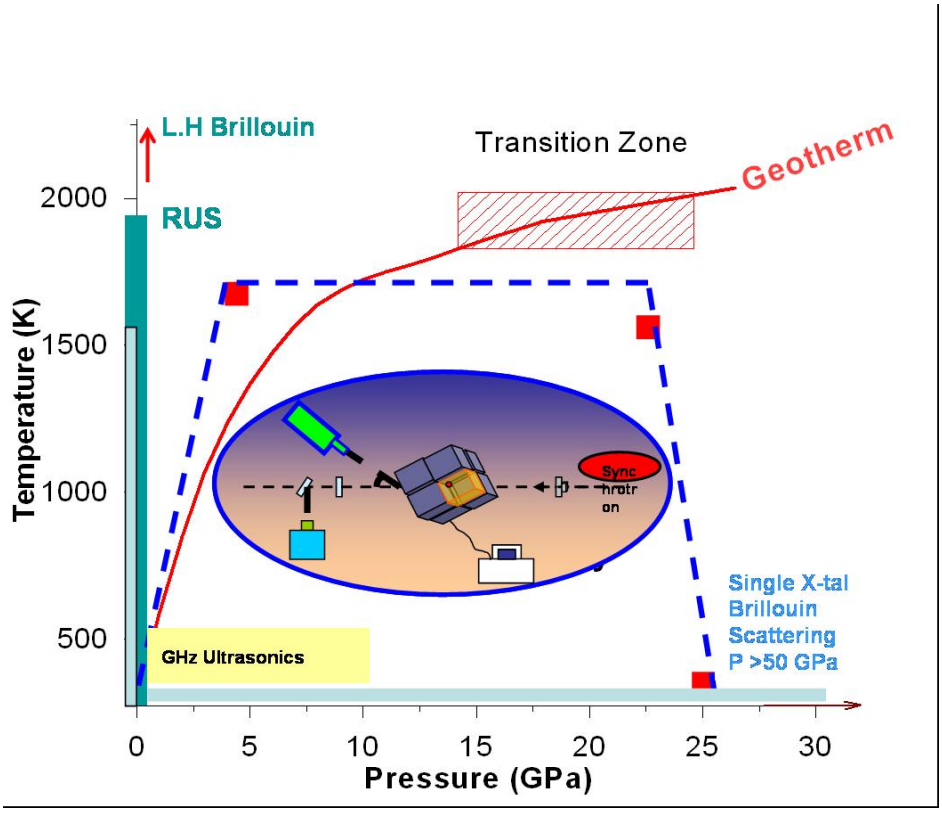

Fig. Current experimental pressure and temperature conditions accessible in laboratory acoustic velocity measurements using various techniques and the mantle conditions with a representative geotherm.

Publication: Li, B., and R. C. Liebermann, Indoor seismology by probing the Earth's interior by using sound velocity measurements at high pressures and temperatures, Proc. National Acad. Sci., 104, 9145-9150, 2007

Acknowledgements. This research was supported by National Science Foundation under grants EAR00135550 (to BL) and EAR02-29704 (to RCL). The experimental data used in this study were obtained using the facilities at X17B1/B2 of NSLS in Brookhaven National Laboratory which is supported by COMPRES under funding from the NSF (EAR01-35554 and 06-49658) and the U.S. Department of Energy, Basic Energy Sciences, and Office of Energy Research under Contract No. DE-AC02-76CH00016.

The Elastic Properties of β-Mg_2SiO_4 from 295 to 660 K and Implications on the Composition of Earth's Upper Mantle

D. G. Isaak[1, 2], G. D. Gwanmesia[3], D. Falde[2], M. G. Davis[2], R. S. Triplett[3], L. Wang[4]

[1]University of California, Los Angeles, [2]Azusa Pacific University,
[3]Delaware State University, [4]Stony Brook University

Elasticity measurements were carried out on a sintered polycrystal β-Mg_2SiO_4 (wadsleyite) from 295- 660 K at ambient pressure using resonant ultrasound spectroscopy (RUS). Room temperature values for the adiabatic bulk (K_S) and shear (G) moduli are 170.2(1.9) GPa and 113.9(0.7) GPa, respectively. The K_S data exhibit linear dependence on temperature (T) with $(\partial K_S/\partial T)_P$=-1.71(5)×10^{-2} GPa K^{-1}. Our result for $(\partial K_S/\partial T)_P$ is consistent with a high magnitude for this derivative which contrasts with -1.20×10^{-2} to -1.30×10^{-2} GPa K^{-1} reported in some earlier studies. The average $(\partial G/\partial T)_P$=-1.57(3)×10^{-2} GPa K^{-1} over the temperature range studied and is consistent with most earlier measurements of $(\partial G/\partial T)_P$ for wadsleyite. Our results for $(\partial K_S/\partial T)_P$ and the average $(\partial G/\partial T)_P$ are consistent with olivine content of 44%-54% at 410-km depth in Earth, given other assumptions made in recent studies about properties of the α- and β-olivine phases for P, T conditions at that depth. The $G(T)$ data exhibit small, but persistent, nonlinear behavior; the magnitude of $(\partial G/\partial T)_P$ increases with T. Greater olivine content than 44%-54% is required to model the 410-km seismic discontinuities if this nonlinear effect is confirmed and demonstrated to apply when extrapolating to Earth's transition zone temperatures.

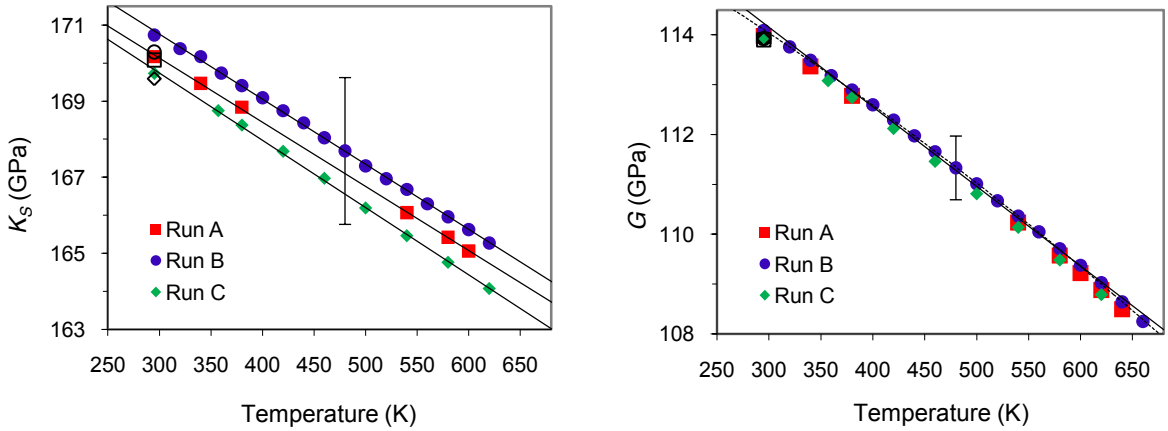

Reference

Isaak, D.G., Gwanmesia, G.D., Falde, D., Davis, M.G., Triplett, R.S., and Wang, L., The elastic properties of β-Mg_2SiO_4 from 295 to 660 K and implications on the composition of Earth's upper mantle. *Physics of the Earth and Planetary Interiors, 162*, 22-31, 2007.

Support

The *x*-ray analysis of the sample in these experiments was done using the X-17B2 beam line at the NSLS (Brookhaven).

The Temperature Dependence of the Elasticity of Fe-Bearing Wadsleyite

D. G. Isaak[1, 2], G. D. Gwanmesia[3], M. G. Davis[2], S. C. Stafford[2], A. A. Stafford[2], R. S. Triplett[3]

[1]University of California, Los Angeles, [2]Azusa Pacific University,
[3]Delaware State University, [4]Stony Brook University

Data were obtained on the elastic properties of β-$(Mg_{0.92}Fe_{0.08})_2SiO_4$ (iron-bearing wadsleyite) from 295 to 640 K at ambient pressure. The elasticity measurements were made on hot-pressed polycrystals using resonant ultrasound spectroscopy (RUS). Multiple temperature excursions were done with data being retrieved during heating (solid symbols in figures) and cooling (open symbols) cycles. Room temperature (RT) values for the adiabatic bulk (K_S) and shear (G) moduli are 170.8(1.2) GPa and 108.9(0.4) GPa, respectively. The average derivatives over the temperature (T) range studied are $(\partial K_S/\partial T)_P$= $-1.75(0.07)\times10^{-2}$ GPa K^{-1} and $(\partial G/\partial T)_P$=$-1.55(0.06)\times10^{-2}$ GPa K^{-1}. Comparing these results with those from our recent Mg-endmember wadsleyite study shows no measurable difference in the average $(\partial K_S/\partial T)_P$ or $(\partial G/\partial T)_P$ from RT to 640 K due to Fe content. The magnitude of $(\partial K_S/\partial T)_P$ measured in our RUS studies at ambient pressure is noticeably larger than found by Liu et al. (*Geophy. Res. Lett., 32: L16301*, 2005; *Phys. Earth Planet. Int., 174*: 98-104, 2009) in studies with Mg-endmember and Fe-bearing wadsleyite [dashed lines in figure for $K_S(T)$]. Slight nonlinearity in the temperature dependences of both K_S and G are observed; second order fits for both $K_S(T)$ and $G(T)$ are statistically justified. Whereas, the current nonlinearity in $G(T)$ for β-$(Mg_{0.92}Fe_{0.08})_2SiO_4$ is similar to that observed for β-Mg_2SiO_4, second order effects in $K_S(T)$ were not observed previously for Mg-endmember wadsleyite.

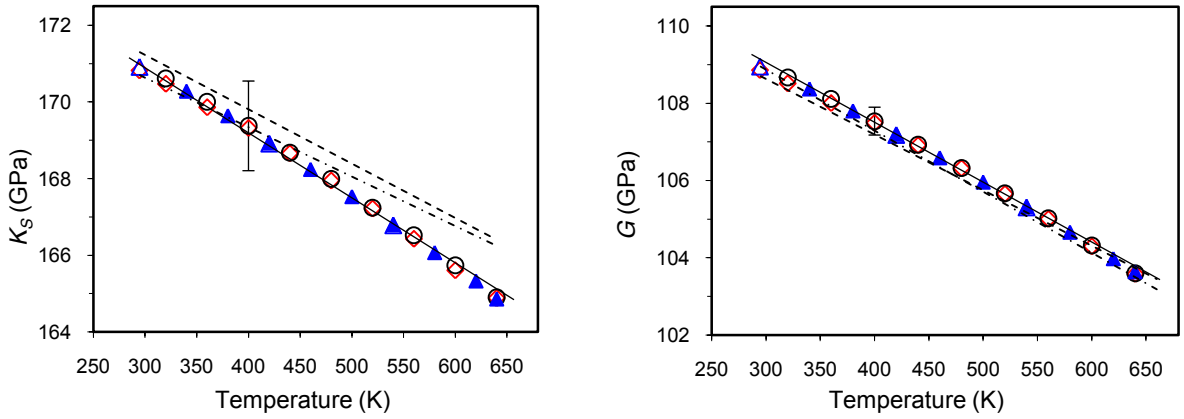

Reference

Isaak, D.G., Gwanmesia, G.D., Davis, M.G., Stafford, S.C., Stafford, A.A, Triplett, The Temperature Dependence of the Elasticity of Fe-Bearing Wadsleyite, *Physics of the Earth and Planetary Interiors, 182*, 107-112, 20010.

Support

The *x*-ray analysis of the sample in these experiments was done using the X-17B2 beam line at the NSLS (Brookhaven).

Physics of the Earth and Planetary Interiors 174 (2009) 98–104

Elasticity of $(Mg_{0.87}Fe_{0.13})_2SiO_4$ wadsleyite to 12 GPa and 1073 K

Wei Liu[a,*], Jennifer Kung[b], Baosheng Li[a], Nori Nishiyama[c,d], Yanbin Wang[c]

[a] Mineral Physics Institute, Stony Brook University, Stony Brook, New York, NY 11794, USA
[b] Department of Earth Sciences, National Cheng-Kung University, Tainan 70101, Taiwan
[c] Center for Advanced Radiation Sources, University of Chicago, Chicago, IL 60637, USA
[d] Geodynamics Research Center, Ehime University, 2-5 Bunkyo-cho, Matsuyama 790-8577, Japan

A B S T R A C T

Elasticity of $(Mg_{0.87}Fe_{0.13})_2SiO_4$ wadsleyite has been measured at simultaneous high pressure and high temperature to 12 GPa and 1073 K using ultrasonic interferometry in conjunction with synchrotron X-radiation. The elastic moduli and their pressure and temperature derivatives are precisely determined using pressure-standard-free third-order and fourth-order finite strain equations. Combined with previous thermoelastic data on olivine, the density, velocity and acoustic impedance contrasts between α- and β-$(Mg_{0.9}Fe_{0.1})_2SiO_4$ at 410-km depth are calculated along a 1673 K adiabatic geotherm. Both the third- and fourth-order finite strain equation fitting results give estimation of ~33–58% olivine content in the upper mantle to account for a seismic discontinuity of ~5% velocity jumps, and 8.5% (*P* wave) and 11.1% (*S* wave) impedance jumps at 410 km depth.

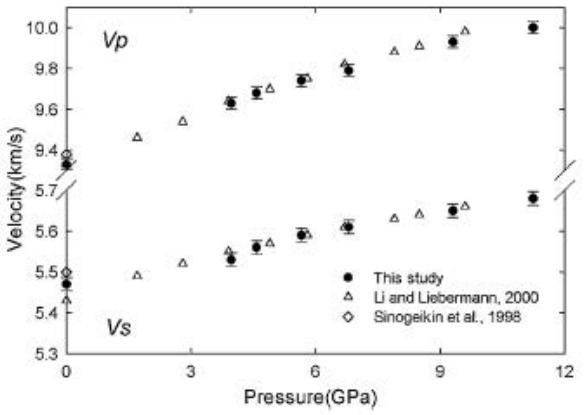

Fig. 4. Comparison of *P* and *S* wave velocities of Fe-bearing wadsleyite from this study with previous data from Sinogeikin et al. (1998) and Li and Liebermann (2000). Error bars indicate two standard deviations.

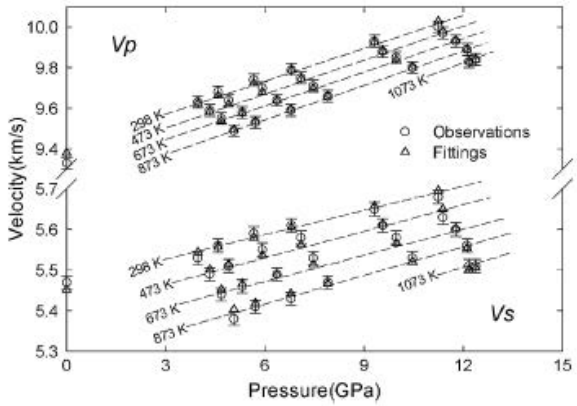

Fig. 5. Comparison of the third-order finite stain fitting (triangle) and measured (circle) results of V_P and V_S as a function of pressure to 12.4 GPa and temperature to 1073 K. Error bars indicate two standard deviations. Dash lines are guide isotherms.

Table 2
Elastic moduli and their pressure and temperature derivatives of wadsleyite.

Ref.	Fe/(Mg+Fe)	K_{S0} (GPa)	G_0 (GPa)	K'_{S0}	G'_0	$(\partial K_S/\partial T)_P$ (GPa K^{-1})	$(\partial G/\partial T)_P$ (GPa K^{-1})	Comments
1	0	174	114					1 bar, RT, BS
2	0	163	110	4.8(2)	1.7(1)			3 GPa, RT, UI
3	0	170(2)	108(1)	4.5(1)	1.6(1)			12 GPa, RT, UI
4	0	170(2)	115(2)	4.3(2)	1.4(2)			14 GPa, RT, BS
5	0	172(2)	113(1)	4.2(1)	1.5(1)	−0.012(1)	−0.017(1)	7 GPa, 873 K, UI
6	0	170.7(11)	111.6(5)	4.56(23)	1.75(9)	−0.0129(17)	−0.0158(10)	7 GPa, 873 K, UI
7[a]	0	170.2(19)	113.9(7)			−0.0171(5)	−0.0157(3)	1 bar, 660 K, RUS
8	8	170(3)	108(2)					1 bar, RT, BS
9	9	165.7(1)	105.66(3)			−0.016(3)	−0.012(1)	1 bar, 318 K, RUS
10	9	165.72(1)	105.43(2)			−0.0175(3)	−0.0159(1)	1 bar, 470 K, RUS
11	12	172(2)	106(1)	4.6(1)	1.6(1)			10 GPa, RT, UI
12	13	175.4(7)	108.0(4)	4.10(11)	1.56(5)	−0.0135(10)	−0.0144(8)	12 GPa, 1073 K, UI
13	13	*171.3*	*108.7*	4.74(8)	1.52(4)	−0.0134(13)	−0.0144(8)	12 GPa, 1073 K, UI

Pressure and Temperature Dependence of the Elasticity of Pyrope-Majorite [$Py_{60}Mj_{40}$ and $Py_{50}Mj_{50}$] Garnets Solid Solution measured by Ultrasonic Interferometry Technique.

Gabriel D. Gwanmesia[1], Liping Wang[2,3], Richard Triplett[1], and Robert C. Liebermann.[2,3]

[1]*Department of Physics & Pre-Engineering, Delaware State University, Dover, Delaware 19901, USA*
[2] *Mineral Physics Institute, Stony Brook University, Stony Brook, New York 11974-2100, USA*
[3] *Department of Geosciences, Stony Brook University, Stony Brook, New York 11974-2100, USA*

Acoustic compressional (P) and shear (S) wave velocities have been measured for two synthetic polycrystalline specimens of pyrope-majorite garnets [$Py_{60}Mj_{40}$ and $Py_{50}Mj_{50}$] by ultrasonic interferometry to 8 GPa and 1000 K, in a DIA-type cubic anvil high pressure apparatus (SAM-85) interfaced with synchrotron x-radiation and x-ray imaging. Elastic bulk (K_S) and shear (G) moduli data obtained at the end of the cooling cycles were fitted to functions of Eulerian strain to 3rd order yielding pressure derivatives of the elastic moduli, $(\partial K_S/\partial P)_T$ = 4.3 (3); $(\partial G/\partial P)_T$ = 1.5 (1) for $Py_{60}Mj_{40}$ garnet and $(\partial K_S/\partial P)_T$ = 4.4 (1); $(\partial G/\partial P)_T$ = 1.3 (1) for $Py_{50}Mj_{40}$ garnet. Both $(\partial K_S/\partial P)_T$ and $(\partial G/\partial P)_T$ are identical for the two garnet compositions and are also consistent with Brillouin scattering data for polycrystalline $Py_{50}Mj_{50}$. Moreover, the new pressure derivatives of the elastic moduli are equal within experimental uncertainties to those of end-member pyrope garnet from ultrasonic studies (*Gwanmesia et al., 2006*) and from Brillouin spectroscopic studies (*Sinogeikin and Bass, 2002a*), thereby demonstrating that the pressure derivatives of the elastic moduli are unaffected by substitution of Si for Mg and Al within the Py-Mj solid solution in the range (Py_{100}-Py_{50}) of the present measurements. Temperature dependence of the elastic obtained from linear regression of entire P-T-K and P-T-G data are: $(\partial K_S/\partial T)_P$ = -14.6 (4) MPa/K, $(\partial G/\partial T)_P$ = -9.4 (4) MPa/K for $Py_{60}Mj_{40}$ garnet, and $(\partial K_S/\partial T)_P$ = -14.6 (4) MPa/K, $(\partial G/\partial T)_P$ = -9.33 (2) MPa/K for $Py_{50}Mj_{50}$ garnet. These values are essentially identical for the two compositions and are also in excellent agreement with the Brillouin scattering data of *Sinogeikin and Bass, 2002b*) for $Py_{50}Mj_{50}$ garnet; however, they are higher than those for pyrope by about 23% for $(\partial K_S/\partial T)_P$ and 11% for $(\partial G/\partial T)_P$ (*Gwanmesia et al., 2006*) .

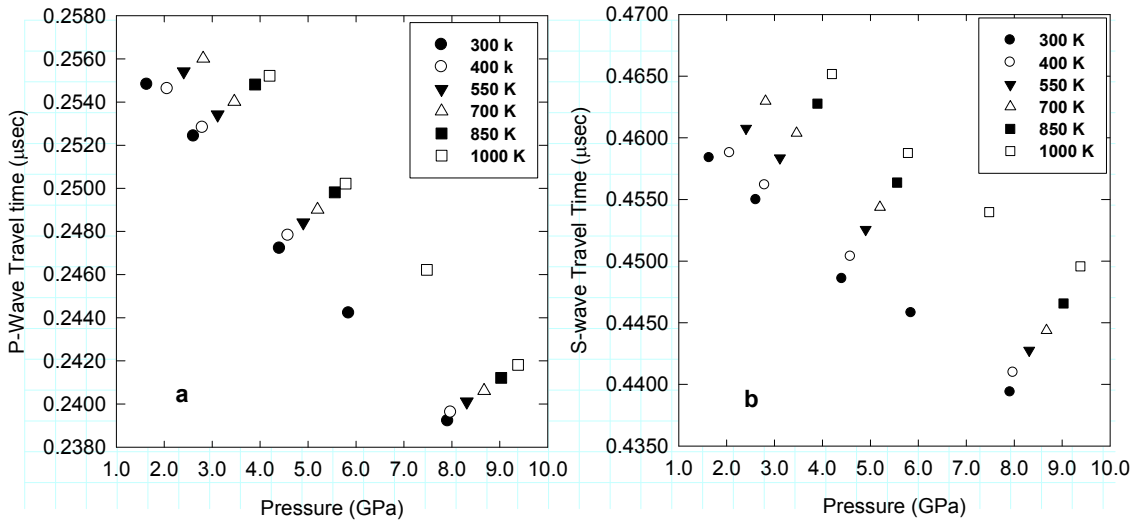

Fig. 1a and b: Travel times of P waves (a) and S waves (b) for $Py_{50}Mj_{50}$ garnet as a function of pressure along experimental isotherms.

Publication: G Gwanmesia, L Wang, R Triplett, R Liebermann (2009), Pressure and temperature dependence of the elasticity of pyrope–majorite [$Py_{60}Mj_{40}$ and $Py_{50}Mj_{50}$] garnets solid solutions measured by ultrasonic interferometry technique, *Phys. Earth Planet. Interiors*, 174, 105-112 (2009).

Acknowledgements: This research was supported by National Science Foundation under grants EAR-0135431 to GDG under the Elasticity Grand Challenge Project and EAR 06-35651 to RCL. The in-situ ultrasonic experiments were carried out at the X-17B2 beamline of the National Synchrotron Light Source (NSLS), which is supported by the US Department of Energy, Division of Materials Sciences and Division of Chemical Sciences under No. DE-AC02-76CH00016, and COMPRES, the Consortium for Materials Properties Research in Earth Sciences under NSF Cooperative Agreements EAR 01-35554 and 06-49658.

Elasticity of stishovite and acoustic mode softening under high pressure

F. Jiang[1], G. D. Gwanmesia[2], T. I. Dyuzheva[3], and T. S. Duffy[1]

[1]Princeton University, [2]Delaware State University, [3]Inst. of High-Pressure Physics, Troitsk

The full set of elastic constants of stishovite, an octahedrally coordinated form of SiO_2, has been measured at high pressures for the first time. Our Brillouin scattering measurements to 12 GPa show that the shear modulus, C_{11}–C_{12}, exhibits softening behavior beginning from ambient pressure and it has decreased by 11% at 12 GPa. The acoustic softening is directly observed in the shear branch for one of the measured planes. Our experimental measurements differ from previous theoretical calculations by up to 10% for the individual elastic constants. Single-crystal x-ray diffraction measurements were carried out at X17c, NSLS to determine the density and orientation of each crystal used. The equation of state determined from our Brillouin and x-ray diffraction data is in excellent agreement with previous studies. These results will provide new constraints on models of the soft-mode driven transformation from stishovite to the $CaCl_2$-type structure in SiO_2.

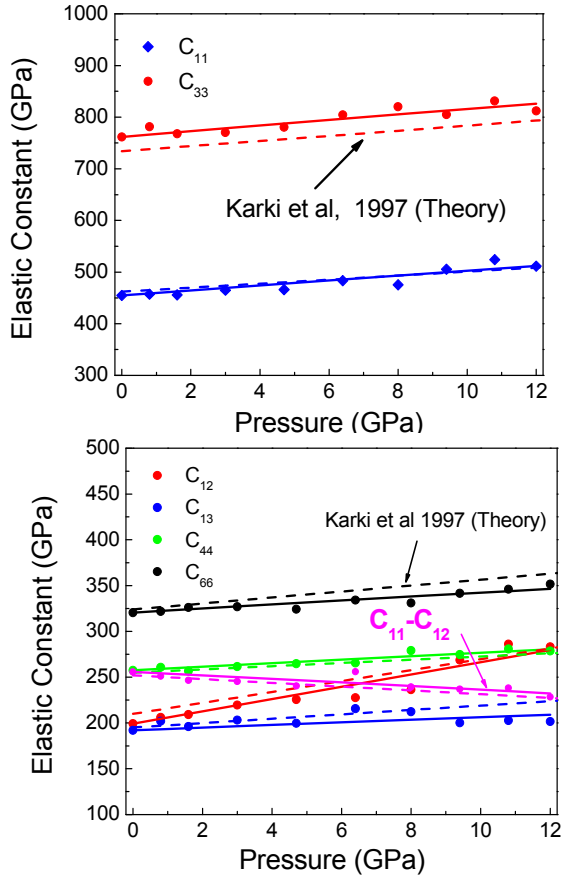

Elastic moduli of stishovite as a function of pressure to 12 GPa compared with theoretical calculations. The softening of C_{11}-C_{12} can be seen in the lower panel.

Jiang, F., G. D. Gwanmesia, T. I. Dyuzheva, and T. S. Duffy, Elasticity of stishovite and acoustic mode softening under high pressure by Brillouin scattering, *Physics of the Earth and Planetary Interiors*, 172, 235-240, 2009.

This work was supported by the NSF (EAR 07-38510) and Carnegie-DOE Alliance Center. NSLS X17C is supported by COMPRES through NSF EAR 06-49658.

Elasticity of diopside to 8 GPa and 1073K and implications for the upper mantle

B. S. Li[1], D. R. Neuville[2]
[1]Mineral Physics Institute, Stony Brook University, New York, USA
[2] CNRS-IPGP, Physique des Minéraux et Magmas, Géochimie et Cosmochimie, France

Clinopyroxene has been found in mantle peridotite xenoliths in various locations and together with orthopyroxene, it is considered to be an important constituent phase in compositional models for the upper mantle. Simultaneous measurements of elastic wave velocities and density have been conducted on diopside by a combined ultrasonic interferometry and X-ray diffraction methods at pressure and temperature conditions relevant to the Earth's upper mantle. The current study not only yielded the first direct measurement of the shear modulus at high pressures, but also enabled a simultaneous determination of the bulk and shear properties and their pressure and temperature derivatives from the measured density and velocities. Finite strain analysis of the experimental data results in K_{S0} = 116.4(7) GPa, K_{S0} = 4.9(1), $(\partial K_S/\partial T)_P$ =−0.012(1) GPa, G_0 = 1.6(1) and $(\partial G/\partial T)_P$ =−0.011(1) GPa/K. With these results and the same finite strain equations, the P and S wave velocities of diopsidic mantle clinopyroxene were calculated along a 1600K adiabatic geotherm. In comparison with other mantle minerals, the seismic velocities of diopsidic clinopyroxene at upper mantle depths are 1–3% higher than those of orthopyroxene, 1–2% and 6–8% lower than those of olivine and majoritic garnet, respectively.

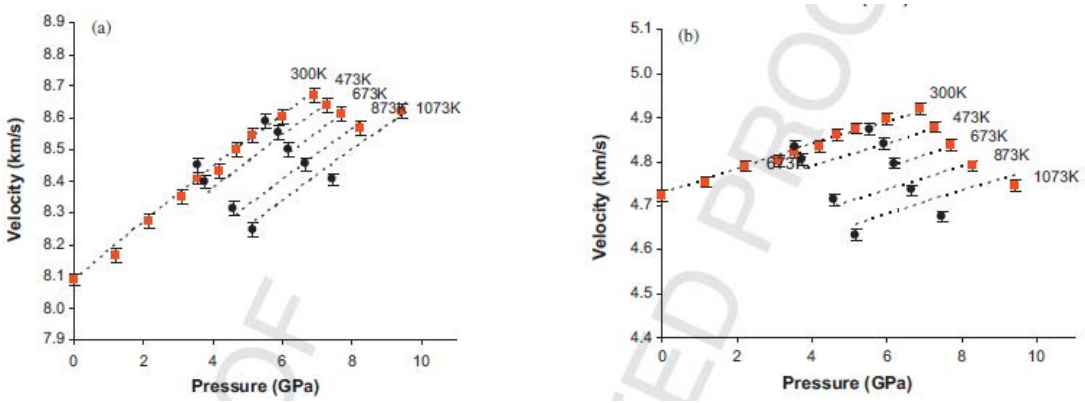

Figure. (a) P and (b) S wave velocities as a function of pressure and temeprature for $CaMgSi_2O_6$ diopside.

B. S. Li, D. R. Neuville, Acoustic Velocities and Elastic Properties of Pyrite (FeS_2) to 9.6 GPa, Physics of the Earth and Planetary Interiors 183, 398–403, 2010.

Synchrotron experiments were conducted at the X17B2 beamline of NSLS which is supported by COMPRES under NSF Cooperative Agreement EAR06-49658.

The Elastic Properties of Diopside, $CaMgSi_2O_6$

Liqin Sang, Carine B. Vanpeteghem, Jay D. Bass, *University of Illinois at Urbana-Champaign*
Stanislas V. Sinogeikin, Geophysical Laboratory, *Carnegie Institution of Washington*

The thirteen single-crystal elastic moduli of two samples of diopsidic pyroxenes close to the ideal composition ($CaMgSi_2O_6$) from different locations have been measured at ambient pressure and room temperature by Brillouin spectroscopy (shown in the table below). There are no major differences in the elastic tensor of the nearly pure diopside composition compared with the second sample containing slightly higher Al and Fe contents. Polycrystalline averaging of the C_{ij} for the bulk modulus K_s and shear modulus G yield values in the table below. The shear moduli reported here are 8% larger than those determined from previous measurements on a similar natural sample, but are in good agreement with recently reported values. We confirm the existence of systematic correlations between the composition of the M2 site and most of the C_{ij} values. No unusual compositional dependence of C_{ij} values or the shear modulus near end-member diopside composition is observed.

	Diopside 1[a]	Diopside 2[a]	Chrome-diopside[b]	Diopside[c]
C_{11}	229.0 ± 0.4	226.1 ± 0.9	228.1 ± 1.0	223 ± 2
C_{22}	179.0 ± 0.4	179.5 ± 0.8	181.1 ± 0.6	171 ± 2
C_{33}	242.5 ± 0.4	239.2 ± 0.9	245.4 ± 1.3	235 ± 2
C_{44}	78.9 ± 0.3	78.1 ± 0.6	78.9 ± 0.3	74 ± 1
C_{55}	68.1 ± 0.2	69.2 ± 0.4	68.2 ± 0.2	67 ± 1
C_{66}	78.2 ± 0.3	76.4 ± 0.8	78.1 ± 0.2	66 ± 2
C_{12}	78.0 ± 0.7	77.4 ± 1	78.8 ± 0.5	77 ± 3
C_{13}	69.8 ± 0.6	70.2 ± 1.3	70.2 ± 0.7	81 ± 2
C_{23}	58.0 ± 0.7	56.7 ± 1.6	61.1 ± 0.7	57 ± 2
C_{15}	9.9 ± 0.3	9.9 ± 0.7	7.9 ± 0.5	17 ± 1
C_{25}	6.1 ± 0.5	5.9 ± 1.2	5.9 ± 0.5	7 ± 2
C_{35}	40.9 ± 0.3	41.0 ± 0.7	39.7 ± 0.4	43 ± 1
C_{46}	6.6 ± 0.2	6.8 ± 0.4	6.4 ± 0.2	7.3 ± 0.9
K_s	114.6 ± 0.6	114.0 ± 1.2	116.5 ± 0.9	113
G	72.7 ± 0.1	72.1 ± 0.3	72.8 ± 0.4	67.0

[a]This work, [b] Isaak and Ohno (2003) and [c] Levien et al. (1979)

Single-crystal elastic moduli (GPa) of diopside for this work in comparison to previous work.

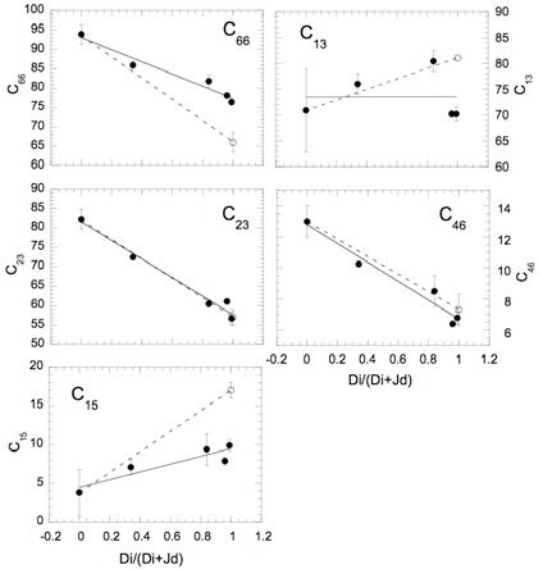

The variation of C_{66}, C_{13}, C_{23}, C_{46} and C_{15} with composition in the diopside-jadeite system. For results near Di/(Di+Jd)=1.0, open circles are from Levien et al (1979), solid circles are diopside #1 of this study, and solid diamonds are diopside #2 of this study. Open circles indicate data at nominal Di/(Di+Jd) ratios of 0.0 (Norris and Bass, 2010); 0.34 (Bhagat et al. 1992); 0.84 (Collins and Brown 1998); and 0.96 (Isaak and Ohno 2003). The solid lines show linear fits using the results of the present study for end-member diopside, excluding the results of Levien et al. (1979). The dashed lines simply connect the data for Jd and the results of Levien et al. (1979).

References: Bhagat, S.S., Bass, J.D., and Smyth, J.R. (1992) Single-crystal elastic properties of omphacite-C2/c by Brillouin spectroscopy. Journal of Geophysical Research, 97, 6843-6848.

Collins, M.D. and Brown, J.M. (1998) Elasticity of an upper mantle clinopyroxene. Physics and Chemistry of Minerals, 26, 7-13.

Isaak, D.G. and Ohno, I. (2003) Elastic constants of chrome-diopside: application of resonant ultrasound spectroscopy to monoclinic single-crystals. Physics and Chemistry of Minerals, 30, 430-439.

Levien, L., Weidner, D.J., and Prewitt, C.T. (1979) Elasticity of diopside. Physics and Chemistry of Minerals, 4, 105-113.

Norris, S. and Bass, J.D. (2010) Sound velocities and elastic properties of single-crystal jadeite. In preparation.

The authors would like to thank I. Steele and J. Jackson for the electron microprobe analyses of the diopside samples. This work was supported by NSF grant EAR 0738871 and partially supported by COMPRES, the Consortium for Materials Properties Research in Earth Sciences under NSF Cooperative Agreement EAR 10-43050.

High-temperature elasticity of polycrystalline orthoenstatite ($MgSiO_3$)

Jennifer Kung[a,c], Ian Jackson[b], Robert C. Liebermann[c]

[a] Department of Earth Sciences, National Cheng Kung University, Taiwan
[b] Research School of Earth Sciences, Australian National University
[c] Mineral Physics Institute and Department of Geosciences, Stony Brook University

Compressional and shear wave velocities of a polycrystalline specimen of MgSiO3 orthoenstatite have been measured by ultrasonic interferometry to 1400 K at 300 MPa in an internally heated gas-medium apparatus. The elastic wave velocities and bulk and shear moduli vary linearly with temperature to 1073 K. Below 1073 K, the temperature derivatives of the elastic moduli [$(\partial KS/\partial T)$=-28.3(7) MPa K^{-1} and $(\partial G/\partial T)$=-14.5(1) MPa K^{-1}, respectively] determined in this study are consistent with averages of single-crystal elastic constants measured by Brillouin spectroscopy by Jackson and her colleagues. The measured temperature dependence of elastic moduli, along with pressure dependence of elastic moduli, thermal expansion and calorimetric data have been assimilated into a finite-strain equation of state of the type proposed by Stixrude and Lithgow-Bertelloni. This analysis suggests significant revisions to the optimal values the zero-pressure Grüneisen parameter $\gamma 0$ and its zero-pressure logarithmic volume derivative q0. The unusually high absolute values of $\partial K/\partial P$ and $\partial K/\partial T$ are related through the extrinsic part of the temperature derivative. Above 1073 K, a pronounced softening of the elastic wave velocities is observed, that is plausibly associated with a phase transformation for which there is microstructural evidence: the recovered specimen was found to have transformed to the low-pressure clinoenstatite polymorph.

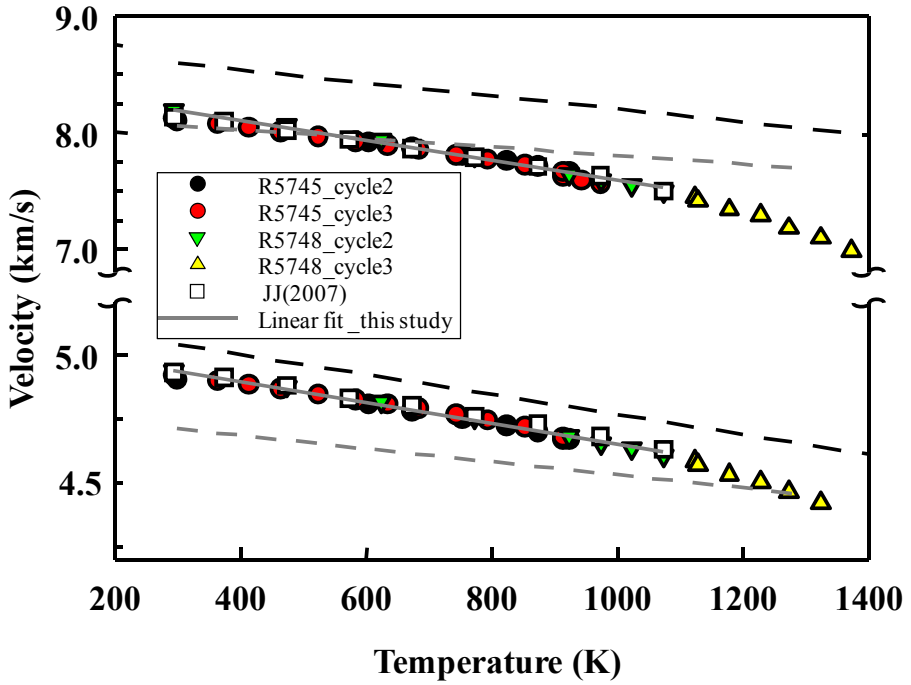

Fig. 1 Derived P and S wave velocities of orthoenstatite (circles and triangles from this study; squares from Jackson et al., 2007), olivine (black dashed line, Isaak et al., 1989) and diopside (gray dashed line, Isaak et al., 2006) plotted as functions of temperature. The P and S wave velocities depart for linear temperature dependence above 1073K.

Publication: Kung, J. I. Jackson, and R. C. Liebermann, High-temperarure elasticity of polycrystalline orthoenstatite (MgSiO3), *American Mineralogist,* in press, October 2010.

Acknowledgements: This experimental work reported in this paper was performed while Jennifer Kung was a postdoctoral research associate at Stony Brook. This research was supported by a NSF grant (INT 02-33849 and EAR 02-29704) to R.C. Liebermann and a grant (LX0348106) from the Australian Research Council to I. Jackson for a collaborative research program between Stony Brook University and the Australian National University and National Science Council (NSC) funding to Jennifer Kung. RCL was supported by COMPRES, the NSF Consortium for Materials Properties Research in Earth Sciences under EAR01-35554 and 06-49658.

Single crystal elasticity and pressure induced phase transition of iron-bearing orthoenstatite

Jin S. Zhang, Jay D. Bass University of Illinois at Urbana-Champaign
Przemyslaw Dera Argonne National Laboratory

Sound velocities and elastic moduli have been measured on iron-bearing orthoenstatite single crystals up to 12Gpa by Brillouin spectroscopy. A fourth order finite strain fit to the data yields to pressure derivatives of 9.09 and 2.90 for the adiabatic bulk modulus (Ks) and shear modulus G respectively. This number is significantly much higher than any of the known major mantle minerals.

A new phase transition was demonstrated by in situ high pressure X-Ray diffraction. The low pressure orthoenstatite phase (Pbca) transformed to a new monoclinic phase ($P2_1/c$) between 9.96 and 11.54 Gpa, which is matched with the sudden increase of anisotropy when pressure increased from 10.5Gpa to 12.0Gpa. The density increase of this phase transition is ~1.7%.

Vp Anisotropy change on plane (100) along with the phase transition

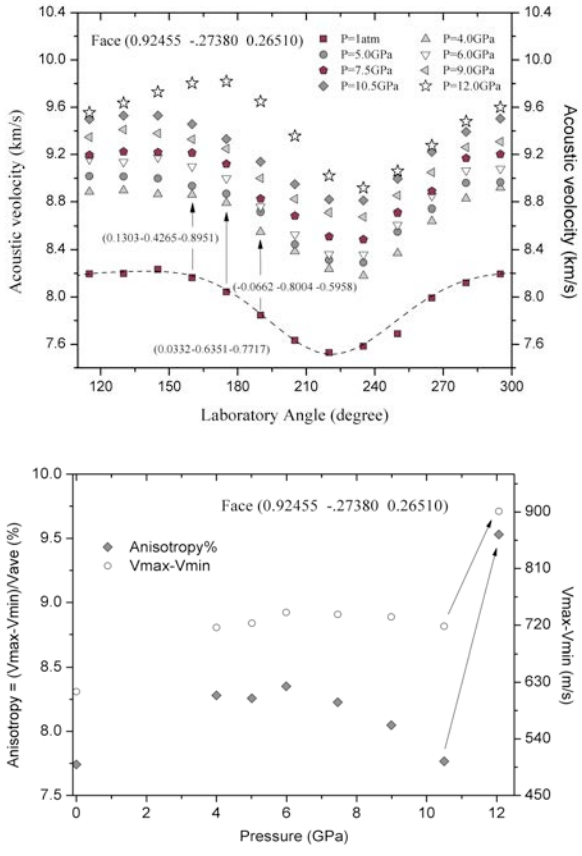

Effect of high pressure on bulk and shear modulus of OEN

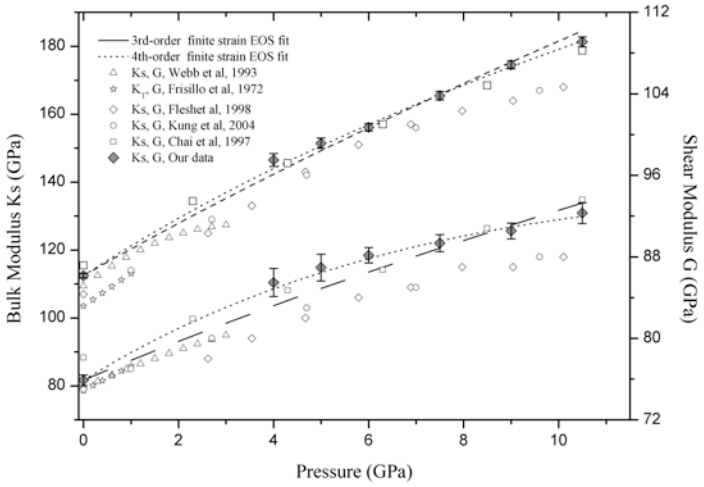

Vs Anisotropy change for single crystal elasticity along with the phase transition

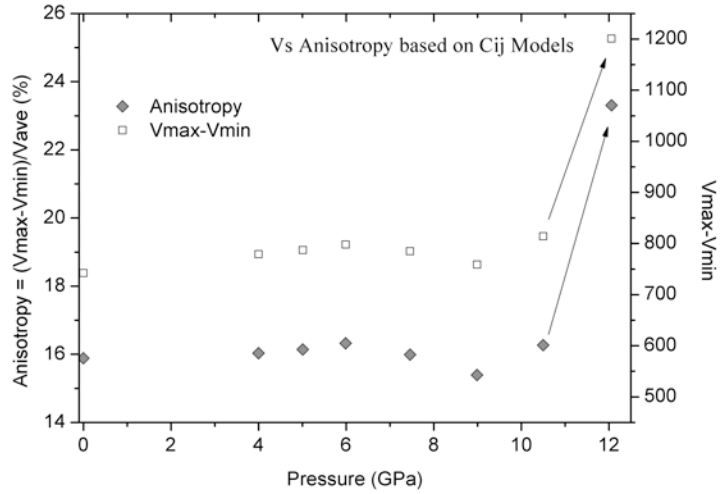

Key references:

Kung, J.,et al. (2004), *Phys. Earth Planet. Inter. 147*, 27-44.
Ulmer, P. and R. Stadler (2001), *Am. Mineral., 86*, 1267-1274.
Pacalo, R. E. G. and T. Gasparik (1990), *Geophys. Res.*, *95*(B10), 15,853–15,858.

High pressure, high temperature equation of state for Fe_2SiO_4 ringwoodite and implications for the Earth's transition zone

Matt M. Armentrout and Abby Kavner, UCLA

Earth & Space Science Department, University of California, Los Angeles 90095

(work performed at GSECARS)

We measured the density of iron-ringwoodite and its pressure and temperature dependence at conditions of the mantle transition zone using the laser-heated diamond anvil cell in conjunction with X-ray diffraction. Our new data combined with previous measurements constrain the thermoelastic properties of ringwoodite as a function of pressure and temperature throughout the transition zone. Our best fit Mie-Grüneisen-Debye equation of state parameters for Fe end-member ringwoodite are V_0 = 42.03 cm^3/mol, K_0 = 202 (4) GPa, K' = 4, g_0 = 1.08 (6), q = 2, and q_D = 685 K. This new equation of state revises calculated densities of the Fe end-member at transition zone conditions upwards by ~0.6% compared with previous formulations. We use this revised equation of state to make predictions of the effect of compositional (iron) and thermal anomalies on the bulk properties of the transition zone.

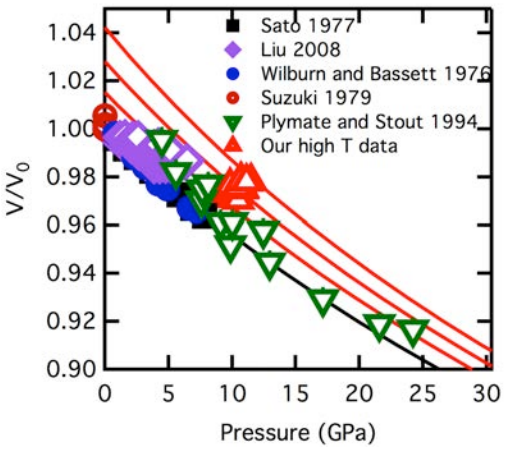

Figure 1. Plot of normalized volume versus pressure for data used in the linear least squares regression. Open and closed symbols refer to high temperature and room temperature measurements respectively. The best fit room-temperature equation of state is shown in black and high temperature contours are plotted in red at 1000, 1500, and 2000 K.

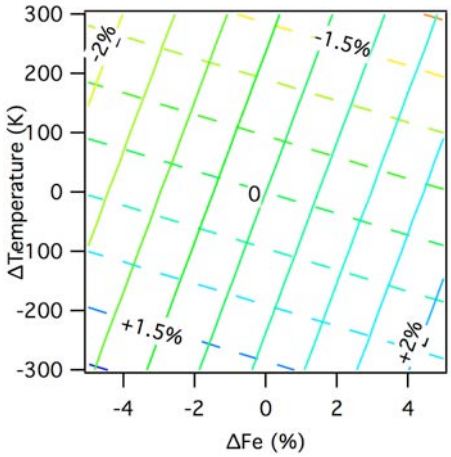

Figure 2. Schematic representation of the effect of changes in composition and temperature on ringwoodite's density (solid) and bulk sound velocity (dashed). Contours of density and bulk sound velocity are plotted in increments of 0.5% difference from 410 km reference values. Different combinations of thermal and compositional anomalies have distinct seismic signature.

References

M. Armentrout* and A. Kavner High pressure, high temperature equation of state for Fe_2SiO_4 ringwoodite and implications for the Earth's transition zone*, Geophys. Res. Lett.*, VOL. 38, L08309, doi:10.1029/2011GL046949 (2011).

Liu, Q., W. Liu, M. L. Whitaker, L. P. Wang, and B. S. Li (2008), *H. Pres. Res., 28*(3), 405-413

Plymate, T. G. and J. H. Stout (1994), *Phys. Chem. Min., 21*(6), 413-420.

Sato, Y. (1977), In: Manghnani M. H., Akimoto, S. (eds)High Pressure Research: applications in geophysics. Academic Press, New York, 307-323

Suzuki, I., Ohtani, E., and Kumazawa, M. (1979), *J. Phys. Earth, 27*, 53-61.

Wilburn, D. R. and W. A. Bassett (1976), *High Temp. – High Pres., 8*(3), 343-348

American Mineralogist, Volume 95, pages 1000–1005, 2010

In situ ultrasonic velocity measurements across the olivine-spinel transformation in Fe_2SiO_4

QIONG LIU,* WEI LIU, MATTHEW L. WHITAKER, LIPING WANG, AND BAOSHENG LI

Mineral Physics Institute, Stony Brook University, Earth & Space Sciences Building, Stony Brook, New York 11794-2100, U.S.A.

Compressional (P) and shear (S) wave velocities across the olivine-spinel transformation in Fe_2SiO_4 were investigated in situ using combined synchrotron X-ray diffraction, X-ray imaging, and ultrasonic interferometry up to 5.5 GPa along the 1173 K isotherm. The onset of the spinel to olivine transformation at 4.5 GPa and olivine to spinel transition for Fe_2SiO_4 at 4.8 GPa was concurrently observed from X-ray diffraction, the amplitude of the ultrasonic signals, the calculated velocities, and the ratio of P and S wave velocities (v_P/v_S). No velocity softening was observed prior to the fayalite to spinel transition. The velocity contrasts across the Fe_2SiO_4 spinel to fayalite phase transition are derived directly from the measured velocities, which are 13 and 12% for P and S waves, respectively, together with a density contrast of 9.4%. A comparison with literature data indicates that the changes in compressional-wave velocity and density across the olivine-spinel transformation in Fe_2SiO_4 are comparable to those with different iron concentrations in the $(Mg,Fe)_2SiO_4$ solid solution, whereas the shear wave velocity contrast decreases slightly with increasing iron concentration.

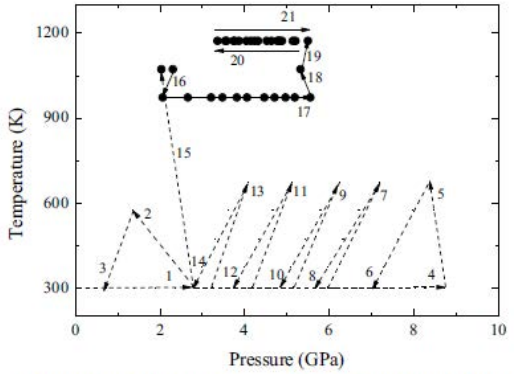

FIGURE 1. Experimental *P-T* path indicating the loading and subsequent heating/cooling cycles (dashed lines with arrows) before the isothermal (973, 1073, and 1173 K) phase transformation processes reported in this study (solid circles).

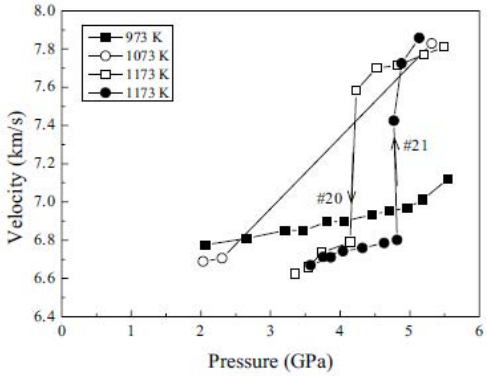

FIGURE 3. P wave velocities for Fe_2SiO_4 phases as a function of pressure at 973, 1073, and 1173 K. The lines connecting the symbols are used for guiding the eyes. The uncertainties in the measured velocities are ~0.5%.

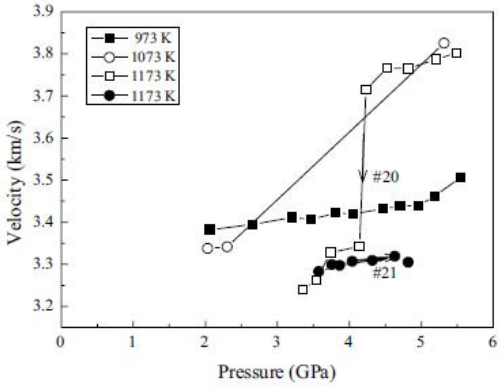

FIGURE 4. S wave velocities for Fe_2SiO_4 phases as a function of pressure at 973, 1073, and 1173 K. The uncertainties in the measured velocities are ~0.5%.

ACKNOWLEDGMENTS

This project was supported by NSF grant to B. Li (EAR0635860). The experiment was conducted at X17B2 of NSLS, Brookhaven National Laboratory, which is supported by the U.S. Department of Energy, Office of Science, Office of Basic Energy Sciences, under contract no. DE-AC02-98CH10886 and by COMPRES, the Consortium for Materials Properties Research in Earth Sciences, under NSF Cooperative Agreement EAR 06-49658,

High Pressure Research Vol. 28, No. 3, September 2008, 405–413

Compressional and shear wave velocities of Fe_2SiO_4 spinel at high pressure and high temperature

Qiong Liu*, Wei Liu, Matthew L. Whitaker, Liping Wang and Baosheng Li

Mineral Physics Institute, Stony Brook University, Stony Brook, NY, USA

Ultrasonic interferometric measurements on polycrystalline Fe_2SiO_4 spinel were conducted simultaneously with synchrotron X-ray diffraction and X-ray imaging up to 6.5 GPa, 1073 K. The compressional and shear wave velocity data and the volume data were fitted to the third-order finite strain equations to derive the bulk and shear modulus and their pressure and temperature derivatives. The fitting results are as follows: $K_{s0} = 204.5(7)$ GPa, $= 73.6(3)$ GPa, $K_s' = 4.3(3)$, $G' = 1.2(1)$, $(\partial K_s/\partial T)_p = -0.027(2)$ GPa/K, and $(\partial G/\partial T)_p = -0.017(1)$ GPa/K. Comparison of our current results with previous data on $(Mg,Fe)_2SiO_4$ spinel with different compositions suggests that the bulk modulus (K_s) increases slightly with increasing iron content, while the shear modulus (G), in contrast, shows a dramatic decrease. However, the pressure and temperature derivatives of K_s and G remain nearly constant from Mg_2SiO_4 to Fe_2SiO_4 spinel with average values of 4.2–4.4, 1.2–1.3, −0.024 GPa/K, and −0.016 GPa/K for K_s', G', $(\partial K_s/\partial T)_p$, and $(\partial G/\partial T)_p$, respectively. The proposed version of equations to describe the effects of iron on the elastic moduli of ringwoodite are: $K_s = 184.7 + 18.0X_{Fe}$, and $G = 118.7 - 41.5\,X_{Fe}$.

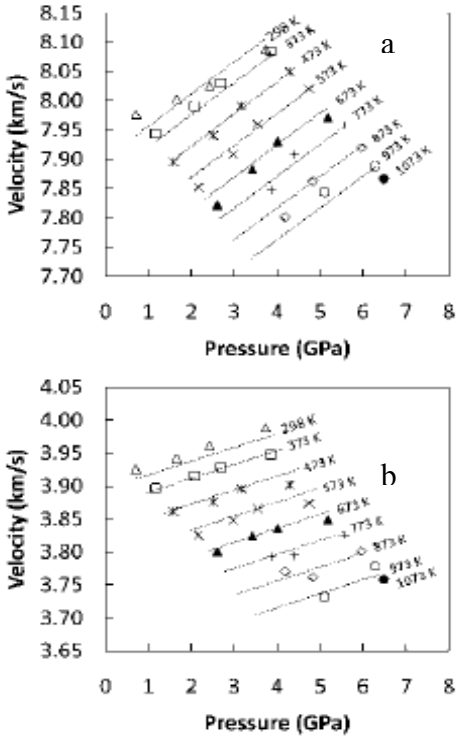

Fig. 1 (a)*P* wave and (b)*S* wave velocities of Fe_2SiO_4 spinel

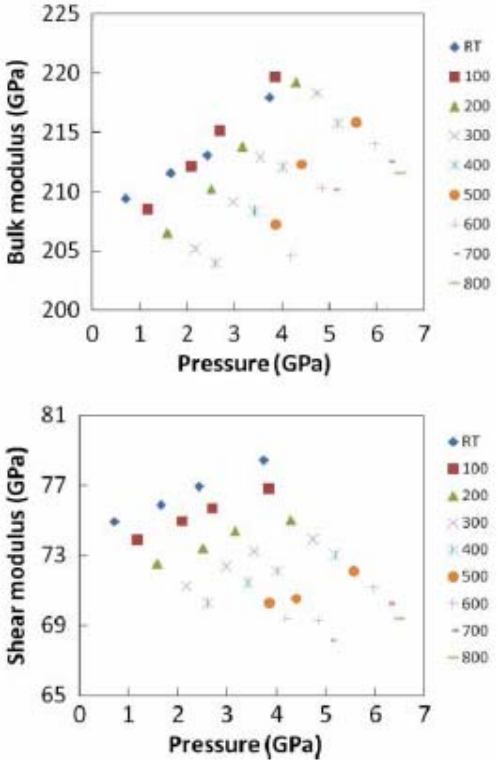

Fig. 2. Elastic moduli of Fe_2SiO_4 spinel

Acknowledgements

This project was supported by NSF grant to B. Li (EAR0635860).

The experiment was conducted at X17B2 of NSLS, Brookhaven National Laboratory which is supported by the U.S. Department of Energy, Office of Science, Office of Basic Energy Sciences, under contract no. DE-AC02-98CH10886 and by COMPRES, the Consortium for Materials Properties Research in Earth Sciences under NSF Cooperative Agreement EAR 06-49658.

Compressibility of nanocrystalline forsterite

Hélène Couvy[1], Jiuhua Chen, Vadym Drozd
CeSMEC, Florida International University, Miami, FL
([1]now at Univeristy of Michigan)

We established an equation of state for nanocrystalline forsterite using multi-anvil press and diamond anvil cell. In situ high pressure and temperature x-ray diffraction experiements were performed at the National Synchrotron Light Source (Brookhaven National Laboratory) at X17B2 beam line using the cubic-anvil multi-anvil press SAM85 and at X17B3 beam line using a Mao-Bell cell with 400 μm anvil culet and 270 μm thick stainless steel gasket pre-indented to 50 μm thickness. Comparative high-pressure and high-temperature experiments show that nanocrystalline forsterite is more compressible than macro-powder forsterite. This difference is attributed to a weakening of the elastic properties of grain boundary and triple junction and their significant contribution in nanocrystalline sample compare to the bulk counterpart. The bulk modulus at zero pressure of forsterite grain boundary was determined to be 83.0 GPa.

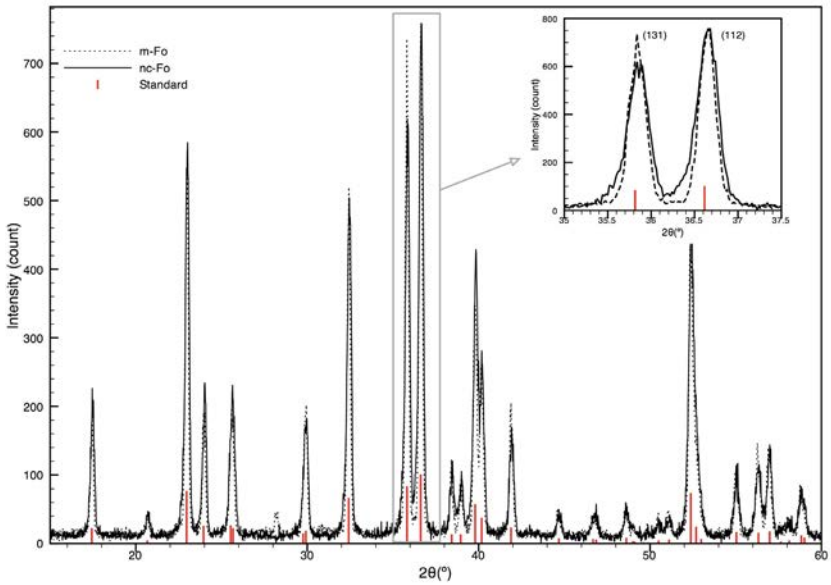

X-ray diffraction patterns of m-Fo (dash line) and nc-Fo (solid line) and forsterite standard peaks position (red sticks). The subview on the upper right corner is a zoom of (131) and (112) peaks.

	m-Fo	nc-Fo
V_0 (Å^3)	290.5 ±0.2	290.5 ±0.3
K_0 (GPa)	129.6 ±3.2	123.3 ±3.4
α_0 (x10^{-5})	2.289 ±0.247	2.471 ±0.288
α_1 (x10^{-8})	0.114 ±0.347	-0.316 ±0.342
dK/dT	-0.011 ±0.005	-0.004 ±0.006

Unit cell volume at zero pressure (V_0), thermal expansion parameters (α_0 and α_1), bulk modulus at zero pressure (K_0), and bulk modulus temperature derivative (dK/dT) of m-Fo and nc-Fo for K' fixed at 3.88.

Acknowledgment:
Research is supported by NSF research grant EAR- 0711321. Use of the National Synchrotron Light Source, Brookhaven National Laboratory, was supported by the U.S. Department of Energy, Office of Science, Office of Basic Energy Sciences, under Contract No. DE-AC02-98CH10886. Use of the X17B2 and X17B3 beamlines were supported by COMPRES, the Consortium for Materials Properties Research in Earth Sciences under NSF Cooperative Agreement EAR 01-35554 and by the Mineral Physics Institute, Stony Brook University.

In search of the mixed derivative $\partial^2 M/\partial P \partial T$ (M = G, K): joint analysis of ultrasonic data for polycrystalline pyrope from gas- and solid-medium apparatus.

G. D. Gwanmesia [Department of Physics & Pre-Engineering, Delaware State University],
I. Jackson [Research School of Earth Sciences, Australian National University],
R. C. Liebermann [Department of Geosciences, Stony Brook University]

Elastic wave velocities for dense (99.8% of theoretical density) isotropic polycrystalline specimens of synthetic pyrope ($Mg_3Al_2Si_3O_{12}$) were measured to 1000 K at 300 MPa by the phase comparison method of ultrasonic interferometry in an internally heated gas-medium apparatus. The temperature derivatives of the elastic moduli [$(\partial Ks/\partial T)_P$ = - 19.3 (4); $(\partial G/\partial T)_P$ = - 10.4 (2) MPa K^{-1}] measured in this study are consistent with previous acoustic measurements on both synthetic polycrystalline pyrope in a DIA-type cubic anvil apparatus (Gwanmesia et al., 2006) and on a natural single crystal by the Rectangular Parallelepiped Resonance (RPR; Suzuki and Anderson 1983) method but $|(\partial Ks/\partial T)_P|$ is significantly larger than from a Brillouin spectroscopy study of single-crystal pyrope (Sinogeikin and Bass, 2002). Alternative approaches to the retrieval of mixed derivatives of the elastic moduli from joint analysis of data from this study and from the solid-medium data of Gwanmesia et al. (2006) yield $\partial^2 G/\partial P \partial T$ = [0.07(12), 0.20(14)] $\times 10^{-3}$ K^{-1} and $\partial^2 K_S/\partial P \partial T$ = [-0.20(24), 0.22(26)] $\times 10^{-3}$ K^{-1}, both of order 10^{-4} K^{-1} and not significantly different from zero. More robust inference of the mixed derivatives will require solid-medium acoustic measurements of precision significantly better than 1%.

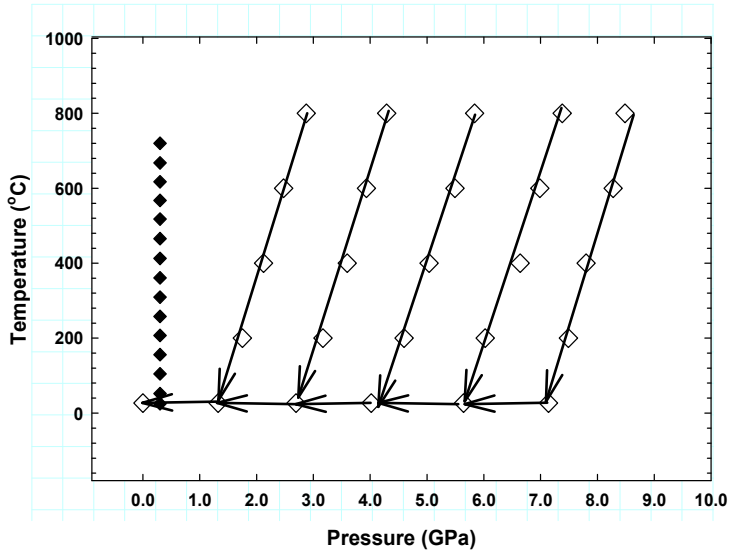

Figure 1. Experimental P and T paths of unloading and cooling cycles in the S-wave and P-wave experiments: experiments conducted in the DIA-type cubic-anvil apparatus (SAM-85), in conjunction with Synchrotron X-radiation (open diamond). Filled diamonds represent data in the internally heated gas-medium apparatus.

Publication: Gwanmesia, G. D., I. Jackson, and R. C. Liebermann, In search of the mixed derivative $\partial^2 M/\partial P \partial T$ (M = G, K): joint analysis of ultrasonic data for polycrystalline pyrope from gas- and solid-medium apparatus, Phys. Chem. Minerals, DOI 10.1007/s00269-006-0130-x, 2007.

Acknowledgements: This research was supported by funding from the Australian Research Council (LX0348106) and partially by a NSF grant (INT 02-33849) to R. C. Liebermann for a collaborative research program with the Australian National University. The in-situ ultrasonic experiments were carried out at the X-17B2 beamline of the National Synchrotron Light Source (NSLS), which is supported by the US Department of Energy, Division of Materials Sciences and Division of Chemical Sciences under No. DE-AC02-76CH00016, and COMPRES, the Consortium for Materials Properties Research in Earth Sciences under NSF Cooperative Agreement EAR 06-49658.

Li, L., L. Wang, and M. T. Vaughan (2008), Elastic softening of peridotite due to the presence of melt phases at high pressure, *Physics of the Earth and Planetary Interiors*, *170*(3-4), 176-180.

The experiment reported here demonstrates many of the capabilities of the D-DIA system. In particular, simultaneous, *in situ,* measurements of the elastic and attenuation properties, with the dynamics of flow within the sample reported. It illustrates many possibilities for future investigations on partially melted samples.

Fluid flow is documented as a Ni dike intrudes a peridotite sample at high pressure and high temperature. The formation of a Ni melt layer coincides with the extension phase of a cyclic stress and the orientation of the liquid plane is normal to the extension direction.

There are apparent correlations between the initiation of the Ni melt and the elastic softening. A previous study (Gribb and Cooper, 2000) reported no unique effect of the melt phase on the attenuation response of olivine. While another study (Jackson et al., 2004) has reported broad energy dissipation peak and dispersion of shear modulus at temperatures above 1000 ^{o}C. In this study, initiation of silicate melting does not trigger pronounced softening of Young's modulus. However, the interaction of the sample and the Ni melt resulted in a drastically reduced the Young's modulus. Accompanied softening of Young's modulus was observed after the Ni intrusion was completed. This study suggests that percolation of a liquid metallic phase is possible within a partially melted mantle rock in the presence of a differential stress field.

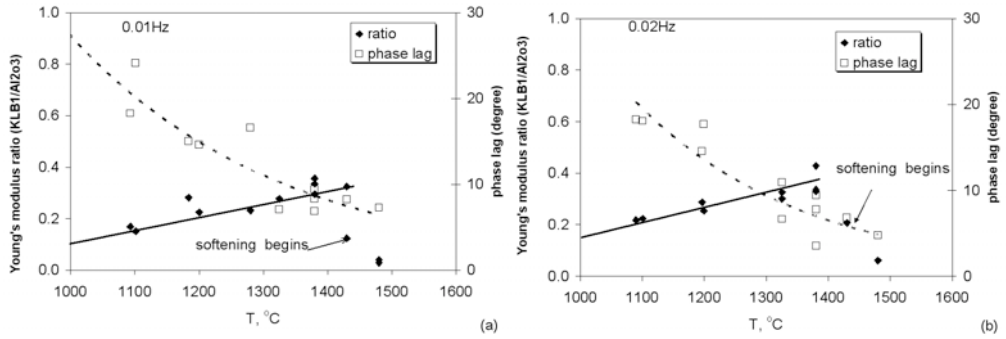

Young's modulus ratio and phase lag of KLB-1 vs. corundum at 2.5 GPa. (a) at 0.01 Hz (b) at 0.02 Hz. It is noticeable that the sample's Young's modulus increases with temperature up to 1380^{o}C at both frequencies while the phase lag decreases. This is expected to be caused by grain growth. Significant softening of Young's modulus of KLB-1 occurs after 1400 ^{o}C while the phase lags do not vary much.

Li, L., and D. J. Weidner (2008), Effect of phase transitions on compressional-wave velocities in the Earth's mantle, *Nature*, *454*(7207), 984-986.

The velocities of seismic waves are governed by the response of the constituent mineral assemblage to perturbations in pressure and stress. The effective bulk modulus is significantly lowered if the pressure of the seismic wave drives a volume reducing phase transformation. A comparison between the amount of time required by phase transitions to reach equilibrium and the sampling period thus becomes crucial in order to define the softening and attenuation of P waves within a two-phase zone. Such phenomena are difficult to assess experimentally since data at earth conditions are required. Here we show synchrotron based experimental data that demonstrate softening of the bulk modulus within the two-phase loop of olivine-ringwoodite at a time scale of 100 seconds. Scaling the amplitude of the pressure perturbation and grain size to those expected in the Earth, the P wave velocities within the discontinuities at 410, 520, and possibly 660 km are likely significantly lower than otherwise expected. The generalization of these observations to Al controlled phase transitions open the possibility of large velocity perturbations throughout the upper 1000 km of the mantle.

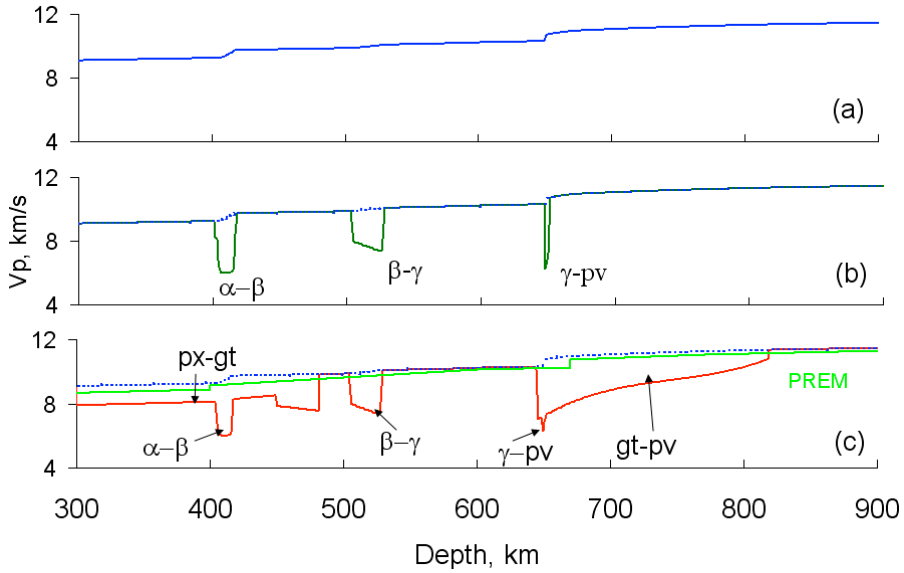

Calculated P wave velocities *vs.* depth in the Earth using pyrolite composition and adiabatic gradient. (a) Assumes the measurement time is much less than the shortest characteristic time (which we estimate to be $< 10^{-2}$ second for P waves). (b) Assumes total phase equilibrium for olivine phases. (c) Same as diagram b except adds total equilibrium for pyroxene-garnet-perovskite transitions. PREM is included. Diagram b and c are calculated from the depth derivative of the density model. The density model is derived from the phase equilibria and equations of state for pyrolite minerals.

Impact of Phase Transitions on P Wave Velocities

Donald J. Weidner and Li Li
Department of Geosciences and Mineral Physics Institute
Stony Brook University, Stony Brook, NY, 11794.

In regions where a high pressure phase is in equilibrium with a low pressure phase, the bulk modulus defined by the P – V relationship is greatly reduced. Here we evaluate the effect of such transitions on the P wave velocity. A model, where cation diffusion is the rate limiting factor, is used to project laboratory data obtained at seismic frequencies, mantle pressure and temperature, but higher stress to the conditions of a seismic wave propagating in the two phase region. We demonstrate that for the minimum expected effect there is a significant reduction of the seismic velocity, as large as 10% over a narrow depth range.

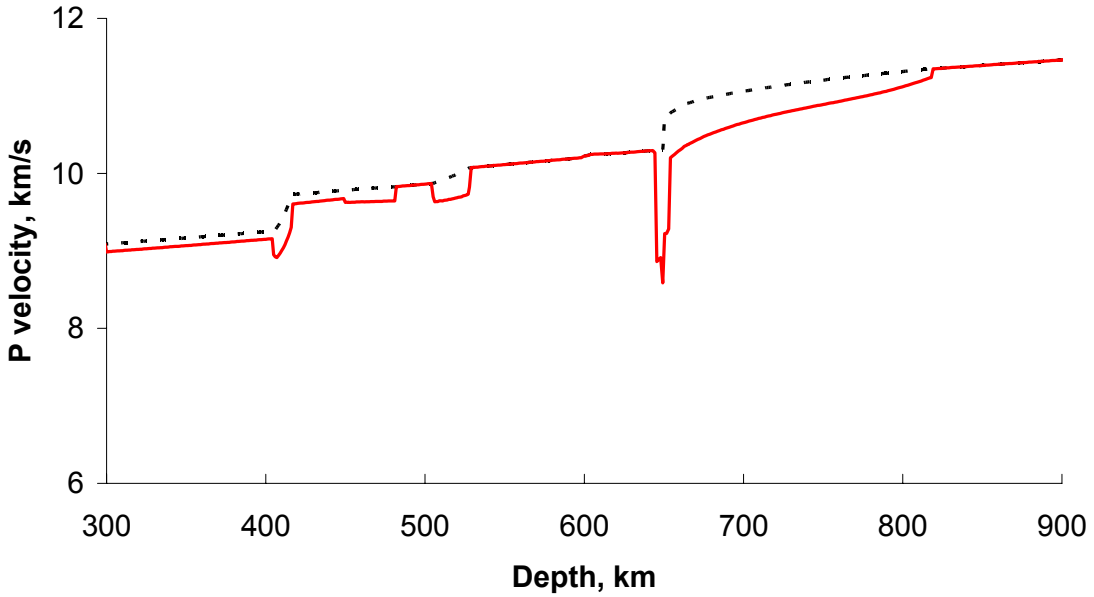

P velocity as a function of depth for a partially relaxed bulk modulus compared with one that is unrelaxed. The relaxed model includes both pyroxene and olivine phase transformations. The bulk modulus for the relaxed model is calculated assuming only 10% of the pyroxene transforms and 5% of the equilibrium amount of olivine transforms during the passage of the P wave. This takes into account the adiabatic character of the P wave and the limited diffusion length for cation exchange. The solid line is the relaxed velocity and the dotted line is the unrelaxed reference velocity. The two curves are identical in depth ranges where these phase transformations are not in progress.

Weidner, D. J., and L. Li (2010), Impact of phase transitions on P wave velocities, Physics of the Earth and Planetary Interiors, 180(3-4), 189-194.

Experiments were conducted at the X17C beamline of NSLS which is supported by COMPRES, the Consortium for Material Property Research in the Earth Sciences under NSF Cooperative Agreement EAR0649658.

Li, L.(2010), Bulk attenuation in the earth's mantle due to phase transitions, *Physics of the Earth and Planetary Interiors*, *183*, 473-477.

Finite bulk attenuation has been agreed to be required to explain the observed damping of radial modes(Anderson, 1980; Durek and Ekstrom, 1995; Sailor and Dziewonski, 1978) even though the dissipation of seismic energy is dominated by shear losses. Bulk attenuation should occur somewhere in the Earth such as the upper mantle (Durek and Ekstrom, 1995; Sailor and Dziewonski, 1978; Widmer et al., 1991); the inner core (Anderson, 1980; Anderson and Hart, 1978a; Dziewonski and Anderson, 1981) or the outer core (Anderson and Given, 1982; Widmer et al., 1991). The plausible mechanisms of attenuation, based on the mineral physics studies (Budiansky and O'Connell, 1980; Budiansky et al., 1983; Heinz et al., 1982), have been proposed as thermoelastic heterogeneity of composite materials for the upper mantle or presence of partial melt or fluid for the core. However, an important mechanism, i.e. phase transitions, has been ignored even though kinetics near equilibrium phase boundaries may be the limiting factor in seismic normal modes (Tamisiea and Wahr, 2002). Moreover, phase transition can contribute to the bulk attenuation due to its volume variation during the process.

The calculated bulk attenuation due to phase transition from mineral physics data is reported here. With relaxation time less than 1 second, the calculated value for a pyrolite mantle is consistent with the inverted bulk attenuation of the upper mantle from seismic observations. The two important mechanisms of phase transitions, diffusion-controlled and kinetics-controlled, have different relaxation time as indicated by the models here. The diffusion controlled is more likely to contribute to the observed seismic bulk attenuation than the kinetic-controlled process based on the available diffusivity and kinetics data. The correlation between the bulk attenuation and relaxation time emphasize the importance of a number of parameters in the mineral physics database such as Fe-Mg diffusivity and kinetics in olivine-wadsleyite-ringwoodite-perovskite, Mg-Ca-Al-Si diffusivity and kinetics in pyroxene-garnet-Ca perovskite, some of which are still unknown.

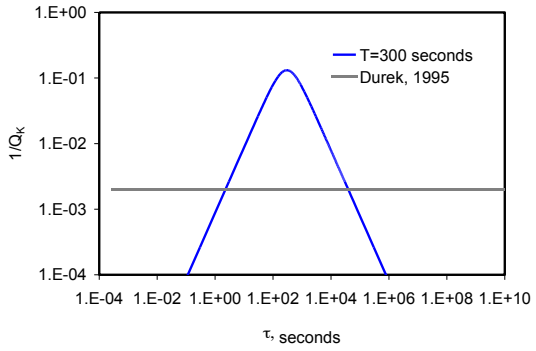

Calculated bulk attenuation for the upper mantle as a function of relaxation time. The sampling wave has a period of 300 seconds. Also plotted are the inverted results from the radial free oscillation (Durek and Ekstrom, 1995). The attenuation due to phase transition must be less than the seismically observed value thus the relaxation is either shorter than 1 second or longer than 10^5 seconds.

Earth’s Deep Water and Carbon Cycles

Is the depth of the seismic X-discontinuity an indicator of mantle H_2O content in $(Mg,Fe)SiO_3$? High-pressure IR studies at U2A

Steven D. Jacobsen
Northwestern University, Department of Earth and Planetary Sciences
Zhenxian Liu, Elizabeth Littlefield*, Russell J. Hemley
*Carnegie Institution of Washington, Geophysical Laboratory (*REU student from Colby College)*
Tiziana Boffa Ballaran,
Bayerisches Geoinstitut, University of Bayreuth, Germany
Lars Ehm
National Synchrotron Light Source, Brookhaven National Laboratory

The mantle X-discontinuity, usually assigned to positive seismic velocity reflectors in the 260–330 km depth range, has proved difficult to explain in terms of a single mineralogical phase transformation in part because of its depth variability. On the basis of high-pressure infrared spectroscopy, X-ray diffraction, and Raman spectroscopy, we show that 1300 ppm variation of H_2O content in $MgSiO_3$ can displace the transition of low-pressure to high-pressure clinoenstatite (LPCen to HPCen) by up to 2 GPa, similar to previous quench experiments on the OEn to HPCen phase transition, where about 30–45 km (1.0–1.5 GPa) of deflection could occur per 0.1 wt% H_2O. If the mantle X-discontinuity results from pyroxene transitions in a depleted harzburgite layer, because of the strong influence of minor amounts of water on the transformation boundary, the depth of the mantle X-discontinuity could serve as a potentially sensitive indicator of water content in the upper mantle.

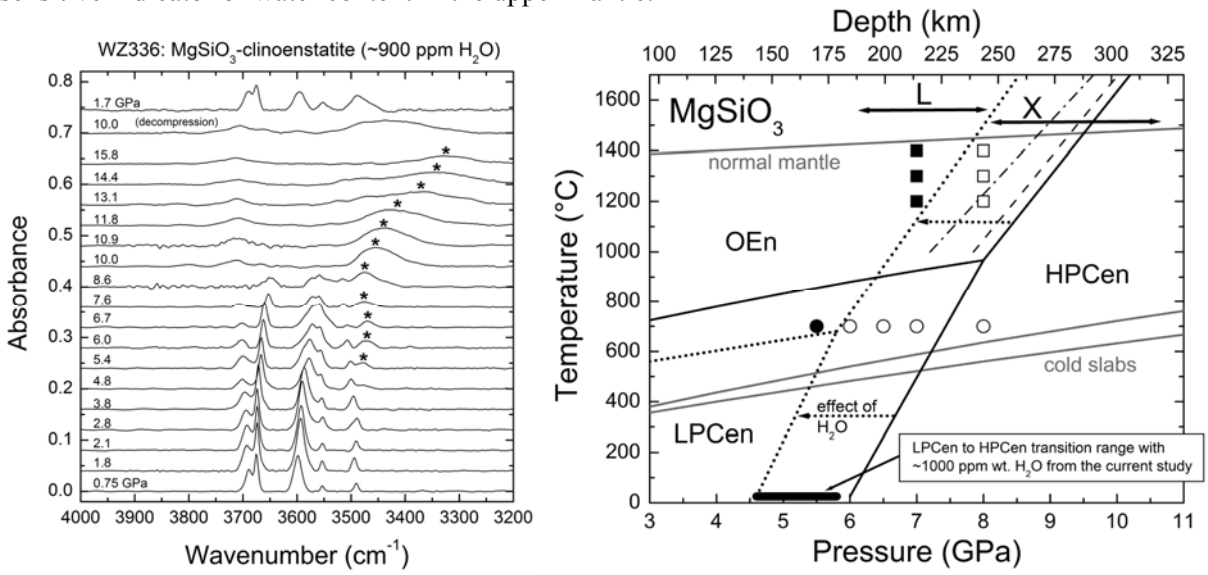

Figures (*Left*) High-pressure IR spectroscopy of LPCen and HPCen, showing the appearance of a broad and low-wavenumber absorption band in the HPCen phase (asterisk), which may signify strong hydrogen bonding in the structure. (*Right*) The effect of water on LPCen-HPCen transitions in this study (dark solid bar) are compared with quench experiments for OEn-HPCen from Withers and Hirschmann (2007) (squares) and Bromiley and Bromiley (2006) (circles). The overall influence of ~0.1wt% H_2O is shown by the dashed line, and may explain depth variability in the seismic Lehman (L) or X-discontinuities.

Reference: Jacobsen, S.D., Z. Liu, T.B. Ballaran, E.F. Littlefield, L. Ehm, and R.J. Hemley (2010) Effect of H_2O on upper mantle phase transitions in $MgSiO_3$: is the depth of the seismic X-discontinuity an indicator of mantle water content? *Physics of the Earth and Planetary Interiors*, 183, 234-244.

Velocity crossover between hydrous and anhydrous forsterite at high pressures

Z. Mao[1], S. D. Jacobsen[2], F. Jiang[1], J. R. Smyth[3], C. M. Holl[2], T. S. Duffy[1]
[1]Princeton University, [2]Northwestern University, [3]University of Colorado,

To determine the effect of water on the sound velocities in the upper mantle, we measured the single-crystal elasticity of forsterite, Mg_2SiO_4, with 0.9 wt.% H_2O to 14 GPa by Brillouin scattering and single crystal X-ray diffraction (X17c, NSLS). At ambient conditions, the addition of this amount of H_2O in forsterite decreases the aggregate bulk and shear moduli by 2.2-2.4% compared with the anhydrous phase (Jacobsen et al., 2008). However, the presence of 0.9 wt.% H_2O increases the pressure derivatives of the bulk and shear moduli. The compressional, V_P and shear wave, V_S velocities of anhydrous and hydrous forsterite as a function of pressure at 300 K are shown in the figure below. V_P and V_S of hydrous forsterite are 0.5% and 0.2% slower than the anhydrous phase at ambient pressure, but become faster at high pressures. At pressure corresponding to 410-km depth, V_P and V_S of forsterite with 0.9 wt.% H_2O are 1.3% and 2.2% faster than those of anhydrous forsterite, respectively. Surprisingly, the addition of H_2O leads to an increase in sound velocity at high pressure. This is an unexpected result that could have important consequences for seismic data.

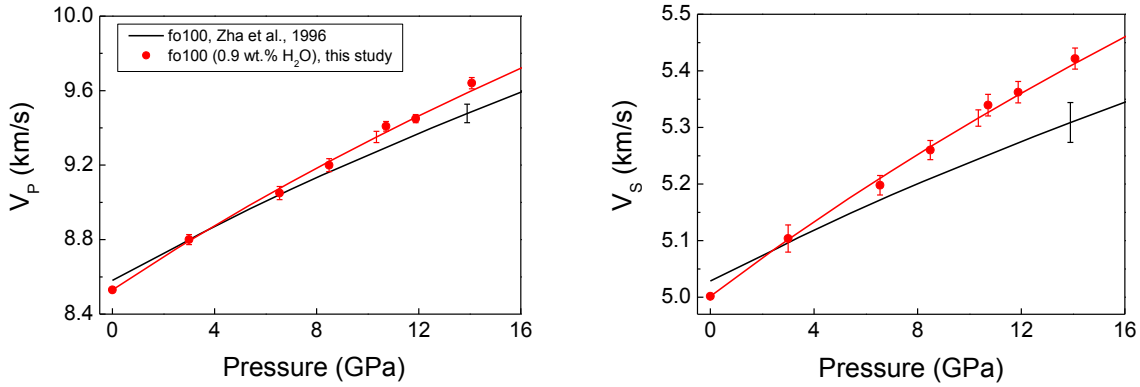

Mao, Z., S. D. Jacobsen, F. Jiang, J. R. Smyth, C. Holl, D. J. Frost, and T. S. Duffy, Velocity crossover between hydrous and anhydrous forsterite at high pressures, *Earth and Planetary Science Letters*, *293*, 250-258, 2010.

This work was supported by NSF. NSLS X17C is supported by COMPRES through NSF EAR 06-49658.

Elasticity of hydrous wadsleyite, β-Mg_2SiO_4, at high pressures

Z. Mao[1], S. D. Jacobsen[2], F. Jiang[1], J. R. Smyth[3], C. M. Holl[2] and T. S. Duffy[1]
[1]Princeton University, [2]Northwestern University, [3]University of Colorado

Wadsleyite, β-Mg_2SiO_4, is potentially a major hydrogen host in the Earth's transition zone (410-660 km depth) due to its large water solubility. Determination of the effect of water on the elasticity of wadsleyite can provide constraints on the water content in the earth's transition zone through comparison with seismic data. We have measured the single-crystal elastic properties of wadsleyite, β-Mg2SiO4, with 0.84 wt.% H_2O measured to 12 GPa from Brillouin scattering and single-crystal x-ray diffraction (X17c, NSLS). Pressure derivatives of the aggregate bulk modulus, K_{S0}, and shear modulus, G_0, of hydrous wadsleyite are indistinguishable within uncertainty from those of anhydrous wadsleyite. Given that the bulk seismic velocity increase at 410-km depth in the mantle is too large for dry pyrolite (60 vol% olivine), we estimate that ~1 wt.% H_2O in wadsleyite at 410-km depth is required to reconcile seismic bulk sound velocities with a pyrolite-composition mantle. If the H_2O content of the mantle is much less than this, then other factors such as other compositional or mineralogical variation need to be considered to explain the 410-km discontinuity. The variations in water content with depth under saturated conditions may also contribute to partial melting and the anomalously steep seismic velocity gradient in the transition zone.

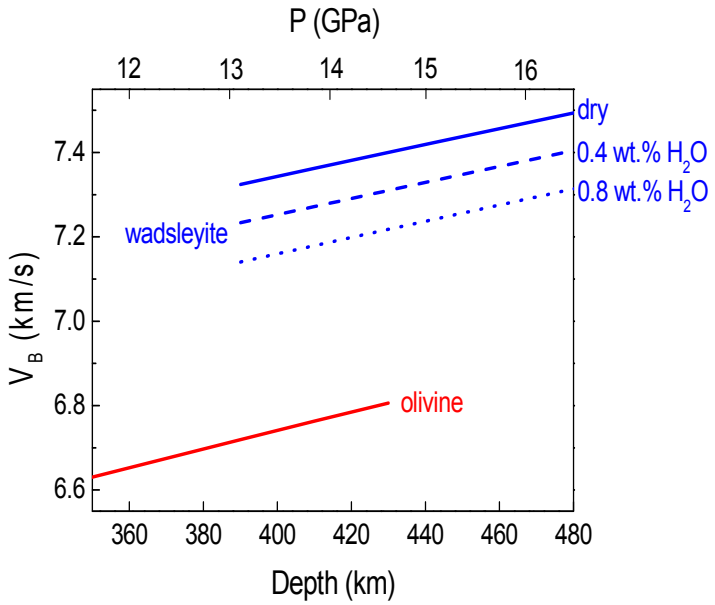

Bulk sound velocities in wadsleyite with different H_2O contents compared with velocities in anhydrous olivine under P-T conditions of the Earth's deep interior

Mao, Z, S. D. Jacobsen, F. Jiang, J. R. Smyth, C. M. Holl, and T. S. Duffy, Elasticity of hydrous wadsleyite to 12 GPa: Implications for Earth's transition zone, *Geophysical Research Letters, 35*, L21305, 2008.

This work was supported by NSF. NSLS X17C is supported by COMPRES through NSF EAR 06-49658.

Hydrogen bonding in Mg_2SiO_4-Ringwoodite: A synthesis of theory and experiment

Wendy Panero[1], Jeffry Pigott[1], Daniel Reaman[1], Zhenxian Liu[2], Joseph Smyth[3]

[1]*School of Earth Sciences, Ohio State University, Columbus, OH 43210*
[2]*Carnegie Institute of Washington, Washington DC*
[3]*Geological Sciences, University of Colorado, Boulder CO*

A combined approach of *ab-initio* calculations and low-temperature, high-pressure infrared spectroscopy, and complementary x-ray diffraction measurements of the equation of state, predicts multiple bonding sites for OH in the ringwoodite structure. Experimentally-derived physical properties and relative energetics are consistent with 51-66% of the hydrogen associated with $V_{Mg}^{''}$ defects, 8-10% associated with $Mg_{Si}^{''}$ defects, and 24-41% associated with $V_{Si}^{''''}$ defects. The understanding of the crystal chemistry and storage of water in the olivine polymorph minerals is of foremost importance to assist in predicting and understanding the effects of variable water content in the interior.

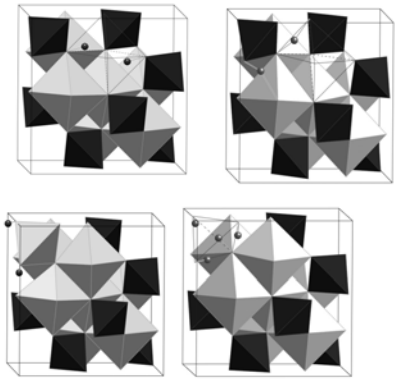

Structure figures for the stable configurations of $V_{Mg}^{''}+2H^{**}$ (2 configurations), $Mg_{Si}^{''}+2H^{**}$, and $V_{Si}^{''''}+4H^{****}$ with polyhedra containing Si in black, those containing Mg in grey, and vacancies outlined in dash lines. Hydrogen atoms and the nearest oxygen bond are labeled with balls and sticks.

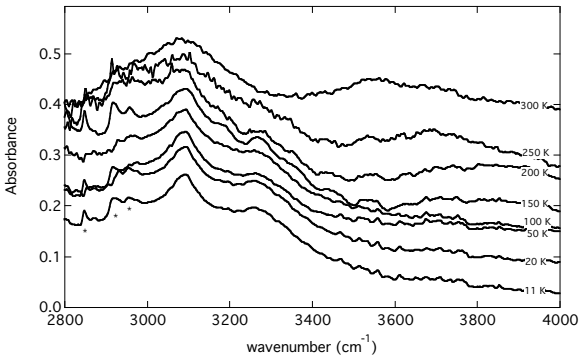

OH absorption with decreasing temperature of ringwoodite with ~1 wt% H2O showing the development of a new peak at ~3260 cm^{-1} as the 3100 cm^{-1} peak narrows with cooling. The process is reversible upon heating and is reproducible through repeated cooling cycles. These multiple peaks are consistent with $V_{Mg}^{''}$, $Mg_{Si}^{''}$, and $V_{Si}^{''''}$ defects. *Stars (*) indicate residual superglue on the sample as well as C-H on the mirrors. Curves are offset vertically for clarity.*

Panero, W. R., First-Principles Determination of the Structure and Elasticity of Hydrous Ringwoodite, *Journal of Geophysical Research, 115*, doi:10.1029/2008JB006282, 2010.

Panero, W. R., J. Smyth, S. Jacobsen, D. Frost, D. M. Reaman*, J. S. Pigott*, S. M. Thomas, Z. Liu, Hydrous Ringwoodite: Clarifying defect mechanisms through combined single-crystal refinement, compressibility, and IR spectroscopy, AGU fall meeting 2009.

This work was supported by NSF EAR-0955647. NSLS X17C and U2A are supported by COMPRES through NSF EAR 06-49658

Brillouin Scattering Measurements on the Single-crystal Elasticity of hydrous ringwoodite at high Pressure-Temperature

Zhu Mao[1], Jung-Fu Lin[1], Steven D. Jacobsen[2], Thomas S. Duffy[3], Yun-Yuan Chang[2], Erik Hauri[4], Vitali B. Prakapenka[5]

[1]The University of Texas at Austin, [2]Northwestern University, [3]Princeton University, [4]Carnegie Institution of Washington, [5]University of Chicago

Single-crystal elasticity of ringwoodite with 1 wt.% H_2O has been measured in an externally-heated diamond anvil cell using the Brillouin spectroscopy system and X-ray diffraction at GSECARS of the Advanced Photon Source, Argonne National Laboratory up to 16 GPa and 673 K. Single-crystal x-ray diffraction was conducted before and after each Brillouin measurements to determine the density of the sample, which is essential for the high pressure-temperature measurements. Brillouin spectra of hydrous ringwoodite were collected at 300 K, 550 K, and 673 K at various pressures, respectively. Our results show two distinct features: 1. a strong reduction by hydration in the elastic moduli at room temperature; 2. significant net effect of temperature and hydration on the elastic moduli at high pressures. This work provides crucial constraints on the transition zone water budget and is essential for understanding the global water circulation.

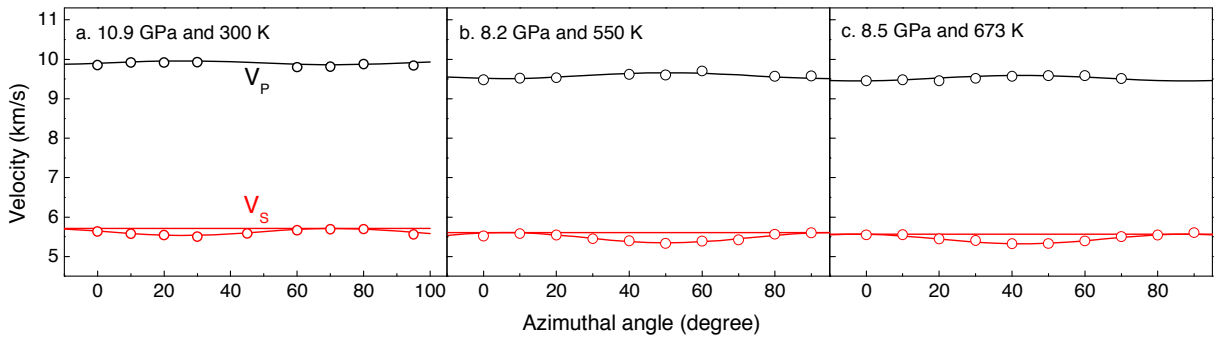

Figure. Measured acoustic velocity (circles) of hydrous ringwoodite compared with fitting results (lines).

Acknowledgements: This work at the UT Austin was supported by the US National Science Foundation (NSF) grants EAR-0838221, Energy Frontier Research in Extreme Environments (EFree), and the Carnegie/DOE Alliance Center (CDAC). This work was also funded by NSF grants EAR-0748707 to S.D Jacobsen and EAR-0738510 to T. S. Duffy. APS is supported by DOE-BES, under Contract No. DE-AC02-06CH11357. We acknowledge I. Kantor and K. K. Zhuravlev for experimental assistance. We thank GSECARS, APS, ANL for providing X-ray diffraction and Brilliouin spectroscopy for the study. Construction of the Brillouin spectrometer at Sector 13 of the Advanced Photon Source was supported by Consortium for Materials Properties Research in Earth Science (COMPRES) as an infrastructure development project.

One page summary of the project

Effect of water in wadsleyite and ringwoodite on the P-T-x coordinates of the wadsleyite-ringwoodite phase transformation: an experimental and thermodynamic study

by Koch-Müller M. Deutsches GeoForschungsZentrum Potsdam, Germany

to support the COMPRES renewal

The seismologically observed discontinuities in the P- and S-wave velocities at depths of 410-, 520- and 660-km are usually attributed to the phase transformations in $(Mg, Fe)_2SiO_4$ from olivine (ol) to wadsleyite (wads), wadsleyite to ringwoodite (ring) and ringwoodite to Mg-perovskite and ferropericlase (post-spinel transformation). However, seismic observations indicate many unusual variations of the depth of these discontinuities, which were explained in the past, by variation in temperature (e.g. Ito and Takahashi, 1989; Bina and Helffrich, 1994). However, recent experimental data (Katsura et al., 2003; Fei et al., 2004; Litasov et al., 2005a) show that the depth variation at least of the 660-km discontinuity cannot be explained by thermal perturbations. Other explanations for the observed variation in depth are variations in the incorporation of minor element and/or volatiles in the corresponding phases (e.g. Ohtani and Litasov, 2006). As experiments show a high but variable solubility of H in the $(Mg,Fe)_2SiO_4$ polymorphs (e.g. Kohlstedt et al., 1996) water is a good candidate to explain the depth variation. In this project we will focuse on the 520-km discontinuity were wadsleyite and ringwoodite coexist. Both phases can incorporate up to 3 wt % of water in their structures (e.g. Inoue et al., 1995) via point defects. Litasov and Ohtani (2003) and Kawamoto (2004) report indications that the wadsleyite to ringwoodite phase transition shifts to high pressures in the presence of water. This could explain the observed depth variation of the 520-km discontinuity (Deuss and Woodhouse, 2001). The reason for the shift of the wadsleyite-ringwoodite phase boundary to higher pressure, however, is unclear as the maximum solubility of water in both phases is comparable.
To fully understand the phase relations more experimental work is needed.
The goals of this project are
(i) to investigate the effect of water on the P-T-x coordinates of the wadsleyite-ringwoodite phase transition in quenched multi-anvil experiments using 10/5 assemblies with COMPRESS Rhenium furnaces,
(ii) to experimentally determine the fractionation of water between coexisting wadsleyite and ringwoodite at the phase boundary,
(iii) to characterize the run products in respect to structure (structural defects, inversion degree) and crystal chemistry
(iv) to characterize the vibrational behavior of hydrous wadsleyite and ringwoodite experimentally, to compare the spectra with spectra calculated using the density functional perturbation theory (DFPT) and finally to use the vibrational density of states to calculate thermodynamic properties, e.g. entropy and heat capacity for hydrous wadsleyite and ringwoodite.

Comparative in situ X-ray diffraction study of San Carlos olivine: Influence of water on the **410 km seismic velocity jump in Earth's mantle**

Jiuhua Chen[1], Haozhe Liu[2], Jennifer Girard[1]
[1] *Florida International University,* [2] *Harbin Institute of Technology*

A comparative study of the equation of states of hydrous (0.4 wt% H_2O) and anhydrous San Carlos olivine (<30 ppm H_2O) was conducted using synchrotron X-rays up to 11 GPa in a diamond anvil cell (DAC) at ambient temperature. Both samples were loaded in the same high-pressure chamber of the DAC to eliminate the possible pressure difference in different experiments. The obtained compression data were fitted to the third-order Birch-Murnaghan equation of state, yielding a bulk modulus K_0 = 123(3) GPa for hydrous olivine and K_0 = 130(4) GPa for anhydrous olivine as K_0' is fixed at 4.6. Therefore, 0.4 wt% H_2O in olivine results in a 5% reduction in bulk modulus. Previous studies reported bulk modulus reduction by water in olivine's high-pressure polymorph (wadsleyite), to which the transformation from olivine gives rise to the seismic discontinuity at 410 km depth. The new data results in a reduction in the magnitude of the discontinuity by 50% in V_P and 30% in V_S (for 1:5 water partitioning between olivine and wadsleyite) with respect to anhydrous mantle. Previous knowledge of the influence of water on this phase transition has been in opposition to a large amount of water [*e.g.*, 200 ppm by Wood (1995)] existing at 410 km depth. Calculation of the seismic velocities based on newly available elasticity data of the hydrous phases indicates that the presence of water is favorable for the mineral composition model (pyrolite) and seismic observations in terms of the magnitude of the 410 km discontinuity.

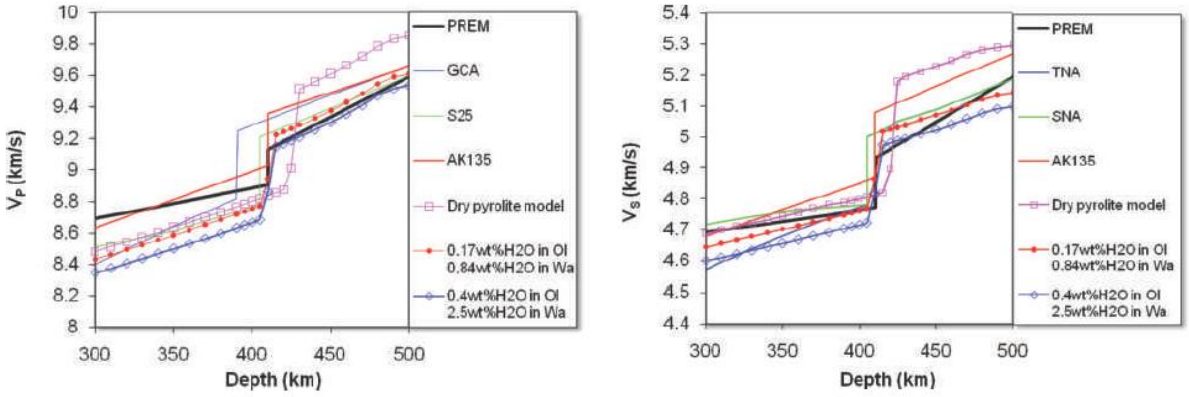

a b

Figure 1. Comparison of (a) P wave velocity and (b) S wave velocity of the pyrolite model (lines with symbols, water contents as indicated) with seismic models (solid lines) PREM (Dziewonski and Anderson 1981), GCA (Walck 1984), S25 (Le Fevre and Helmberger 1989), AK135 (Kennett et al. 1995), TNA (Grand and Helmberger 1984), SNA (Grand and Helmberger 1984). The pyrolite model with 0.17wt%H_2O in olivine and 0.84 wt%H_2O in wadsleyite matches the seismic models well. Therefore the long-standing discrepancies between the mineral physics model of pyrolite composition and seismic models may be reconciled by the presence of water at an undersaturated level.

Reference: Jiuhua Chen, Haozhe Liu, Jennifer Girard, Comparative in situ X-ray diffraction study of San Carlos olivine: Influence of water on the 410 km seismic velocity jump in Earth's mantle, *American Mineralogist*, 96 (2011), 697–702.

Research is supported by NSF (EAR-0711321 and EAR-1015509). Use of high pressure beamline X17C of NSLS is supported by COMPRES, the Consortium for Materials Properties Research in Earth Sciences under NSF Cooperative Agreement EAR 10-43050.

Water Solubility Studies in $MgSiO_3$ Perovskite by FTIR Spectroscopy

*G. Amulele, K. Otsuka, C. Sanchez, K. K. M. Lee, S. Karato: Department of Geology and Geophysics, Yale University, New Haven, CT.

Z. Liu, Z. Chen: National Synchrotron Light Source, Brookhaven National Laboratory, Upton, NY.

Although water solubility in lower mantle minerals is critical for understanding global water circulation, the water solubility in lower mantle minerals is poorly constrained. Preliminary investigations on water solubility in $MgSiO_3$-perovskite synthesized in a multi-anvil apparatus at 1500 - 1600 ^oC and 24 - 25 GPa under SiO_2 or MgO saturated conditions have been carried out by FTIR spectroscopy both at ambient as well as modest pressures of up to 10 GPa in a diamond-anvil cell using KBr as a pressure medium. The FTIR spectra show one dominant band at 3440 cm^{-1} in $MgSiO_3$-perovskite corresponding to about 50 - 70 ppm wt% water in the perovskite. This is consistent with the results by Litasov et al. (2003) who obtained solubility of about 100 ppm wt% water in $MgSiO_3$-perovskite, but much larger than the values reported by Bolfan-Casanova et al. (2000). Based on the in-situ FTIR in a diamond-anvil cell using KCl as a pressure medium, Reid et al. (2006) reported infrared absorption peaks at 3160 and 3066 cm^{-1} at high pressures that broaden and weaken at low (<3 GPa) pressures. They interpreted that these peaks are caused by an unquenchable hydroxyl-related species. However, we did not find these peaks but instead we found these peaks from the FTIR spectroscopy of KCl. We conclude that 3160 and 3060 cm^{-1} peaks are due to KCl, and $MgSiO_3$ perovskite has a small but finite water solubility (~50-70 ppm wt%).

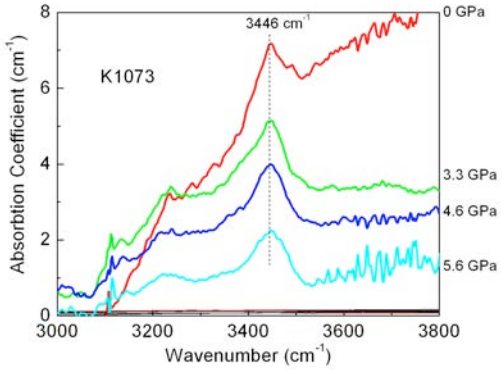

FTIR Spectra of $MgSiO_3$ under pressure.

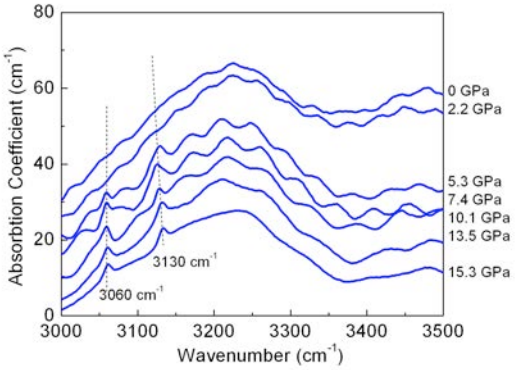

FTIR Spectra of KCl under pressure.

Reference: Annual Geophysical Union, Fall Meeting, San Francisco, 2010, MR31A-1981

Acknowledgement: Supported by NSF under Grant HSF-EAR-0911465

High-Pressure Infrared Spectroscopy of the Dense Hydrous Magnesium Silicates Phase D and Phase E

Sean R. Shieh Department of Earth Sciences, University of Western Ontario
Thomas S. Duffy Department of Geosciences, Princeton University
Zhenxian Liu Geophysical Laboratory, Carnegie Institution of Washington
Eiji Ohtani Department of Mineralogy, Tohoku University

Phase D and E are hydrous magnesium silicates that are stable at high pressure-temperature conditions and could serve as H_2O carriers in the Earth's mantle, especially in subducting slabs. The infrared (IR) spectra of phase D and E were studied to 42 and 41 GPa, respectively, using synchrotron IR facility at beamline U2A, National Synchrotron Light Source. Our results show thta both phases, at least 3 broad OH stretch vibrations were observed at elevated pressures indicating that each phase has multiple hydrogen positions that exhibit disorder. No structural phase transition or amorphization was observed for either phase over the measured pressure range. The mode Grüneisen parameters of phase D and E are in the range of -0.12 - 1.14 and -0.17 - 0.83, respectively with mean values of 0.41 (phase D) and 0.31 (phase E). Using empirical correlations of OH frequency and O...H and O…O bond lengths; the six OH vibrations of phase D at ambient pressure have corresponding O…H and O…O bond distances in the range of 1.519-1.946 Å and 2.225-2.817 Å, whereas the four OH vibrations of phase E have the corresponding O…H and O…O bond distances in the range of 1.572 - 2.693 Å and 2.557 - 2.986 Å. These ranges encompass values reported from single-crystal x-ray diffraction measurements. At high pressures, the observable OH stretching vibrations exhibit both positive and negative pressure slopes. Our high-pressure infrared spectra for phase D do not support the occurrence of hydrogen symmetrization as predicted by first-principles calculations.

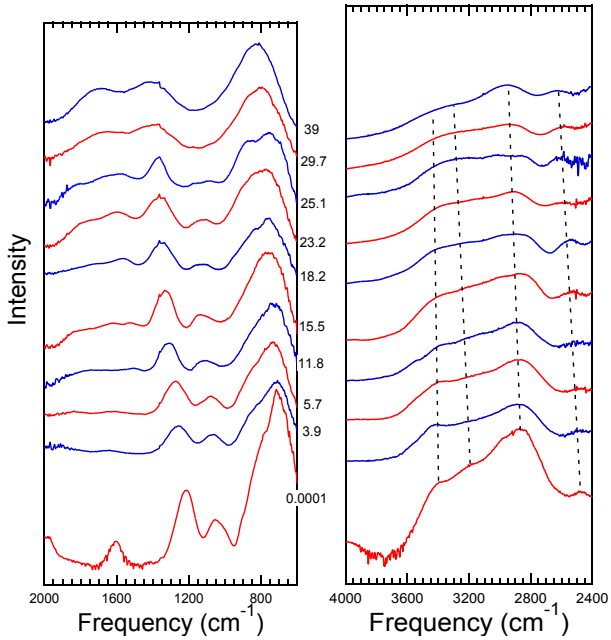

Representative spectra of phase D under compression to 39 GPa. The pressure (in GPa) is labeled on the right side of the left panel. (a) Internal modes (b) OH stretching modes. Dashed lines are guides for the eye.

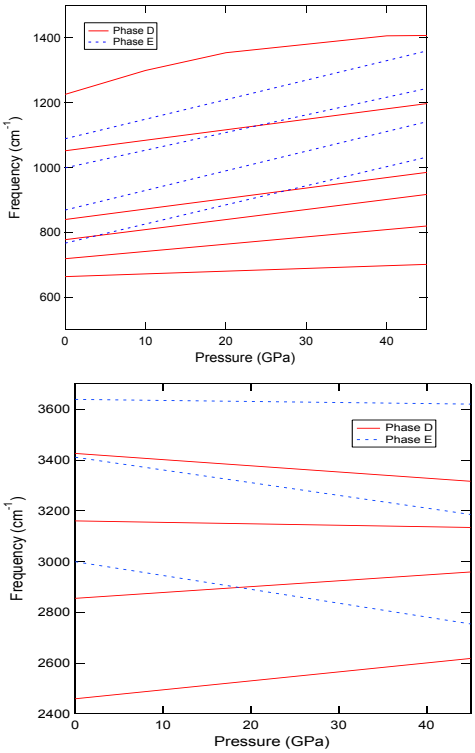

Comparison of the frequency shifts of internal modes and OH vibrational modes as a function of pressure for phases D and E.

Reference: Shieh, S.R., T.S. Duffy, Z. Liu, and E. Ohtani, High-pressure infrared spectroscopy of the dense hydrous magnesium silicates phase D and phase E, *Phys. Earth Plane. Inter.* 175, 106-114, 2009.

Single-crystal elasticity of diaspore, AlOOH, to 12 GPa by Brillouin scattering

F. Jiang, J. Majzlan, S. Speziale, D. He, and T. S. Duffy,
Princeton University

Hydroxides are materials that readily form in natural environments in both the bulk state and on surfaces. These minerals span a range of chemistries and possess diverse bonding and structural properties. Aluminum hydroxides and oxyhydroxides are widely found in soils and sediments. Diaspore, α-AlOOH, is an aluminum hydroxide stable to at least 65 GPa at room temperature and to at least 14 GPa at 950°C. Hydrous phases in the Al_2O_3-SiO_2-H_2O system are also geologically relevant to understanding subducted pelitic sediments and Al-rich basalts.

The high-pressure elasticity of diaspore (AlOOH) has been determined by Brillouin spectroscopy to 12 GPa in diamond anvil cells. Acoustic velocities were measured in three approximately orthogonal principal planes at ambient and 8 elevated pressures, yielding the full elastic tensor as a function of compression. X-ray diffraction was carried out at X17c, NSLS to determine the density and orientation of each crystal plane. From calculated linear compressibilities, the *a*-axis is the most compressible. The *b*-axis becomes the least compressible axis at high pressures. Both volume and axial compression curves calculated using our Brillouin results are in good agreement with the results from static compression studies. High-pressure sound velocities in diaspore exceed those of other hydrous minerals as well as many anhydrous phases relevant to Earth's upper mantle.

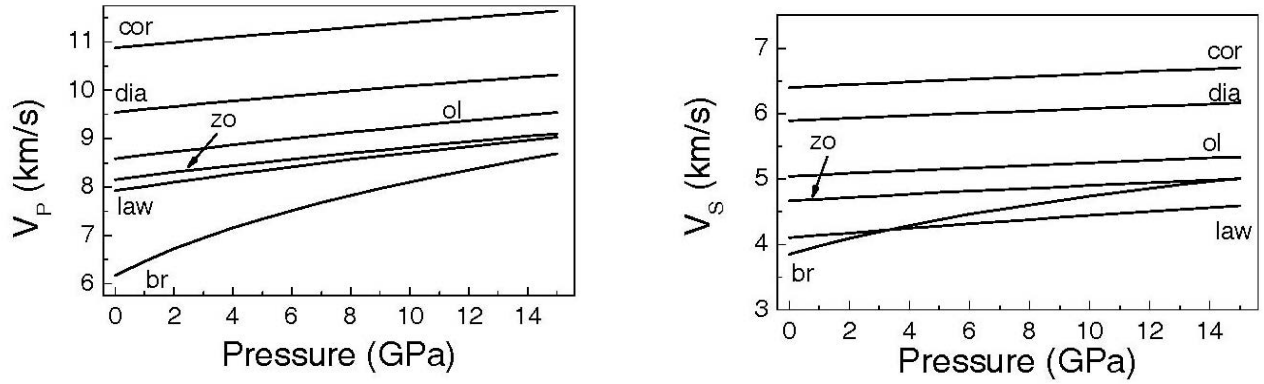

Compressional and shear sound velocities of diaspore (dia) at 300 K in comparison with corundum: cor; α-olivine: ol; brucite: br; zoisite: zo; lawsonite: law.

Jiang, F., J. Majzlan, S. Speziale, D. He, and T. S. Duffy, Single-crystal elasticity of diaspore, AlOOH, to 12 GPa by Brillouin scattering, *Physics of the Earth and Planetary Interiors*, *170*, 220-228, 2008.

This research was support by NSF (EAR 07-38510). NSLS X17c is supported by COMPRES through NSF EAR 06-49658.

Single-crystal elastic constants of zoisite $Ca_2Al_3Si_3O_{12}(OH)$

Zhu Mao, Fuming Jiang, and Thomas S. Duffy, Princeton University

Hydrous minerals in subduction zones are potential agents for transporting water to the deep earth. Properties of these minerals, especially elastic moduli, are needed to model seismic wave speeds in subduction zones and hence place constraints on cycling of H_2O through subduction zones. Zoisite is a metamorphic mineral of the epidote group containing 2 wt% water. It is likely to be one of the important phases in subduction zone environments. The stability field of zoisite extends up to 6.6 GPa and 950°C (Poli et al., 1998). In basaltic compositions, zoisite is found under conditions as high as 3.1 GPa and 650°C (Forneris and Holloway, 2003).

In this study, the single-crystal elastic constants of zoisite $Ca_2Al_3Si_3O_{12}(OH)$ were determined by Brillouin scattering under ambient conditions. Brillouin spectra were recorded in 37 directions for three separate crystal planes. The density of the sample and the orientation of each plane were determined by single-crystal diffraction using energy dispersive techniques at X17C of the National Synchrotron Light Source. The complete elastic tensor was then obtained by an inversion of the acoustic velocity and orientation data. The Voigt-Reuss-Hill averages of the aggregate bulk modulus, shear modulus and Poisson's ratio were determined to be K_S = 125.3(3) GPa, G=71.9(1) GPa and σ=0.26, respectively. Our results are consistent with some previous static compression studies (Pawley et al., 1998; Grevel et al., 2000), although we find higher *c* axis compressibility. Our results provide the first determination of the shear modulus of zoisite. Compared with lawsonite, zoisite has a similar bulk modulus (~125 GPa), but a 30% larger shear modulus than lawsonite (~52 GPa). The V_P/V_S ratio is 1.76 for zoisite and compared with1.45 for lawsonite.

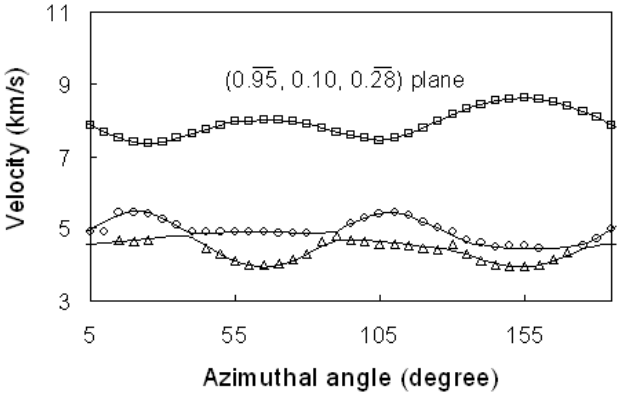

Figure: Acoustic velocities in zoisite. Symbols are measured data, lines are from best-fitting elastic constants.

Mao, Z., F. Jiang, and T. S. Duffy, Single-crystal elasticity of zoisite, $Ca_2Al_3Si_3O_{12}(OH)$, by Brillouin scattering, *American Mineralogist*, *92*, 570-576, 2007.

Experiments were conducted at the X17C beamline of NSLS which is supported by COMPRES, the Consortium for Material Property Research in the Earth Sciences under NSF Cooperative Agreement EAR06-49658.

High pressure synchrotron X-ray powder diffraction and infrared spectroscopy study on brucite

Maining Ma[1, 2], Wei Liu[1], Zhiqiang Chen[3], Zhenxian Liu[4], Baosheng Li[1]

1. Mineral Physics Institute, Stony Brook University, Stony Brook, NY 11794, USA
2. Key Laboratory of Computational Geodynamics, Chinese Academy of Sciences, Beijing 100049, China
3. Department of GeoScience, Stony Brook University, Stony Brook, NY 11794, USA
4. Geophysical Laboratory, Carnegie Institution of Washington, Washington DC 20015, USA

Synchrotron X-ray powder diffraction and infrared (IR) spectroscopy study of brucite were conducted at ambient temperature up to 31 GPa using a diamond anvil cell (DAC) at beamlines X17C and U2A of National Synchrotron Light Source (NSLS). Within the current experimental pressure range, the unit-cell volume of brucite shows a monatonic decrease with increasing pressure with c-axis more compressible than a-axis. Both experimental and calculation results show that c/a shows anomalous behavior with increasing pressure. The OH stretching frequency shows pressure-induced redshift in IR spectra and a new peak is observed above 4 GPa with a different linear redshift which implies that one of OH structures has been tilted at larger angle under high pressure. However, neither X-ray diffraction nor discontinuity in the refined unit cell volume indicating a structural phase change can be observed throughout the entire pressure range.

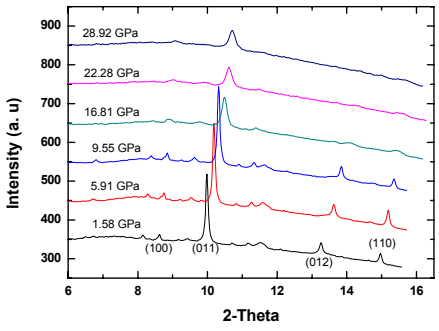

Fig. 1 X-ray diffraction of brucite at high pressure and ambient temperature.

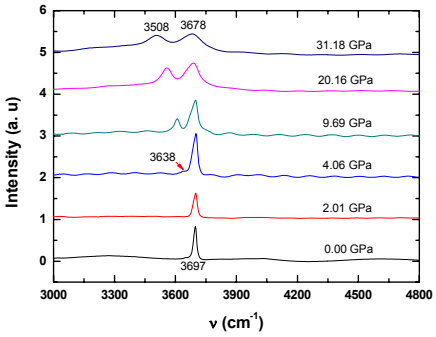

Fig. 2 IR spectroscopy of brucite at high pressure and ambient temperature along compression.

This work was supported by NSF (EAR0635860 to BL) and National Natural Science Foundation of China (Grant No. 40774047 to MM). The experiments were conducted at NSLS supported by COMPRES. Use of the National Synchrotron Light Source, Brookhaven National Laboratory, was supported by the U.S. Department of Energy.

High-pressure behavior of portlandite under quasi-hydrostatic stress conditions

Sang-Heon Dan Shim and Krystle Catalli, *Massachusetts Institute of Technology*
Vitali Prakapenka, *GSECARS, University of Chicago*

Pressure-induced amorphization of important water carrying minerals, such as serpentine, has been proposed as the source of deep focused earthquakes based on earlier measurements made in the diamond-anvil cell without a pressure transmitting medium. Yet, a more recent multi-anvil study found no amorphization. Pressure-induced amorphization was also reported in portlandite [$Ca(OH)_2$], which has served as an archetype for hydrous minerals.

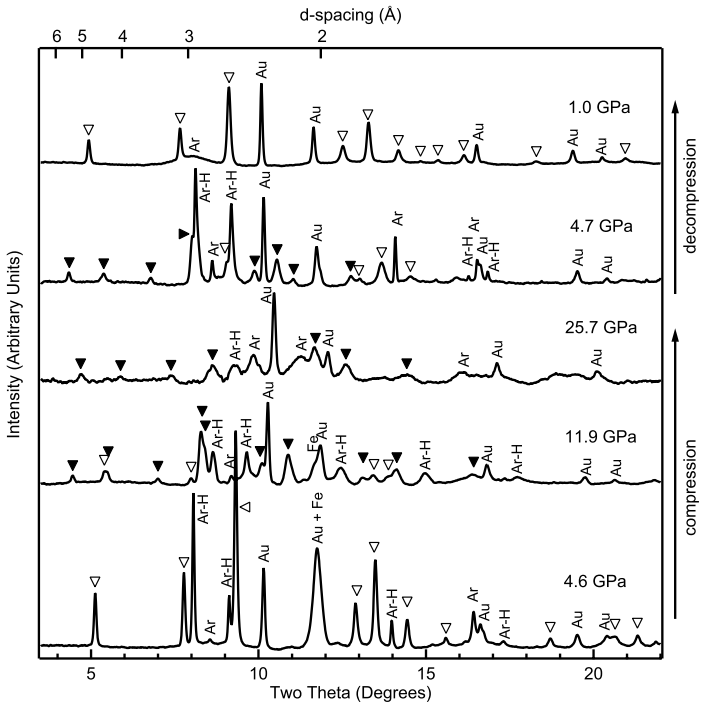

X-ray diffraction patterns of $Ca(OH)_2$ measured at high pressure.

We conducted synchrotron X-ray diffraction (beamline 12.2.2 of the Advanced Light Source and the GSECARS sector of the Advanced Photon Source) and Raman spectroscopy measurements on $Ca(OH)_2$ in the diamond-anvil cell under quasi-hydrostatic stress conditions using Ar as a pressure transmitting medium. We found that under quasi-hydrostatic stress conditions, portlandite undergoes a transition to a new crystalline phase instead of amorphization. Analysis of stress conditions in the sample suggests that the earlier observation of amorphization without a pressure transmitting medium was likely due to strong non-hydrostatic stress. This also implies that the earlier observation of amorphization of serpentine is likely due to non-hydrostatic stress.

Publications

K. Catalli, S.-H. Shim, and V. B. Prakapenka. A crystalline-to-crystalline phase transition in $Ca(OH)_2$ at 8 GPa and room temperature. Geophys. Res. Lett. 35, L05312, 2008.

High Pressure Synchrotron Infrared Studies of Talc and Lawsonite

Henry P. Scott [*Department of Physics and Astronomy, Indiana University South Bend, South Bend, Indiana*], Zhenxian Liu, Russell R. Hemley [*Geophysical Laboratory, Carnegie Institution of Washington*], and Quentin Williams [*Department of Earth Sciences, University of California at Santa Cruz, Santa Cruz, California*]

The high-pressure stability of hydrated metamorphic phases is essential to understand Earth's deep water cycle. Yet, the manner in which hydrogen is retained within these phases is a topic of considerable uncertainty. In particular, the role of hydrogen bonding (and its pressure dependence) in stabilizing these metamorphic phases at high pressure remains unclear. Here we present high-pressure infrared spectra of two geologically important hydrous minerals: talc, $Mg_3Si_4O_{10}(OH)_2$, and lawsonite, $CaAl_2Si_2O_7(OH)_2 \cdot H_2O$, at room temperature. For lawsonite, our data span the far infrared region from 150 to 550 cm^{-1} and extend to 25 GPa. We combine our new spectroscopic data with previously published high-pressure mid-infrared and Raman data to constrain the Grüneisen parameter and vibrational density of states under pressure. In the case of talc, we present high-pressure infrared data that span both the mid and far infrared from 150 to 3800 cm^{-1}, covering lattice, silicate, and hydroxyl stretching vibrations to a maximum pressure of 30 GPa. Both phases show remarkable metastability well beyond their nominal maximum thermodynamic stability at simultaneous high-pressure and high-temperature conditions.

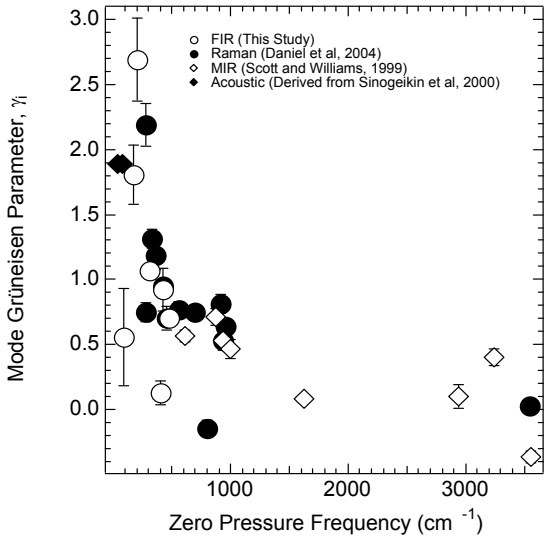

Figure 1. Compilation of mode Grüneisen parameters versus zero pressure frequency obtained by the FIR measurements of the current study, MIR measurements from Scott and Williams (1999), Raman measurements from Daniel et al (2000) and acoustic values derived from Sinogeikin et al (2000). Error bars represent plus or minus one standard deviation. Note the strong frequency dependence of mode Grüneisen parameters; the low frequency modes provided by FIR are critically important to constrain the vibrational density of states.

Reference

Scott, H. P., Z. Liu, R. J. Hemley, and Q. Williams, High-pressure infrared spectra of talc and lawsonite, *American Mineralogist*, *92*(11-12), 1814-1820, (2007).

Acknowledgments

Operation of beamline U2A at the NSLS is supported by COMPRES under NSF Cooperative Agreement Grant No. EAR 06-49658, and by the U.S. Department of Energy through the Carnegie/DOE Alliance Center (CDAC) contract DE-FC03-03N00144. We thank Y. Fei for providing the talc sample used in these experiments.

Talc growth during olivine and magnesite hydrolysis by silica-rich fluids at mid-crustal pressures and temperatures

Ryan J. Kerrigan, Philip A. Candela, and Philip M. Piccoli
Laboratory for Mineral Deposits Research, Department of Geology
University of Maryland, College Park, MD, 20742

Experiments in the simplified systems MgO-SiO_2-H_2O (MSH) and MgO-SiO_2-H_2O-CO_2 (MSHC) have been conducted by using hydrothermal diamond anvil cells to investigate reaction rates and the resulting textures at temperatures and pressures consistent with the temperatures and pressures of the Earth's crust. The conditions and simplified systems of the experiments serve as approximations for geologic environments wherein magnesium-rich rocks (i.e., mafic, ultramafic, and magnesium-rich carbonate rocks) are hydrothermally altered by silica-rich fluids. The hydrolysis reaction rates and textures that result from the irreversible interactions of olivine and magnesite with aqueous fluids in the presence of quartz have been characterized.

Reaction rates have been determined by a new approach developed during this study, which uses *in situ* observation of reactant volume loss to determine the growth rate of the products of hydrolysis reactions. In addition, some experiments were analyzed by real-time synchrotron radiation analysis to identify the phases in the reactions and to provide semi-quantitative constraints on the kinetic data. Experiments performed in this study resulted in the development of several textural varieties. Talc grown during this study exhibited both fibrous and platy habits, textural variations that appeared to be controlled by: variations in the density of the aqueous phase, surface area of starting materials, rate of temperature increase, and the presence of strong chemical gradients. Previous studies have suggested that the growth of fibrous talc is due to the pseudomorphism of preexisting fibrous minerals (Stemple and Brindley, 1960; Ross et al., 1968; Sanford, 1981). The primary growth of fibrous talc in these experiments demonstrates that the production of fibrous talc does not require the pseudomorphism of a fibrous precursor as previously suggested.

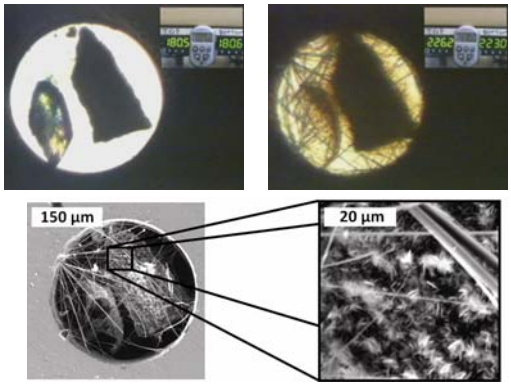

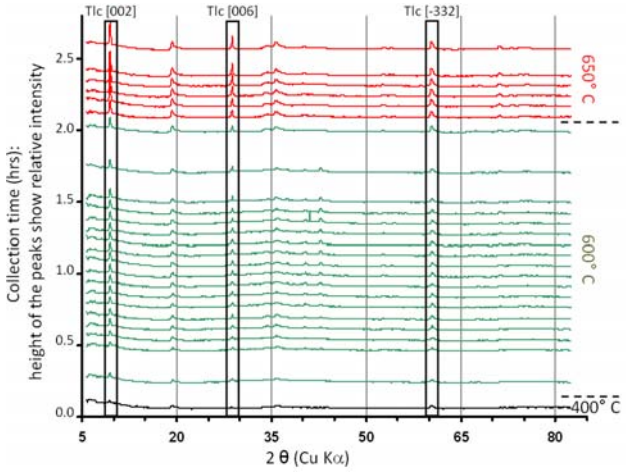

Kerrigan, R. J. (2011) Reaction rates and textural development of hydrolysis reactions in the system MgO-SiO_2-H_2O. University of Maryland, College Park, Ph.D. Dissertation, 205 pgs.

This work was supported by the University of Maryland. NSLS X17C is supported by COMPRES through NSF EAR 06-49658.

The pressure-induced spin transition in rhombohedral carbonates

Barbara Lavina[1], Przemyslaw Dera[2], Robert T. Downs[3], Yusheng Zhao[1]

[1]*HiPSEC and Dept. of Physics and Astronomy, University of Nevada, Las Vegas, Nevada 89154, USA;* [2]*GSECARS, University of Chicago, Argonne, Illinois 60439, USA;* [3]*Geosciences, University of Arizona, Tucson, Arizona 85721-0077, USA*

One of the most fascinating aspects of high pressure science is to witness dramatic variations of elements properties as an effect of external load. The phenomenon of spin pairing of iron's bonding electrons in the Earth's interior was predicted to occur half a century ago[1]. Directly affecting the properties of the most abundant transition element, the electronic transition has major geophysical implications[2-4]. Our single-crystal structural analysis of siderite-magnesite solid solutions[5-7], (Fe, Mg)CO_3, allowed unprecedented observations on the transition nature, of geophysical and solid state physics relevance.

10% shrinkage at 44 GPa

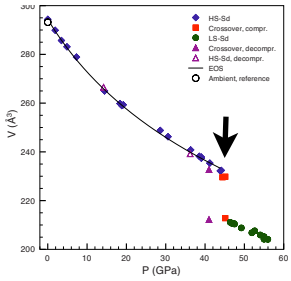

raise of absorption bands in the visible range

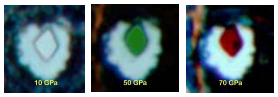

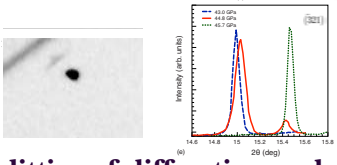

splitting of diffraction peaks: formation of high and low spins domains

anisotropic octahedral compression

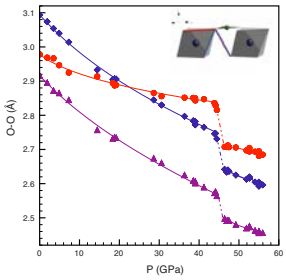

We have provided the first evidence of the lack of an intermediate spin state or a random spin distribution in a pressure-induced spin transition.

Iron rich minerals with regular octahedral Fe^{2+} coordinations are likely to show sharp transitions in the Earth's mantle.

Graphics modified from refs. 5, 6

Exceptional phenomena are associated with the pressure-induced spin-pairing transition in $FeCO_3$: i) the colorless crystals assume intense pressure-dependent coloration, ii) the transition causes 10% volume decrease, iii) the spin pairing occurs over a narrow pressure range in which domains of siderite in the two states coexist, iv) the transition shows ~ 3 GPa hysteresis, v) in the diluted system the transition is shifted to ~ 5 GPa higher pressure. These observations are interpreted as due to a strong cooperative effect of adjacent clusters, which has implications on the width of the transition in the Earth's mantle. Considering that many thermally induced spin transitions also show a cooperative contribution, rather sharp transitions may be expected in Fe-rich compositions of phases with iron in highly symmetric octahedral environments.

The unique observations were made possible by the newly developed monochromatic single crystal diffraction technique and the availability at the APS of the GSECARS/COMPRES gas loading system[8].

The UNLV High Pressure Science and Engineering Center (HiPSEC) is supported by DOE-NNSA under Cooperative Agreement No. DE-FC52-06NA262740. This research was partially supported by COMPRES, the Consortium for Materials Properties Research in Earth Sciences under NSF Cooperative Agreement EAR 10-43050.

[1] W. Fyfe, Geoch. et Cosmoch. Ac. 1960, 19, 141–143. [2] J. Badro et al., Science, 2003, 300, 789–791. [3] J. Badro et al. Science, 2004, 305, 383–386. [4] W. Sturhahn, J. Jackson, J. Lin, Geophys Res Lett, 2005, 32, L12307. [5] B. Lavina et al., Geophys. Res. Lett., 2009, 36, 039652.[6] B. Lavina et al., Phys. Rev. B, 2010, 82, 064110. [7] B. Lavina et al. High Pressure Res., 2010, 30, 224–229. [8] M. Rivers et al., High Pressure Res, 2008, 28, 273–292.

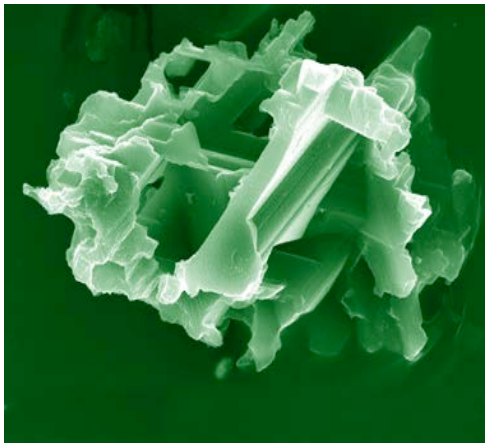

"L. Dobrzhinetskaya and R. Wirth, 2010. Ultradeep Rocks and Diamonds in the Light of Advanced Scientific Technologies. In: *New Frontiers in Integrated Solid Earth Sciences* (Eds: S. Cloetingh and J. Negendank) p. 373-395, Springer, New York."

Unusual microdiamonds and ultradeep rocks found by geologists in many mountain chains formed during lithospheric plate collisions have re-opened a new page of deep Earth's history. We have learned new details due to implementation of high-resolution electron microscopy and synchrotron assisted analytical methods which together represent unprecedented synergy of science and innovative technology.

Microdiamonds from ultrahigh pressure collisional terranes contain different suite of nanoscale inclusions (oxides and K-Cl-S-C-OH fluid) than kimberlitic diamonds of larger size formed inside of thick subcontinental lithosphere. The latter contain inclusions of silicate minerals, associated with native iron, carbides as well as fluid indicating oxygen deficiency conditions, and partial melting of the deep mantle triggered by local excess of H_2O. Microdiamonds from continental collisional zones are formed from a supercritical fluid enriched with local elements of continental crust and organic carbon subducted to the depth more than 200-250 km. Influence of components derived from mantle plume and/or mantle wedge on microdiamond crystallization is also established.

Studies of microdiamonds with Synchrotron Infrared Spectroscopy and nano Secondary Ion Mass Spectrometry strongly suggest that, both carbon and OH-fluid from which these diamonds were crystallized, originate from shallow crustal material which was subducted to deep mantle. In that depth (>200-250 km) where temperature and pressure are high enough, the organic carbon was stabilized in a form of diamond. Therefore, microdiamonds preserve evidence of the pathway by which shallow sediments containing organic carbon and water can be stored in its deep mantle. The proposed concept helps better understanding the geodynamic aspects of deep carbon cycling, thermodynamics of carbon-rich geochemical systems and other thermo-mechanical processes operated at convergent plate boundaries.

Biological carbon storage in Earth's mantle: evidence from diamond synthesis in synchrotron X-ray *in situ* DAC experiments

Larissa Dobrzhinetskaya *University of California Riverside, Department of Earth Sciences*

Global carbon cycle is in a focus of multidisciplinary studies because it related to sustainability of Earth's conditions for human life. We have conducted experiments on diamond synthesis from graphite and amorphous carbon mixed with 3 wt% of organic matter (glucouse $C_6H_{12}O_6$ & oxalic acid dihydrate [$(COOH)_2 \cdot 2H_2O$]) in DAC at pressure 9-11 GPa and temperature 1200-1400K (Fig.1). At high PT conditions glucouse (Eq.1) and oxalic acid dehydrate (Eq.2) produce fluid according to reactions: Eq.1: $(x+y)C_6H_{12}O_6=6xC+6xH_2O+3yCH_4+3yCO_2$ & Eq.2: $(COOH)_2 \cdot 2H_2O=3/2CO_2+3H_2O+1/2C$. Experiments show that both organic substances at high PT conditions promote diamond nucleation which is faster in the run products containing amorphous carbon than graphite. The induction time required for a supercritical COH fluid formation prior the diamond nucleation is ~20 min in DAC whereas it took up to 2-7 hrs in our earlier multianvil apparatus experiments at similar conditions. These huge differences are due to the high sensitivity of synchrotron *in situ* X-ray analysis in detecting a very small diamond. Experimental results show that biological carbon delivered to the Earth's mantle together with surface sediments through deep subduction zones can be stored there in a stable high-pressure form of carbon - diamond. Moreover the biological carbon substances promote graphite and probably any other amorphous carbon transformation to diamond, therefore creating a light carbon isotope reservoirs in deep Earth.

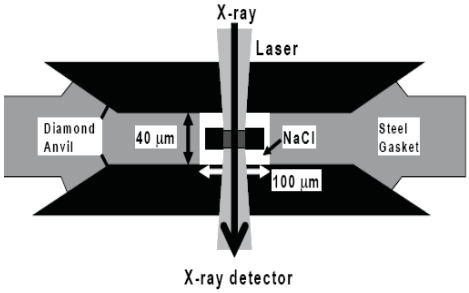

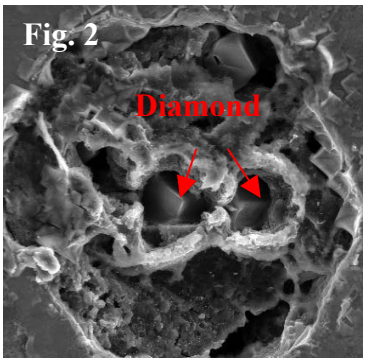

1. J Zhang, V Prakapenka, A Kubo, A Kavner, H Green, L Dobrzhinetskaya, Carbon and Graphite in Presence of COH Fluids: An In-Situ High-Pressure and -Temperature Laser-Heated Diamond Anvil Cell Experimental Study. In: *L Dobrzhinetskaya et al. (Eds)* Ultrahigh-pressure metamorphism: 25 years after the discovery of coesite and diamond. Elsevier Inc (2011). DOI:10.1016/B978-0-12-385144-4.00003-5.

This study is strongly related to our other COMPRES facilities project which involves synchrotron infrared and Raman spectroscopy studies of microdiamonds from ultrahigh-pressure metamorphic terranes incorporated collisional orogenic belts. **See publications below:**

2. L Dobrzhinetskaya, R Wirth, Ultradeep Rocks and Diamonds in the Light of Advanced Scientific Technologies, New Frontiers in Integrated Solid Earth Sciences, p.373-395, Springer, N-York (2010).

3. L Dobrzhinetskaya, R Wirth, D Rhede, Z Liu, H Green, Phlogopite and Quartz Lamellae in Diamond-bearing Diopside from Marbles of the Kokchetav Massif, Kazakhstan: Exsolution or replacement Replacement Reaction?, J Metamorph. Geol., 27, 607-620 (2009).

4. . L Dobrzhinetskaya, R Wirth, H Green II, A Look inside of Diamond-Forming media in Subduction Zones. Proc Natl Acad Sci USA, 104(22), 9128-9132 (2007). - ***our Diamond is on the Cover page of this PNAS issue.***

5. L Dobrzhinetskaya, Z Liu, P Cartigny, J Zhang, D Tchkhetia, R Hemley, H Green, Synchrotron infrared and Raman spectroscopy of microdiamonds from Erzgebirge, Germany, Earth Planet Sci. Lett., 248, 325-334 (2006).

New Insights into the Deep Mantle

Effects of Fe spin transition on the elasticity of (Mg,Fe)O magnesiowüstites and implications for the seismological properties of the Earth's lower mantle

S. Speziale[1,5], V.E. Lee[1], S.M. Clark[2], J.F. Lin[3], M.P. Pasternak[4], and R. Jeanloz[1]
[1]Univ. California, Berkeley, U.S.A.
[2]Lawrence Berkeley Natl. Laboratory, U.S.A.
[3]Lawrence Livermore Natl. Laboratory, U.S.A.
[4]Tel Aviv University, Israel
[5]GFZ-Potsdam, Germany

X-ray diffraction of $(Mg_{0.8}Fe_{0.2})O$ measured at lower mantle pressures reveals a discontinuous pressure dependence of the bulk modulus at 40 (± 5) GPa that is related to the spin-pairing transition of Fe^{2+}. By combining two different experimental datasets we could place constraints on the equation of state of $(Mg_{0.8}Fe_{0.2})O$ with Fe^{2+} in low-spin configuration. Modeling the effect of temperature on the pressure extension of the mixed-spin regime, we could estimate the effect of the transition on the elastic properties of bulk lower mantle rocks. The inclusion of the effects of Fe^{2+} spin transition would imply a substantial correction to the current compositional model of the lower mantle. Up to 10 mol percent increment of the content of magnesiowüstite would be required to match seismological data.

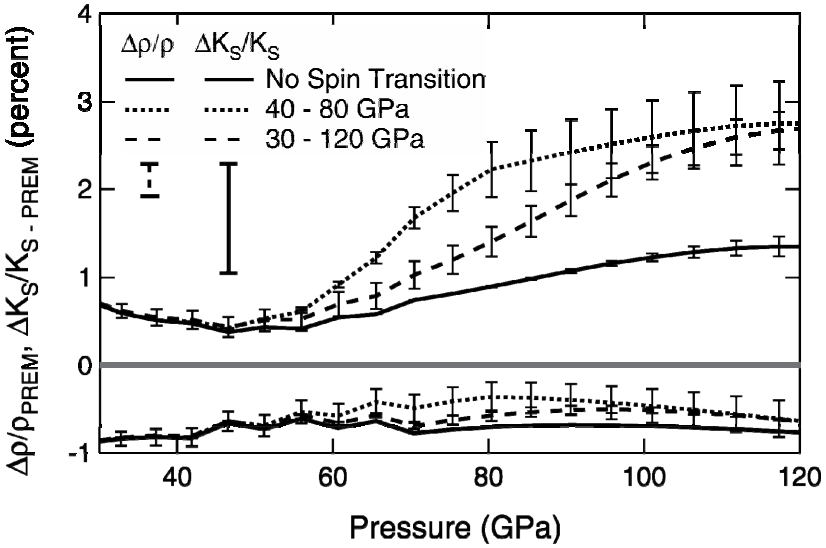

Figure 1. Relative density and bulk modulus variation between a pyrolitic mineralogical model and the PREM seismological model (see text for details). The three sets of curves represent: model with no spin transition in magnesiowüstite, a model with progressive spin transition across the pressure range 40–80 GPa and a model with spin transition across the range between 30 and 120 GPa.

Citation: Speziale S., V.L. Lee, S.M. Clark, J.F. Lin, M.P. Pasternak, and R. Jeanloz, Effects of Fe spin transition on the elasticity of (Mg,Fe)O magnesiowüstite and implications for the seismological properties of the Earth's lower mantle, J. Geophys. Res., 112, 10212, doi:1029/2006JB004730, 2007.

Experimental work was performed at A.L.S. Beamline 12.2.2 supported by COMPRES, within the NSF cooperative agreement EAR 06-49658.

Sound velocities and density of $(Mg_{0.65}Fe_{0.35})O$ up to 1.4 Mbar

Bin Chen[1], Jennifer M. Jackson[1], Wolfgang Sturhahn[2], Dongzhou Zhang[1], Jiyong Zhao[3], Caitlin. A. Murphy[1], and June K. Wicks[1]

1. Seismological Laboratory, California Institute of Technology, Pasadena, CA 91125
2. Jet Propulsion Laboratory, Pasadena, CA 91109
3. Advanced Photon Source, Argonne National Laboratory, Argonne, IL 60439

Sound velocities and density measurements of lower mantle component minerals are essential to interpret the seismic complexities observed in Earth's lower mantle. We determined the elastic and vibrational properties of $(Mg_{0.65}Fe_{0.35})O$-ferropericlase up to 1.4 Mbar using nuclear resonant inelastic X-ray scattering (NRIXS) and in-situ X-ray diffraction (XRD) techniques in diamond anvil cells with neon as the pressure medium. $(Mg_{0.65}Fe_{0.35})O$ contains the amount of iron within the estimated range expected for an aluminum-poor lower mantle assemblage. From the low-energy region of the partial phonon density of states (PDoS), in situ XRD measurements, and our separate equation-of-state study with smaller pressure increments (Fig. 1), we derived its shear and compressional velocities at lowermost mantle pressures (Fig. 2). From integration of the PDoS, we also determined Fe-weighted vibrational parameters as a function of pressure for this ferropericlase. Our data provide new knowledge about the effects of the spin crossover and iron content on the density and sound velocities of ferropericlase in a previous uncharted pressure-composition sector. In light of our results and seismic observations, a better understanding of the compositional variations in Earth's lowermost mantle can be achieved.

Reference: Chen, B., Jackson, J. M., Sturhahn, W., Zhang, D., Zhao, J., Murphy, C.A., and Wicks, J.K. (2010) Sound velocities and density of $(Mg_{0.65}Fe_{0.35})O$ ferropericlase up to 1.4 Mbar. EOS Trans. AGU, Fall Meeting. Suppl. MR13A-1911.

The NRIXS measurements were conducted at Sector 3-ID-B, APS, Argonne National Laboratory and the XRD measurements were conducted at ALS beamline 12.2.2, Lawrence Berkeley National Laboratory, both partially supported by infrastructure and development programs through COMPRES.

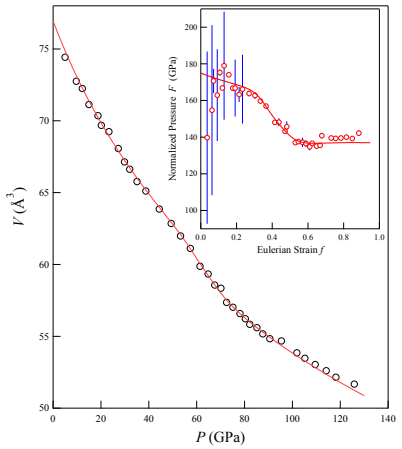

Fig. 1. The compression data of $(Mg_{0.65}Fe_{0.35})O$ up to 126 GPa and its equation of state.

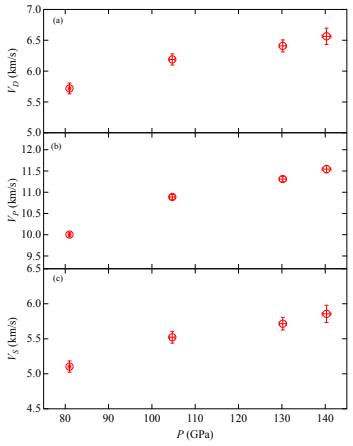

Fig. 2. Debye, compressional and shear sound velocities of ferropericlase at lowermost mantle pressures.

Single-crystal Brillouin Spectroscopy of $(Mg_{0.9}Fe_{0.1})O$ to high-pressures and temperatures

H. Marquardt, S. Speziale (German Research Center for Geosciences GFZ Potsdam, Germany)
D. Frost (Bayerisches Geoinstitut, Bayreuth, Germany)

We successfully collected both Brillouin spectra and single-crystal x-ray diffraction images of ferropericlase up to a pressure of ~15 GPa at a temperature of 700 K (see fig. 1 for typical spectrum). A first analysis of the data shows that increasing temperature decreases c_{11}, c_{44}, c_s, K and G, but increases c_{12}. These first results indicate that the slowest shear wave propagating in [011], polarized along [1-10], which is determined by the shear constant c_s, is significantly lowered when temperature is increased. The fastest shear wave propagating in [001], which is given by the constant c_{44}, is much less sensitive to temperature [as it is to pressure (Marquardt et al. 2009a; Marquardt et al. 2009b)]. This results in an increase of shear wave anisotropy of ferropericlase with increasing temperature. However, it is known that the anisotropy of ferropericlase changes sign at around 20 GPa (Karki et al. 1999; Marquardt et al. 2009b), meaning that the previously slowest shear wave propagation direction becomes the fastest. The shear anisotropy of ferropericlase in the lower mantle would then be lower along a geotherm than determined from high pressure measurements performed at ambient temperature, as it has been predicted for iron-free MgO (Karki et al. 1999). However, temperature might also affect the pressure derivative of the shear wave velocities, similar to what does the substitution of magnesium with iron (Marquardt et al. 2009b).

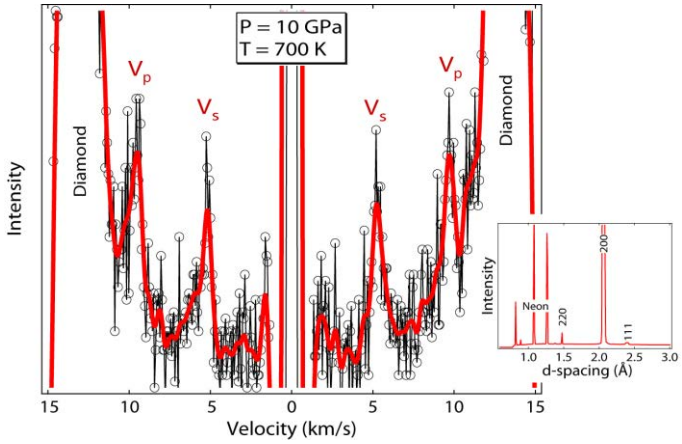

Fig. 1: Brillouin spectrum collected at simultaneously high-pressure and high-temperature in an externally heated diamond-anvil cell. The black circles represent the raw data and the red line (filtered) is shown for illustration. Single-crystal x-ray diffraction (inset) was collected simultaneously to determine the sample density and orientation at the same experimental conditions where Brillouin scattering was carried out.

Karki, B. B., R. M. Wentzcovitch, et al. (1999). "First-principles determination of elastic anisotropy and wave velocities of MgO at lower mantle conditions." *Science* **286**(5445): 1705-1707.

Marquardt, H., S. Speziale, et al. (2009a). "Single-crystal elasticity of $(Mg_{0.9}Fe_{0.1})O$ to 81 GPa." *Earth Planet. Sci. Lett.* **287**(3-4): 345-352.

Marquardt, H., S. Speziale, et al. (2009b). "Elastic Shear Anisotropy of Ferropericlase in Earth's Lower Mantle." *Science* **324**(5924): 224-226.

Very low sound velocities in iron-rich (Mg,Fe)O: Implications for the core-mantle boundary region*

June K. Wicks
wicks@caltech.edu
Division of Geological and Planetary Sciences, California Institute of Technology, Pasadena, CA 91125, USA

Jennifer M. Jackson
Seismological Laboratory Division of Geological and Planetary Sciences, California Institute of Technology, Pasadena, CA 91125, USA

Wolfgang Sturhahn
Advanced Photon Source, Argonne National Laboratory, Argonne, IL 60439, USA, now at Jet Propulsion Laboratory, Pasadena, CA 91109, USA

Very low sound velocities were measured in $(Mg_{0.16}{}^{57}Fe_{0.84})O$ at high pressures, suggesting that the presence of iron-rich (Mg,Fe)O can explain the characteristic sound speeds of ultra-low velocity zones (ULVZs) near Earth's core-mantle boundary.

Nuclear resonant scattering experiments were conducted at beamline 3-ID-B of the Advanced Photon Source, Argonne National Laboratory, at ambient temperature over the pressure range 0 to 121 GPa. Nuclear resonant inelastic x-ray scattering (NRIXS) was used to determine the Debye sound velocity, V_D, at each pressure, and the effect of iron's electronic environment on the sound velocities was observed using synchrotron Mössbauer spectroscopy. Corresponding compressional (V_P) and shear (V_S) velocities at each pressure were determined from the V_D and an equation of state reported for iron-rich (Mg,Fe)O (Figure 1).

We found that V_S decreases with increasing pressure approaching a magnetic transition at 28 GPa (at 300K) that may be related to the B1 to rhombohedral structural distortion. In the measured pressure range of 100 to 121 GPa, we noted decreasing V_P that may be due to the high to low Fe spin transition of $(Mg_{0.16}Fe_{0.84})O$. Apart from the effect of magnetic transitions, the very low pressure derivatives of V_P and V_S for $(Mg_{0.16}Fe_{0.84})O$ ensure that this material retains ultra-low sound velocities up to core-mantle boundary pressures.

Without defining a formation mechanism, the simplest way to explore the effect of iron-rich (Mg,Fe)O is to mix the measured velocities of $(Mg_{0.16}Fe_{0.84})O$ with the modeled velocities of PREM. We show that small amounts of $(Mg_{0.16}Fe_{0.84})O$ can bring down the average sound velocity of an assemblage and match properties of ULVZs.

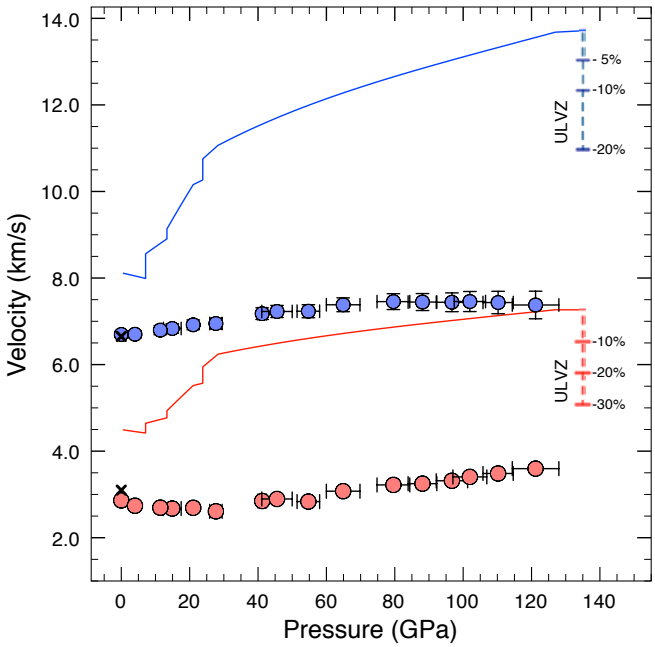

Figure 1. V_P (blue) and V_S (red) of $(Mg_{0.16}{}^{57}Fe_{0.84})O$ determined from V_D plotted alongside V_P and V_S of the Preliminary reference Earth model (PREM) *[Dziewonski and Anderson (1981), PEPI, 25, 297]*. Seismic determinations of ULVZ velocities vary by study but typically have been reported as having ~5-20% lower V_P and ~10-30% lower V_S than PREM, which we indicate at 135 GPa. At 0 GPa, we plot predicted sound velocities for $(Mg_{0.16}Fe_{0.84})O$ from an ultrasonic study on the (Mg,Fe)O solid solution *[Jacobsen et al. (2002), JGR, 107(B2), 2037].*

**summary and figure adapted from Wicks et al.(2010), GRL, 37, L15304.*

A geodynamic and mineral physics model of a solid-state ultralow-velocity zone*

Dan J. Bower, June K. Wicks, Michael Gurnis and Jennifer M. Jackson
Division of Geological and Planetary Sciences, Caltech, USA

Recent results (*Wicks et al.*, 2010) suggest that a mixture of iron-enriched (Mg,Fe)O and ambient mantle is consistent with wavespeed reductions and density increases inferred for ultralow-velocity zones (ULVZs). We explore this hypothesis by simulating convection to deduce the stability and morphology of such chemically-distinct structures. The buoyancy number (B), or chemical density anomaly, largely dictates ULVZ shape, and the prescribed initial thickness (proxy for volume) of the chemically-distinct layer controls its size. We synthesize our dynamic results with various Voigt-Reuss-Hill mixing models to provide insight into the inherent seismic tradeoff between ULVZ thickness and wavespeed reduction. Seismic data are compatible with a solid-state origin for ULVZs, and a suite of these structures may scatter seismic energy to produce broadband PKP precursors.

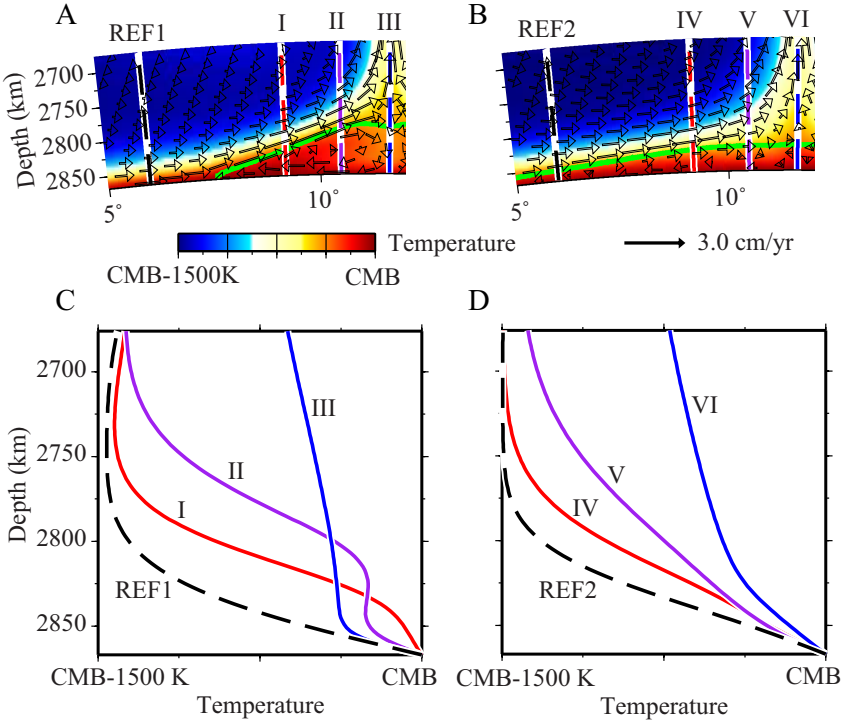

Figure 1: Steady-state behavior of a thin (Mg,Fe)O-containing layer. (A) Counter-circulation driven by viscous coupling ($B = 1.25$, $d_{ch} = 16$ km, impermeable domain). The ULVZ component is contained within the area outlined in green and the CMB. (C) Temperature profiles: reference REF1, upwelling I, center II, and downwelling III. (B) Sluggish convection ($B = 4$, $d_{ch} = 16$ km, permeable domain). (D) Temperature profiles (REF2, IV, V, VI) are at the same locations as in (C).

References

Bower, D. J., J. K. Wicks, M. Gurnis, and J. M. Jackson (2011), A geodynamic and mineral physics model of a solid-state ultralow-velocity zone, *Earth Planet. Sc. Lett.*, *303*, 193–202, doi:10.1016/j.epsl.2010.12.035.

Wicks, J. K., J. M. Jackson, and W. Sturhahn (2010), Very low sound velocities in iron-rich (Mg,Fe)O: Implications for the core-mantle boundary region, *Geophys. Res. Lett.*, *37*, L15304, doi:10.1029/2010GL043689.

Bower et al. (2011)

Enhanced convection and fast plumes in the lower mantle induced by the spin transition in ferropericlase*

Dan J. Bower†, Michael Gurnis†, Jennifer M. Jackson† and Wolfgang Sturhahn‡
†Division of Geological and Planetary Sciences, Caltech, USA
‡ Jet Propulsion Laboratory, Pasadena, USA

Using a numerical model we explore the consequences of the intrinsic density change ($\Delta\rho/\rho \approx 2-4\%$) caused by the Fe^{2+} spin transition in ferropericlase on the style and vigor of mantle convection. The effective Clapeyron slope of the transition from high to low spin is strongly positive in pressure-temperature space and broadens with high temperature. This introduces a net spin-state driving density difference for both upwellings and downwellings. In 2-D cylindrical geometry spin-buoyancy dominantly enhances the positive thermal buoyancy of plumes. Although the additional buoyancy does not fundamentally alter large-scale dynamics, the Nusselt number increases by 5-10%, and vertical velocities by 10-40% in the lower mantle. Advective heat transport is more effective and temperatures in the core-mantle boundary region are reduced by up to 12%. Our findings are relevant to the stability of lowermost mantle structures.

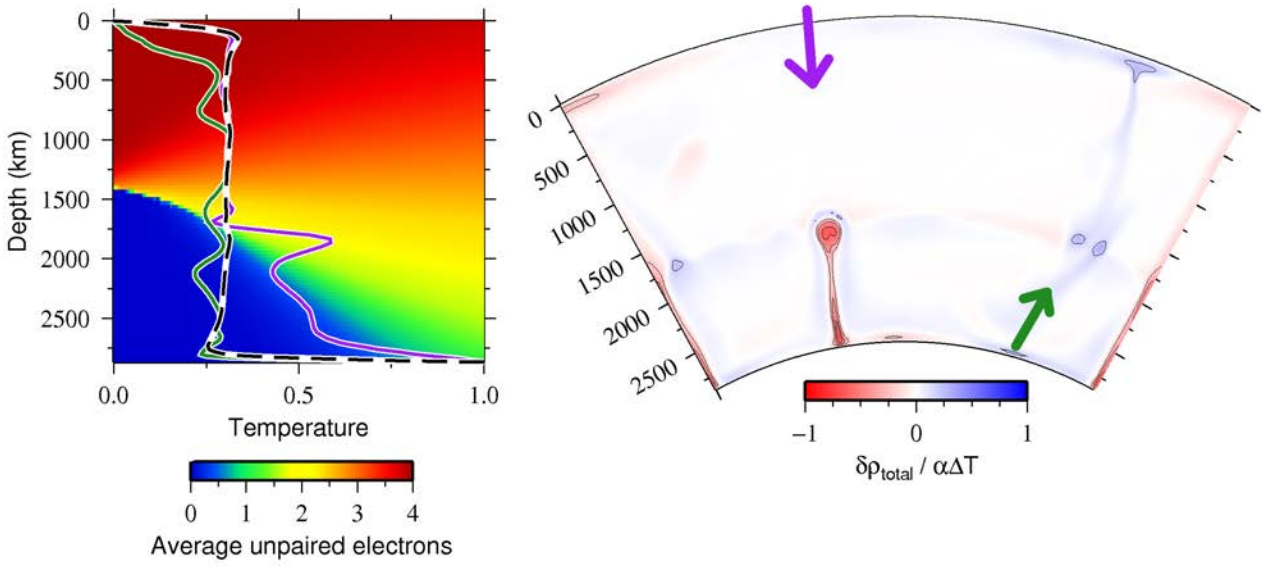

Figure 1: Snapshot from a model at quasi-steady state. (left) Geotherms with *Sturhahn et al.* (2005) spin-state model. Black dashed line is the reference geotherm. (right) Total density anomaly, scaled by $1/\alpha\Delta T$, relative to the horizontally-averaged profile.

References

Bower, D. J., M. Gurnis, J. M. Jackson, and W. Sturhahn (2009), Enhanced convection and fast plumes in the lower mantle induced by the spin transition in ferropericlase, *Geophys. Res. Lett.*, *36*, L10306, doi:10.1029/2009GL037706.

Sturhahn, W., J. M. Jackson, and J.-F. Lin (2005), The spin state of iron in minerals of Earth's lower mantle, *Geophys. Res. Lett.*, *32*, L12307, doi:10.1029/2005GL022802.

Bower et al. (2009)

Electronic Spin and Valence States of Iron in the Earth's Lower Mantle

Jung-Fu "Afu" Lin, Assistant Professor
Department of Geological Sciences, The University of Texas at Austin

Silicate perovskite and ferropericlase are believed to be the abundant minerals in the lower mantle, whereas silicate post-perovskite likely exists in the lowermost mantle. The properties of the deep mantle can be strongly influenced by the presence of iron in these phases, which in turn affects our understanding of the nature of the Earth's deep mantle. The electronic spin crossover in ferropericlase have been observed to result in significant changes in its elastic, electrical, thermal, and transport properties, although the electronic states and associated effects on the properties of perovskite and post-perovskite remain highly debated. Here we have studied the spin and valence states of iron in these lower-mantle minerals at relevant pressure-temperature (P-T) conditions using synchrotron Mossbauer spectroscopy (SMS). The synchrotron X-ray spectroscopic results, including the hyperfine parameters (quadrupole splittings (QS) and chemical shifts (CS)) have played important roles as site-specific fingerprints for assignments of the valence and spin states of iron in the lower-mantle minerals. In particularly, our recent synchrotron Mossbauer results consistently show that Fe2+ predominantly exhibits extremely high quadruple splittings and relatively high chemical shifts whereas a certain amount of Fe3+ also occurs in the perovskite and post-perovskite phases. Combing these results with thermodynamic modellings and seismic observations of the lower mantle, the electronic states of iron and their associated effects in lower-mantle minerals can affect our understanding on the seismology, geochemistry, and geodynamics of the Earth's deep mantle.

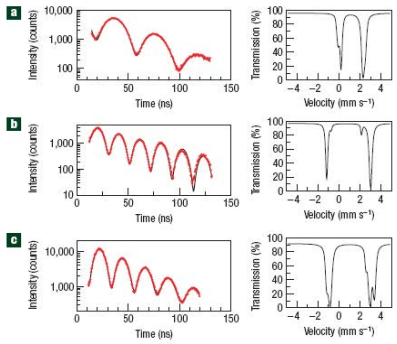

Figure 1 Representative synchrotron Mossbauer spectra. a*, Enstatite at ambient conditions.* ***b****, Silicate perovskite at 110 GPa.* ***c****, Silicate post-perovskite at 134 GPa. Corresponding energy spectra calculated from the fits are shown in the left panels.*

References

[1] J.F. Lin, H.C. Watson, G. Vankó, E.E. Alp, V.B. Prakapenka, P. Dera, V.V. Struzhkin, A. Kubo, J. Zhao, C. McCammon, W.J. Evans, Intermediate-spin ferrous iron in lowermost mantle post-perovskite and perovskite, *Nature Geoscience*, 1, 688-691, 2008.
[2] J.F. Lin, Z. Mao, I. Jarrige, Y. Xiao, P. Chow, T. Okuchi, N. Hiraoka, and S.D. Jacobsen, *Am. Miner.*, **95**, 1125-1131 (2010).
[3] Z. Mao, J.F. Lin, C. Jacobs, H. Watson, Y. Xiao, P. Chow, E.E. Alp, and V.B. Prakapenka, *Geophys. Res. Lett.*, **37**, L22304 (2010).
[4] J.F. Lin, Z. Mao, and E.E. Alp, submitted (2011).

Bulk sound speed changes at the perovskite to post-perovskite phase transition

Sang-Heon Dan Shim, Justin Hustoft, and Krystle Catalli, *Massachusetts Institute of Technology*
Vitali Prakapenka, *GSECARS, University of Chicago*

The discovery of a phase transition in the dominant mantle silicate from the perovskite structure to the post-perovskite structure has impacted our understanding of the complex seismic structures observed in the lowermost mantle. Unlike most discontinuities in the mantle, the D" discontinuity found at 200-400 km above the core-mantle boundary shows a decrease in bulk sound speed and very little change in P-wave velocity, while S-wave velocity increases.

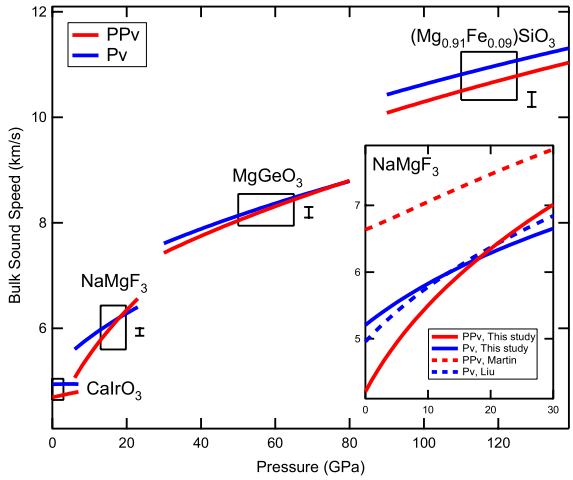

Bulk sound speeds of the perovskite phase (blue lines) and the post-perovskite phase (red lines) in different materials.

In order to systematically investigate the bulk sound speed change at the perovskite to post-perovskite phase transition, we conducted synchrotron X-ray diffraction measurements at the GSECARS sector of the Advanced Photon Source and beamline 12.2.2 of the Advanced Light Source. We found that bulk sound speed decreases at the phase transition in both $(Mg_{0.91}Fe_{0.09})SiO_3$ and $NaMgF_3$. Previous studies have also shown that bulk sound speed decreases at the phase transition in $MgGeO_3$ and $CaIrO_3$. This indicates that the bulk sound speed decrease is common in the perovskite-to-post-perovskite transition systems. This also suggests that the bulk sound speed decrease is controlled by the structural change, not by composition. Therefore, the bulk sound speed decrease should be a robust property for the D" discontinuity resulting from the perovskite to post-perovskite transition without being significantly affected by compositional variations in the lowermost mantle.

Publications

S.-H. Shim, K. Catalli, J. Hustoft, A. Kubo, V. B. Prakapenka, W. A. Caldwell, and M. Kunz. Crystal structure and thermoelastic properties of $(Mg_{0.91}Fe_{0.09})SiO_3$ postperovskite up to 135 GPa and 2700 K. P. Natl. Acad. Sci. 105, 7382–7386, 2008.
J. Hustoft, K. Catalli, S.-H. Shim, A. Kubo, V. B. Prakapenka, and M. Kunz. Equation of state of $NaMgF_3$ postperovskite - implications for the seismic velocity changes in the D" region. Geophys. Res. Lett. 35, L10309, 2008.

The behavior of iron in $(Mg,Fe)SiO_3$ post-perovskite assemblages at Mbar pressures

Jennifer M. Jackson[1,*], Wolfgang Sturhahn[2], Oliver Tschauner[3], Michael Lerche[4], and Yingwei Fei[5]

[1] Seismological Laboratory, California Institute of Technology, CA 91125
[2] Advanced Photon Source, Argonne National Laboratory, Argonne, IL 60439
[3] High Pressure Science and Engineering Center, University of Nevada, NV 89154
[4] HPSynC, Carnegie Institution of Washington, Argonne, IL 60439
[5] Geophysical Laboratory, Carnegie Institution of Washington, Washington, D.C. 20015

The electronic environment of the iron sites in post-perovskite (PPv) structured $(^{57}Fe,Mg)SiO_3$ have been measured in-situ at 1.12 and 1.19 Mbar at room temperature, using ^{57}Fe synchrotron Mössbauer spectroscopy (Fig. 1a). The measurements were conducted at sector 3-ID-B of the Advanced Photon Source at Argonne National Laboratory. Evaluation of the time spectra reveals two distinct iron sites, which are well distinguished by their hyperfine fields. The dominant site is consistent with an Fe^{3+}-like site in a high spin state. The second site is characterized by a small negative isomer shift with respect to α-iron and no quadrupole splitting, consistent with a metallic iron phase. Combined with SEM/EDS analyses of the quenched assemblage, (Fig. 1b) our results are consistent with the presence of a metallic iron phase co-existing with a ferric-rich PPv. Such a reaction pathway may aid in our understanding of the behavior of iron at Earth's core-mantle-boundary region.

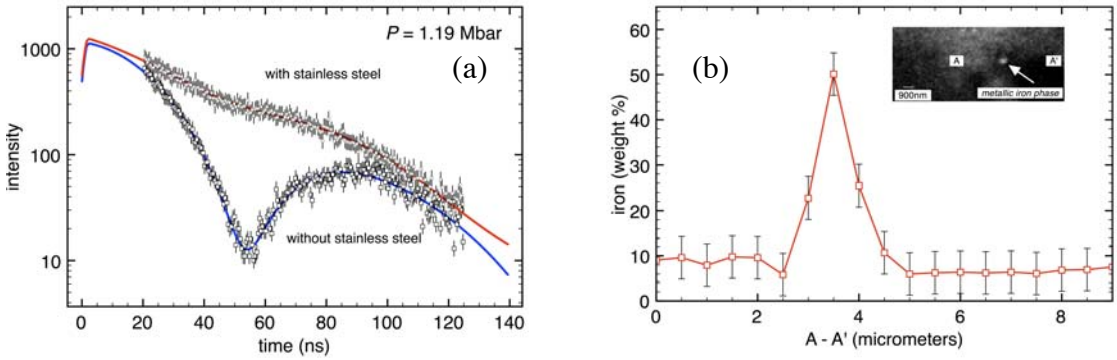

Figure 1 (adapted from Jackson *et al*. *GRL* 2009[*]). (a) Synchrotron Mössbauer spectra of $(^{57}Fe,Mg)SiO_3$-PPv with and without stainless steel prepared in two different diamond-anvil-cells, at P = 1.19 Mbar (synthesized at 1350 ± 200 K). The lines through the data represent the best-fit hyperfine parameters. (b) EDS results of the iron content across a trace (A-A'on SEM image inset) in the recovered quenched PPv phase assemblage from Fig1a. The inset SEM image shows the amorphous quenched PPv and an iron-rich cluster (bright spots).

[*]Jackson *et al*. (2009) *Geophys*. *Res*. *Lett*., 36, L10301, doi:10.1029/2009GL037815

Spin transition of iron in magnesium silicate perovskite and post-perovskite

Sang-Heon Dan Shim, Krystle Catalli, and Brent Grocholski, *Massachusetts Institute of Technology*
Vitali Prakapenka, *GSECARS, University of Chicago*
Wolfgang Sturhahn, *Sector 3, Argonne National Lab*
Paul Chow, Yuming Xiao and Haozhe Liu, *HPCAT, Argonne National Lab*
Hyunchae Cynn and William Evans, *Livermore National Lab*

Iron is known to undergo a spin transition in ferropericlase at lower mantle pressures. However, the spin transition is still unclear in the dominant mantle silicates, perovskite and post-perovskite. One of the main reasons for the difficulty is that perovskite and post-perovskite contains both Fe^{2+} and Fe^{3+} which have different spin behaviors.

We synthesized perovskite and post-perovskite with controlled oxidation state of iron, which makes it possible to distinguish the behaviors of Fe^{2+} and Fe^{3+} and their effects on the physical properties. We performed various different measurements in the laser-heated diamond-anvil cell at Sectors 3 (Nuclear Forward Scattering), 13 (GSECARS; X-Ray Diffraction), and 16 (HPCAT; X-ray diffraction, Nuclear Forward Scattering, and X-ray Emission Spectroscopy) of the Advanced Photon Source.

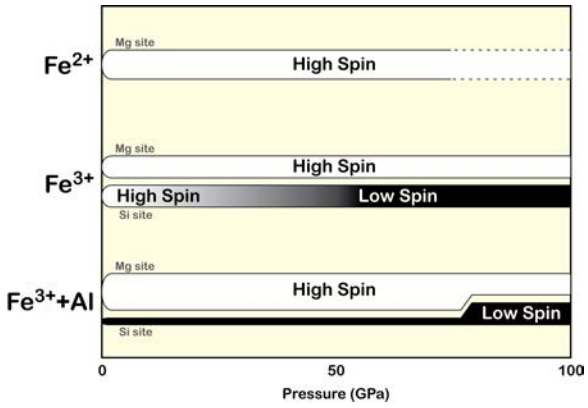

Schematic diagram of spin behaviors of Fe^{2+} and Fe^{3+} in mantle silicate perovskite.

We found that Fe^{2+} remains high spin at least up to 70 GPa, while Fe^{3+} in the Si site undergoes a gradual transition to low spin up to 55 GPa in perovskite. The gradual spin transition results in stiffening of perovskite. In post-perovskite, we found that Fe^{3+} in the Mg site remains high spin, while Fe^{3+} in the Si site is low spin. We found that Fe^{3+} increases the density of post-perovskite much more than Fe^{2+}. These findings imply that mantle heterogeneities containing elevated amount of Fe^{3+} may have distinctive elastic properties and density, making them detectable in seismic imaging.

Publications

Lundin, S., Catalli, K., Santillán, J., Shim, S.-H., Prakapenka, V. B., Kunz, M., and Meng, Y. Effect of Fe on the equation of state of mantle silicate perovskite over 1 Mbar. Phys. Earth Planet. Inter. 168, 97-102, 2008.

Catalli, K., Shim, S.-H., Prakapenka, V. B., Zhao, J. and Sturhahn, W. X-ray diffraction and Mössbauer spectroscopy of Fe^{3+}-bearing Mg-silicate post-perovskite at 128-138 GPa. Am. Mineral. 95, 418-421, 2010.

Catalli, K., Shim, S.-H., Prakapenka, V. B., Zhao, J., Sturhahn, W., Chow, P., Xiao, Y., Liu, H., Cynn, H. and Evans, W. J. Spin state of ferric iron in $MgSiO_3$ perovskite and its effect on elastic properties. Earth Planet. Sc. Lett. 289, 68-75, 2010.

Grocholski, B., Shim, S.-H., Sturhahn, W., Zhao, J., Xiao, Y. and Chow, P. C. Spin and valence states of iron in $(Mg_{0.8}Fe_{0.2})SiO_3$ perovskite. Geophys. Res. Lett. 36, L24303, 2009.

Seismic detectability of the perovskite to post-perovskite transition

Sang-Heon Dan Shim and Krystle Catalli, *Massachusetts Institute of Technology*

Since its discovery in 2004, the post-perovskite transition has stimulated many exciting discoveries in seismology, geochemistry, and mineral physics. The phase transition has been attributed to the source of a discontinuous increase in S-wave velocity found in the lowermost mantle, the origin of which has been unknown for decades. However, most high pressure measurements on the post-perovskite phase have been conducted in compositionally simple systems. In order for a phase transition to generate seismic discontinuity, it should occur at a depth (or pressure) where a related seismic discontinuity exists and have sufficiently small thickness otherwise it would be observed as a seismic gradient in the mantle.

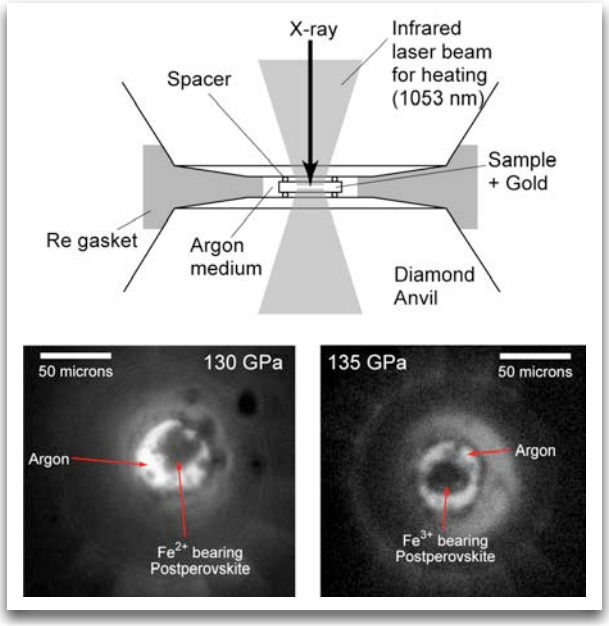

Schematic diagram of sample setup (top) and microphotographs of the samples in the laser heated diamond-anvil cell (bottom).

We have conducted X-ray diffraction measurements at lower mantle pressure and temperature conditions on the post-perovskite phase boundary in the laser-heated diamond-anvil cell at the GSECARS sector of the Advanced Photon Source.

We found that the amounts of iron and aluminum expected for a standard mantle composition (pyrolite) increase the thickness of the post-perovskite boundary to 400-600 km. Therefore, the observation of the seismic discontinuity resulting from the post-perovskite transition indicates that the lowermost mantle would be depleted in aluminum or have distinct mineralogy compared with the rest of the mantle. The compositional constraints we obtained in this study is important for using seismic imaging to infer the composition of the lowermost mantle which is believed to be the source region for some hotspot volcanism (such as Hawaii) and the graveyard for the subducting slabs.

Publications

Catalli, K., Shim, S.-H. and Prakapenka, V. Thickness and Clapeyron slope of the postperovskite transition. Nature, 2009, 462, 782-785

Deformation of Lower-Mantle Ferropericlase across the Electronic Spin Transition

Jung-Fu Lin[1], Hans-Rudolf Wenk[2], Marco Voltolini[2], Sergio Speziale[3], Jinfu Shu[4], Thomas Duffy[5]

[1]*Lawrence Livermore National Laboratory, Livermore, California 94550, USA*

[2]*Department of Earth and Planetary Science, University of California, Berkeley, California 94720, USA*

[3]*GeoForschungsZentrum Potsdam, Telegrafenberg, 14473 Potsdam, Germany*

[4]*Geophysical Laboratory, Carnegie Institution of Washington, Washington, DC 20015, USA*

[5]*Department of Geosciences, Princeton University, Princeton, New Jersey 08544, USA*

We investigated the deformation of lower-mantle ferropericlase [$(Mg_{0.83},Fe_{0.17})O$] through the spin transition under non-hydrostatic conditions in a diamond cell using radial X-ray diffraction techniques at X17c of the NSLS. We observe unexpectedly lower stress and strength of ferropericlase, together with active slip systems and high elastic anisotropy. These results indicate that ferropericlase would play more dominant roles in the deformation and seismic anisotropy of the lower mantle, including subducting slabs, than what is expected by studying the high-spin ferropericlase.

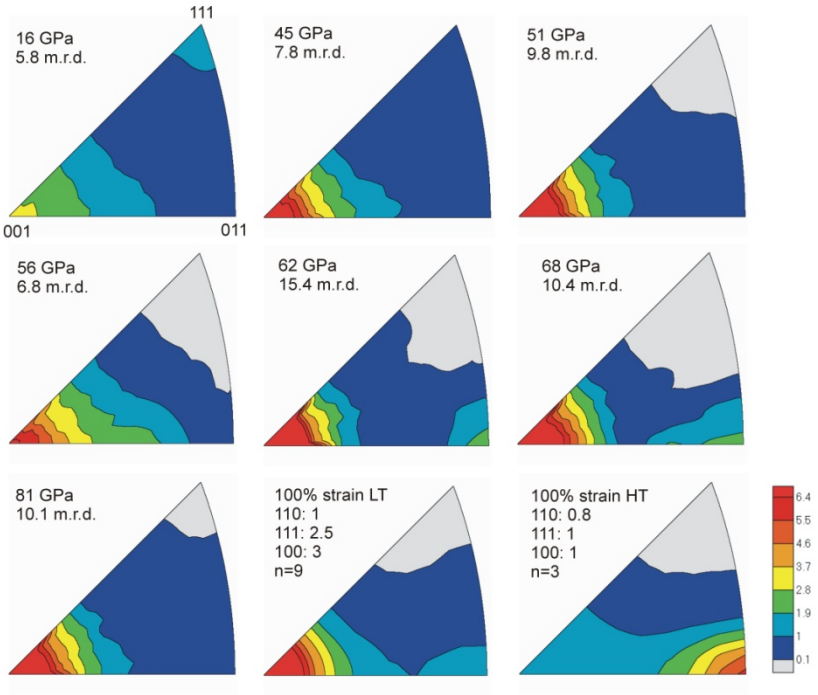

Figure: Inverse pole figures of the compression direction for $(Mg_{0.83},Fe_{0.17})O$ at high pressures in equal area projection.

Reference: J. F. Lin, H.-R. Wenk, M. Voltolini, S. Speziale, J. Shu, T. Duffy, Deformation of the lower-mantle ferropericlase across the electronic spin transition, Phys. Chem. Minerals, 36, 585, 2009.

Experiments were conducted at the X17C beamline of NSLS which is supported by COMPRES, the Consortium for Material Property Research in the Earth Sciences under NSF Cooperative Agreement EAR06-49658.

Weakening of calcium iridate during its transformation from perovskite to post-perovskite.

Hunt, S. A.[1], D. J. Weidner[2], L. Li[2], L. Wang[2], N. P. Walte[3], J. P. Brodholt[1], and D. P. Dobson[1]

1. University College London, UK. 2. SUNY at Stony Brook. 3. Bayerisches Geoinstitut, Germany.

The D'' region at 2,700-2,900 km depth in the Earth contains the thermal boundary at the base of the mantle. With superadiabatic gradients of 1,000 K or more, this boundary is a source of mantle upwellings that have their surface expression in regions of significant intraplate volcanism. In addition, subducted oceanic crust is thought to penetrate to D'', from where it is recycled by means of plume volcanism. The discovery of a phase transformation in $MgSiO_3$ at 120 GPa suggests that D'' contains the new, $CaIrO_3$-structured, post-perovskite phase. The thermal structure of D'' means that strain will localize to its lowermost part just atop the core-mantle boundary, where the mantle is hottest and hence weakest. This is consistent with the observed gradient in seismic anisotropy. Although it is generally true that the increased temperature of the D'' layer will result in the D'' material being weaker, the effect of the phase transition on the strength of the mantle has not been determined. Indeed, recent inversions of the geoid suggest that cooler regions of D'' (which would contain more post-perovskite) are weaker than hotter, perovskite-bearing regions. We performed studies of concurrent deformation and transformation from perovskite to post-perovskite in the low-pressure analogue $CaIrO_3$ at beamline X17b2 of the NSLS. We find that post-perovskite is up to 10 times weaker than perovskite in this system (figure 1). This results is in good agreement with our subsequent ab inito studies of diffusion creep in the $MgSiO_3$ system, where the post-perovskite can be up to several orders of magnitude weaker, depending on the orientation of the stress field relative to the crystallographic axes. This weakening of $MgSiO_3$ in D'' will have significant implications for the dynamics of the core-mantle boundary.

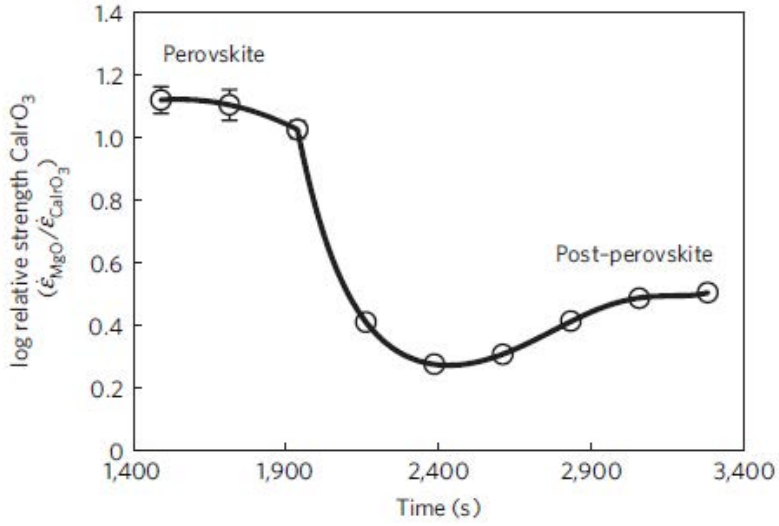

Figure 1. Strength of $CaIrO_3$ relative to MgO as it transforms from the perovskite structure to the post-perovskite structure. Note the strength scale is in log units.

This work was supported by NSF. NSLS X17b is supported by COMPRES through NSF EAR 06-49658.

Deformation mechanisms in post-perovskite and anisotropy in the lowermost mantle

L. Miyagi[1], W. Kanitpanyacharoen[2], P. Kaercher[2], K.M.M. Lee[1], H.R. Wenk[2]

[1]Yale University, [2]University of California, Berkeley

$MgSiO_3$ post-perovskite (pPv) is thought to be a major phase in the Earth's lowermost mantle (D" region). It is critically important to understand the plastic deformation properties of pPv in order to interpret the rheology and seismic anisotropy of this region. Previously the Berkeley high pressure research group performed room temperature diamond anvil cell (DAC) deformation experiments to 150 GPa on $MgGeO_3$ pPv (Merkel et al. 2005) and $MgSiO_3$ pPv (Merkel et al. 2007). These experiments produced textures consistent with slip on (100) and/or {110} lattice planes. However, D-DIA experiments on the pPv analog $CaIrO_3$ pPv identified (010)[100] slip (Miyagi et al. 2008a).

To resolve this controversy new deformation experiments were performed on $MgSiO_3$ pPv at the COMPRES-supported high pressure beamline 12.2.2 at the Berkeley Advanced Light Source. This beamline is well-suited for radial diffraction DAC experiments because of the convenient geometry of sample stage and laser heating system. A membrane control system has been developed to change pressure *in situ* as well as laser heating which is necessary to induce the pPv phase transformation (Miyagi et al 2008b). In these new ALS experiments Miyagi et al. 2010 observed that at large strains a texture evolves with a maximum at 001 (Fig. 1a-c), which is consistent with (001) slip as confirmed with polycrystal plasticity simulations (Fig. 1d). Thus previous conclusions had to be revised. It appears that the weak (100) textures observed previously were due to the phase transformation under stress, rather than deformation. Calcium iridate pPv seems to be a poor analog for $MgSiO_3$ pPv because of different bonding characteristics. Previously assumed deformation mechanisms failed to explain seismic observations, but the new (001) slip system is compatible with observed seismic anisotropy in the D" zone, i.e. fast S-waves polarized parallel to the core-mantle boundary and an opposite anisotropy behavior for fast S-waves and P-waves. The new results open new possibilities for modeling anisotropy evolution during convection in the lowermost mantle, linking microscopic mineral physics properties to large macroscopic observations.

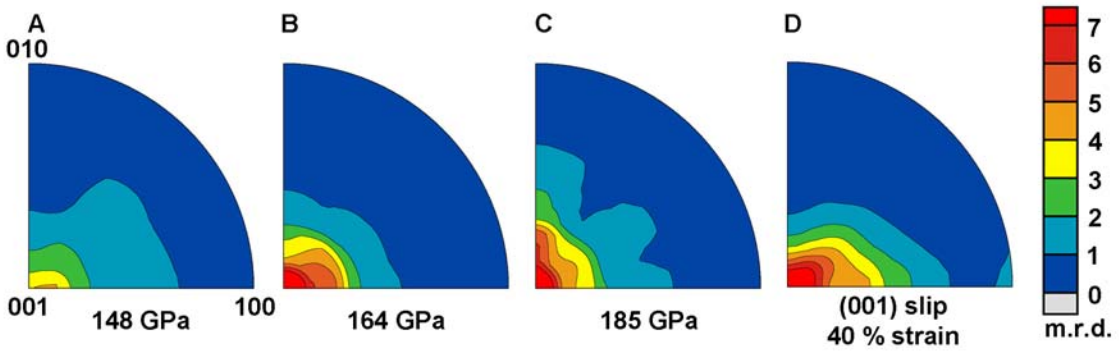

Fig. 1. (a-c) Inverse pole figures of post-perovskite deformed in the DAC. (d) Polycrystal plasticity simulations to identify active slip systems (Miyagi et al. 2010).

Miyagi L, Kanitpanyacharoen W, Kaercher P, Lee KKM, Wenk HR (2010). Slip systems in MgSiO3 post-perovskite: Implications for D" anisotropy. Science 329, 1639-1641.

Experiments were conducted at the X17C beamline of NSLS which is supported by COMPRES, the Consortium for Material Property Research in the Earth Sciences under NSF Cooperative Agreement EAR06-49658.

Characteristics of lateral heterogeneities with thermal and chemical origins in the pyrolitic lower mantle

B. S. Li
Mineral Physics Institute, Stony Brook University, New York, USA

Seismic tomography reveals various degrees of lateral heterogeneities of seismic velocities in the lower mantle, especially at the bottom of the lower mantle under the Central Pacific and beneath Africa. The relative changes between shear and compressional velocities ($R_{SP} = d\ln V_S/d\ln V_P$), bulk sound and shear velocities ($R_{CS} = d\ln V_C/d\ln V_S$), and density versus shear wave velocity ($R\rho_S = d\ln\rho/d\ln V_S$) in response to thermal and chemical variations were investigated for the pyrolitic lower mantle. For heterogeneities with thermal origins, R_{SP} increases from 1.7 to 2.0 together with $R\rho_S$ decreasing from 0.4 to 0.2 and R_{CS} = ~0.27 from the top to the bottom of the lower mantle. In comparison, chemical variations (bulk iron or silica contents) are characterized by $R_{SP} < 1.5$ and $R_{CS} > 0.5$ at lower mantle depths. Negative values of $R\rho_S$ and R_{CS} are indicative of chemical anomalies in the lower mantle, but a combination of thermal and chemical heterogeneities may be required to produce velocity and density anomalies at the magnitudes observed in seismic data. Further refinement of these characteristics requires data on the higher order pressure and temperature derivatives of the elastic moduli of the constituent phases.

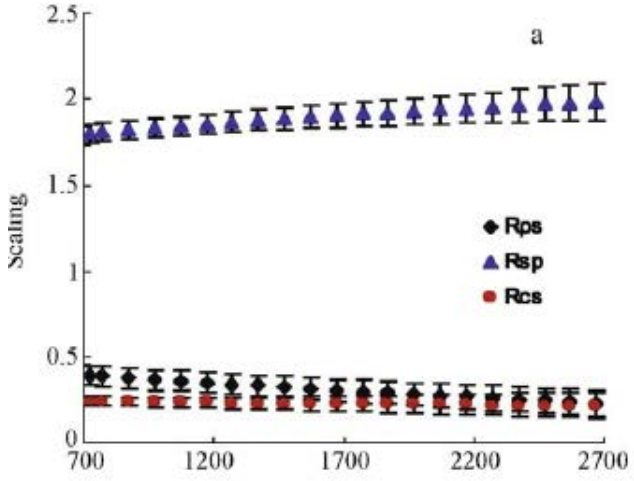

Figure. Characteristic values of R_{SP}, $R\rho_S$, and R_{CS} for lateral heterogeneities originated from temperature

B. S. Li, Characteristics of lateral heterogeneities with thermal and chemical origins in the pyrolitic lower mantle. Progress in Natural Science 19, 1603–1611, 2009.

Synchrotron experiments for collecting the data used in this study were conducted at the X17B2 beamline of NSLS which is supported by COMPRES under NSF Cooperative Agreement EAR06-49658.

Magnetic ordering and spin state of iron in Fe_2O_3 post-perovskite

Sang-Heon Dan Shim and Krystle Catalli, *Massachusetts Institute of Technology*
Dane Morgan and Amy Bengtson, *University of Wisconsin*
Vitali Prakapenka, *GSECARS, University of Chicago*
Wolfgang Sturhahn, *Sector 3, Argonne National Lab*

Magnetic ordering in Fe_2O_3 has been used to understand the paleomagnetic fields of Earth and other planets. However, the record can be later altered by various processes, most notably including impact. For example, while strongly magnetized crust was discovered on Mars, some basins found unmagnetized. Because those basins may be formed by impact, it has been inferred that impact may demagnetize magnetic record carrier minerals in the basins. However, effects of pressure on magnetic ordering have not been well understood.

We have conducted Nuclear Forward Scattering (Sectors 3 of APS) and X-ray diffraction

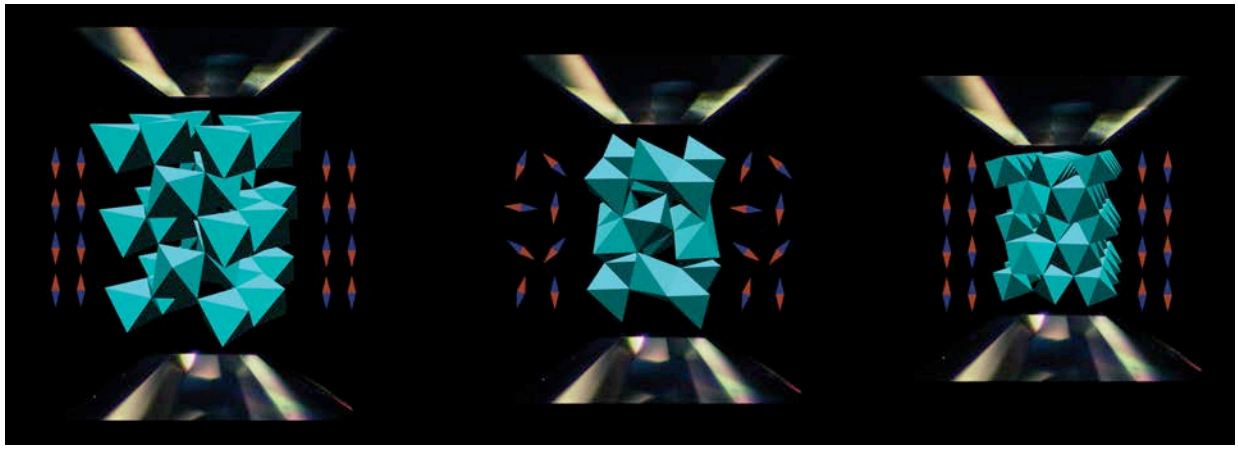

High pressure phase transitions in Fe_2O_3. (Left) corundum type (Middle) Rh_2O_3-II type (Right) post-perovskite

GSECARS of APS) combined with *ab initio* calculations in order to determine how the magnetic ordering changes in different high pressure phases of Fe_2O_3.

We found that Fe_2O_3 undergoes demagnetization at the corundum-type to Rh_2O_3-II type phase transition at 50 GPa. However, Fe_2O_3 is remagnetized at the Rh_2O_3-II-type to the post-perovskite-type transition. This suggests that pressure does not necessarily monotonically destroy magnetic ordering in the crystal lattice.

Publications

S.-H. Shim, A. Bengtson, D. Morgan, W. Sturhahn, K. Catalli, J. Zhao, M. Lerche, and V. B. Prakapenka. Electronic and magnetic structures of the postperovskite-type Fe_2O_3 and implications for planetary magnetic records and deep interiors. P. Natl. Acad. Sci., 106:5508–5512, 2009.

Far-Infrared Dielectric and Vibrational Properties of Wüstite at High Pressure

Christopher T. Seagle, Zhenxian Liu *Carnegie Institution of Washington*
Wenxuan Zhang, Dion L. Heinz *University of Chicago*

The far infrared reflectivity of $Fe_{0.91}O$ was investigated from atmospheric pressure up to 33 GPa using synchrotron techniques in conjunction with the diamond anvil cell from 100 – 700 cm^{-1} at the U2A beamline of NSLS. The frequency of the fundamental transverse optic (TO) mode was found to be nearly independent of pressure up to 4.6 GPa, followed by an increase in the TO mode frequence with pressure up to the rhombohedral phase transition at ~8 GPa. In addition, a second weak mode at 583 cm^{-1} (at 1 bar) was well resolved and found to shift to higher frequency and increase in strength with pressure. This localized mode arises from the high concentration of vacancies in the crystal structure, and the relative strength suggests pressure-induced charge localization near vacancy sites.

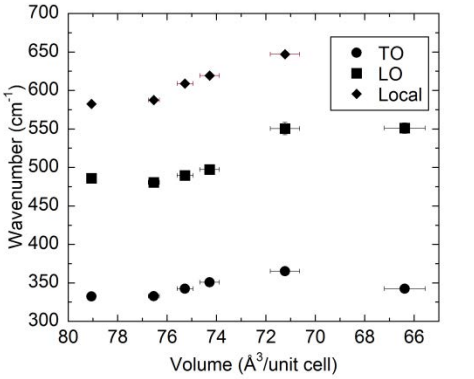

Optical and Localized mode frequencies for $Fe_{0.91}O$ as a function of volume.

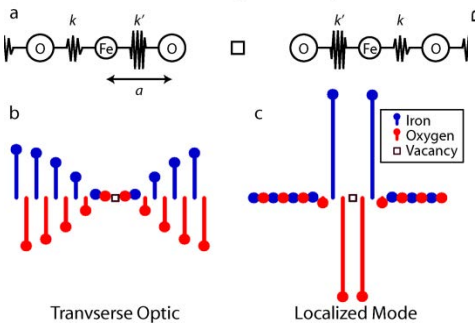

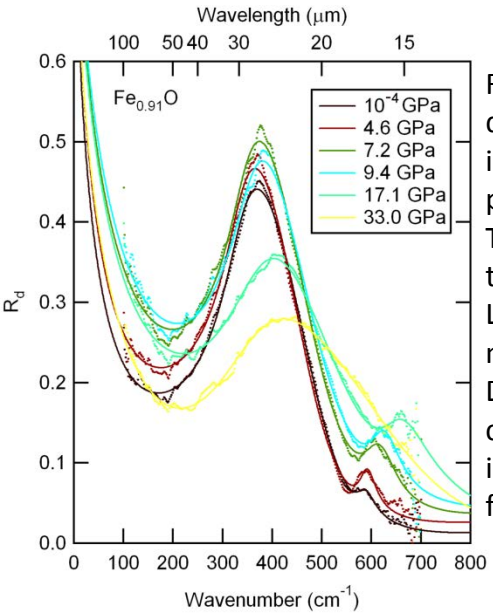

Reflectivity of the diamond-wüstite interface as various pressures (dots). The solid lines are the best fit to a Lorentz oscillator model with a Drude-like free-carrier contribution in the low frequency limit.

Origin of the localized mode at ~585 cm^{-1}. (a) Spring model for $Fe_{0.9}O$. [(b) and (c)] atomic displacements plotted in the vertical direction for the two strongest normal modes.

Reference: Seagle, C.T., W. Zhang, D.L. Heinz, and Z. Liu (2009) Far-infrared dielectric and vibrational properties of nonstoichiometric wüstite at high pressure, *Phys. Rev. B*, **79**, 014104.

This work was partially supported by DOE-NNSA(CDAC). This research was partially supported by the Consortium of Materials Properties Research in Earth Sciences (COMPRES) under National Science Foundation (NSF) Cooperative Agreement EAR 06-49658. Use of the National Synchrotron Light Source, Brookhaven National Laboratory, was supported by the U.S. Department of Energy (DOE), Office of Science, Office of Basic Energy Sciences, under contract DE-AC02-98CH10886.

Iron, Iron Alloys and Earth's Core

Elasticity of Iron in Earth's Core by Inelastic X-ray Scattering

Jung-Fu "Afu" Lin, Assistant Professor
Department of Geological Sciences, The University of Texas at Austin

Deep-Earth scientists have increasingly relied on synchrotron-based high-resolution inelastic X-ray scattering spectroscopy (HERIX) to investigate the properties of the Earth's interior which is naturally subject to high pressure-temperature conditions. In particular, laboratory-measured sound velocities of candidate iron alloys and oxides/silicates at relevant pressure-temperature conditions of the Earth's core and mantle are needed to directly decipher the behavior of seismic waves travelling through the deep Earth. Of particular importance is our recent study on the compressional wave velocity (Vp) of hcp-Fe, the most abundant constitute of the Earth's core, to over 100 GPa and high temperatures using phonon dispersion curves measured from HERIX and sample density from XRD in an externally-heated DAC at 3IDD of the APS. The velocity-density profiles of iron alloys are among the most fundamental parameters to constrain the chemical composition and seismic behavior of the Earth's core, although reliable experimental studies remain limited. Alternatively, an empirical linear approximation, called Birch's law, has been commonly used to model the composition of the Earth's core without considering extended pressure-temperature effects on the velocity behavior of iron alloys. Here we have discovered a nonlinear, temperature-dependent behavior of the compressional-wave velocity (V_P) and density (ρ) of hcp-Fe at high pressures and temperatures. These unexpected findings carry a series of critical geophysical, geochemical and geodynamic implications. Coupling the HERIX system with the laser-heated DAC would provide a true arsenal to directly measure sound velocities of candidate materials of the deep Earth at relevant pressure-temperature conditions. It should be noted that these new capabilities can be readily applied to study a plethora of outstanding questions in material science, condensed matter physics, chemistry, and energy materials.

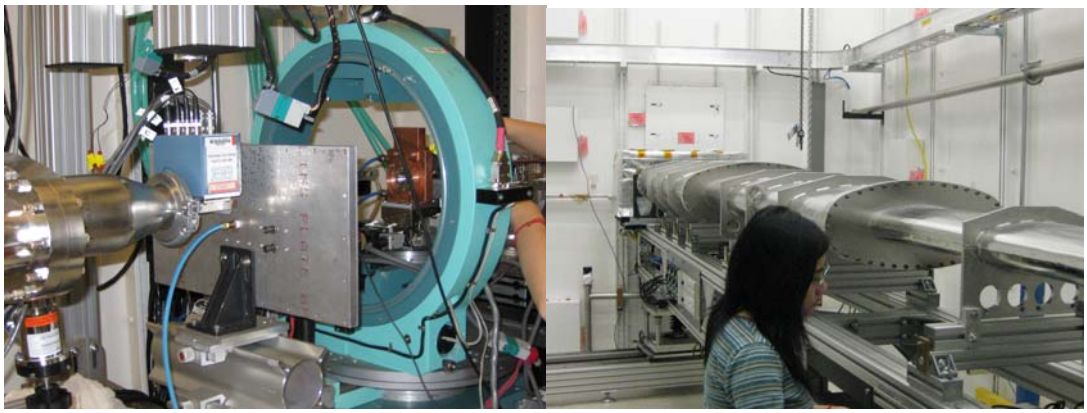

Figure 1 *(Left) HERIXS setup for EH DAC with an online image plate (held by the central Al plate holder). (Right) Four-analyzer spectrometer with a 6-meter arm.*

Selected References:

J. F. Lin, Z. Mao, H. Yavas, J. Zhao, and L. Dubrovinsky, Shear wave anisotropy of textured hcp-Fe in Earth's inner core, *Earth Planet. Sci. Lett.*, 298, 361-366, 2010.

Z. Mao, J. F. Lin, and A. Alatas, and J. Zhao, Power-law velocity-density behavior of iron in Earth's inner core, submitted, 2011.

Experimental determination of elasticity of iron at high pressure

Arianna Gleason *Geological and Environmental Sciences, Stanford University*
Wendy L. Mao *Geological and Environmental Sciences, Stanford University; Photon Science, SLAC National Accelerator Laboratory*

Information on the high P-T rheological, elastic and vibrational behavior of iron is essential for interpreting seismological and geomagnetic observations of Earth's core, but have been challenges due to the lack of in-situ experimental probes at extreme conditions. Despite all the pioneering experimental measurements and theoretical calculations made over the past decade, there is still a lack of consensus on the elasticity of hcp-iron at core conditions. Improvements in the accuracy of elasticity measurements are critical for improving constraints on Earth's core.

We demonstrated that by coupling hydrostatic axial XRD, radial XRD, nuclear-resonant inelastic x-ray scattering (NRIXS), and phonon inelastic x-ray scattering to study the elastic anisotropy of hcp-iron up to 52 GPa (W. Mao, 2008). Comparison of the results from this new method with the elasticity determined by lattice strain analysis of radial X-ray diffraction measurements showed significant differences, highlighting the importance of strength anisotropy in hcp iron. We found that our method which combines results from inelastic scattering and pressure-volume measurements gives a shape in the velocity anisotropy close to sigmoidal (with a faster *c* and slower *a* axis) and a smaller magnitude in the anisotropy compared to velocities based on the lattice strain method which gives a bell shape velocity distribution with the fast direction between the *c* and *a* axes.

We recently measured the NRIXS of ^{57}Fe loaded hydrostatically (with either He or Ne as the pressure medium) to 93 GPa (Fig. 1) and determined the Debye sound velocity (V_D) as a function of pressure. V_D is heavily dependent on the aggregate shear wave velocity (V_S) giving us a more accurate constraint of V_S of hcp-iron under hydrostatic conditions. Comparison of our results to previous data (Fig. 2) indicate that our more hydrostatically loaded samples have velocities that trend higher than non-hydrostatic experiments, providing a new baseline for comparison of iron at high temperature and with iron + impurities at core conditions.

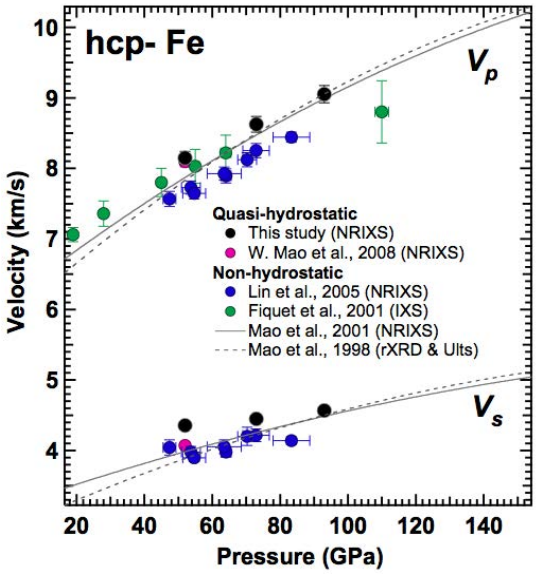

Fig. 1. Hydrostatic high pressure phonon DOS for hcp-Fe.

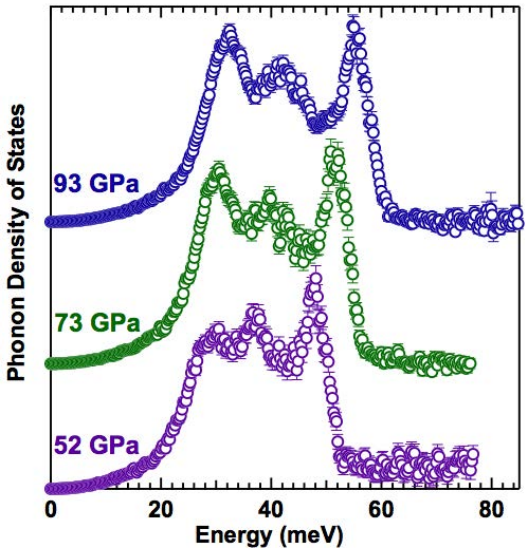

Fig. 2. Comparison of aggregate compressional and shear wave velocities determined from our NRIXS measurements.

W. L. Mao, V. V. Struzhkin, A. Q. R. Baron, S. Tsutsui, C. E. Tommaseo, H-R. Wenk, M. Hu, P. Chow, W. Sturhahn, J. Shu, R. J. Hemley, D. L. Heinz, and H-k. Mao, Experimental determination of elasticity of iron at high pressure, *J. Geophys. Res.* **113**, B09213, doi:10.1029/2007JB005229, 2008.

This research was supported by W. Mao is supported through the Geophysics program at NSF (EAR-0738873) and COMPRES, the Consortium for Materials Properties Research in Earth Sciences under NSF Cooperative Agreement EAR 10-43050.

In-situ laser heating and pressure increase with radial diffraction at ALS beamline 12.2.2 and application to iron

Lowell Miyagi, Martin Kunz, Jason Knight, James Nasiatka, Marco Voltolini, and Hans-Rudolf Wenk
Department of Earth and Planetary Science, University of California, Berkeley, California 94720, USA
Advanced Light Source, Lawrence Berkeley Laboratory, Berkeley, California 94720, USA

Radial diffraction in conjunction with the diamond anvil cell (DAC) is a useful technique to study the development of lattice strains and lattice preferred orientation (LPO), *in-situ* at pressures relevant to the deep earth. These experiments provide useful rheological information on high-pressure mineral phases that can be used to constrain deformation mechanisms in the deep earth and interpret observed seismic anisotropies. However, previous work using the DAC and radial diffraction were performed at ambient temperature. It is questionable whether room temperature studies are appropriate for extrapolation to behavior in planetary interiors where materials are deforming at both high pressure and temperature. In order to address this limitation we have developed a novel combination of remote pressure increase utilizing a gas membrane driven panoramic DAC and single sided *in-situ* laser heating for radial diffraction. The device has been used to study bcc (α), fcc (γ) and hcp (ε) iron at a range of pressures and temperatures up to 30 GPa and 1900 K . We have documented orientation relationships during phase transformations by in situ observation of textures (i.e. Burgers and Kurdjumov-Sachs). Also, in contrast to room temperature measurements on hcp iron which indicate texture is developed primarily through basal (0001)⟨2-1-10⟩ slip , it appears that at high temperature pyramidal ⟨a+c⟩ {2-1-12}⟨2-1-13⟩ slip is activated and becomes dominant (Fig. 1). This illustrates the importance of texture measurements at high temperatures where different slip system may become active. We also observe that the high temperature fcc phase develops a 110 texture typical for fcc metals deformed in compression. This device is now available to users at ALS beamline 12.2.2.

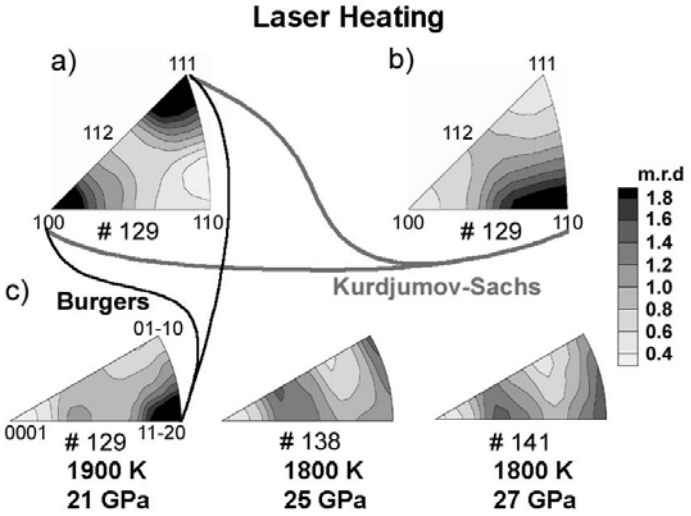

Figure 2: IPFs selected from the high temperature run for a) bcc Fe, b) fcc Fe, and c) hcp Fe. Lines connecting IPFs show the Burgers relation for the bcc-hcp transformation, and Kurdjumov-Sachs relation for the bcc-fcc transformation. With heating hcp Fe develops a maximum at 01-10 (#138) this can be attributed to recrystallization. With further deformation (#141) a girdle develops around the periphery while the girdle 30° offset from 0001 remains, indicating activation of pyramidal ⟨a+c⟩ {2-1-12}⟨2-1-13⟩ slip.

Thermal pressure of ε-Fe determined from the phonon density of states

Caitlin A. Murphy[1,*], Jennifer M. Jackson[1], Wolfgang Sturhahn[2], and Bin Chen[1]

[1] Seismological Laboratory, California Institute of Technology, Pasadena, CA 91125
[2] Argonne National Laboratory, Argonne, IL 60439. Now at Jet Propulsion Laboratory.
([*] caitlinm@caltech.edu)

The phonon density of states (DoS) of hexagonal close-packed iron (ε-Fe) was probed directly with high statistical quality between pressures of 30 GPa and 151 GPa using nuclear resonant inelastic x-ray scattering with simultaneous volume determination by x-ray diffraction at 300 K. Measurements were conducted at sector 3-ID-B of the Advanced Photon Source. Neon was used as a pressure-transmitting medium for a subset of our measurements. From each measured phonon DoS, we extracted salient thermodynamic parameters. For example, we determined the volume-dependence of ε-Fe's vibrational thermal pressure (Fig. 1), which is an important parameter in determining accurate equations of state at high-pressures and the core density deficit. In a forthcoming paper (Murphy *et al*. 2011, *under review*), we will present a unique approach to determining the melting of ε-iron at high-pressures from the measured phonon DoS.

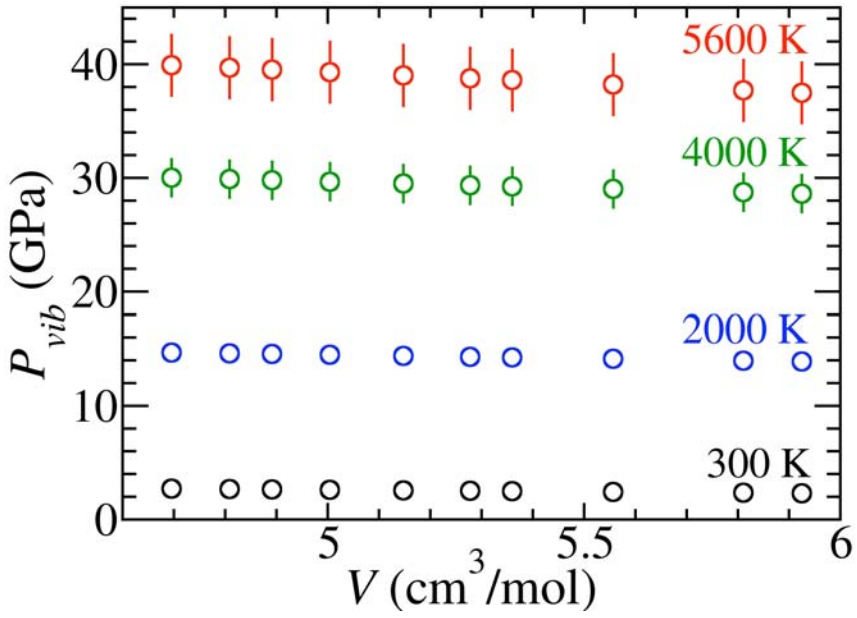

Figure 1. ε-Fe's volume- and temperature-dependent vibrational thermal pressure (P_{vib}). Values for P_{vib} (T > 300 K) account for anharmonic effects, and errors calculated from best-fit parameters are smaller than the symbol if not visible (Murphy *et al.* 2011, *under review*).

Unraveling the role of carbon in the Earth's inner core with x-rays

Lili Gao[1,2] (liligao2@aps.anl.gov); Jie Li[1,3], Associate Professor (PI) (jackieli@umich.edu)

[1]*Department of Geology, University of Illinois, Urbana, IL;* [2]*Advanced Photon Source, Argonne National Laboratory, Argonne, IL;*
[3]*Department of Geological Sciences, University of Michigan, Ann Arbor, MI*

The Earth's magnetic field originates in the liquid outer core. The driving forces for the geodynamo include thermal convection associated with secular cooling, and chemical convection due to the release of elements lighter than iron during inner core growth. The nature and abundance of light elements in the core remain poorly constrained.

To test the hypotheses of a iron-carbon inner core, we studied the densities at high pressures and sound velocities at high pressures and high temperatures. Our results suggest that the addition of carbon to iron brings a closer match of sound velocity and density to the inner core, supporting a carbon-rich inner core.

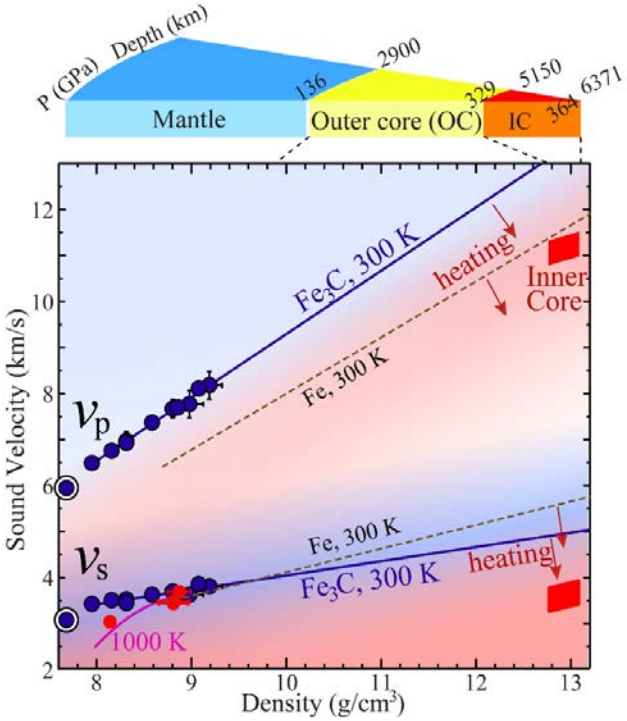

Fig 1. Compressional (v_p) and shear (v_s) velocities of Fe_3C determined with NRIXS method, compared with those of iron and the seismically observed values of the inner core.

Using nuclear resonant inelastic x-ray scattering (NRIXS) method, an established and unique way of measuring sound velocities at high pressures, we studied the compressional velocities (v_p) and shear velocities (v_s) of Fe_3C to a pressure of 50 GPa at 300 K, and to a previously uncharted high temperature range of up to 1450 K and 47 GPa (Fig. 1) [1-3]. These results reveal a deviation of the high-temperature v_s from Birch's law (linear dependence of sound velocity on density), and further suggest a non-linear temperature effect on v_s. With temperature effect considered, Fe_3C provides a closer match of both v_p and v_s to the inner core.

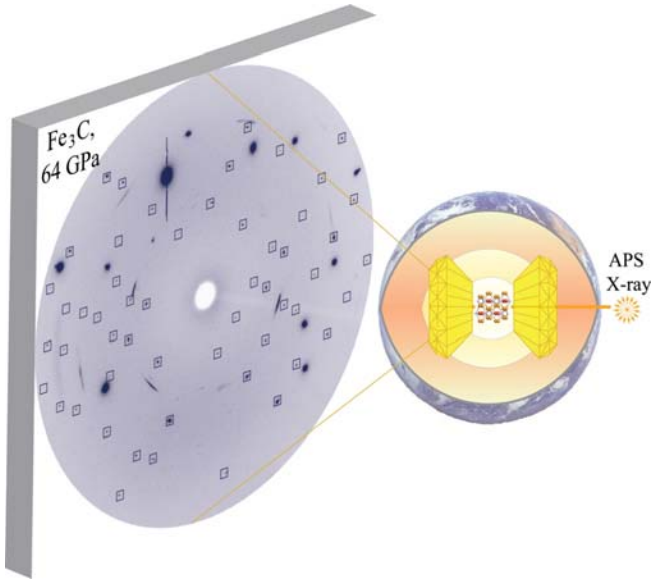

Fig 2. X-ray diffraction pattern on a single crystal of Fe_3C at 64 GPa and 300 K collected at GSECARS of the APS.

To measure the densities of Fe_3C, we collected x-ray diffraction data on quasi single crystals of Fe_3C (Fig. 2) up to 200 GPa at 300 K, well into the pressure range of the Earth's core (136 GPa - 364 GPa) [4]. Extrapolated to the pressure and temperature conditions of the inner core, our results suggest that a mixture of Fe_3C and iron may match the density of the inner core.

This work was conducted at sector 3 and GSECARS of the APS, which are partially supported by COMPRES, the Consortium for Materials Properties Research in Earth Sciences, under NSF Cooperative Agreement EAR 10-43050. We thank 11-BM-B of the APS for the help with sample characterization with high-resolution x-ray diffraction method on our synthetic Fe_3C samples. Use of the APS is supported by the U.S. Department of Energy, Office of Science, Office of Basic Energy Science, under contract No. DE-AC02-06CH11357. This work is supported by NSF grants EAR0609639/EAR1023729 and EAR0738973/EAR1025639.

References:

[1] **L. Gao**, B. Chen, J. Wang, E.E. Alp, J. Zhao, M. Lerche, W. Sturhahn, H.P. Scott., F. Huang, Y. Ding, S.V. Sinogeikin, C. Lundstrom, J.D. Bass and **J. Li**, Geophysical Research Letters, 35, L17306, (2008)
[2] **L. Gao**, B. Chen, M. Lerche, E.E. Alp, W. Sturhahn, J. Zhao, Y. Hasan and **J. Li**, Journal of Synchrotron Radiation, 16, 714-722 (2009)
[3] **L. Gao**, B. Chen, J. Zhao, E.E. Alp, W. Sturhah, and **J. Li**, 2011 (submitted)
[4] **L. Gao**, B. Chen, P. Dera, B. Lavina, V. Prakapenka, W. Sturhahn, E.E. Alp, J. Zhao and **J. Li** (in prep.)

Combined *in situ* synchrotron X-ray diffraction and ultrasonic interferometry study of ε-FeSi at high pressure

Matthew L. Whitaker, Wei Liu, Qiong Liu, Liping Wang, Baosheng Li *Mineral Physics Institute, Stony Brook University*

Ultrasonic interferometry was used in combination with synchrotron X-radiation in a multi-anvil apparatus to determine the compressional and shear wave velocities and unit-cell volumes of ε-FeSi (fersilicite; cubic B20 structure) at room temperature and pressures up to ~12 GPa. This experiment was conducted at the COMPRES-supported beamline X17B2 of the National Synchrotron Light Source at Brookhaven National Laboratory. The data collected during compression are compared with those collected during decompression after heating to release stress within the sample cell. By fitting all of the decompression unit-cell volume and sound velocity data to third-order finite-strain equations, we obtain the adiabatic zero-pressure bulk and shear moduli and their first pressure derivatives: K_{S0} = 169.3(8) GPa, G_0 = 116.3(4) GPa, K_{S0}' = 6.5(3), G_0' = 3.0(1). The bulk modulus obtained here is in good agreement with those of some previous experimental studies, but lower than those obtained by first-principles calculations. This study presents the first direct measurement of the shear properties of this phase.

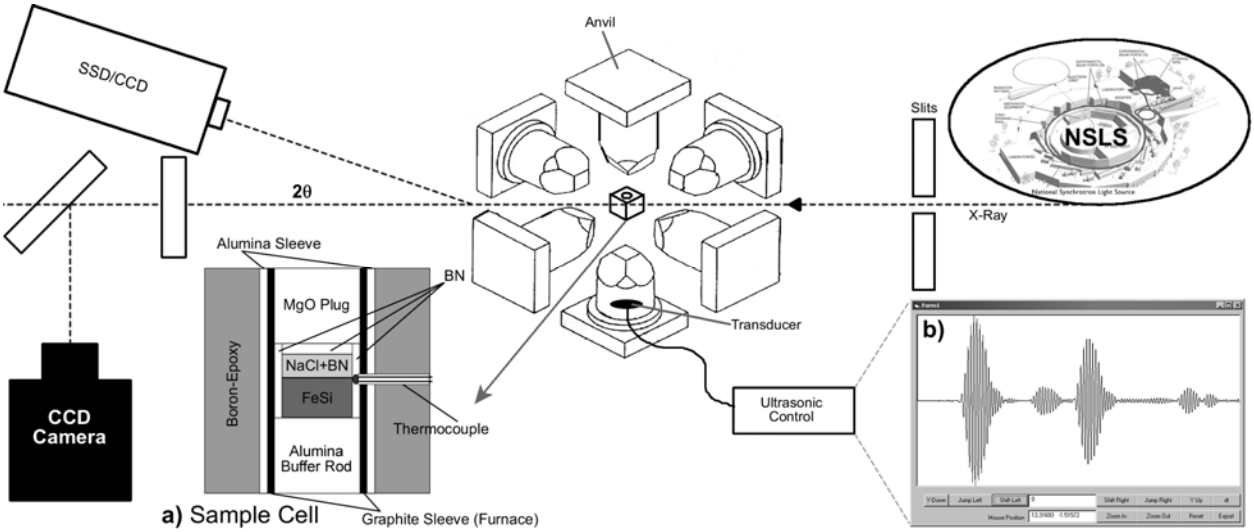

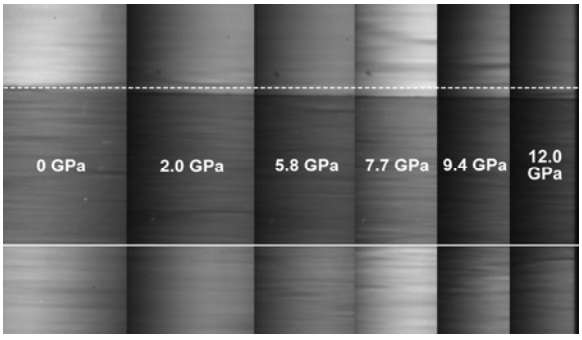

ABOVE: Outline of the experimental DDIA-type SAM85 setup at beamline X17B2 at the NSLS. a) Schematic diagram of the experimental cell assembly used in this study. b) Simultaneous ultrasonic measurement of both P and S Wave data using a dual-mode transducer in the frequency range from 20 to 70 MHz. In the ultrasonic signal shown here, the first pulse is anvil/buffer rod interface, second is buffer rod/sample interface, third is sample/salt interface.

RIGHT: X-radiographic imaging of the sample during compression. Pressure is listed for each image. Change in sample length is evident as pressure increases.

ACKNOWLEDGMENTS: This research is supported by NSF grants EAR00135550 and EAR0635860 to BL. Use of the National Synchrotron Light Source, Brookhaven National Laboratory, was supported by the U.S. Department of Energy, Office of Science, Office of Basic Energy Sciences, under Contract No. DE-AC02-98CH10886. Use of the X17B2 beamline was supported by COMPRES, the Consortium for Materials Properties Research in Earth Sciences under NSF Cooperative Agreement EAR 01-35554 and by the Mineral Physics Institute, Stony Brook University. MPI Publication No. 470.

Reference: M.L. Whitaker, W. Liu, Q. Liu, L. Wang, and B. Li (2008) High Pressure Research 28(3) 385-395

Thermoelasticity of ε-FeSi to 8 GPa and 1273 K

Matthew L. Whitaker, Wei Liu, Qiong Liu, Liping Wang, Baosheng Li *Mineral Physics Institute, Stony Brook University*

The elastic properties of ε-FeSi (fersilicite; cubic B20 structure) were investigated at high temperature and pressure using a combination of ultrasonic interferometry and synchrotron radiation in a multi-anvil apparatus up to 8 GPa and 1273 K. This experiment was conducted at the COMPRES-supported beamline X17B2 of the National Synchrotron Light Source at Brookhaven National Laboratory. The unit-cell volumes and sound velocity data were fit to third-order finite-strain equations with adiabatic temperature conversions to maintain a thermodynamically internally consistent data set. The adiabatic zero-pressure bulk and shear moduli and their first pressure and temperature derivatives were obtained from this fitting: K_{S0} = 168.9 (7) GPa, G_0 = 116.5 (3) GPa, K_{S0}' = 6.6 (2), G_0' = 2.9 (1), $(\partial K_{S0}/\partial T)_P$ = ‑0.023 (1) GPa K^{-1}, $(\partial G_0/\partial T)_P$ = ‑0.030 (1) GPa K^{-1}. This study presents the first complete thermodynamically consistent set of elastic moduli and their temperature and pressure derivatives for this phase.

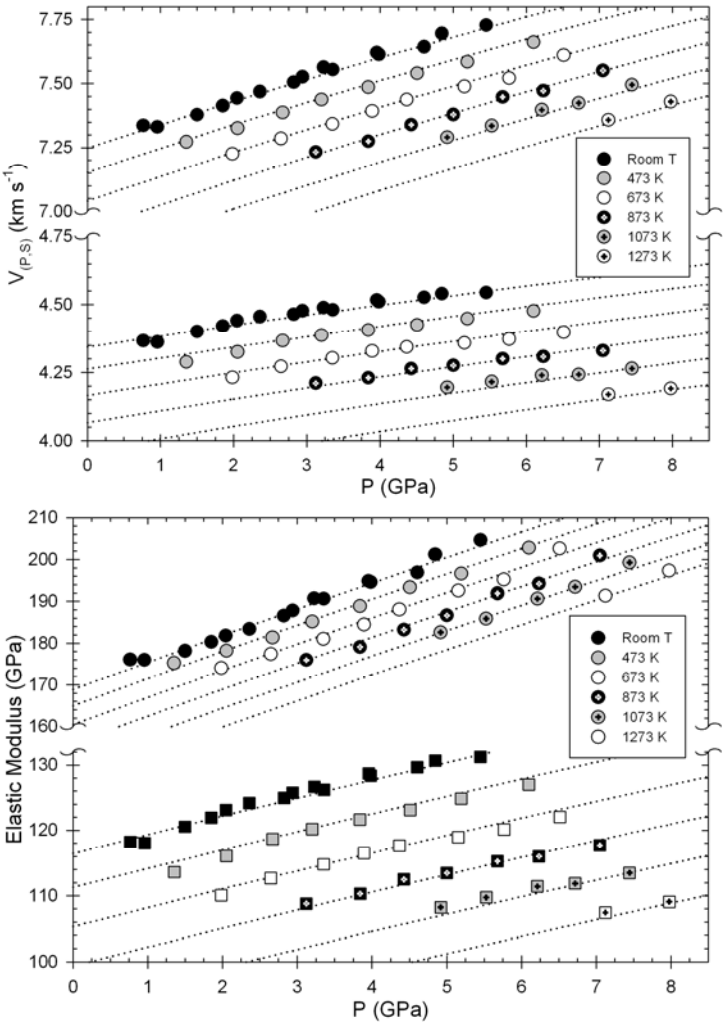

TOP LEFT: Variation of elastic compressional (V_P) and shear (V_S) wave velocities for ε-FeSi as a function of pressure and temperature from the ultrasonic measurements and X-ray data to 8 GPa and 1273 K. Data above the break are P-wave velocities, and data below the break are S-wave velocities. Data symbols are coded by temperature as shown in the legend; velocities obtained from the finite-strain fitting of the thermoelastic data are shown as dashed lines.

BOTTOM LEFT: Variation of experimental measurements of elastic bulk (K_S) and shear (G) moduli as a function of pressure. Circles are adiabatic bulk modulus measurements, squares are shear modulus values; symbols are coded by temperature, using the same coding for both elastic moduli. The third-order finite-strain fits of these experimental data are shown as dashed lines.

ACKNOWLEDGMENTS: This research is supported by NSF grants EAR00135550 and EAR0635860 to BL. Use of the National Synchrotron Light Source, Brookhaven National Laboratory, was supported by the U.S. Department of Energy, Office of Science, Office of Basic Energy Sciences, under Contract No. DE-AC02-98CH10886. Use of the X17B2 beamline was supported by COMPRES, the Consortium for Materials Properties Research in Earth Sciences under NSF Cooperative Agreement EAR 01-35554 and by the Mineral Physics Institute, Stony Brook University. MPI Publication No. 475.

Reference: M.L. Whitaker, W. Liu, Q. Liu, L. Wang, and B. Li (2009) American Mineralogist 94(7) 1039-1044

Acoustic Velocities and Elastic Properties of Pyrite (FeS_2) to 9.6 GPa

Matthew L. Whitaker *Mineral Physics Institute, Stony Brook University; Geodynamics Research Center, Ehime University, Matsuyama, Japan*
Wei Liu, Liping Wang, Baosheng Li *Mineral Physics Institute, Stony Brook University*

Ultrasonic interferometry was utilized in conjunction with synchrotron-based X-ray diffraction and X-radiographic imaging in a multi-anvil apparatus to determine the compressional and shear wave velocities and unit-cell volumes of pyrite (FeS_2) at room temperature and pressures up to 9.6 GPa. This experiment was conducted at the COMPRES-supported beamline X17B2 of the National Synchrotron Light Source at Brookhaven National Laboratory. Fitting all of the experimental volume and velocity data to third-order finite-strain equations yielded the adiabatic zero-pressure bulk and shear moduli and their first pressure derivatives: $K_{S0} = 138.9(7)$ GPa, $G_0 = 112.3(3)$ GPa, $(\partial K_{S0}/\partial P)_T = K_{S0}' = 6.0(1)$, $(\partial G_0/\partial P)_T = G_0' = 3.0(<1)$, where the numbers in parentheses represent the 1σ uncertainty in the last significant digit. These results are in good agreement with several previous static compression studies on this material but differ quite strongly from the results obtained via first principles calculations. This study presents the first direct measurement of the bulk shear properties of this material.

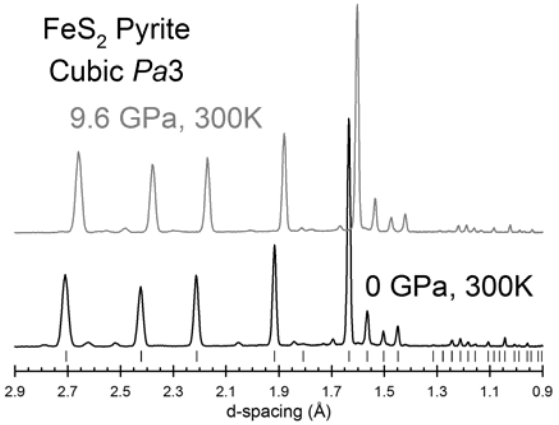

ABOVE: X-ray diffraction patterns of FeS_2 sample at 0 and 9.6 GPa. Vertical lines below diffraction pattern indicate peak positions in the standard powder diffraction file that were used to index the pattern. Unmarked peaks are the result of parasitic scattering from the surrounding material in the cell assembly.

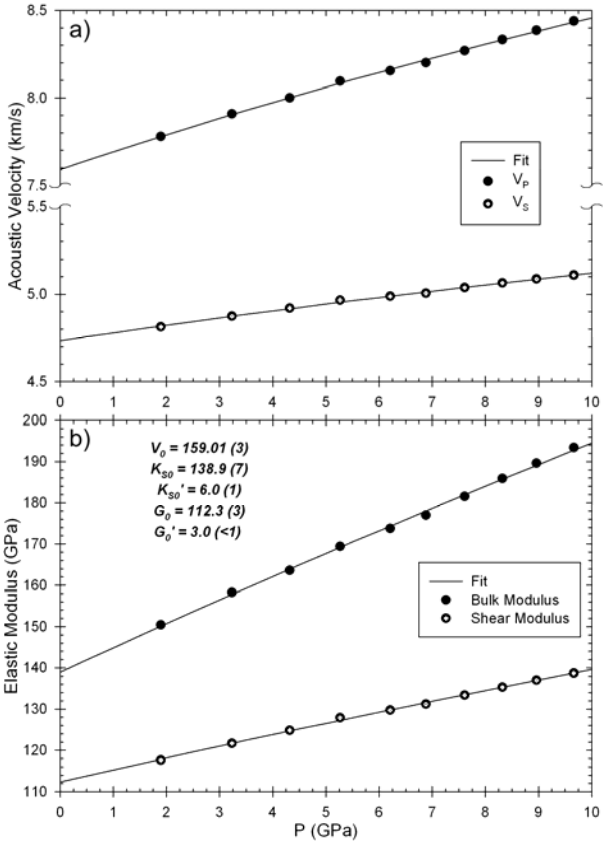

RIGHT: (a) Acoustic velocities in FeS_2 versus pressure. Black circles represent P-wave velocities; circles with crosshairs represent S-wave data. (b) Elastic modulus of FeS_2 versus pressure. Black circles are adiabatic bulk modulus; circles with crosshairs represent shear modulus. Fitting results are shown on (b). The continuous curves are calculated from these fitted parameters.

ACKNOWLEDGMENTS: This research is supported by NSF grants EAR00135550 and EAR0635860 to BL. Use of the National Synchrotron Light Source, Brookhaven National Laboratory, was supported by the U.S. Department of Energy, Office of Science, Office of Basic Energy Sciences, under Contract No. DE-AC02-98CH10886. Use of the X17B2 beamline was supported by COMPRES, the Consortium for Materials Properties Research in Earth Sciences under NSF Cooperative Agreement EAR 01-35554 and by the Mineral Physics Institute, Stony Brook University. MPI Publication No. 480.

Reference: M.L. Whitaker, W. Liu, L. Wang, and B. Li (2010) Journal of Earth Science 21(5) 792-800

Bridging the Gap Between Multi-Anvil and Diamond Anvil Experiments

Matthew L. Whitaker & Baosheng Li *Mineral Physics Institute, Stony Brook University*

The literature on several iron/light-element alloy (ILEA) compounds at high pressures and temperatures show a marked discrepancy between the results obtained via experiments in Diamond Anvil Cells (DAC) versus those obtained in Multi-Anvil Cells (MAC). Four such materials (Fe_3P, FeS_2, FeS and ε-FeSi) were studied using a combination of synchrotron-based static compression experiments in the DAC and combined ultrasonic interferometry and synchrotron X-radiation in the MAC. The MAC experiments were conducted at beamline X17B2 of the National Synchrotron Light Source at Brookhaven National Laboratory, and the DAC experiments were conducted at beamline X17C of the same facility; both are COMPRES-supported beamlines. The results obtained from these two different types of experiments were remarkably similar, showing much better agreement than has ever before been seen between MAC and DAC experiments on these types of materials. The results of these experiments have provided an important benchmark for future studies on these materials and have resolved some of the controversy regarding the physical properties of these phases under extreme conditions.

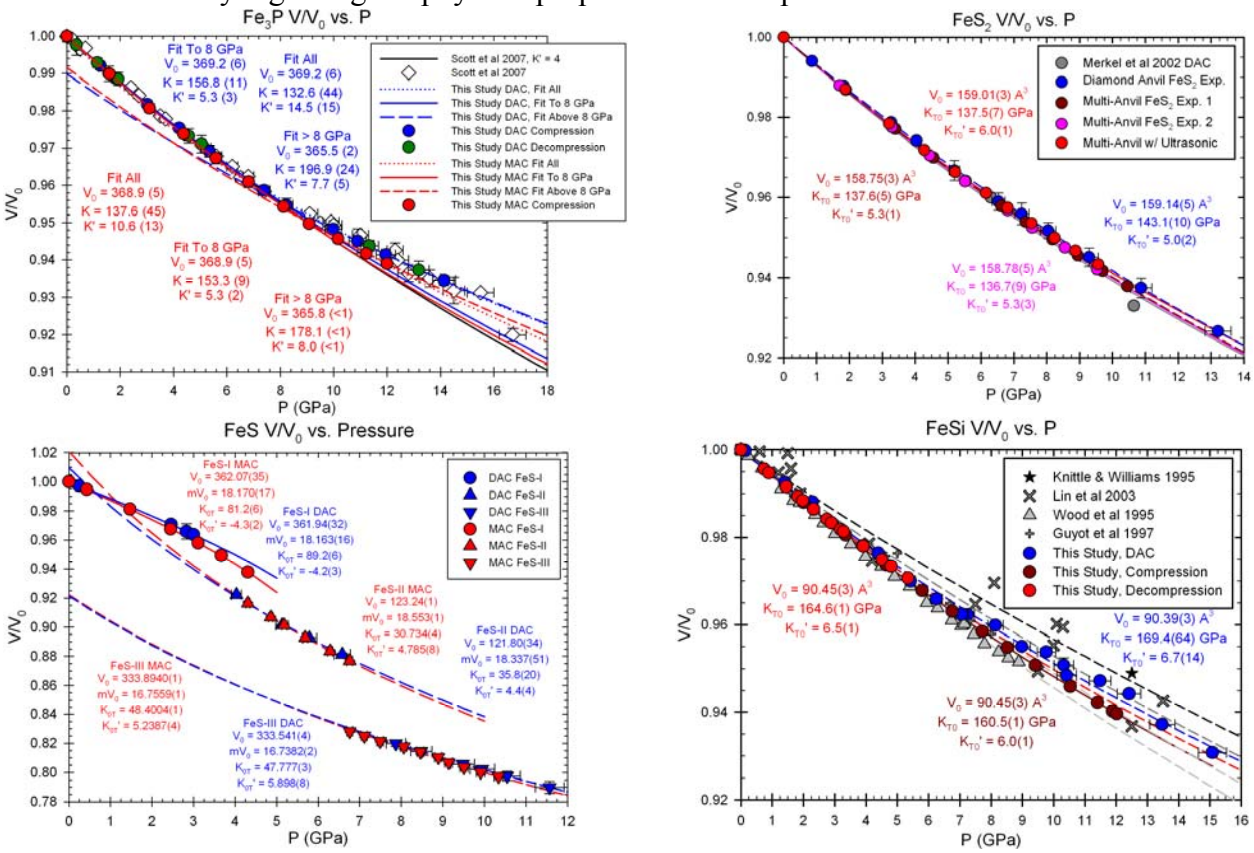

FIGURES: Volume change vs. pressure plots showing results of both DAC (blue) and MAC (red) experiments on Fe_3P (top left), FeS_2 (top right), FeS (bottom left) and ε-FeSi (bottom right). Parameters obtained from third-order Birch-Murnaghan fits are shown on diagrams for each dataset.

ACKNOWLEDGMENTS: This research is supported by NSF grants EAR00135550 and EAR0635860 to BL. Use of the National Synchrotron Light Source, Brookhaven National Laboratory, was supported by the U.S. Department of Energy, Office of Science, Office of Basic Energy Sciences, under Contract No. DE-AC02-98CH10886. Use of X17B2 & X17C beamlines supported by COMPRES, the Consortium for Materials Properties Research in Earth Sciences under NSF Cooperative Agreement EAR 01-35554 and by the Mineral Physics Institute, Stony Brook Univ.

Reference: M.L. Whitaker (2009) Ph.D. Dissertation. Dept. of Geosciences, p. xviii + 139. Stony Brook University

New Insights into the Composition of the Earth's Inner Core

Matthew L. Whitaker & Baosheng Li *Mineral Physics Institute, Stony Brook University*

Results of ultrasonic experiments on iron/light-element (ILEA) alloys at high pressure and temperature conducted at COMPRES-supported beamline X17B2 were extrapolated to pressures and temperatures relevant to the Earth's inner core, and a compositional-density-velocity model was constructed for the solid portion of the core. Previous models of core composition have been conducted under the assumption that Birch's Law, which states that acoustic velocity is solely a function of density, is valid for Fe and ILEA phases, and have thus far been unable to account for all aspects of the PREM model. The present ultrasonic data suggests that Birch's Law does not apply to ILEA materials. By treating the existing data on pure Fe differently than previous studies and accounting for the fact that iron also does not seem to follow Birch's Law, a model accounting for all aspects of PREM in the inner core, including the shear velocities, has been generated. This model, designed to account for experimentally observed deviations from Birch's Law, yields an inner core model that satisfies geochemical constraints on the composition of the core as well as the density deficits observed in seismic profiles of both the inner and outer cores.

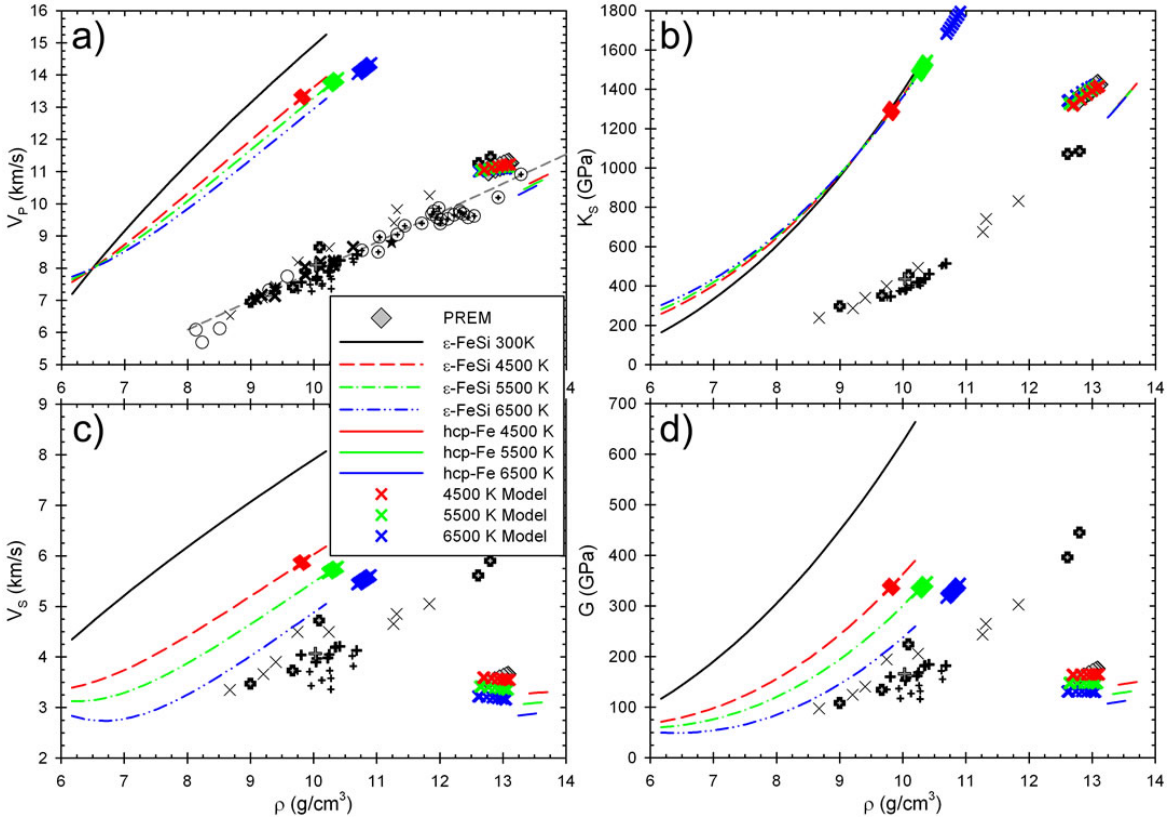

FIGURE: a) P-wave velocity, b) Adiabatic bulk modulus, c) S-wave velocity, and d) Shear modulus as functions of density. 300 K extrapolation of ε-FeSi data6, along with calculated "Birch's Law" deviations at 4500 K (all red data), 5500 K (all green data), and 6500 K (all blue data). These deviations were also calculated for Fe using the previous data. Model results are shown on the diagram as x's. Symbols in background are results of previous studies.

ACKNOWLEDGMENTS: This research is supported by NSF grants EAR00135550 and EAR0635860 to BL. Use of the National Synchrotron Light Source, Brookhaven National Laboratory, was supported by the U.S. Department of Energy, Office of Science, Office of Basic Energy Sciences, under Contract No. DE-AC02-98CH10886. Use of the X17B2 beamline was supported by COMPRES, the Consortium for Materials Properties Research in Earth Sciences under NSF Cooperative Agreement EAR 01-35554 and by the Mineral Physics Institute, Stony Brook Univ.

Reference: M.L. Whitaker (2009) Ph.D. Dissertation. Dept. of Geosciences, p. xviii + 139. Stony Brook University

Infrared Reflectivity of Iron at High Pressure

Christopher T. Seagle, Russell J. Hemley, Zhenxian Liu *Carnegie Institution of Washington*
Dion L. Heinz *University of Chicago*

The infrared reflectance of iron was studied using high-pressure synchrotron radiation methods up to 50 GPa at room temperature in a diamond anvil cell from 1000 – 8000 cm^{-1} (1.25 – 10 μm) at the U2A beamline of NSLS. The magnitude of the reflectivity show a weak pressure dependence up to the transition from the body centered cubic (bcc) to hexagonal close packed (hcp) phase transition, where a discontinuous change in optical properties was observed. Reflectance spectra were corrected for diamond absorption and treated with a Kramers-Kronig analysis to extract the optical constants. The emissivity of iron, an important parameter for temperature measurement in the laser heated diamond anvil cell using spectroradiometry, was found to be independent of wavelength for hcp iron in the infrared but strongly wavelength dependent for bcc iron below ~13 GPa.

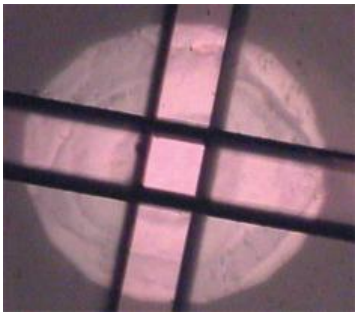

Optical photograph of an iron foil sample with an IR window. The window limits propagation of IR light to the central ~50 × 50 μm (central square). The diameter of the diamond culet is 300 μm. Near the culet edge, the outline of the iron foil is visible.

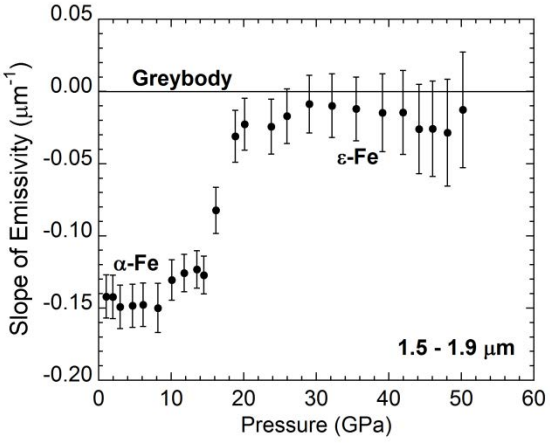

Slope of the emissivity of iron in the 1.5 – 1.9 μm range as a function of pressure. A slope of zero corresponds to an ideal greybody.

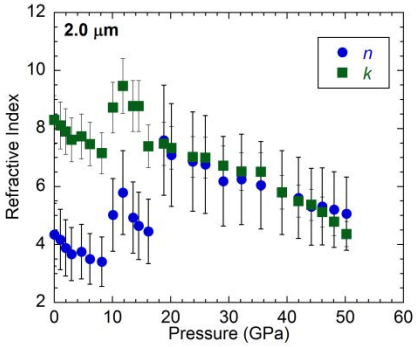

Real (*n*) and imaginary (*k*) parts of the refractive index of iron as a function of pressure at a wavelength of 2.0 μm.

Reference: Seagle, C.T., D.L. Heinz, Z. Liu, and R.J. Hemley (2009) Synchrotron infrared reflectivity measurements of iron at high pressures, *Applied Optics*, **48**, 545-552.

This work was supported by Department of Energy – National Nuclear Security Administration (Carnegie – Department of Energy Alliance Center) (CDAC). This research was partially supported by the Consortium of Materials Properties Research in Earth Sciences (COMPRES) under National Science Foundation (NSF) Cooperative Agreement EAR 06-49658. Use of the National Synchrotron Light Source, Brookhaven National Laboratory, was supported by the U.S. Department of Energy (DOE), Office of Sciences, under contract DE-AC02-98CH100886.

High Spatial Resolution X-ray absorption Imaging on ALS 12.2.2

D Walker [Lamont-Doherty Observatory, Columbia U.], MJ Walter & O Lord [Bristol U], SM Clark [ALS, Lawrence Berkeley Lab]

ALS beamline 12.2.2 has been enhanced with the capacity to make 1-2 micron spatial resolution X-ray absorption images. Thin phosphor imaging screens and low-divergence X-ray illumination are key attributes of the system conducive to high resolution images. Our objective has been to use the imaging system to observe diamond anvil cell (DAC) experiments in progress. Laser heating to first melting of the interface between spatially-resolved crystalline starting materials produces liquids saturated in both phases. The spatial distribution of reactants and product liquids yield the sign of the melting reaction. In binary systems like Fe-FeS, Fe-FeC or Fe-FeO, the image density can be used to determine liquid chemistry. This work recovers the known answers in Fe-FeS, establishes the C solubility in Fe-carbide melts to ~1/2 megabar, and shows that there is negligible solubility of Oxygen in eutectic Fe-FeO to ~ 2/3 megabar. The Earth's outer core in therefore unlikely to have much oxygen in solution.

References:

Core-mantle chemical issues. (2005) Walker D *Canadian Mineralogist*, (Fleet volume), 43(5), 1553-1564.

X-ray absorption contrast images of binary chemical reactions. (2009) D Walker, OT Lord, MJ Walter, and SM Clark. *Chemical Geology*, **269**, 211-220. doi:10.1016/j.chemgeo.2008.12.025

Melting in the Fe-C system to 70 GPa (2009) OT Lord, MJ Walter, R Dasgupta, D Walker, and SM Clark. *EPSL*, 284, 157-167, doi:10.1016/j.epsl.2009.04.017

Imaging experiments were conducted on ALS beamline 12.2.2. We are very grateful for the development work to make possible the imaging system on 12.2.2 by R. Celestre, A. McDowell, E. Doming, M. Kunz, Jason Knight, and W.A Caldwell. This work was supported by the COMPRES initiative, by the National Science Foundation under grant EAR02-07546 to DW, and by the Advanced Light Source, which is supported by the Director, Office of Science, Office of Basic Energy Sciences, Materials Sciences Division, of the U.S. Department of Energy under Contract No. DE-AC03-76SF00098 at Lawrence Berkeley National Laboratory.

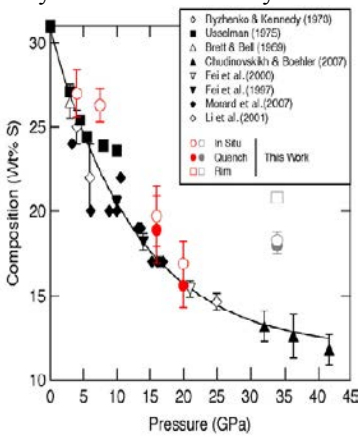

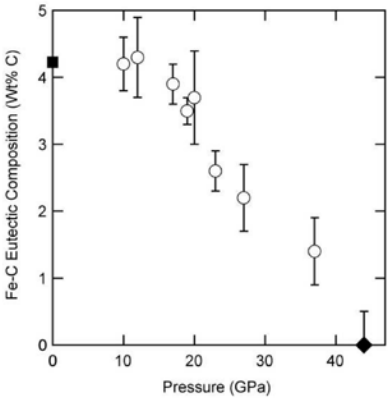

High-pressure melting behavior in the Fe-S system using synchrotron X-ray radiography

Bin Chen[1], Lili Gao[1], Kurt Leinenweber[2], Yanbin Wang[3], Takeshi sanehira[3], Jie Li[1]

1. Department of Geology, University of Illinois, Urbana, IL
2. Department of Chemistry, Arizona State University, Tempe, AZ
3. Center for Advanced Radiation Sources, The University of Chicago, Chicago, IL

We studied the high-pressure melting behavior of Fe-S mixtures containing 9wt% sulfur using the synchrotron X-ray radiographic method in a large volume press. By opening two graphite windows along the X-ray path and using boron nitride capsules, we were able to observe segregation of sulfur-rich liquid and iron-rich solid upon initial melting and determine the eutectic temperature of the Fe-S system at pressures between 13 and 16 GPa. Our results are in excellent agreement with the existing data from quench experiments, and are further supported by in situ X-ray diffraction measurements. The liquidus temperatures of this composition, determined on the basis of the disappearance of the solid phase on the radiographs, are also consistent with literature values. By observing radiographic changes with time, we monitored the approach to equilibrium and obtained preliminary data on the kinetics of the melting process.

Reference: Chen, B., Gao, L., Leinenweber, K., Wang, Y., Sanehira, T., Li, J. (2008) In situ investigation of high-pressure melting behavior in the Fe-S system using synchrotron X-ray radiography, *High Press. Res.* **28**(3): 315-326.

The radiography experiments were conducted at Sector 13-ID-D of APS, Argonne National Laboratory. The multi-anvil cell assemblies used in this study were from the Multi-anvil Cell Assembly Development Project, which were supported by COMPRES.

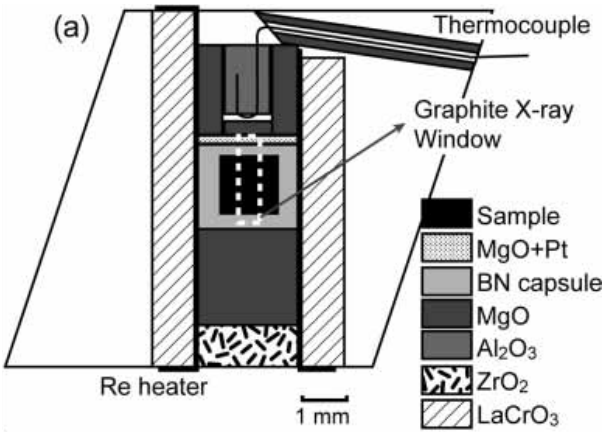

(Left) The 10/5 multi-anvil assembly for X-ray radiography experiments with graphite X-ray windows in Re heater.

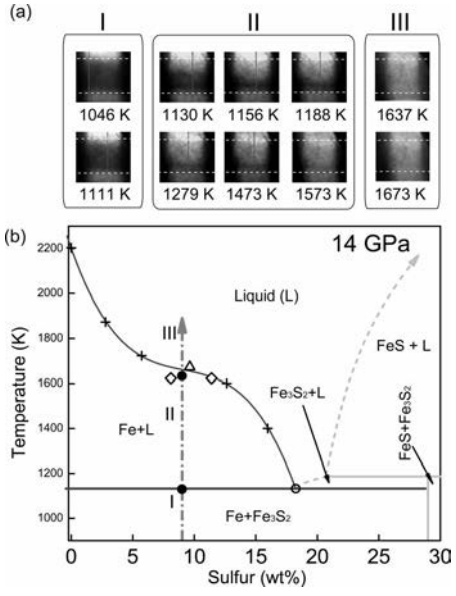

(Right) X-ray radiographs and the melting behavior of the Fe-S system at 14 GPa.

Rapid Core Formation through Diapirism from High-Pressure X-ray Radiography: J. Li[1], B. Chen[2], Kurt Leinenweber[3] and Yanbin Wang[4], [1]Department of Geological Sciences, University of Michigan, 1100 N. University Ave, Ann Arbor MI 48109, USA. jackieli@umich.edu, [2]Division of Geological and Planetary Sciences, California Institute of Technology, [3]Department of Chemistry, Arizona State University, [4]Center for Advanced Radiation Sources, The University of Chicago

Introduction: Geochemical observations based on Hf/W isotopic measurements suggest that the Earth's core formed in less than 30 Ma after the birth of the solar system [1]. This rapid core-mantle differentiation requires an efficient mechanism.

In this study we investigate the process of diapiric core segregation using high-pressure X-ray radiography and X-ray computed microtomography (CMT) techniques. Experiments were carried out at the Sector 13 (GSECARS) of the Advanced Photon Source, Argonne National Laboratory, using the 1000-ton Large Volume Press (LVP) combined with the 14/8 and 10/5 equatorial cell assemblies developed by COMPRES (cf. Fig. 1). This system allows the in-situ pressure determination from diffraction and observation of melting textures in real time from x-ray radiography.

The sample consisted of a layer of San Carlos olivine (Fo90) containing a Fe-S "diapir" and sandwiched between two layers of Fe-S powder (Fig. 2). Radiographs were collected at 5 s time intervals during melting at high pressure and temperature, and were performed until the upper Fe-S layer sank through the olivine layer and merged completely with the thin Fe-S layer below. Microtomography and post-run analysis on the final configuration confirms the phase separation and provides 3-dimensional details of the final textures.

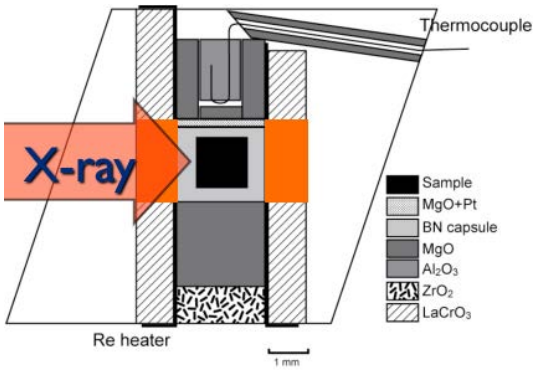

Figure 1 Multi-anvil 10/5 cell assembly for in situ X-ray radiography experiments.

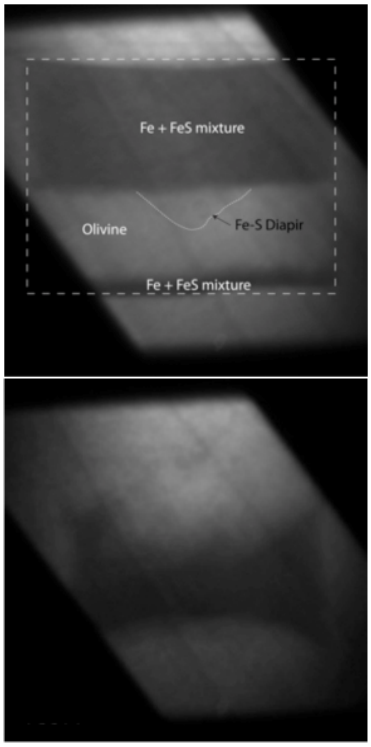

Figure 2 Radiographs of Run T1031 at 10 GPa and 1900 K. Upper: Before melting of Fe-S alloy; Lower: 40 min after melting. Dashed lines enclose an area of 1.2 mm x 1.0 mm.

We observed that at 10 and 14 GPa sub-millimeter sized Fe-S diapir sank through underlying solid olivine/wadsleyite layer in less than one hour, equivalent to a rate of thousands of km per million years. Diapirism appears to be an efficient mechanism for core segregate through partially molten or solid mantle. By applying the general scaling laws for diapir sinking velocities $V_0 = 1/3 \cdot \Delta\rho \cdot g \cdot r^2/\eta$, new constraints can be placed on the timing of the core formation [2].

References: [1] Yin et al. (2002) *Nature* 418, 949-952; Kleine et al. (2002) *Nature* 418, 952-955. [2] Samuel, H. and Tackley P. J. (2008) G^3, 9(6), Q06011; Golabek G. J. et al. (2008) *Earth. Planet. Sci. Lett.* 271, 24-33; Golabek et al. (2009) G^3, 10(11), Q11007.

Acknowledgements: We thank L. Gao, T. Yu, M. Rivers, X. Chen, J. Liu, and Z. Li for their assistance with the experiments and data processing. This work is supported by NASA - NNX09AB946, NNX10AG97G and COMPRES. Chen acknowledges support by the Caltech GPS Texaco Postdoctoral Fellowship.

New Techniques Enabled by COMPRES

Precise Stress Measurements with White Synchrotron X-rays

Donald J. Weidner[1], Michael T. Vaughan[1], Liping Wang[1], Hongbo Long[1], Li Li[1], Nathaniel A. Dixon[2], and William B. Durham[2]
[1] Mineral Physics Institute, Stony Brook University, Stony Brook, NY 11794
[2] Dept. of Earth, Atmospheric, and Planetary Sciences, Massachusetts Institute of Technology, 77 Massachusetts Ave., Cambridge, MA 02139

In situ measurement of stress in polycrystalline samples forms the basis for studies of the mechanical properties of materials with very broad earth science and materials science applications. Synchrotron x rays have been used to define the local elastic strain in these samples, which in turn define stress. We have developed a new, energy dispersive detection system for white radiation, which has been installed at the National Synchrotron Light Source. The new system provides differential strain measurements with a precision of 3×10^{-5} for volumes that are 50×50×500 microns. This gives a stress precision of about 10 MPa for silicate minerals. This system enables accurate steady-state, high pressure and high temperature rheological studies of Earth minerals at mantle conditions.

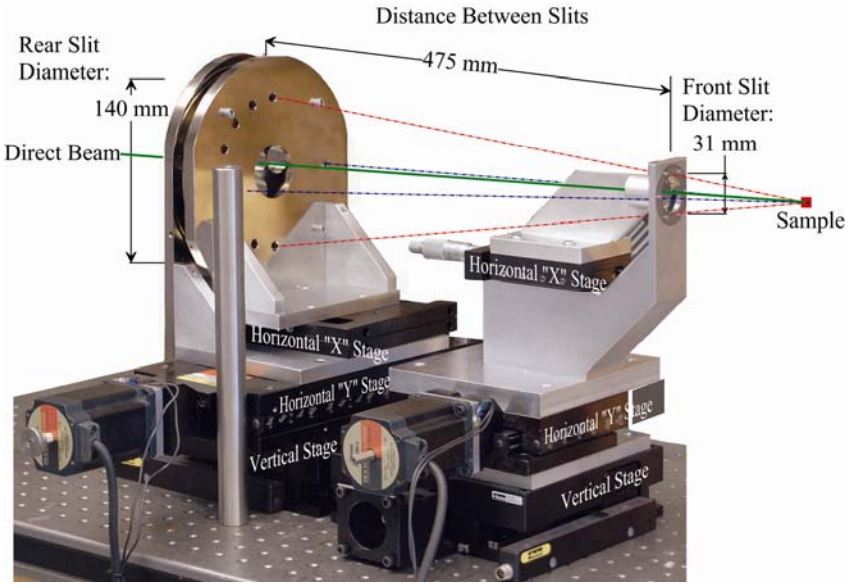

Conical slit system. Dash-Dot lines represent the diffracted x-rays (red, vertical, blue, horizontal), pointing at the sample. Remotely controlled stages move each slit normal to the direct X-ray beam (green). Slit opening controlled by motion of inner and outer slit components relative to each other.

Weidner, D. J., M. T. Vaughan, L. Wang, H. Long, L. Li, N. A. Dixon, and W. B. Durham (2010), Precise stress measurements with white synchrotron x rays, Rev. Sci. Instrum., 81(1), 013903

Experiments were conducted at the X17C beamline of NSLS which is supported by COMPRES, the Consortium for Material Property Research in the Earth Sciences under NSF Cooperative Agreement EAR0649658.

Li, L., and D. J. Weidner (2010), Note: Synchronized stress-strain measurements in dynamic loading at high pressure using D-DIA, *Rev. Sci. Instrum.*, *81*(9), 096102.

The time evolution of a system in a sinusoidal stress field potentially yields a rich array of information ranging from kinetics, anelasticity, and lattice preferred orientation induced by grain rotation. X-ray diffraction data are useful for extracting this information at high pressure and temperature. In high pressure dynamic loading experiments, stresses are often inferred from the strain of a stress-proxy such as alumina. While alumina was considered as a good choice for its relative low loss, its inherent loss still limits the stress estimation. Moreover, the stress field in the sample may differ from that in the proxy due to irregularities associated with the interfaces between the sample and the proxy or interference from the pressure medium. In a typical experiment, a sinusoidal stress is applied to a stack of alumina and sample. The strain of the alumina and sample are measured with the resulting amplitude ratio indicating the ratio of the elastic moduli and phase lag indicating the attenuation.

A new data collection protocol for forced oscillation experiments using a multi-anvil high pressure device is reported. We derive stress of the sample at high pressure and temperature from synchrotron X-ray diffraction which is synchronized with sample strain measurements from X-ray radiographs. This method yields stress directly from the sample rather than a stress proxy. Furthermore, the diffraction pattern yields useful information concerning time evolution of structurally related phenomena. We illustrate some of these possibilities with high pressure experimental data in this paper.

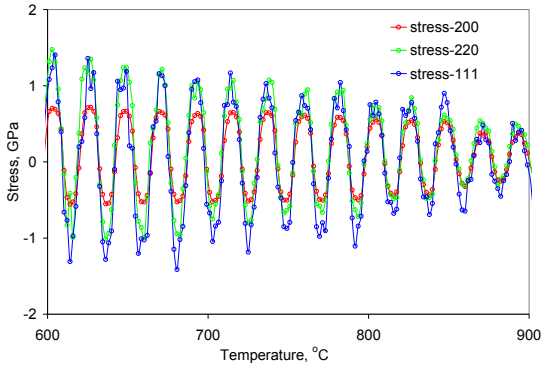

Stress as a function of temperature determined for MgO at 2.5 GPa. Three diffraction peaks (200), (220) and (111) are shown. Temperature was ramped down as the DDIA rams were driven by a sinusoidal signal. Zero stress corresponds to hydrostatic pressure and positive stress is extensional. The period of the sine wave is 1440 seconds.

Li, L., and D. J. Weidner (2007), Energy dissipation of materials at high pressure and high temperature, *Rev. Sci. Instrum.*, *78*(5), 053902.

The dynamic response of materials to an applied stress, especially a cyclic loading force, bears fundamental information about their physical properties. These mineral properties at mantle pressure and temperature control the dynamics of the Earth. Previous studies have developed various methods for studying the dynamical response of the materials at relatively low pressure (less than 300 MPa). The main challenge in measuring anelastic properties at high pressure (>300MPa) is the need of a technique for measuring stress and strain with sufficient precision, and with sufficiently short measurement time, yet with no mechanical loss in the measurement system.

We report an experimental method to study the anelastic properties of materials at high pressure and high temperature. The multi-anvil high pressure deformation device, used to apply a cyclic loading force onto the sample, can reach 15 GPa and 2000K. A synchrotron X-ray radiation source provides time resolved images of the sample and reference material. The images yield stress and strain as a function of time, stresses are derived from the reference material, strains from the sample. This method has been tested by applying a sinusoidal stress at mHz-Hz frequency on a San Carlos olivine specimen at 5 GPa and up to 2000K. Strain as small as 10^{-5} can be resolved. We have obtained experimental results which exhibit resolvable attenuation factor (Q^{-1}) and shear modulus (M) at deep Earth conditions. These results are in quantitative agreement with previously reported lower pressure data and suggest that temperature and grain size have dominating effect on these properties.

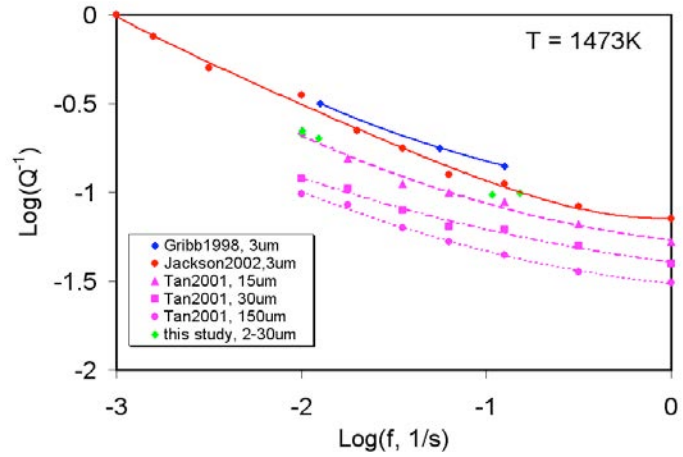

Comparison of Q^{-1} of olivine at various grain sizes. This study is measured at 5GPa. Other studies are at pressures lower than 300 MPa.

Li, L., L. Wang, and M. Vaughan (2009), An exploratory study of the viscoelasticity of phase transforming material, *Physics of the Earth and Planetary Interiors*, *174*(1-4), 174-180.

Time dependent volume changes accompanying pressure variations can give rise to bulk modulus attenuation and dispersion. Phase transformations in a two phase region are candidates for such phenomena. Here we report laboratory data that are consistent with bulk modulus softening as pressure is cycled in a region of coexisting olivine and spinel. We use $Fa_{70}Fo_{30}$ olivine as our sample. Experiments are performed in a multi-anvil high pressure apparatus (Deformation DIA) using synchrotron (NSLS) X-ray radiation as the probing tool. Pressure is up to 12 GPa and temperature is up to 1450 ^{o}C. Measurements were carried out within the binary loop where the olivine and spinel phases coexist. We apply a uniaxial oscillation stress onto the sample and Young's modulus and Q^{-1} are measured at frequencies of 0.1-0.01Hz. Our results indicate that the sample in olivine-ringwoodite region has much lower bulk modulus and higher Q^{-1} than in the single phase regions.

Our data show that:

- All determinations of Young's modulus decrease with increasing temperature indicating a softening due to a relaxation process. The amount of softening of the two phase region is greater than what would be expected from a simple mixture of the two phases. The two phase sample shows the greatest softening and the effect is most pronounced for the 100 second oscillation. This suggests that the transformation may be contributing to the strain during the oscillation.
- The phase lag, indicating attenuation, provides less clear signals. The olivine phase lag actually decreases with increasing temperature. This may reflect grain growth at higher temperature. The two phase region always exhibits higher attenuation at higher temperature, but the magnitude of the phase lag is not exceptionally different from what would be expected for a two phase mechanical mixture.
- The long period oscillation data taken on a Fe rich olivine sample in the olivine field, the ringwoodite field, and the two phase field are consistent with a model in which the phase transformation is driven by the oscillating pressure field. Scaling the model to the Earth, mostly through the reduced amplitude of the oscillation, implies that seismic waves sample the relaxed modulus in the two phase zone associated with phase transformations. The principle implication is that the bulk modulus will be considerably reduced in this region.

Li, L. (2009), Studies of mineral properties at mantle condition using Deformation multi-anvil apparatus, *Progress in Natural Science*, *19*(11), 1467-1475.

In order to understand the structure and dynamics of the Earth, one has to understand various mechanical properties of the rocks of which the Earth is made. Two typical mechanical properties are rheological and viscoelastic properties. The frontier has been defined by the bringing together of new tools to study these properties at high pressure and temperature.

A series of breakthroughs have enabled this new technology. They include:

- Use of a DIA – a cubic multi-anvil high-pressure device – in conjunction with a synchrotron source that enables x-ray analysis of the sample.
- Development of D-DIA for deformation experiments.
- Analysis of stress using x-ray diffraction.
- Analysis of strain from x-ray images.
- Use of x-ray transparent anvils in the multi-anvil system in order to obtain the necessary diffraction data for stress analysis.
- The understanding of the effect of plasticity on X-ray stress measurements.
- Implementation of conical slits to allow white energy-dispersive or 2-D detectors to allow monochromatic angle-dispersive measurements.

This paper reviews recent studies of the rheological and viscoelastic properties of minerals at mantle pressure and temperature using deformation multi-anvil apparatus (D-DIA). Stress-strain-time relations were measured using synchrotron X-ray radiation to determine these properties. Rheological properties of San Carlos olivine have been measured at pressure up to 10 GPa and indicated that the effect of pressure on the viscosity of olivine is much smaller than previous reported. The unique capability of synchrotron X-ray can resolve the stress heterogeneity within a polycrystalline material as well as a multi-phase mixture and elucidate the stress-strain distribution in an aggregate. Anelasticity measurements were carried out using olivine as the sample at mantle pressure and temperatures. The results showed that grain boundary activity rather than pressure dominate the relaxation processes. The aim of this paper is to illustrate the methods using new tools for high pressure research.

Measurement of thermal diffusivity at high pressures and temperatures using synchrotron radiography

Dobson, D. P.[1], S. A. Hunt[1], L. Li[2], and D. Weidner[2].
1. University College London, UK. 2. SUNY at Stony Brook.

The thermal transport properties of the Earth's mantle are very important for understanding mantle convection, secular cooling and the heat budget of the core. However, they are amongst the most poorly known of mantle properties due to the difficulty of performing the measurements. We have developed a synchrotron-based method for measuring thermal diffusivity at high pressure which significantly simplifies the measurement (and implemented it at X17b2 of the NSLS). In the Ångstrom method as implemented in traditional high-pressure thermal diffusivity measurements two thermocouples are placed co-axially within the sample, at the axis and at some arbitrary radius. The sample is then heated in a cylindrical furnace and the temperature is allowed to vary sinusoidally with time. The phase difference of the temperature wave between the two thermocouples provides a measure of the thermal diffusivity of the sample. The problem is that it is often very difficult to produce long cylinders high pressure samples. Furthermore their weak metastability and high hardness makes drilling coaxial holes of <100mm diameter and ~3 mm length in the samples nearly impossible in many cases. We have modified the method as follows: we have dispensed with the thermocouples and instead use the thermal expansion of the sample as a proxy for the temperature. The length of the sample is imaged by placing thin strips of Pt foil across the diameter of the sample (oriented perpendicular to the incident X-ray beam) at ~1mm intervals along the sample. The highly absorbing foils show up on X-radiographs and by measuring the relative displacement between foils as the thermal wave diffuses into the sample the phase of the wave can be determined for all radii in a single measurement.

Here we performed a proof-of-concept experiment on NaCl at 4 GPa. While NaCl has a large thermal expansivity compared to many mantle silicates this is offset by its much smaller bulk modulus, meaning that much of the temperature effect is taken up by thermal pressure in the sample rather than thermal expansion (Voigt-like situation). Results are very encouraging suggesting that the method could be used for measuring thermal diffusivity in mantle silicates at high pressure.

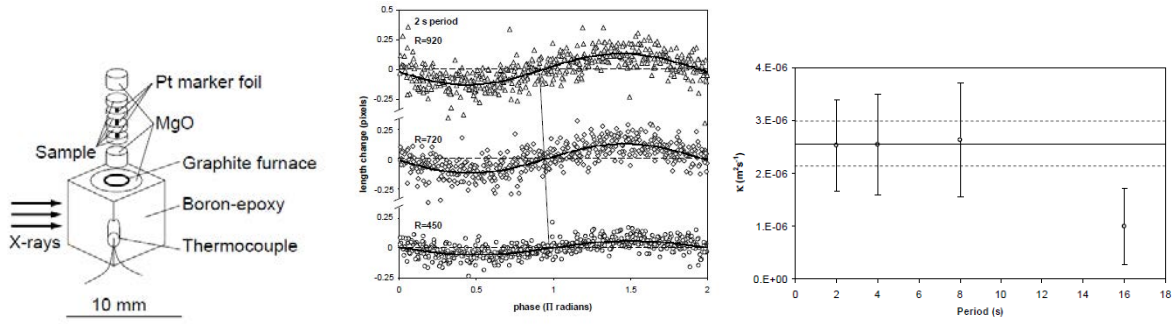

Figure 1. Left: schematic drawing of the cell used in high-pressure experiments. Centre: the displacements of the foils at three arbitrary radii. The change in phase angle is due to the diffusion of the temperature wave into the sample. Right: the thermal diffusivity determined at 4 GPa at different periods of the thermal wave in this experiment compared to the value extrapolated to pressure from literature data (solid line).

This work was supported by NSF. NSLS X17b is supported by COMPRES through NSF EAR 06-49658.

Simultaneous Ultrasonic Interferometry and X-radiation Measurements at X17B2 of NSLS to 20 GPa 1773K

Baosheng Li, Ultrasonic Group of Mineral Physics Institute at Stony Brook University

We have developed techniques to conduct simultaneous ultrasonic interferometry, X-ray diffraction and X-ray imaging measurement on solid and liquids at high pressure and high temperature. A series of experiments on minerals relevant to the Earth's deep interior as well as other functional materials under high-pressure and temperature have been performed and unprecedented data have been obtained. It is worth noting that similar techniques implemented at other synchrotron facilities around the world have all used X17B2/NSLS as a model experimental set-up. The greatest advantage of the current setup is that a combined analysis of the ultrasonic velocity and X-ray diffraction data on crystalline materials provides a unique means to determine the thermalelasticity with a direct determination of pressure using the sample itself. These techniques can also be applied to (1) reliably determine the density equation of state for glass/amorphous materials through the measurements of ultrasonic velocities with direct sample length measurements, (2) establish absolute pressure scales, and (3) conduct in-situ investigation on time-dependent processes such as phase transformation and melting. The newest development has enabled us to conduct these measurements up to 20 GPa in pressure and 1773 K in temperature.

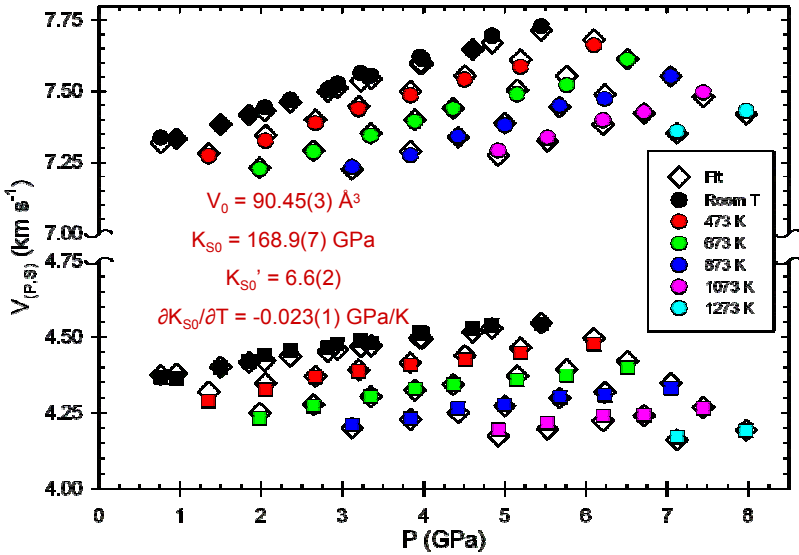

Sound velocities in Fe as a function of P and T

Experiments were conducted at the X17C beamline of NSLS which is supported by COMPRES, the Consortium for Material Property Research in the Earth Sciences under NSF Cooperative Agreement EAR0649658.

Paper

Appl. Phys. Lett. 93, 191904, 2008, doi:10.1063/1.3023049)

Work performed on beamlines X17B2.

Characterizing High Pressure Melt/liquid Properties with a Paris-Edinburgh Cell at the Advanced Photon Source

Yanbin Wang (University of Chicago)
Guoyin Shen (Carnegie Institution of Washington)

A Paris-Edinburgh (PE) cell (model VX-3) has been recently installed at HPCAT 16BM-B and successfully integrated with x-ray measurements for comprehensive characterization of melt/liquid properties, allowing users to study structure (by x-ray diffraction), elasticity (by ultrasonic interferometry), and viscosity (by radiographic imaging) at high pressure and temperature. Density determination for melts/liquids is being commissioned by x-ray absorption measurements.

The PE press and the sample container assembly are designed to contain the sample volume ranging from 0.03 mm^3 to 1.2 mm^3 while the entire volume can be monitored through X-ray windows widely open in radial direction (see figure). Currently, the sample pressure and temperature can reach up to either 7 GPa and 2,300K or 10 GPa and 1,000K, respectively, depending on the choice of anvil and sample assembly dimensions. For diffraction experiment, the APS bending magnet white beam provides a broad hard X-ray spectrum up to 120 keV with appreciable fluxes. Combining with the maximum available 2θ angle of ~40 degrees, the maximum momentum transfer, $Q=4\pi\sin(\theta)/\lambda$, can reach up to ~40 $Å^{-1}$. A real-time white-beam radiography imaging system is established with 7x magnification, ~3 μm imaging resolution, and a frame rate of up to 1,000 per second depending on the incident beam filtering. This real time imaging system is useful for viscosity measurements, and to define the sample dimension as well as to monitor the stability of system under high pressure and temperature conditions. A table top channel-cut monochromator which can provide 30-70 keV energy range has been installed for multi-energy X-ray absorption/transmission measurement.

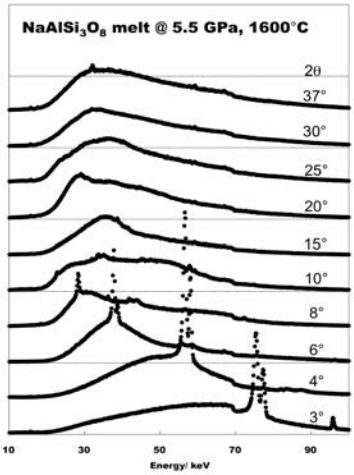

Energy dispersive data at multiple angles for melt/liquid structure measurements.

The feasibility of the facility has been tested with several silicate melts. For example, melt structures of albite and anorthite have been determined to 6 GPa and 2000 K (Yamada et al 2011). The melt structures along the jadeite – diopside join has been systematically measured and a manuscript is ready to be submitted. High quality acoustic signals were recorded in a commissioning study with an ultrasonic setup with the PE press.

Yamada, A, et al (2011) *Rev. Sci. Instrum.*, **82**, 015103(1-7).

DDIA-30: a Versatile Megabar Multi-Anvil Device for In-Situ High-Pressure Studies with White and Monochromatic Synchrotron Radiation

Y. Wang[1], Z. Jing[1], N. Hilairet[1,], T. Yu[1], N. Nishiyama[1,2], Y. Tange[2], T. Sakamaki[1], M. Rivers[1], S. Sutton[1]*
[1]Center for Advanced Radiation Sources, The University of Chicago , USA
[2]Global Center of Excellence, Geodynamics Research Center, Ehime University, Japan
[*] Now at Unite Materiaux et Transformations, CNRS UMR 8207 – Universite Lille 1, France

We report installation and test results of the DDIA-30 apparatus, a new high pressure device jointly supported by GSECARS and COMPRES. This module is now operational in the 1000 ton press at the insertion device beamline (13-ID-D) of the Advanced Photon Source. As a double-stage, hydrostatic device, the system is tested with second stage anvils made of sintered diamonds. Initial tests were conducted with pressure and temperature conditions up to 35 GPa and 1800 K, respectively. This is the first such device in the US. Experiments in Japan show that double-stage configuration with sintered diamond anvils is capable of generating megabar (100 GPa) pressures [1]. Melting experiments were conducted on gold to 20+ GPa, using both diffraction and imaging as criteria for detecting melting. This device can also be used for deformation experiments, like the deformation DIA [2].

Design & capability

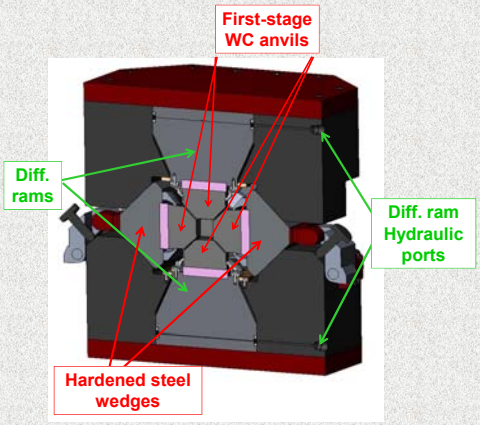

- Max load capacity: 1000 ton
- Max diff. ram travel: 10 mm
- Max first-stage anvil truncation: 45 mm
- Accommodates 14 mm sintered diamond second-stage anvils

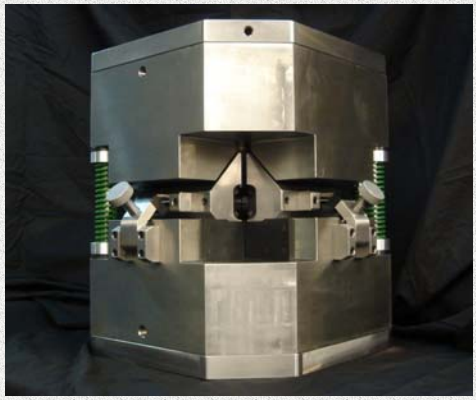

Hardware installation

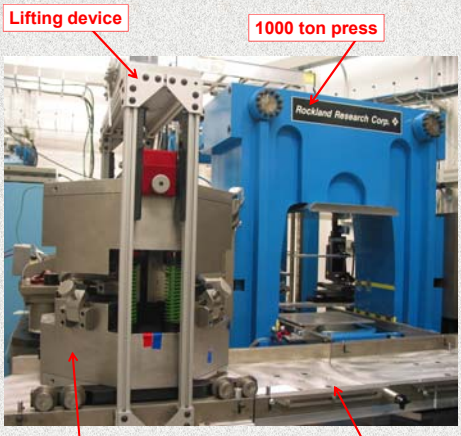

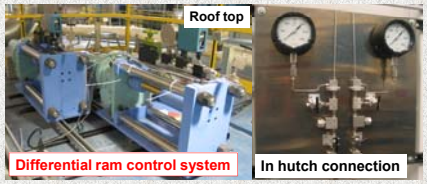

Test results

Double-stage configuration

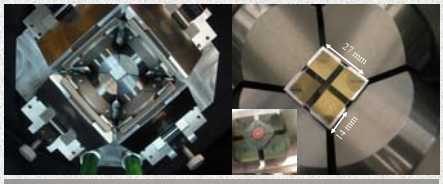

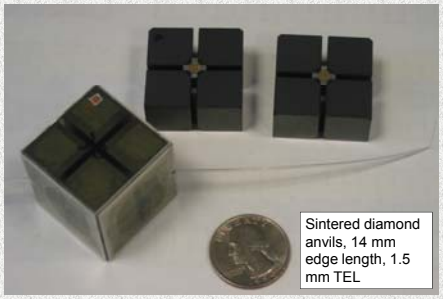

Pressure tests

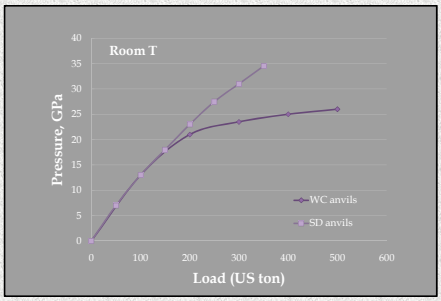

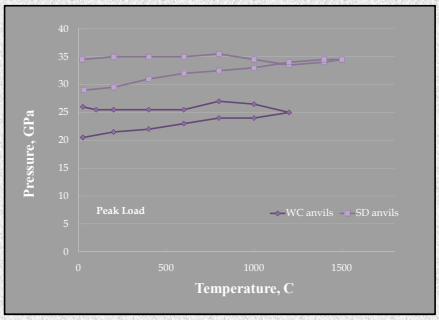

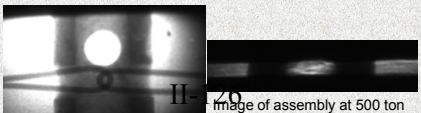

Image of assembly at 0 load

Image of assembly at 500 ton (with WC second-stage anvils)

Temperature tests

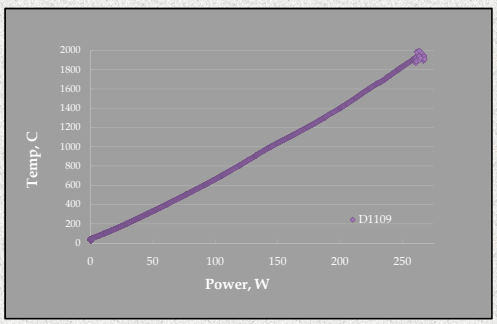

Both $LaCrO_3$ and TiB_2 heaters have been tested. Stable temperatures up to 2500 K and 2000 K can be generated using WC and SD anvils, respectively.

Applications: Double-stage system

Melting curves of gold and iron have been determined up to ~30 GPa and 2500 K. Results were presented by Jing et al. at Fall AGU Meeting, 2010

Potential for high pressure studies

Enormous efforts have been invested by researchers in Japan who have demonstrated that the 6-8 configuration is capable to ~100 GPa and >2000 K (e.g., Ito & Yamazaki, 2010). As the first double-stage multi-anvil system in the US, DDIA-30 will play a pivotal role in "ultrahigh "pressure multi-anvil research especially for deep mantle property studies.

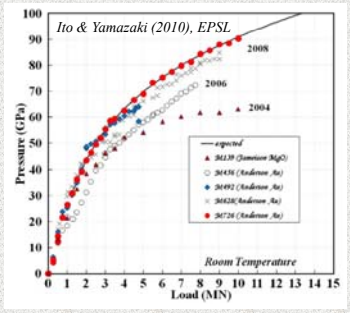

Further development: deformation tests

Control system for differential rams are under testing. 6-6 MA cells have been tested using small D-DIA and will be used for deformation experiments.

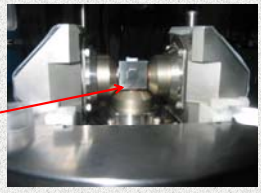

Nishiyama et al., HPR, 2008

Acknowledgments. We thank the financial support from COMPRES and GSECARS, valuable training experience provided by T. Irifune at Geodynamics Research Center, Ehime Univ., heater materials from Kurt Leinenweber (ASU), and technical support from Guy Macha. Work partially support by NSF grant EAR-0652574 and 0968456.

Nanoscale Manipulation of the Properties of Solids at High Pressure with Relativistic Heavy Ions

M. Lang, F.X. Zhang, J. Zhang, J. Wang, U. Becker, R.C. Ewing *University of Michigan*
B. Schuster, C. Trautmann, R. Neumann *GSI Helmholtz Center for Heavy Ion Research*

Zirconate pyrochlore, $Gd_2Zr_2O_7$, pressurized in a diamond-anvil cell (DAC) up to 40 GPa was irradiated at one of the world's largest ion accelerator facilities with energetic uranium and xenon ions with kinetic energy of 45 GeV. The high velocity (~50% speed of light) of the ion beam allows traversal of mm-thick diamond anvils of the DAC before reaching the pressurized sample. As the projectiles lose kinetic energy along their trajectories, they induce intense electronic excitations and ionizations, which trigger complex processes within the solid. *In situ* synchrotron X-ray diffraction experiments (COMPRES beamline X17C, NSLS) on irradiated and non-irradiated reference samples revealed that a previously unquenchable, pyrochlore high-pressure phase was recovered to ambient pressure after ion-beam exposure. Transmission electron microscopy evidenced a radiation-induced, nano-crystalline texture. Quantum-mechanical calculations confirm that the surface energy at the nanoscale is the cause of the remarkable stabilization of the high-pressure phase. This work highlights the combined use of high-pressure and high-energy ion irradiation as a new strategy for manipulating and stabilizing novel materials to ambient conditions that otherwise could not be recovered.

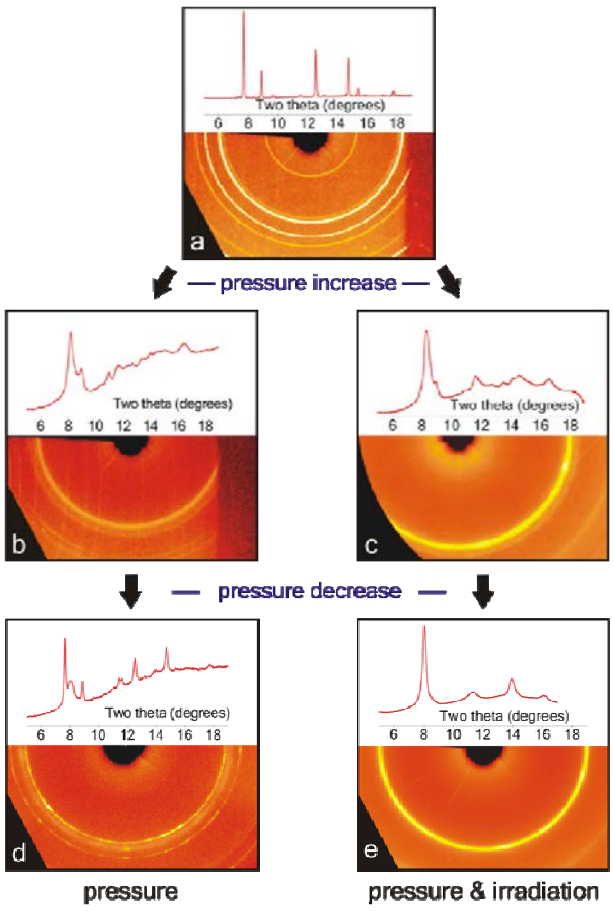

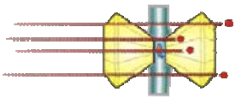

Figures: (above) Experimental scheme for the irradiation of pressurized samples inserted in the DAC with relativistic heavy ions. (left) Synchrotron XRD images and patterns of $Gd_2Zr_2O_7$. (a) Pyrochlore-structured starting material upon releasing pressure (b,d) without and (c,e) with irradiation. (d) The diffraction image and pattern of the quenched unirradiated pyrochlore shows the typical maxima of the defect-fluorite structure, whereas (e) a new cubic high-pressure phase was observed in the irradiated sample after pressure release.

Reference: M. Lang, F.X. Zhang, J.M. Zhang, J.W. Wang, B. Schuster, C. Trautmann, R. Neumann, U. Becker, R.C. Ewing, *Nature Materials* 8 (2009) 793-797.

Acknowledgements: This work was supported by the Office of Basic Energy Sciences, USDOE under DOE grant DE-FG02-97ER45656. The use of NSLS at X17C station is supported by NSF COMPRES EAR01-35554 and by US-DOE contract DE-AC02-10886. This research was supported in part by the National Science Foundation through TeraGrid resources provided by NCSA and NICS.

Studying the Earth using a multi-technique setup at sector 3 of the APS

Lili Gao[1,2], Esen E. Alp[1], Wolfgang Sturhahn[1], Jiyong Zhao[1], Thomas Toellner[1], Michael Lerche[1,3], Hasan Yavas[1]
[1]*Advanced Photon Source, Argonne National Laboratory, Argonne, IL;* [2]*Department of Geology, University of Illinois, Urbana, IL;*
[3]*High Pressure Synergetic Consortium, Carnegie Institution of Washington, Argonne, IL*

Deciphering the composition and nature of the Earth's interior requires knowledge on the elastic properties and thermo-dynamic properties of relevant materials. At pressures of mega-bars, as in the Earth's lower mantle and core, nuclear resonant inelastic x-ray scattering (NRIXS) is a unique method in measuring sound velocity and shear modulus; it also yields thermo-dynamic parameters. With synchrotron Mössbauer spectroscopy (SMS), we can obtain valence state, spin state and magnetic properties, which serve as input parameters for geophysical modeling. For such experiments, a focused x-ray source with high energy resolution and bunched time structure is required. With a focal x-ray beam size of < 10 microns, an energy resolution of 1 meV and x-ray bunches separated by 153 nanoseconds, sector 3 of the Advanced Photon source (APS) is one of the few places in the world that provide such capability.

In determining sound velocity with NRIXS method, knowledge on density and compressibility is required. With the recent integration of an x-ray diffraction (XRD) system, density and compressibility can be obtained simultaneously with the NRIXS data, enhancing the accuracy of measured sound velocities. The on-line XRD system also provides in situ pressure determination, especially at high temperatures or very high pressures where the conventional ruby pressure calibrant can no longer provide such information.

Also integrated in this setup is the double-sided laser heating system. Even more challenging than reaching the high pressures is to approach the extreme temperatures in the interior of the Earth. The ever-improving laser heating technique at sector 3 of the APS provides a way to study materials under high temperatures, helping to understand the nature of the Earth's interior.

With this setup, the sound velocities of a number of core-candidate materials, including pure iron, Fe-Ni alloy, FeH_x, Fe_3C, Fe-Si alloy and Fe_3S, have been studied to decipher the myth of light alloying element(s) composition in the core. The valence state and spin state of a series of Earth-related materials, including (Mg,Fe)O, Fe_2O_3, Fe_3O_4, perovskite / post-perovskite $(Mg,Fe)_2(Al,Si)O_4$ and

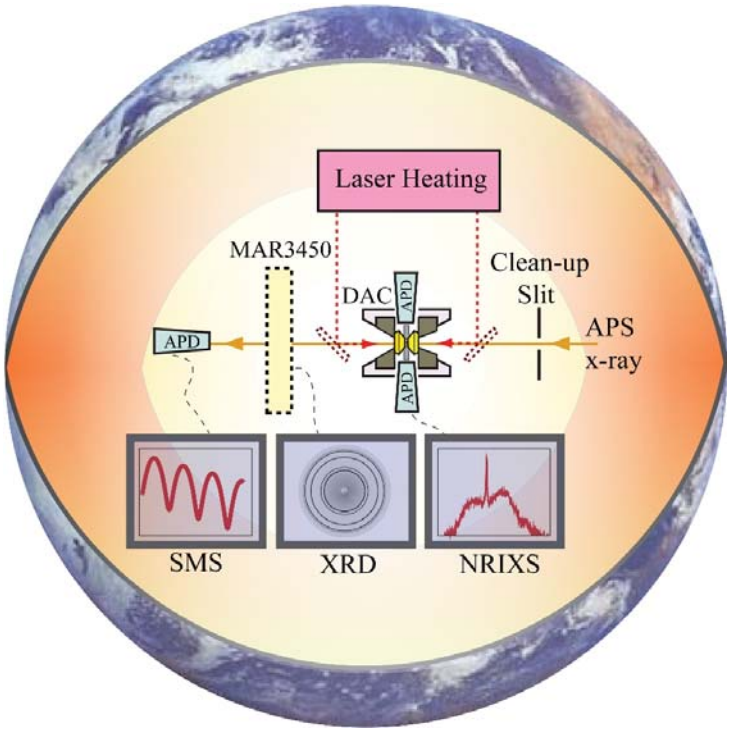

Fig. 1. The experimental setup at beamline 3-ID-B of the APS, integrating SMS, XRD, NRIXS, DAC and laser heating techniques. This setup is widely used in research at extreme pressure and temperature conditions with geophysical applications.

meteorites have been investigated using the SMS method. In addition, these methods have also been used to study the magnetic and vibrational properties of other materials with interesting physical properties, including $FePO_4$, $FeBO_3$, $Fe(OH)_2$, Fe-S, Fe-Dy, Fe-Tb, Fe-Mg, Fe-Au, Fe-Pt and $CaFe_2As_2$.

Use of the APS was supported by the U.S. Department of Energy, Office of Science, Office of Basic Energy Science, under contract No. DE-AC02-06CH11357. This work was partially supported by COMPRES, the Consortium for Materials Properties Research in Earth Sciences, under NSF cooperative agreement EAR 10-43050.

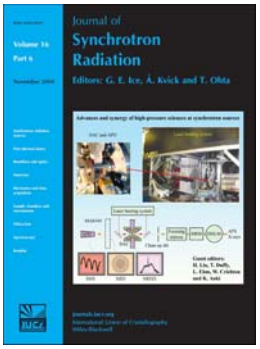

Reference: L. Gao, B. Chen, M. Lerche, E.E. Alp, W. Sturhahn, J. Zhao, Y. Hasan and J. Li, Sound velocities of compressed Fe_3C from simultaneous synchrotron x-ray diffraction and nuclear resonant scattering measurements, Journal of Synchrotron Radiation, 16, 714-722 (2009) **(cover article of the 2009 November issue)**

Geophysics Opportunities at Sector 3-ID of APS
Inelastic X-Ray and Nuclear Resonant Spectroscopy

A. Alatas[1], E. Alp[1], L. Gao[1,2], L. Yan[1,3], T. Toellner[1], J. Zhao[1],
[1]Advanced Photon Source, Argonne National Laboratory, [2] University of Illinois, Urbana Champaign,
[3]University of California, Davis

Nuclear Resonant Scattering

The nuclear resonant x-ray scattering program at Sector-3-ID at the APS has been actively developing applications for mineral physicists, particularly those who are working with high pressures using DAC's since 2000.

The beamline has adopted a multiple focusing scheme to deliver ~ 10 micrometers beam at three different stations. Coupled with advanced milli-eV resolution "tunable, in-line" monochromators, we can excite the nuclear resonances for Kr, Fe, Eu, Sn and Dy.

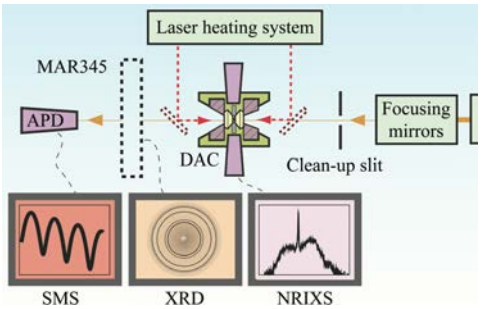

There are two different techniques applied to mineralogical problems: Synchrotron Mössbauer Spectroscopy (SMS), and Nuclear Resonant Inelastic X-Ray Scattering (NRIXS). **SMS** measures valence, spin state, magnetism and local atomic environment, while **NRIXS** yields thermoelastic properties: phonon density of states, Debye sound velocity, vibrational entropy, kinetic energy and force constants. These two techniques are complemented with x-ray diffraction, **XRD**, so that bulk compressibility and density can be measured as well, allowing simultaneous determination of shear and compressional sound velocity.

Inelastic X-Ray Scattering: HERIX-3

The momentum resolved high-resolution inelastic x-ray scattering, **IXS**, program at Sector-3-ID is now available for geophysics and materials community, particularly those working with high pressures using DAC since 2010.

The HERIX-3 spectrometer has an overall resolution of 2.2 meV at 21.651 keV It is suitable for single crystal work to measure elastic constants and compressional sound velocity from powder samples under high pressure and temperature.

The momentum-resolved **IXS** spectroscopy measures the phonon dispersion relations in single or polycrystalline samples as well as in liquids and glasses. The HERIX-3 spectrometer at Sector 3 is compatible with DAC's. Thus, sound velocity, elastic constants, relaxation times in liquids, dynamic viscosity can be measured. Relaxation behavior of liquids and glasses under pressure and temperature can be studied at this station. The beam size recently has been reduced to 17 micrometer, providing HERIX-3 to have the highest flux density in the world among the total 4 IXS instruments in the world..

Anomalous sound speed in (Mg,Fe)O

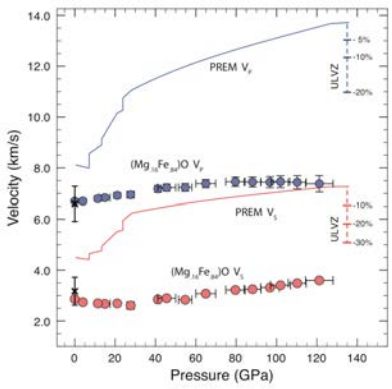

As a unique method to measure sound velocity at Mbar pressures, NRIXS is used to determine the shear and compressional velocity of $(Mg_{0.16}{}^{57}Fe_{0.84})O$ to shed light on the observed ultra-low velocity zone (ULVZ) at 2900 km depths.

(Courtesy: J. Jackson, Caltech)

Sound velocity of Fe at high temperature

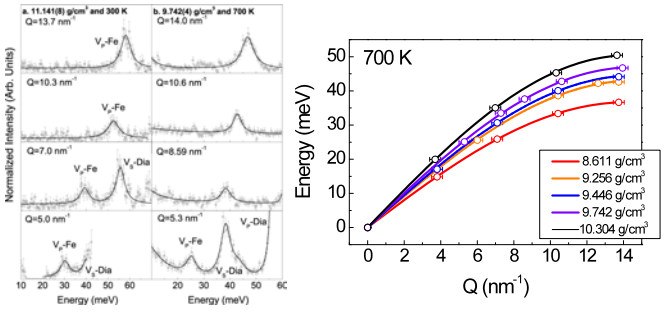

(Courtesy: Z. Mao, J.F. Lin, U Texas-Austin)

The nuclear resonance of iron has been very popular with COMPRES community, due to its wide applicability. To date, many systems have been studied, among them: Fe, FeO, Fe_2O_3, Fe_3O_4, $FePO_4$, $FeBO_3$, Fe(OH), (Mg,Fe)O, $(Mg,Fe)_2SiO_4$, FeS, Fe_3S, Fe-Ni, Fe-H, Fe-Dy, Fe-Tb, Fe-Mg, Fe-Au, Fe-Pt, and $CaFe_2As_2$.

Anvils and More: Essential Materials for High-Pressure Research

Cubic boron nitride as a primary calibrant for a high temperature pressure scale

Alexander F. Goncharov[1], Kirill K. Zhuravlev[1,2], Stanislav Sinogeikin[1], Jonathan C. Crowhurst[3], Muhtar Ahart[1], Dmitry Lakshtanov[4], Vitali Prakapenka[2], Jay D. Bass[4], Pierre Beck[1], Sergei N. Tkachev[1,2], Joseph M. Zaug[3], Yingwei Fei[1]

[1]Geophysical Laboratory, Carnegie Institution of Washington, 5251 Broad Branch Rd, NW, Washington, DC, 20015
[2]Center for Advanced Radiation Sources, University of Chicago, Chicago, Illinois 60637, USA
[3]Lawrence Livermore National Laboratory, University of California, 7000 East Ave., Livermore, CA 94551, USA
[4]Geology Dept., University of Illinois at Urbana-Champaign, 1301 W.Green st. Urbana, Illinois 61801, USA.

We present results establishing a new high pressure scale at high temperature based on the thermal equation of state and elastic properties of cubic boron nitride (cBN) and silicon carbide (SiC-3C). This scale is derived from concomitant measurements of density and sound velocities at high pressure and temperature independent of any previous pressure scale. The present results for cBN obtained at room temperature to 27 GPa suggest the validity of the current ruby scale (within ±4% at 100 GPa). At high temperature, the data obtained at 16 GPa to 723 K are in fair agreement with the thermal equation of state of cBN reported in our previous work. We have also shown that cBN can serve as a convenient pressure gauge in x-ray and optical studies using the laser heated diamond anvil cell [1]. Recently, we have performed concomitant measurements of density and Raman active vibrational modes of cBN and SiC-3C to 80 GPa at 300 K [2], which provide a foundation for extension of our pressure scale to a Mbar pressure range.

References:

1. Goncharov, A. F., S. Sinogeikin, J. C. Crowhurst, M. Ahart, D. Lakshtanov, V. Prakapenka, J. Bass, P. Beck, S. N. Tkachev, J. M. Zaug, Y. Fei "Cubic boron nitride as a primary calibrant for a high temperature pressure scale." *High Pressure Research*, **27**, 409–417 (2007).
2. Zhuravlev, K.K., Goncharov, A. F., Tkachev, S. N., Prakapenka, V., *Cubic silicon carbide and boron nitride as possible primary pressure calibrants for high pressure and temperature scale.* Abstract MR13A-1901 presented at 2010 Fall Meeting, AGU, San Francisco, Calif., 13-17 Dec., 2010.

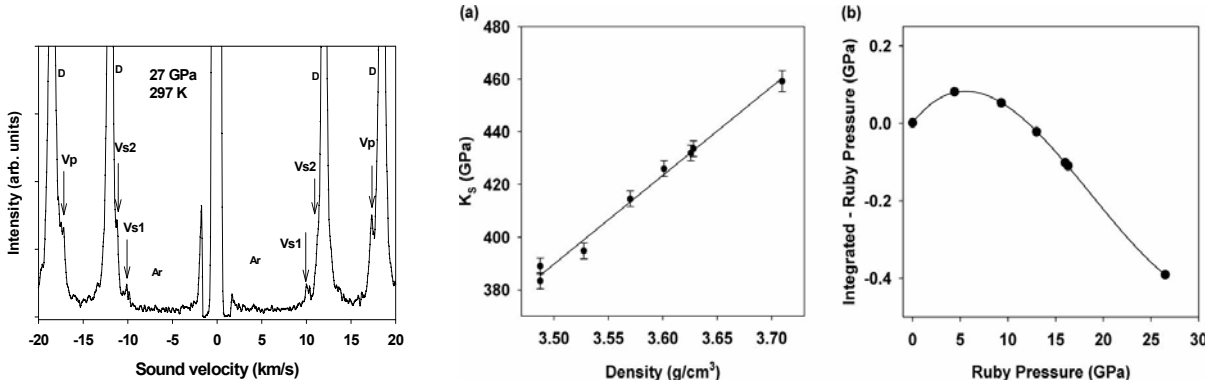

Left: Brillouin spectra of cBN single crystals in the DAC at 27 GPa . Middle and Right: Bulk modulus of cBN determined experimentally. (a) Density dependence of the adiabatic bulk modulus, K_S . (b) A difference of pressure determined by direct integration of the experimentally determined bulk modulus and pressure determined by the ruby fluorescence technique

Synchrotron x-ray diffraction and Brillouin spectroscopy were performed at GSECARS (APS, supported by DOE Contract No. W-31-109- Eng-38). This research was partially supported by National Science Foundation under grantEAR01-35642 (to JDB), which provided funds for the construction of the Brillouin facility at Sector 13 of the APS, and support for this particular study. This work at GL & UIUC is supported by National Science Foundation under grants EAR-0842057, EAR08-42345, and EAR07-38871.

Elasticity of cubic boron nitride under ambient conditions

Jin S. Zhang, Jay D. Bass University of Illinois at Urbana-Champaign
Takashi Taniguchi National Institute for Materials Science
Alexander F. Goncharov Carnegie Institution of Washington
Yun-Yuan Chang, Steven D. Jacobsen Northwestern University

As a superhard material with properties similar to diamond, including chemical inertness, cubic boron nitride (cBN) is an excellent candidate as a pressure calibration standard for high-temperature high-pressure research using its PVT equation of state. However, the elastic properties of cBN at ambient conditions reported in the literature vary by up to 8%, which can likely be attributed in part to variability in cBN composition and defect structure as well as measurement uncertainties. We have measured the single-crystal elastic moduli of high-purity cBN with high precision by Brillouin scattering measurements, making an effort to minimize experimental uncertainties. We obtain values of C_{11}=798.4±1.7GPa, C_{44}=469.0±1.0GPa, C_{12}= 172.4±1.1GPa, from which the isotropic aggregate bulk modulus Ks=381.1±1.3GPa and shear modulus G=398.8±1.2GPa (Hill average) were calculated. Our results improve the precision and reduce the uncertainties in the elastic moduli of high-purity cBN as a reference for future high P-T press ure scales.

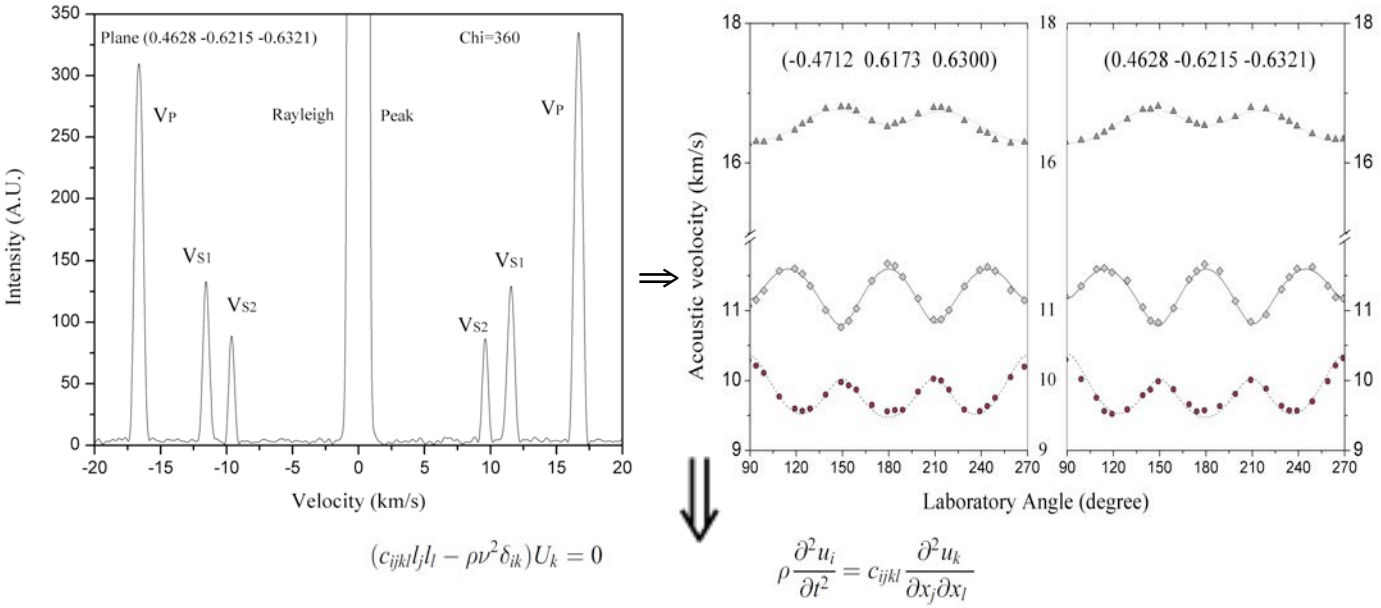

C_{11}=798.4±1.7GPa, C_{44}=469.0±1.0GPa, C_{12}= 172.4±1.1GPa, Ks=381.1±1.3GPa G=398.8±1.2GPa

Key references:

Grimsditch et al., J. Appl. Phys. 76, 832(1994). Goncharov et al., High. Pres. Res. 27, 409 (2007).

Toward a self-consistent pressure scale: elastic moduli and equation of state of MgO by simultaneous x-ray density and Brillouin sound velocity measurements at high-pressure high-temperature conditions

Stanislav Sinogeikin[1,3] , Dmitry Lakshtanov[1], Carmen Sanches-Valle[1], Vitali Prakapenka[2], Guoyin Shen[3], Jinguing Wang[1], Jay Bass[1]

[1] University of Illinois at Urbana-Champaign; .[2] GSECARS, The University of Chicag; [3] HPCAT, Geophysical Laboratory, Carnegie Institution of Washington; [4] Geophysical Laboratory, Carnegie Institution of Washington.

Accurate phase diagrams and PVT equations of state (EOS) of materials strongly depend on the PVT calibrations of standard materials (e.g. MgO, NaCl, Au, Pt), which currently do not predict identical pressures at the same experimental conditions. MgO is commonly used as a pressure standard in a variety of high pressure and high-temperature experiments. Despite being one of the simplest and most studied materials, its accurate EOS is still uncertain, especially at high PT. The direct way of obtaining a self consistent pressure scale is by measuring acoustic velocities (Vp and Vs) and density simultaneously. Such P-V-T-Vp-Vs measurements allow one to determine the pressure directly, without resort to a separate calibration standard.

Recently, as part of a major COMPRES initiative, we have constructed a Brillouin spectrometer at GSECARS, APS (13-BM-D) which allows accurate simultaneous sound velocity and lattice parameter measurements at high pressures and high temperatures. Such measurements were performed on single crystal MgO at simultaneously high pressures (up to 30 GPa) and high temperatures (up to 873K) in diamond cells with Ne or Ar as pressure medium. At each PT point we measured the unit cell parameters and the acoustic velocities of MgO in several crystallographic directions, and directly obtained all three single crystal elastic moduli, as well as isotropic adiabatic bulk (Ks) and shear (μ) moduli. Unit cell parameters of pressure medium (Ne, Ar) and additional pressure calibrants (Au, Pt, NaCl) were measured at each PT for cross calibration. These results allowed us to constrain a self-consistent high P-T equation of state of MgO.

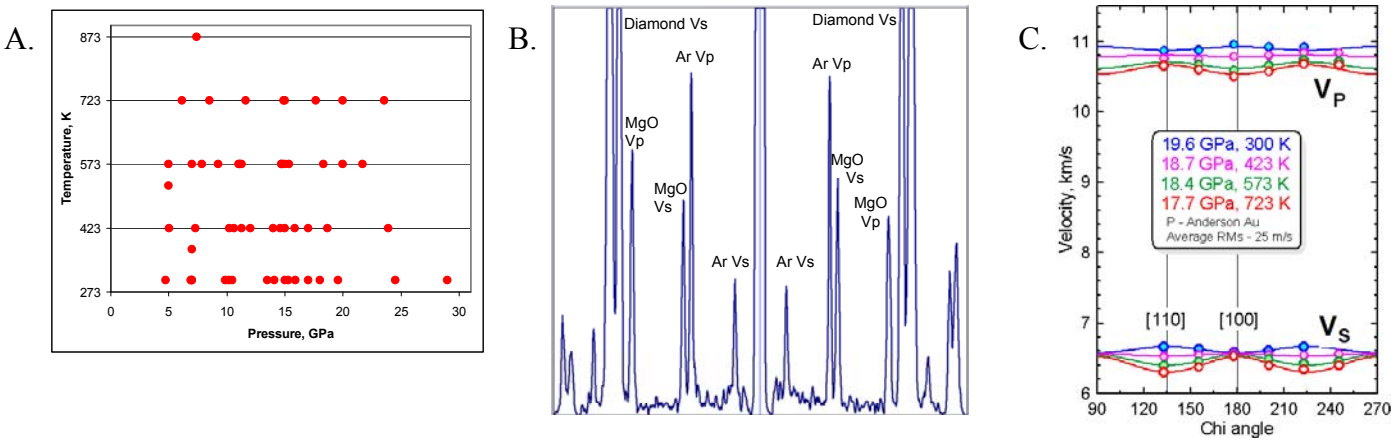

P-T range of single-crystal P-T-V-Vp-Vs measurements on MgO (A), Brillouin spectrum of single-crystal MgO In [100] at 17.7 GPa, 723 K (B), and measured and fitted velocities in MgO as a function of crystallographic direction at pressure about 18 GPa and different temperatures (C).

Reference: Sinogeikin et al., (2006) Brillouin spectrometer interfaced with synchrotron radiation for simultaneous x-ray density and acoustic velocity measurements. Rev, Sci. Instrum. 77: 103905.

This work was supported by COMPRES and the National Science Foundation. GeoSoilEnviroCARS [Sector 13, Advanced Photon Source (APS), Argonne National Laboratory] is supported by the National Science Foundation—Earth Sciences (EAR-0217473), Department of Energy—Geosciences (DE-FG02-94ER14466), and the State of Illinois. Use of the Advanced Photon Source was supported by the U.S. Department of Energy, Office of Science, Office of Basic Energy Sciences, under Contract No. W-31-109-ENG-38.

Elastic moduli and equation of state of NaCl to 30 GPa by simultaneous x-ray density and Brillouin sound velocity and measurements

Stanislav Sinogeikin[1,3] , Dmitry Lakshtanov[1], Carmen Sanches-Valle[1], Vitali Prakapenka[2], Guoyin Shen[3], Eugene Gregoryanz[4], Jay Bass[1]

[1] University of Illinois at Urbana-Champaign; .[2] GSECARS, The University of Chicag; [3] HPCAT, Geophysical Laboratory, Carnegie Institution of Washington; [4] Geophysical Laboratory, Carnegie Institution of Washington.

NaCl is commonly used as a pressure standard in a variety of high pressure experiments. Some recent experimental studies suggest that the commonly used Decker equation of state of NaCl in the B1 structure is outdated and possibly inaccurate at pressures above 15-20 GPa. This would result in erroneous phase diagrams and PVT equations of state for materials when NaCl is used for pressure determination. Moreover, most previous acoustic velocity measurements of NaCl have been limited to pressures below 10 GPa, making the elastic properties of NaCl at higher pressure, especially in the vicinity of B1-B2 transition, highly uncertain.

Recently we have constructed a Brillouin spectrometer at GSECARS, APS (station 13-BM-D) which allows accurate simultaneous sound velocity and lattice parameter measurements at high pressures. Such measurements were performed on single crystal NaCl (B1) to a maximum pressure of 30 GPa in a diamond cell with Ne as a hydrostatic pressure medium. At each pressure we measured the acoustic velocities of NaCl in several crystallographic directions, and also the unit cell parameters. From these measurements we directly obtained the complete set of single crystal elastic moduli, as well as isotropic adiabatic bulk (K_S) and shear (μ) moduli. Unit cell parameters of Ne, Au and Pt were measured at each pressure for cross calibration.

At high pressure NaCl exhibits a number of unusual properties. First, it shows extreme elastic anisotropy which is 3.3 times higher than that at ambient pressure. Secondly, above ~15 GPa the density – velocity relations deviate from linearity and violate Birch's law. Thirdly above 20 GPa in the vicinity of B1-B2 transition the acoustic velocities and elastic (especially shear) moduli show unusual behavior (mode softening) that is not adequately described by finite strain equations of state.

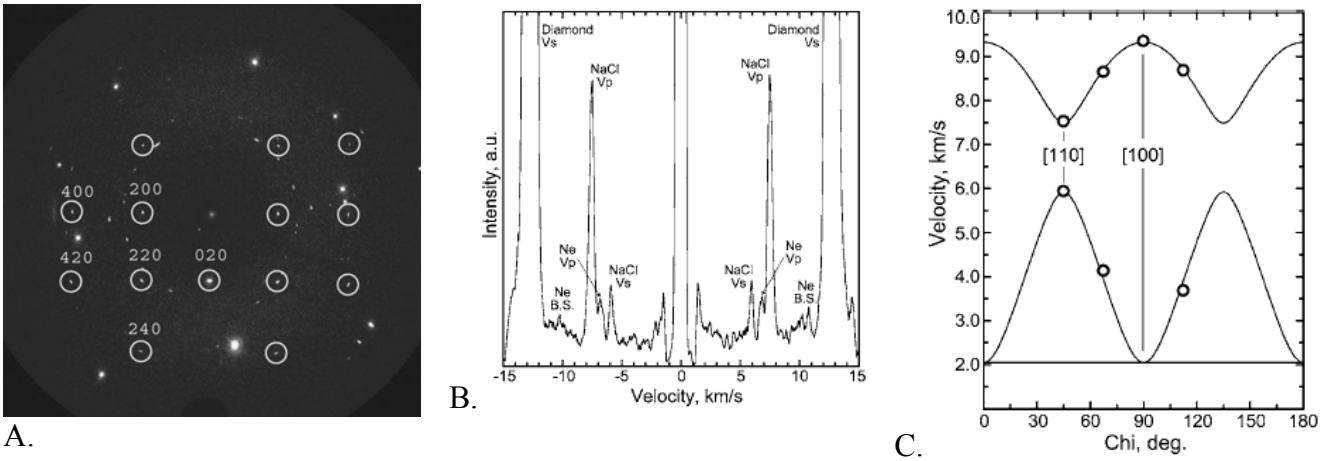

A. B. C.

X-ray diffraction (A), Brillouin spectrum in the [110]direction (B), and acoustic velocities as a function of crystallographic direction (C) of single crystal NaCl (B1) at 26 GPa in Neon pressure transmitting medium.

Reference: Sinogeikin et al., (2006) Brillouin spectrometer interfaced with synchrotron radiation for simultaneous x-ray density and acoustic velocity measurements. Rev, Sci. Instrum. 77: 103905.

This work was supported by COMPRES and the National Science Foundation. GeoSoilEnviroCARS [Sector 13, Advanced Photon Source (APS), Argonne National Laboratory] is supported by the National Science Foundation—Earth Sciences (EAR-0217473), Department of Energy—Geosciences (DE-FG02-94ER14466), and the State of Illinois. Use of the Advanced Photon Source was supported by the U.S. Department of Energy, Office of Science, Office of Basic Energy Sciences, under Contract No. W-31-109-ENG-38.

Strength of NaCl at Mantle Pressures

Zhongying Mi, Sean R Shieh, University of Western Ontario
Thomas S. Duffy, Princeton University
Boris Kiefer, New Mexico State University

NaCl was measured up to 44 GPa by radial x-ray diffraction technique using a symmetric diamond anvil cell (DAC) at beamline X17C, National Synchrotron Light Source. In this study, phase transformation from B1 (rock salt structure) to B2 (CsCl structure) starts at 29.4 GPa and is completed at about 31.8 GPa, which is in agreement with previous reports. The differential stresses of NaCl are obtained by using lattice strain theory. Our results show that the ratio of differential stress to shear modulus, t/G of NaCl-B1 gently increases with pressures, indicating that NaCl is a soft materials at pressures below ~30 GPa. While near the transition pressure the abrupt drop of the t/G values suggest the weakening effect of stress arising from the B1-B2 phase transformation. Later, the ratios of t/G exhibit slightly increment at higher pressures and have higher values than B1 phase above 40 GPa. The differential stress supported by NaCl show similar trends and results is still less than 1 GPa at applied pressure to 44 GPa. We also calculated the differential stress on different planes of NaCl; for B1 phase, (111) is the strongest plane and (200) is the weakest plane.

(a) (b)

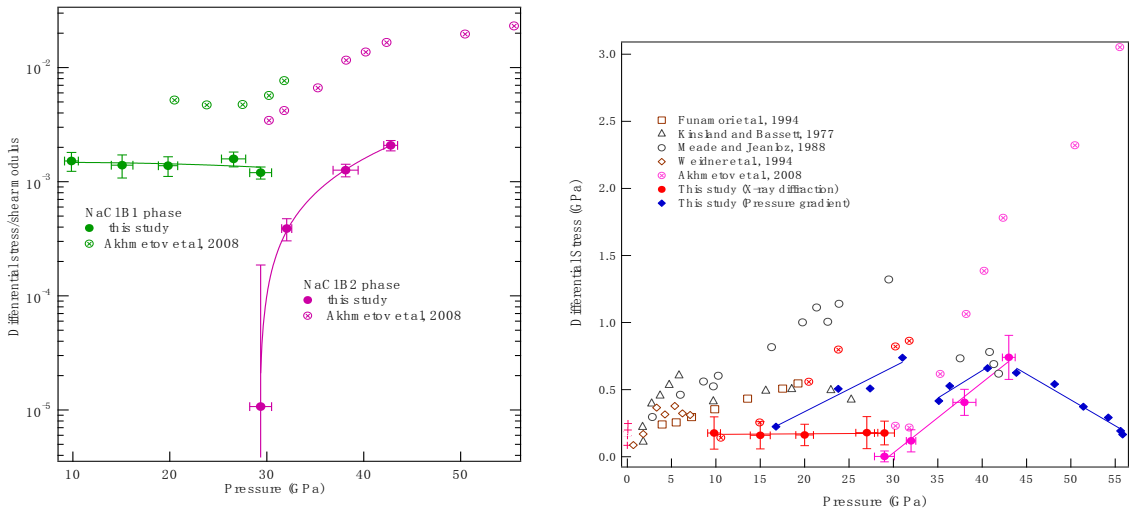

(a) The ratios of differential stress to shear modulus as a function of pressure for NaCl B1 and B2 phase show a sharp decrease across NaCl B1-B2 transition.
(b) Comparisons of differential stress of NaCl obtained from this study (solid symbols) and previous reports (open symbols).

Reference: Mi, Z., S.R. Shieh, T. S. Duffy and B. Kiefer, Strength study of NaCl to lower mantle pressure, *EOS, Transactions, Am. Geophys. Union*, 2010.

We thank to S. Dorfman for sample preparation and to Z. Chen for his help at beamline X17C, NSLS. This work was supported by NSERC and also by COMPRES, the Consortium for Materials Property Research in Earth Sciences.

Brillouin Spectroscopy and X-ray Diffraction of fcc-argon to 56 GPa and 700 K

H. Marquardt, S. Speziale (German Research Center for Geosciences GFZ Potsdam, Germany)
A. Gleason (University of Berkeley, California, USA)

We simultaneously performed Brillouin scattering and synchrotron x-ray diffraction on polycrystalline argon loaded in the diamond-anvil cell at Sector 13 of the Advanced Photon Source at Argonne National Laboratory. An externally heated cell was used, which allowed us to accurately control the temperature and enabled us to run experiments at different pressures along a 700 K isotherm up to a maximum pressure of 56 GPa (fig. 1). The temperature was measured with two thermocouples that were attached to different positions on the diamond close to its culet, pressure was calibrated both with a gold standard and with ruby fluorescence.
As expected, we find that the sound wave velocities are lower along the 700K isotherm than reported at 300K, but follow a similar trend with increasing pressure. The collected x-ray diffraction data allow us to directly derive the density at each pressure where Brillouin scattering was performed and also provides information about the polycrystalline nature of the sample. Our data can help to better understand the behaviour of noble gases at simultaneously high pressure and temperature and provide a basis to estimate the behaviour of argon as a pressure-transmitting medium in diamond-anvil cell experiments where temperature-annealing is performed. In addition, the simultaneous collection of acoustic wave velocities and x-ray diffraction promises to enhance our understanding of the potentials and problems of Brillouin Spectroscopy on polycrystals/powders in general (analysis in progress).

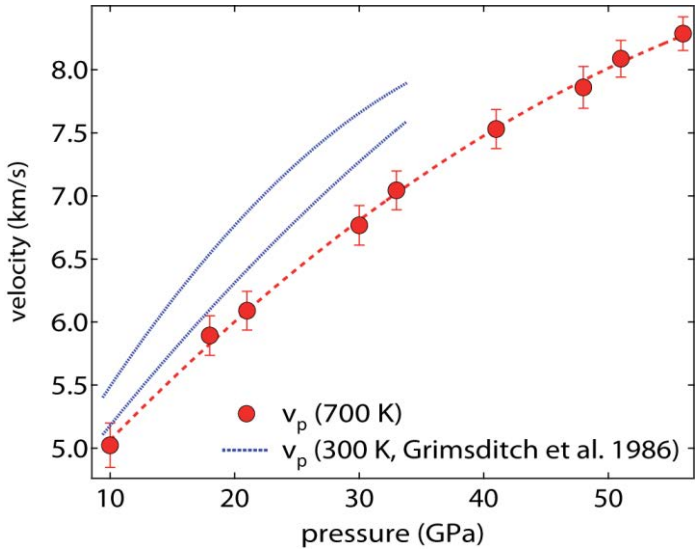

Fig. 1: Compressional velocity of solid argon along a 700 K isotherm.

Strength measurements of solid noble gas pressure media to Mbar pressures

S. M. Dorfman, A. Kubo, T. S. Duffy *Princeton University*
Y. Meng *HPCAT, Argonne National Laboratory*

In order to simulate the hydrostatic stress conditions of the Earth's interior in the uniaxial diamond anvil cell, samples must be suspended in a soft pressure medium, as the hydrostaticity of the sample environment is limited by the strength of the medium at high pressure. Because they are both soft and non-reactive, solid noble gases are widely used pressure media, but their strengths at Mbar pressures are not well-known. We have measured deviatoric stresses sustained by Ar and Ne media in the diamond anvil cell. Ar was loaded cryogenically with Pt and ruby standards in a Be gasket in a diamond anvil cell. We performed energy-dispersive radial diffraction at beamline X17C of the National Synchrotron Light Source (NSLS) at pressures up to 60 GPa. Ne was loaded with Au and NaCl standards at high pressure in the COMPRES/GSECARS gas loading system in a Re gasket. Angle-dispersive axial diffraction was performed at beamline 16-ID-B of the HPCAT sector of the Advanced Photon Source (APS) at up to 268 GPa. Deviatoric stresses were evaluated by relative shifts of diffraction lines due to anisotropic compression and by peak width analysis. Differential stress, *t*, measured in Ar reaches 4 GPa at 60 GPa, while weaker Ne has the same strength at 100 GPa. To achieve more hydrostatic stress conditions in these media at Mbar pressures, annealing is required.

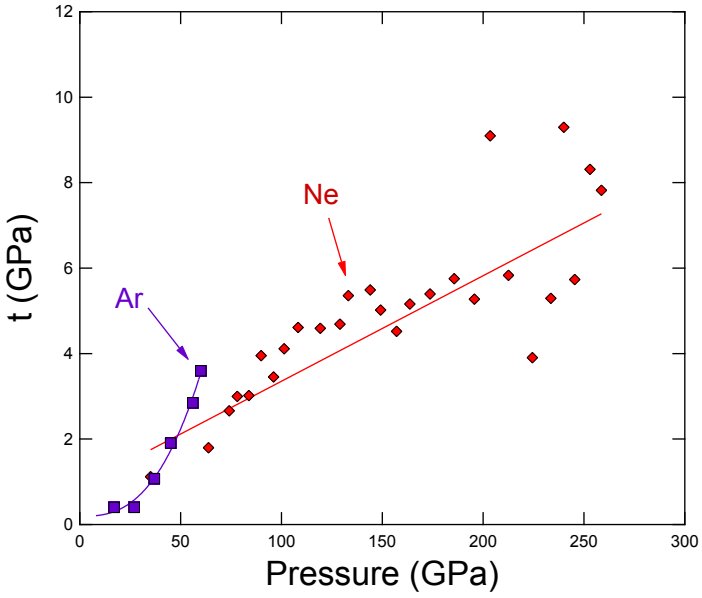

Figure: Differential stress, *t*, measured in Ar and Ne by diffraction line shift analysis (Singh 1993).

Acknowledgements: Jingzhu Hu assisted with experiments at X17C. The COMPRES/GSECARS gas loading system is supported by COMPRES (NSF EAR 0649658) and GeoSoilEnviroCARS (NSF EAR 0622171, DOE DE-FG02-94ER14466). Use of the Advanced Photon Source was supported by the U.S. Department of Energy, Office of Science, Office of Basic Energy Sciences, under contract no. DE-AC02-06CH11357). The use of X17C is supported by NSF COMPRES EAR01-35554 and by US-DOE contract DEAC02-10886.

Single-crystal elasticity of LiF at elevated pressures.

Anastasia Kantor[1], Innokenty Kantor[2], Vitali Prakapenka, *GSECARS, University of Chicago*

[1]Present address: Bayerisches Geoinstitut, University of Bayreuth, Germany
[2]Present address: European Synchrotron Radiation Facility, Grenoble, France

A Brillouin scattering (BS) setup installed at the 13-BMD station at the Advanced Photon Source is a unique tool allowing measuring elasticity of transparent materials and X-ray diffraction (XRD) from them at the same time in a diamond anvil cell under high-pressure. This combination gives not only a possibility to measure elastic constants (with the velocity input from BS and density input from XRD), but also to establish a primary pressure scale from the density-bulk modulus relations (Zha et al., 2000). Lithium fluoride (LiF) was chosen as a material for this task for many reasons, mainly because it's a rare case of a simple cubic material without high-pressure phase transitions (unlike NaCl) and with relatively low sound velocities, that wouldn't be hidden under the S-wave diamond peak at moderate pressures (unlike MgO). Unfortunately, LiF appeared to be an extremely weak Brillouin scatterrer, so the collecting time became enormously high on elevated pressures, and a poor signal to noise ration does not allow data collection above ~12 GPa even when laser power was increased by an order of magnitude. Nevertheless, we managed to obtain the high-quality single-crystal elastic modules of LiF up to 12 GPa. Our data significantly extend and correct previous measurements on LiF (Muller and Smith, 1964).

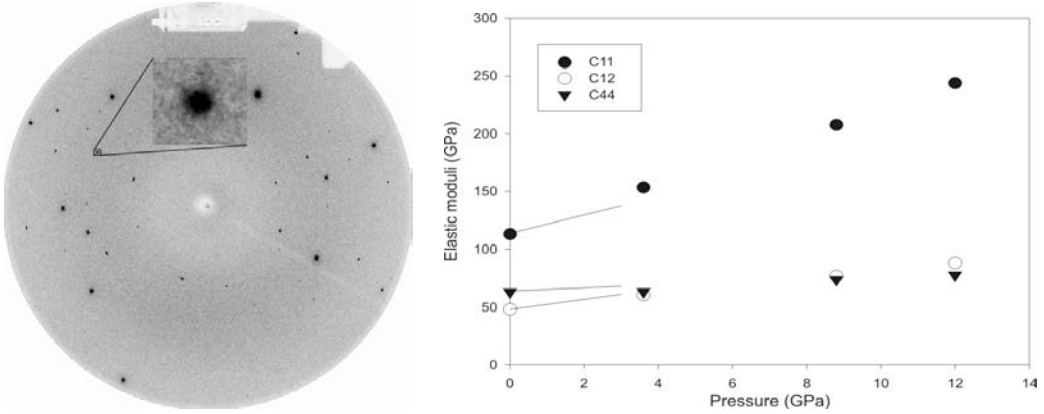

Fig. 1. Left: typical X-ray diffraction pattern from a LiF crystal in Ne pressure medium. Bright spots are diamond reflection, one of the LiF reflections in magnified to show the perfect crystal quality. Right: single-crystal elastic constants of LiF. Solid lines show previous measurements up to 3 GPa (Muller and Smith, 1964). Error bars are approximately half of the symbol size.

Muller R.A. and Smith C.S. (1964) J. Phys. Chem. Solids **25**, 1279-1292.

Zha C.S., Mao H.K., Hemley R.J. (2000) PNAS **97**, 13494-13499.

Strength of Pt by radial x-ray diffraction

S. M. Dorfman, T. S. Duffy *Princeton University*
S. Shieh *University of Western Ontario*

Pt is commonly used as a pressure calibrant in diamond anvil cell experiments and had been previously observed to have an anomalously high strength despite a low shear modulus. We compressed Pt powder of grain size 0.15-0.45, 0.5-1.2, and 44 microns (-324 mesh) to 60 GPa in the diamond anvil cell under non-hydrostatic conditions. Both angle- and energy-dispersive X-ray diffraction experiments were performed at NSLS X17C and X17B3 in the radial geometry through a Be gasket. The strength of bulk grain size Pt is lower than previously observed, but higher strengths were measured for smaller grain sizes.

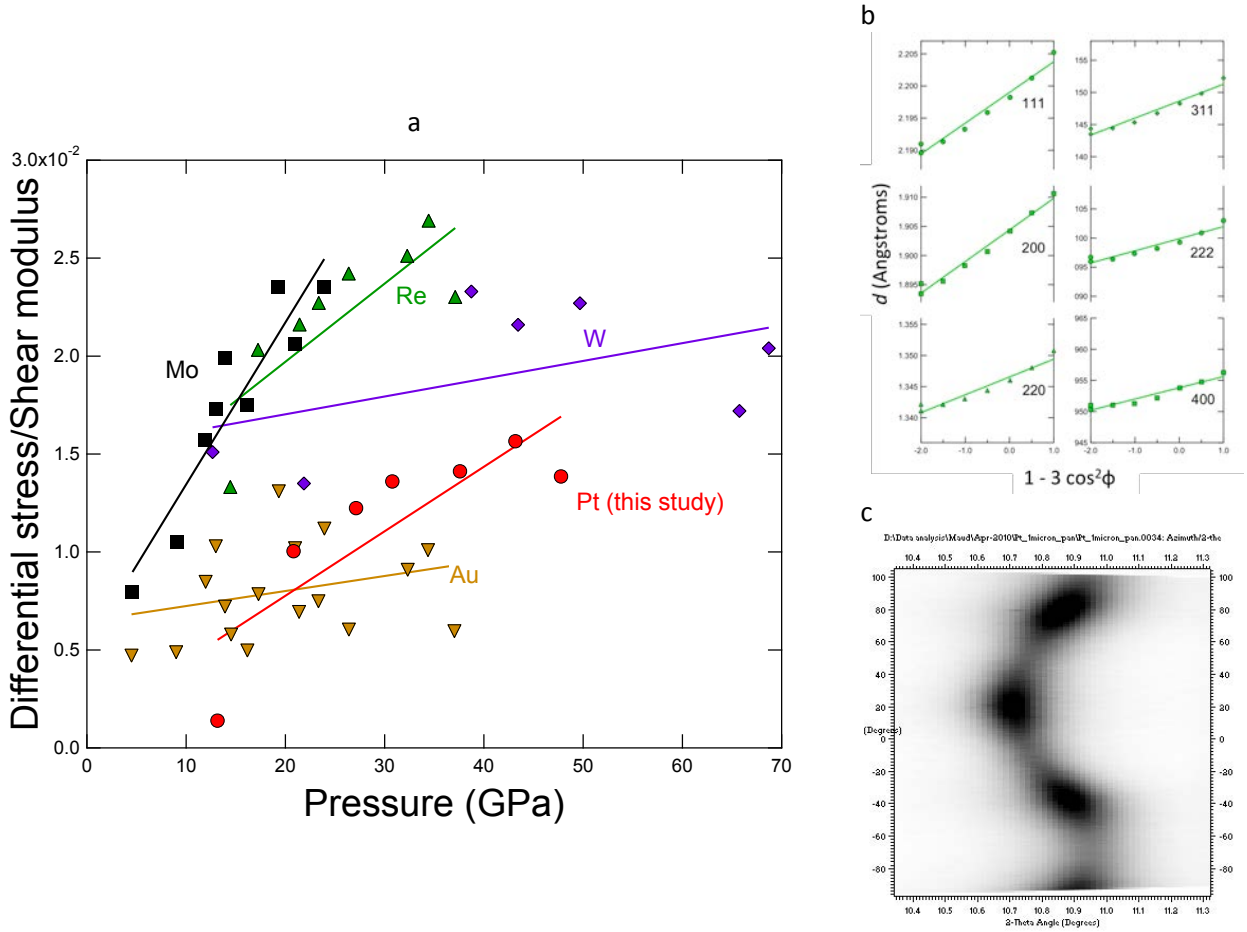

Figures: a) Differential stress measurements on bulk grain size Pt sample give low strength, as in FCC Au but unlike BCC and HCP metals Mo, W and Re. b) From energy-dispersive diffraction experiments, shift in diffraction line positions as a function of orientation with respect to the loading axis is used to measure differential strain and stress. c) From angle-dispersive diffraction experiments, texture and curvature of Pt 111 line at 60 GPa indicates both plastic and elastic deformation.

Acknowledgements: The use of X17C is supported by NSF COMPRES EAR01-35554 and by US-DOE contract DEAC02-10886.

JOURNAL OF APPLIED PHYSICS 106, 043506 (2009)

Experimental and theoretical studies on the elasticity of molybdenum to 12 GPa

Wei Liu,[1,a)] Qiong Liu,[1] Matthew L. Whitaker,[1,2] Yusheng Zhao,[3] and Baosheng Li[1]
[1]*Mineral Physics Institute, Stony Brook University, Stony Brook, New York 11794, USA*
[2]*Department of Geosciences, Stony Brook University, Stony Brook, New York 11794, USA*
[3]*LANSCE, Los Alamos National Lab, Los Alamos, New Mexico 87545, USA*

(Received 26 May 2009; accepted 1 July 2009; published online 19 August 2009)

Experiments have been conducted to measure compressional (V_P) and shear wave (V_S) velocities as well as unit-cell volumes (densities) of molybdenum to 12.0 GPa at room temperature using ultrasonic interferometry in conjunction with synchrotron x-radiation. Both V_P and V_S as well as the adiabatic bulk (K_S) and shear (G) moduli exhibit monotonic increase with increasing pressure. A finite strain equation of state analysis of the directly measured velocities and densities yields K_{S0} =260.7(5) GPa, G_0=125.1(2) GPa, K'_{S0}=4.7(1), and G'_0=1.5(1) for the elastic bulk and shear moduli and their pressure derivatives at ambient conditions. Complimentary to the experimental data, V_P and V_S as well as the elastic bulk and shear moduli were also computed using density functional theory (DFT) at pressures comparable to the current experiment. Comparing with experimental results, the velocities and elastic moduli from DFT calculations exhibit close agreement with the current experimental data both in their values as well as in their pressure dependence. © *2009 American Institute of Physics*. [DOI: 10.1063/1.3197135]

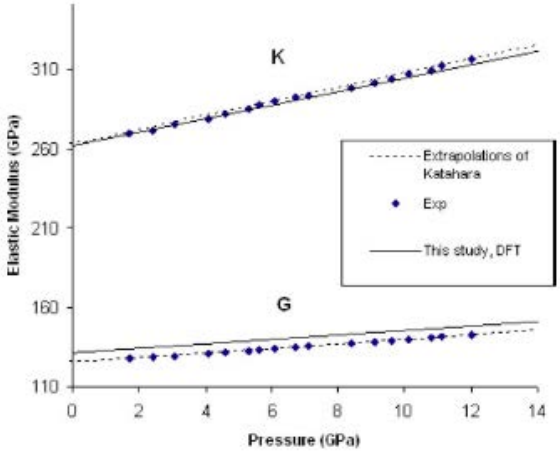

FIG. 3. (Color online) Variation of bulk (K_S) and shear (G) modulus for molybdenum as a function of pressure. Symbols are from experimental studies, solid line represents the results from current DFT calculations, and dashed lines are the extrapolations of results from Katahara *et al.* (1979).

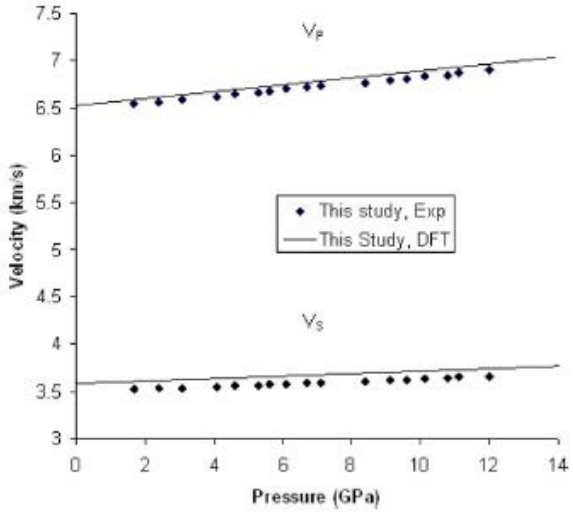

FIG. 2. (Color online) Elastic compressional (V_P) and shear (V_S) wave velocities for molybdenum as a function of pressure from the current ultrasonic and x-ray measurements to 12.0 GPa (symbols) and from DFT calculations (lines).

Acknowledgments

This research is supported by DoE/NNSA (DEFG5206NA2621 to BL). These experiments were carried out at the National Synchrotron Light Source (NSLS), which is supported by the US Department of Energy, Division of Materials Sciences and Division of Chemical Sciences under Contract No. DE-AC02-76CH00016. X-17B2 is supported by COMPRES.

Systemtatics of the Static Strength of Materials to Mbar Pressures in the Diamond Cell

Thomas S. Duffy (Princeton University)

Strength properties of materials under static and dynamic loading are essential quantities for characterizing mechanical behavior. Quantitative measurements of static strengths achieved in the diamond anvil cell can be made using x-ray diffraction in a radial geometry for samples under non-hydrostatic compression. This work provides a synthesis and summary of results for a range of materials including metals and strong ceramics (Duffy, 2007). Measurements were carried out at X17c, NSLS using x-ray diffraction in a radial geometry in the diamond anvil cell. Results for metals up to 68 GPa show that the ratio of yield strength to shear modulus ranges from 0.01-0.03 and increases weakly with compression. Trends at lower pressure for Re, W, and hcp-Fe are consistent with available data above 1 Mbar. Strong ceramics such as B_6O, c-Si_3N_4, and TiB_2 achieve yield strengths as large at 10% of the shear modulus at pressures up to ~70 GPa. Strengths of materials used as pressure media can now be quantitatively compared and evaluated.

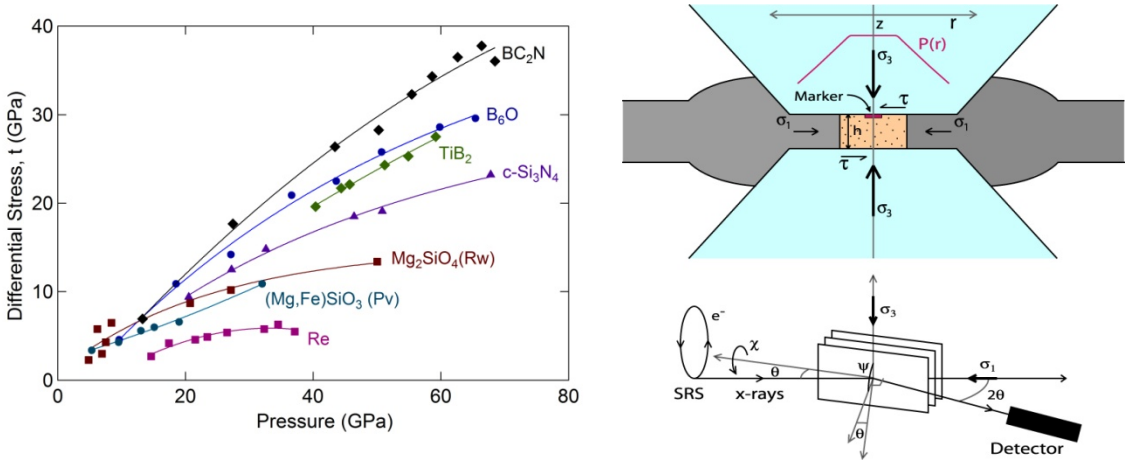

Left: Summary of differential stress measurements for strong solids (oxides, nitrides, borides, silicates) obtained using energy dispersive x-ray diffraction in the diamond anvil cell. Differential stress values for Re metal are shown for comparison. Rw—ringwoodite; Pv-perovskite; c-Si_3N_4 –cubic (spinel-type) silicon nitride.
Right: Geometry for radial x-ray diffraction experiments.

Duffy, T. S., Strength of materials under static loading in the diamond anvil cell, in *Shock Compression of Condensed Matter – 2007*, edited by M. D. Furnish, M. L. Elert, T. P. Russell, and C. T. White, AIP, New York, 639-644, 2007.

This work was supported by the NSF and Carnegie-DOE Alliance Center. NSLS X17C is supported by COMPRES through NSF EAR 06-49658.

Elastic moduli and strength of nanocrystalline cubic BC_2N from x-ray diffraction under nonhydrostatic compression

H. Dong, D. He, T.S. Duffy (Princeton), and Y. Zhao (LANL)

Cubic B-C-N phases are reported to have hardness higher than cubic boron nitride (*c*BN), along with better chemical stability and ability to withstand oxidation at a higher temperature than diamond. This significantly adds the attractiveness of cubic B-C-N phases as superhard materials for potential industrial applications. In this study the stress behavior of nanocrystalline cubic boron carbon nitride (*c*-BC_2N) was investigated using x-ray diffraction at X17C, NSLS. Experiments using radial and axial geometries in the diamond anvil cell were carried out under nonhydrostatic compression up to ~75 GPa. The radial x-ray diffraction data yields a bulk modulus, K_0=276±20 GPa with a fixed pressure derivative, K_0'=3.4 at ψ =54.7°, which corresponds to the hydrostatic compression curve. A comparative study of the observed compression curves from radial and axial diffraction shows that the ruby fluorescence pressure scale may reflect the maximum stress under nonhydrostatic compression. It was found that the nanostructured *c*-BC_2N sample could support a maximum differential stress of ~38 GPa when it started to yield at ~ 66 GPa under uniaxial compression. Moreover, the aggregate elastic moduli of the nanocrystalline *c*-BC_2N have been determined from the radial x-ray diffraction data at high pressures.

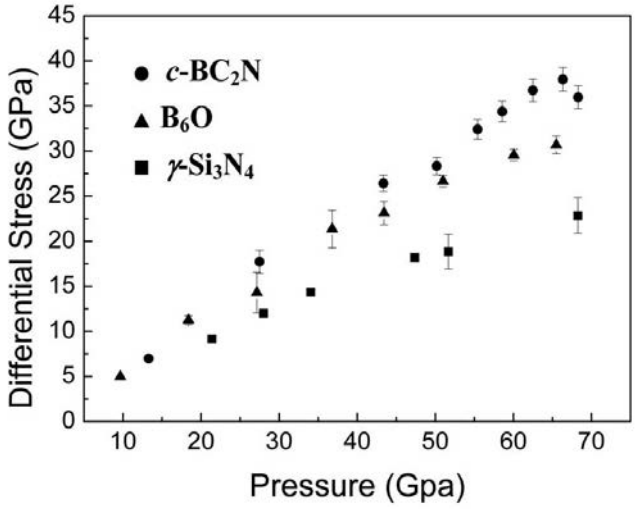

Differential stress in nanocrystalline BC_2N under non-hydrostatic compression compared to selected other strong solids.

Dong, H., D. He, T. S. Duffy, and Y. Zhao, Elastic moduli and strength of nanocrystalline cubic BC_2N from x-ray diffraction under nonhydrostatic compression, *Physical Review B*, 79, 014105, 2009.

This work was supported by the NSF and Carnegie-DOE Alliance Center. Experiments were conducted at the X17C beamline of NSLS which is supported by COMPRES, the Consortium for Material Property Research in the Earth Sciences under NSF Cooperative Agreement EAR06-49658.

Superhard diamond/tungsten carbide nanocomposites

Z. J. Lin,[1,2,a]_ J. Z. Zhang,[1] B. S. Li,[3] L. P. Wang,[3,4] Ho-Kwang Mao,[2] Russell J. Hemley,[2] and Yusheng Zhao, [1,4,a]

[1]*LANSCE-Lujan Center, Los Alamos National Laboratory, Los Alamos, New Mexico, USA*
[2]*Geophysical Laboratory, Carnegie Institution of Washington, NW Washington, DC, USA*
[3]*Mineral Physics Institute, State University of New York, Stony Brook, New York, USA*
[4] *HiPSEC, University of Nevada, Las Vegas, Nevada, USA*

We conducted high *P-T* reactive sintering experiments between diamond and tungsten at 1500 and1650 °C, both at a pressure of about 6.0 GPa. We investigated the processing conditions of diamond/tungsten carbide WC composites using *in situ* synchrotron x-ray diffraction XRD and reactive sintering techniques at high pressure and high temperatures. The as-synthesized composites were characterized by synchrotron XRD, scanning electron microscopy, high-resolution transmission electron microscopy, and indentation hardness measurements. Through tuning of the reaction temperature and time, we produced fully reacted, well-sintered, and nanostructured diamond composites with Vickers hardness of about 55 GPa and the grain size of WC binding matrix smaller than 50 nm. A specific set of orientation relationships between WC and tungsten is identified to gain microstructural insight into the reaction mechanism between diamond and tungsten.

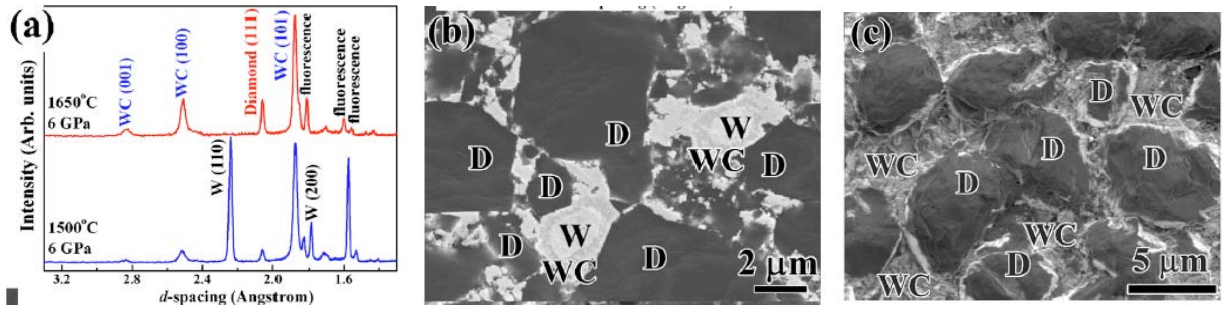

Figure (a) Synchrotron XRD patterns of diamond/WC composites sintered at 6 GPa and selected temperatures. (b) and (c) are SEM images of diamond/WC composite synthesized at 1500 and 1650 °C, respectively. "D" denotes diamond.

Z. J. Lin, J. Z. Zhang, B. S. Li, L. P. Wang, Ho-Kwang Mao, Russell J. Hemley, Superhard diamond/tungsten carbide nanocomposites, Applied Physics Letters 98, 121914, 2011

Synchrotron experiments were conducted at the X17B2 beamline of NSLS which is supported by COMPRES under NSF Cooperative Agreement EAR06-49658.

Synthesis using COMPRES multi-anvil cell assembly

– Transparent nano-polycrystalline diamond

Jiuhua Chen (FIU), Helene Couvy (FIU, now at U of Michigan), Kurt Leinenweber (ASU)

COMPRES multi-anvil cell assembly project integrates multi-anvil expertise from the community and produces experimentally proved reliable high pressure cell assembly to the community. Using these cell assemblies, we have successfully synthesized transparent nano-polycrystalline diamond through direct conversion from graphite (a rod of polycrystalline graphite, 99.9995%) at high pressure and temperature (19 GPa and 2400ºC) without any catalyst. The experiments were conducted using the Walker module high pressure apparatus at the Center for the Study of Matter at Extreme Conditions (CeSMEC) of Florida International University. Such transparent polycrystalline diamond was previously produced in Japan (1) but not in the US community.

Young's modulus (E) and nano-hardness (H_N) of the nano-polycrystalline diamond sample were measured through nanoindentation test using a Hysitron Triboindenter. Compared with commercial superhard (sintered diamond and cBN) anvils used at the COMPRES multi-anvil beamline at NSLS, the Young's modulus and nano-hardness of the nano-polycrystalline diamond has greater Young's modulus and hardness (E=707 GPa and H_N=62 GPa).

Reference

1. Irifune T, Kurio A, Sakamoto S, Inoue T et al. (2003) Ultra hard polycrystalline diamond from graphite. Nature 421: 599-600.
2. Hélène Couvy, Debrupa Lahiri, Jiuhua Chen, Arvind Agarwal, Gautam Sen, Nano-hardness and Young's modulus of nano-polycrystalline diamond, *Scripta Materialia*, 2011, in press.

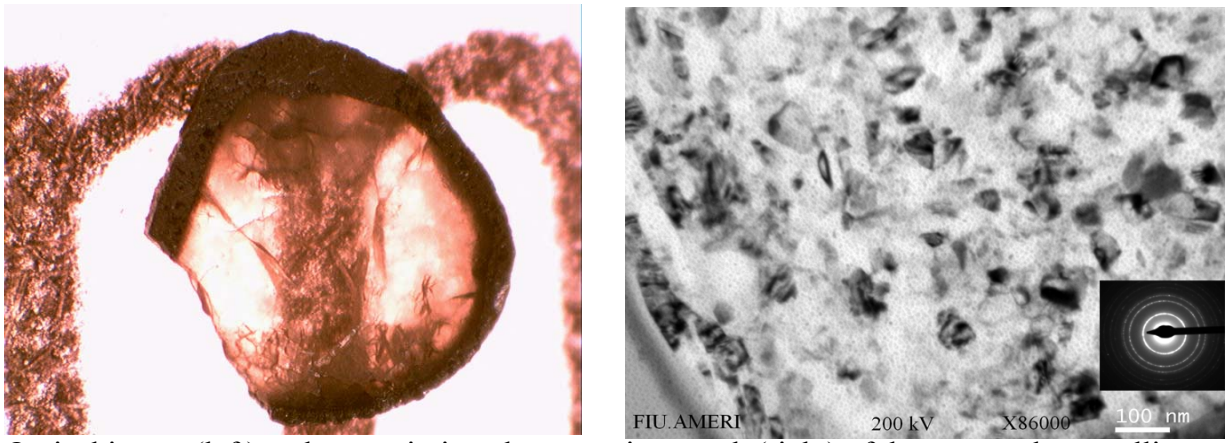

Optical image (left) and transmission electron micrograph (right) of the nano-polycrystalline diamond.

Research is supported by COMPRES and EFree, an Energy Frontier Research Center funded by DOE-BES under Award Number DE-SC000105.

Enhancing the Mechanical Properties of Single-crystal CVD Diamond

Qi Liang, Chih-shiue Yan, Yufei Meng, Joseph Lai, Szczesny Krasnicki, Ho-kwang Mao and Russell J. Hemley *Geophysical Laboratory, Carnegie Institution of Washington, Washington, DC 20015*

Approaches for enhancing the strength and toughness of single-crystal diamond produced by chemical vapor deposition (CVD) at high growth rates are described. CVD processes used to grow single-crystal diamond in high density plasmas were modi ed to incorporate boron and nitrogen. Semi-quantitative studies of mechanical properties were carried out using Vickers indentation techniques. The introduction of boron in single-crystal CVD diamond can signi cantly enhance the fracture toughness of this material without sacri cing its high hardness (~78 GPa). Growth conditions were varied to investigate its effect on boron incorporation and optical properties by means of photoluminescence, synchrotron infrared, and ultraviolet–visible absorption spectroscopy. Boron can be readily incorporated into single-crystal diamond by the methods used, but with nitrogen addition, the incorporation of boron was hindered. The spectroscopic measurements indicate that nitrogen and boron coexist in the diamond structure, which helps explain the origin of the enhanced fracture toughness of this material. Further, low pressure/high temperature annealing can enhance the intrinsic hardness of single-crystal CVD diamond by a factor of two without appreciable loss in fracture toughness. This doping and post-growth treatment of diamond may lead to new technological applications that require enhanced mechanical properties of diamond.

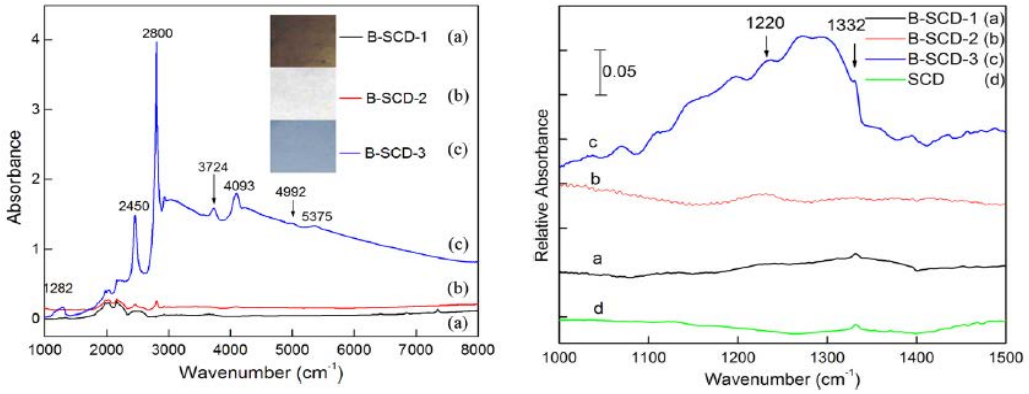

Left: IR absorption spectra for representative materials B-SCD-1, B-SCD-2, and B-SCD-3 (300 K). All materials have identical thickness (~0.3 mm). The inset shows surface images of the three materials in this measurement, the color of these materials are brown, transparent, and blue, respectively.
Right: Detail of the IR absorption spectra in the 1000-1500 cm^{-1} region for representative materials B-SCD-1, B-SCD-2, B-SCD-3, and SCD (300 K). Material SCD was grown under the same conditions as B-SCD-1 but is free of boron incorporation.

Reference

Liang, Q., C. Yan, Y. Meng, J. Lai, S. Krasnicki, H. Mao, and R. J. Hemley, *J. Phys.: Condens. Matter*, *21*(36), 364215, (2009).

Acknowledgments

This research was partially supported by COMPRES under NSF Cooperative Agreement Grant No. EAR 06-49658, and by the U.S. Department of Energy through the Carnegie/DOE Alliance Center (CDAC) contract DE-FC03-03N00144.

Planets and Planetary Materials

Ultrafast Growth of Wadsleyite in Shock-produced Melts and Its Implications for Early Solar System Impact Processes

Oliver Tschauner[a,b], Paul D. Asimow[b], Natalya Kostandova[b], Thomas J. Ahrens[b,c], Chi. Ma[b], Stanislas Sinogeikin[d], Zhenxian Liu[e], Sirine Fakra[f] and Nobumichi Tamura[f]
[a]High Pressure Science and Engineering Center, Department of Physics, University of Nevada, Las Vegas, NV 89154; [b]Division of Geological and Planetary Sciences, and [c]Lindhurst Laboratory of Experimental Geophysics, Seismological Laboratory, California Institute of Technology, Pasadena, CA 91125; [d]High Pressure Collaborative Access Team, Advanced Photon Source, Argonne National Laboratory, Argonne, IL 60439; [e]Geophysical Laboratory, Carnegie Institution of Washington, Washington, DC 20015; and [f]Advanced Light Source, Lawrence Berkeley National Laboratory, Berkeley, CA 94720

Wadsleyite is widely believed to be the most abundant mineral in the Earth between 410 and 520 km depth. The conditions where wadsleyite forms are known from long-duration high-pressure experiments, but it had never before been recovered from a laboratory-scale shock experiment, which lasts for less than one microsecond. The only confirmed natural occurrence of wadsleyite is in shocked meteorites, which are debris from collisions of rocky bodies in the early solar system. Based on synchrotron X-ray diffractometry and infrared spectroscopy, we found small quantities of the mineral wadsleyite after a high-pressure laboratory shock experiment on thin layers of magnesium oxide and fused quartz. The time duration needed to form wadsleyite was much shorter than was previously assumed necessary with an estimated growth rare in the range of several m/s. On the basis of these experiments, the wadsleyite in those meteorites could be generated by collisions between bodies one to five meters in diameter, or a thousand times smaller than calculated by earlier theoretical modelers. The results suggest that high-velocity, destructive collisions among the bodies that eventually merged to form Earth may have developed early in their growth and evolution.

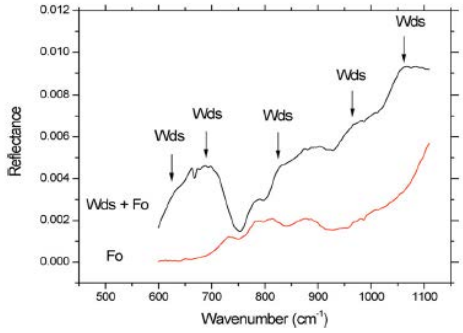

Figure 1. Reflectance IR spectrum of a wadsleyite-bearing region compared with spectrum of forsterite collected from different regions of sample. This spectrum proves abundance of wadsleyite in the shock-synthesized sample. The spectrum was taken at U2A, NSLS. Spatial resolution was 8 × 10 μm^2.

Reference

Tschauner, O., P. D. Asimow, N. Kostandova, T. J. Ahrens, C. Ma, S. Sinogeikin, Z. Liu, S. Fakra, and N. Tamura, *Proceedings of the National Academy of Sciences*, *106*(33), 13691-13695, (2009).

Acknowledgments

This research was partially supported by COMPRES under NSF Cooperative Agreement Grant No. EAR 06-49658, and by the U.S. Department of Energy through the Carnegie/DOE Alliance Center (CDAC) contract DE-FC03-03N00144.

The distinct morphological and petrological features of shock melt veins in the Suizhou L6 chondrite

Xiande XIE[1]*, Zhenya SUN[2], and Ming CHEN[1]
[1]Guangzhou Institute of Geochemistry, Chinese Academy of Sciences, P.O. Box 1131, Guangzhou GD 510640, China
[2]Center for Materials Research and Analysis, Wuhan University of Technology, Wuhan HB 430070, China

The morphology and petrology of distinct melt veins in the Suizhou L6 chondrite have been investigated using scanning electron microscopy, electron microprobe analyses, and Raman spectroscopy, synchrotron energy-dispersive diffraction, and transmission electron microscopy. It is found that the melt veins in the Suizhou meteorite morphologically are the simplest, straightest, and thinnest among all shock veins known from meteorites.

At first glance, these veins look like fine fractures, but petrologically they are solid melt veins of chondritic composition and consist of fully crystalline materials of two distinct lithological assemblages, with no glassy material remaining. The Suizhou melt veins contain the most abundant high-pressure mineral species when compared with all other veins known in chondrites. Thus, these veins in Suizhou are classified as shock veins. All rock-forming and almost all accessory minerals in the Suizhou shock veins have been transformed to their high-pressure polymorphs, and no fragments of the precursor minerals remain in the veins. Among the 11 high-pressure mineral phases identified in the Suizhou veins, three are new high-pressure minerals, namely, tuite after whitlockite, xieite, and the CF phase after chromite. On the basis of transformation of plagioclase into maskelynite, it is estimated that the Suizhou meteorite experienced shock pressures and shock temperatures up to 22 GPa and 1000 _C, respectively. Shearing and friction along shock veins raised the temperature up to 1900–2000 _C and the pressure up to 24 GPa within the veins. Hence, phase transition and crystallization of high-pressure minerals took place only in the Suizhou shock veins. Fast cooling of the extremely thin shock veins is regarded as the main reason that up to 11 shock-induced high-pressure mineral phases could be preserved in these veins.

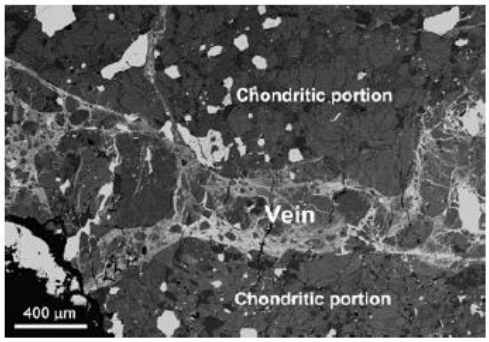

Fig. 1. Backscattered electron (BSE) image of a polished thin section of the Sixiangkou L6 chondrite showing the occurrence of a melt vein (Vein). Note the curved and jagged boundaries between the vein and the chondritic portion and a branched veinlet.

Table 1. Synchrotron radiation X-ray diffraction data of majorite-pyrope (Maj-Prp) garnets in the Suizhou vein matrix.

Maj-Prp garnet #1 in vein matrix		Maj-Prp garnet #2 in vein matrix		Majorite garnet JCPDS No. 25-0843	
d (Å)	*I*	*d* (Å)	*I*	*d* (Å)	*I*
2.880	70	2.880	70	2.881	70
2.572	100	2.571	100	2.575	100
2.453	50	2.451	40	2.454	45
2.350	35	2.349	35	2.352	30
2.256	35	2.255	30	2.262	35
2.104	10	2.105	10	2.103	18
2.038	20	2.037	30	2.038	25
1.865	50	1.863	25	1.868	25
1.821	10	1.820	10	1.820	10
1.662	20	1.661	20	1.663	20
1.597	40	1.596	30	1.597	40
1.539	70	1.538	50	1.540	60
1.438	10	1.438	10	1.439	17
1.288	10	1.288	15	1.288	15
1.257	15	1.256	10	1.258	20
1.228	15	1.228	10	1.228	14

IR-reflectivity of solid versus liquid methane on U2A of the NSLS

Kimberly Adams, Steven D. Jacobsen
Northwestern University, Department of Earth and Planetary Sciences
Zhenxian Liu, Maddury Somayazulu
Carnegie Institution of Washington, Geophysical Laboratory

Hydrocarbons including methane (CH_4) are among the most important energy resources today. Knowledge of CH_4 properties and phase stability has further application to Earth and planetary sciences in identifying states of molecular compounds on icy bodies of the outer solar system. In 2008, *Cassini* revealed dark, lake-shaped patches through the 2 and 5 μm windows of Titan's atmosphere [Brown et al. 2008, *Nature* 454, 607]. Interpreting these dark patches in terms of possible hydrocarbon lakes requires laboratory-based, IR-reflectivity of methane and ethane at relevant conditions. We loaded CH_4 into diamond cells for synchrotron-IR reflectance measurements at 50-100 K on the U2A beamline of the NSLS. We studied co-existing states of vapor and liquid CH_4 at temperatures down to 94 K. Upon crystallization below 94 K, we observed a dramatic increase in reflectance of CH_4 at the diamond-sample interface (R_{sd}). Whereas the position of characteristic absorption bands of CH_4 are unchanged upon phase change, darkening of CH_4 upon melting is consistent with Titan's observed dark surface features, which may represent large polar lakes forming seasonally through a methane cycle on Titan.

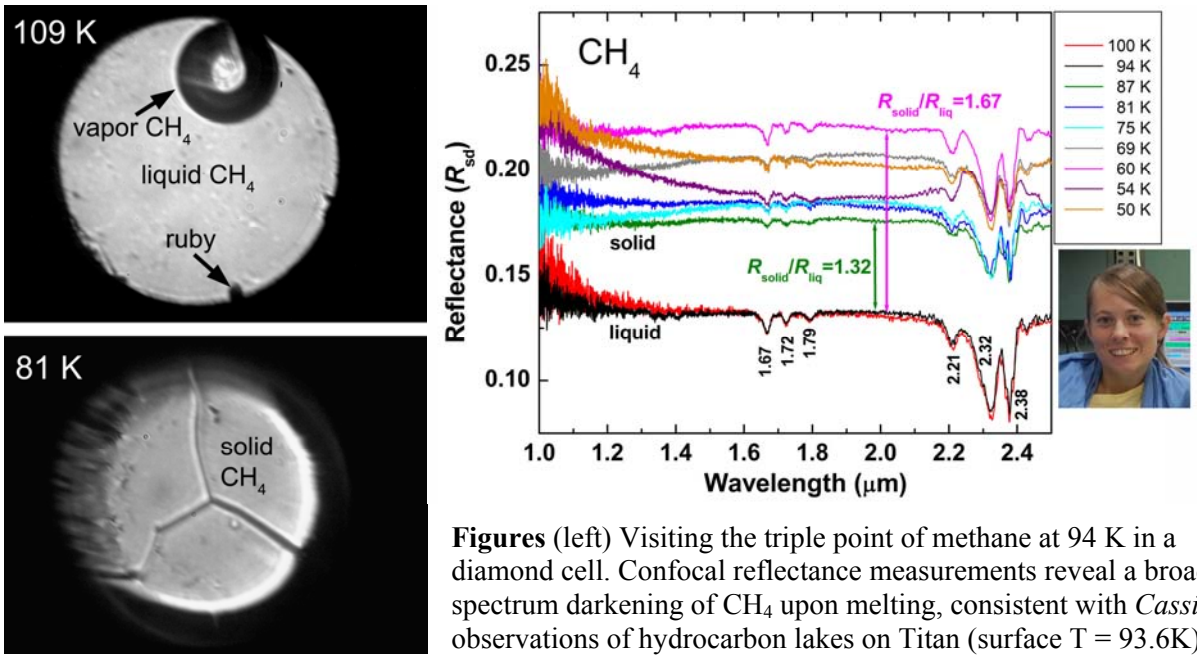

Figures (left) Visiting the triple point of methane at 94 K in a diamond cell. Confocal reflectance measurements reveal a broad-spectrum darkening of CH_4 upon melting, consistent with *Cassini* observations of hydrocarbon lakes on Titan (surface T = 93.6K).

This research was supported in part by NSF EAR-0748707 (CAREER) to S.D.J. Use of the NSLS was supported by the DOE, Office of Science, Office of Basic Energy Sciences, under Contract No. DE-AC02-98CH10886. Operation of beamline U2A at the NSLS is supported by COMPRES under NSF Cooperative Agreement Grant No. EAR 06-49658, and by the U.S. Department of Energy through the Carnegie/DOE Alliance Center (CDAC) contract DE-FC03-03N00144. Accommodations for K.A.A. at NSLS were also supported by COMPRES.

Reference: Adams, K.A., et al., Visible and near-infrared reflectivity of solid and liquid methane: application to spectroscopy of Titan's hydrocarbon lakes. *Submitted* 2011.

Structural Stability of Methane Hydrate at High Pressures

Jinfu Shu[1], Xiao-Jia Chen[1], I-Ming Chou[2], Wenge Yang[3], Jingzhu Hu[4], Russell J. Hemley[1], and Ho-kwang Mao[1]
[1] Geophysical Laboratory, Carnegie Institution of Washington, Washington, DC 20015
[2] 954 National Center, U.S. Geological Survey, Reston, VA 20192
[3] HPSynC, Geophysical Laboratory, Carnegie Institution of Washington, Argonne, IL 60439
[4] National Synchrotron Light Source, Brookhaven National Laboratory, Upton, NY 11973

The structural stability of methane hydrate under pressure at room temperature was examined by both in-situ single-crystal and powder x-ray diffraction techniques on samples with structure types I, II, and H in diamond-anvil cells. Energy dispersive x-ray diffraction (EDXD) was utilized to study the single crystals with white beams at the superconducting wiggler beamline X17C, National Synchrotron Light Source (NSLS), Brookhaven National Laboratory. Above 3 GPa, the methane hydrate decomposed to solid methane and ice powders. Angle dispersive x-ray diffraction (ADXD) was utilized for the structure analysis. 40 keV monochromatic x-ray beams were focused to around 10 microns in diameter (FWHM) for the diffraction study at 16BM-D beamline, High Pressure Collaborative Access Team (HPCAT) of the Advanced Photon Source (APS), Argonne National Laboratory.

The diffraction data for types II (sII) and H (sH) were refined to the known structures with space groups *Fd3m* and *P6₃/mmc*, respectively. Upon compression, sI methane hydrate transforms to the sII phase at 120 MPa, and then to the sH phase at 600 MPa. The sII methane hydrate was found to coexist locally with sI phase up to 500 MPa and with sH phase up to 600 MPa. The pure sH structure was found to be stable between 600 and 900 MPa. Methane hydrate decomposes at pressure above 3 GPa and forms methane with the orientationally disordered *Fm3m* structure and ice VII (*Pn3m*). The results highlight the role of guest (CH_4)-host (H_2O) interactions in the stabilization of the hydrate structures under pressure.

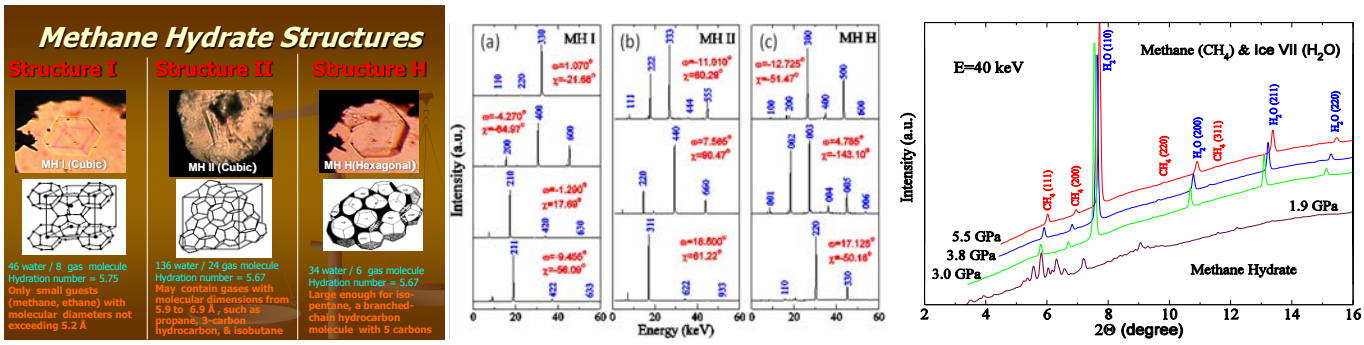

Figure a. The three type (I, II and H) methane hydrate structure.

Figure b. The characteristic EDXD profiles of methane hydrate phases I, II and H.

Figure c. The powder diffraction patterns of methane and ice powders decomposed from methane hydrate above 3 GPa, measured with ADXD with x-ray energy of 40 keV.

Shu, J., X. Chen, I.-M. Chou, W. Yang, J. Hu, R. J. Hemley, and H.-kwang Mao (2011), Structural stability of methane hydrate at high pressures, *Geoscience Frontiers, 2,* 93-100.

This work on the X17C beamline of NSLS which is supported by COMPRES through NSF EAR06-49658.

Simultaneous Measurements of Sound Velocity and X-ray Diffraction of Ice VII to 19 GPa and 873 K

Liqin Sang, Jin Zhang, Jay D. Bass, *University of Illinois at Urbana-Champaign*

Daniel L. Farber, Chantel Aracne, *Lawrence Livermore National Laboratory*

Inno Kantor, Vitali Prakapenka, *GSECARS, APS*

We have measured the sound velocity of Ice VII by Brillouin spectroscopy using membrane-style diamond anvil cell with an external Mo-wire resistance heater at elevated temperatures to 873 K at pressures of 2 GPa to 19 GPa. The unit cells of Ice VII and Au were determined by synchrotron X-ray diffraction, using Au as an in situ pressure gauge. All our samples contained were contained within and chemically insulated from the Re-gasket hole by a gold liner. We determined the melting of Ice VII by monitoring the sound velocity drop and the disappearance of diffraction pattern of Ice VII upon melting. Below ~8 GPa, our results are consistent with the previously determined melting curves. However, our determination of the melting temperature at 12.5 GPa results in a discrepancy of at least 130 K. Given the care taken in the present experiments to avoid potential contamination of the water sample due to reactions at high temperatures between the sample and the gaskets and/or pressure gauges, our new measurements likely provide the first measurements on pure water which displaies an extended stability field of the solid phase. Thus, our new measurements suggest that the melting curve of H_2O at high pressure needs to be reevaluated.

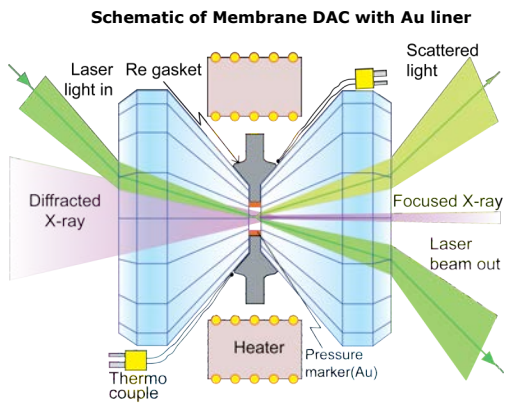

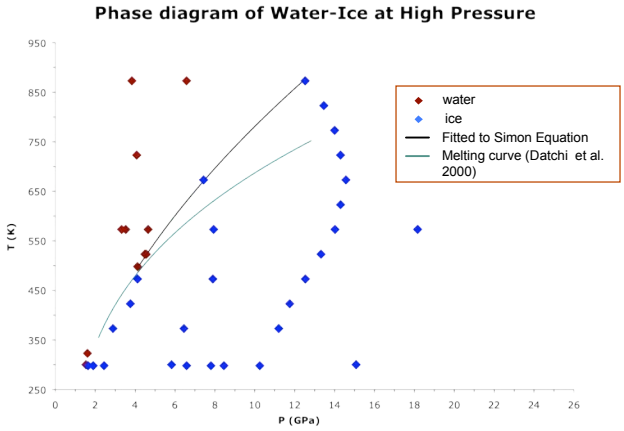

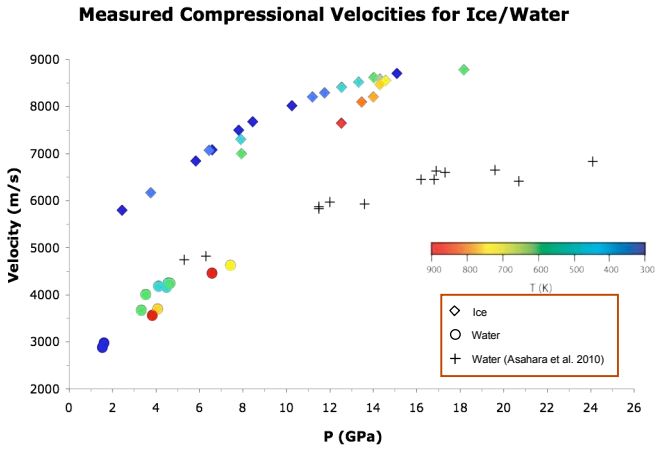

References: Asahara, Y., M. Murakami, Y. Ohishi, N. Hirao, and K. Hirose (2010), Sound velocity measurement in liquid water up to 25 GPa and 900 K: Implications for densities of water at lower mantle conditions, Earth and Planetary Science Letters, 289(3-4), 479-485.

Datchi, F., P. Loubeyre, and R. LeToullec (2000), Extended and accurate determination of the melting curves of argon, helium, ice (H2O), and hydrogen (H-2), Physical Review B, 61(10), 6535-6546.

Fei, Y. W., A. Ricolleau, M. Frank, K. Mibe, G. Y. Shen, and V. Prakapenka (2007), Toward an internally consistent pressure scale, Proceedings of the National Academy of Sciences of the United States of America, 104(22), 9182-9186.

This study was supported by Department of Energy, Basic Energy Science office and partially supported by COMPRES, the Consortium for Materials Properties Research in Earth Sciences under NSF Cooperative Agreement EAR 10-43050. We thank all the staff at 13-BMD GSECARS for their kindly help on our experiment.

Investigations of planetary differentiation from high P-T phase equilibria of natural materials

Lisa R. Danielson[1], Kevin Righter[1], Yanbin Wang[2], and Kurt Leinenweber[3]: [1]NASA Johnson Space Center, [2]GSECARS, APS, University of Chicago, [3]Arizona State University

Chondritic material is thought to be the fundamental building blocks of terrestrial planets and planetessimals. Therefore, crystallization of chondritic material can be used to simulate an accreting and segregating bulk planet. Although chondritic and peridotitic phase equilibria below 20 GPa have been studied in detail (Zhang and Herzberg, 1994; Agee et al., 1995; Wasserman et al., 2001; Litasov and Ohtani, 2002; Asahara et al., 2004; Danielson et al., 2004; Lee et al., 2004), experiments above 20 GPa, and particularly ≥27 GPa, are lacking. Because this pressure range represents the transition into the Earth's lower mantle, experiments conducted in this pressure range are critical to understanding early crystallization of the deepest planetary mantles. Therefore, the objective of this study is to conduct in situ measurements of the liquidus phases and temperatures for a number of planetary mantle analog materials at pressures above 20 GPa.

Experiments were carried out at the Large Volume Press at the Advanced Photon Source, Argonne National Laboratory. Energy dispersive X-ray diffraction data were collected between 1500 °C and 2350 °C. A 3mm TEL beamline modified "Fei-type" assembly was used in experiments and developed by Leinenweber and Soignard as part of the COMPRES cooperative agreement (figure inset below). X-ray windows are a slit in the Re furnace and aluminaor graphite plugs in the lanthanum chromite. The view through the slit can be seen in the radiography image of the uncompressed or heated assembly below, left – the darker grey regions in the column are areas of more Re foil overlap. A 1:1 by weight mixture of MgO and diamond powder was used as a pressure standard and packed between the capsule and thermocouple and/or under the capsule.

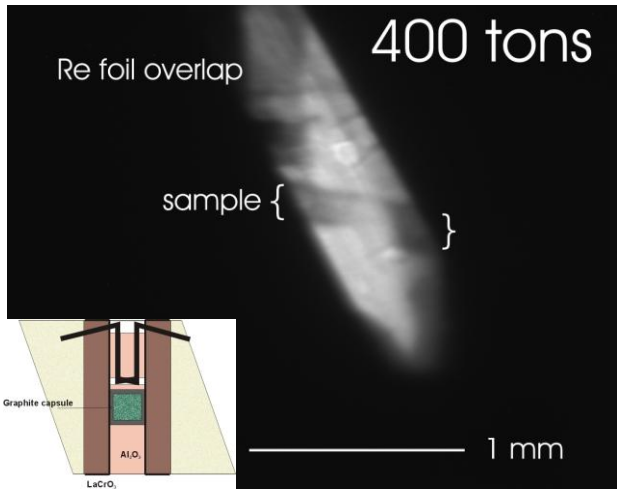

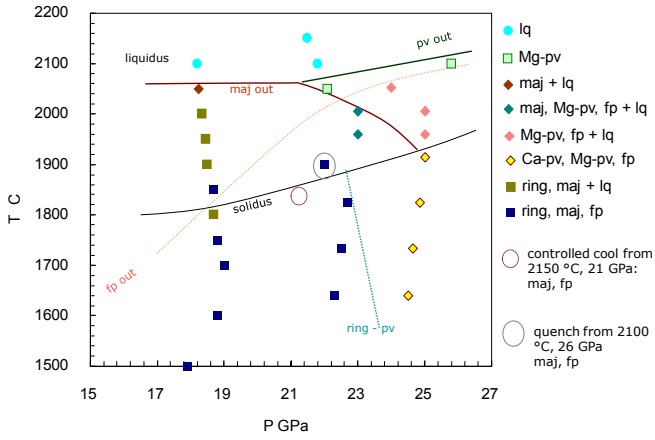

Mg,Fe perovskite is the liquidus phase above 21 GPa and 2050 °C for Allende, but ferropericlase slope may become the liquidus phase above 25 GPa. Both liquidus slopes for Allende and peridotite are at lower temperatures than previously extrapolated values. A shallow liquidus slope is consistent with deeper, hotter magma ocean. In a magma ocean crystallizing from the bottom up, this scenario may not crystallize enough perovskite to drive an oxidation pump of the mantle.

Agee et al. (1995) *J. Geophys. Res.*, 100, 17725-17740. Asahara et al. (2004) *Phys. Earth Planet. Int.*, 143-144, 421-432. Danielson et al. (2004) *Eos Trans. AGU*, 85(47), Fall Meet. Suppl., V43C-1432. Litasov and Ohtani (2002) *Phys. Earth Planet. Int*, 134, 105-127. Lee et al. (2004) *Earth Planet. Sci. Lett*, 223, 381-393. Zhang and Herzberg (1994) *J. Geophys. Res*, 99, 17729-17742.

Origin of Earth's water from highly siderophile element partitioning between core and mantle. K. Righter (NASA-JSC), M. Humayun (Florida State Univ.), L.R. Danielson (NASA-JC).

Three models have been advanced to explain the origin of water on Earth. The first of these is suggests that the Earth acquired its water early, during the accretion process (1). A second model proposes that water arrived just at the end of accretion, after the huge metallic core of the Earth had finished forming (2). The third model is the traditional model in which the Earth's origin has been attributed to comets or another kind of volatile-bearing body that arrived late and well after accretion was complete (3). The second and third hypotheses is linked to a class of elements called the highly siderophile elements; these elements are thought to reside mainly in the Earth's core, but they are also present in the mantle at concentrations similar to those that would be expected if small amounts of chondritic material were added to the mantle after the core had formed. These models were originally proposed in the 1970s, at a time at which relevant high P-T data were unavailable (2).

To test this model more thoroughly, we studied the distribution of the HSE palladium (Pd) to test whether its abundance in the Earth's mantle requires the addition of later chondritic material, or whether its presence can be explained by simple metal-silicate equilibrium between the mantle and the core during accretion. The results, including multi-anvil experiments at 12 to 15 GPa, have shown that the concentration of Pd in the Earth's mantle can be explained by high P-T distribution between the core and the mantle early in the history of the planet (4). The implications are that late additions of water- and HSE-bearing material are not necessary, and that water and HSE concentrations in the Earth's mantle were established very early during accretion. Other elements (e.g., gold, platinum, iridium, and rhodium) are being investigated to determine whether they are also compatible with this simple, and early, origin of water on Earth.

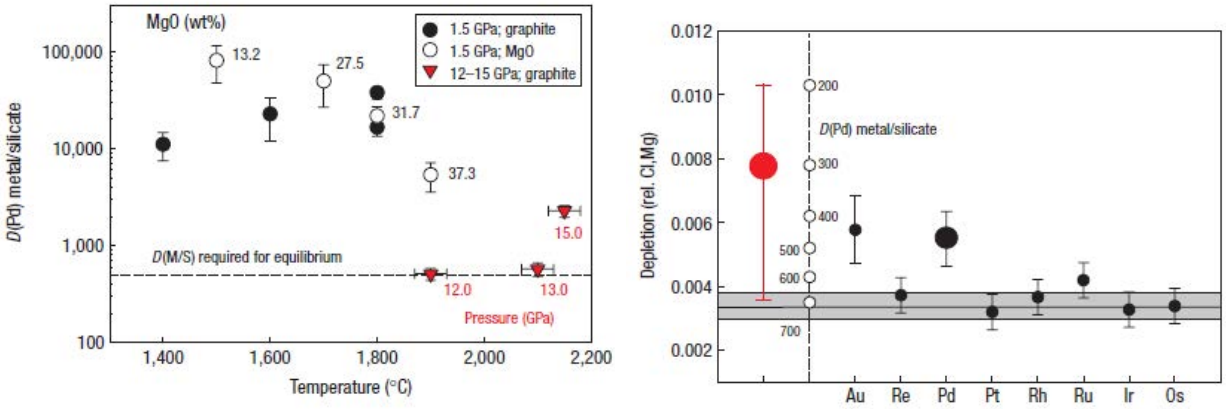

Figure 1(left): Metal-silicate partition coefficients from this study showing the decrease in D(Pd) at higher temperature (and pressure) to values required if an equilibrium scenario can be valid. Figure 2(right): The calculated mantle content of Pd using a high P-T D(Pd) (red circle) compared to the measured Pd content (black).

The multi-anvil experiments in this study were carried out at NASA JSC, utilized COMPRES assembly parts (5), and benefitted from discussions and interactions with K. Leinenweber, ASU. This research is supported by NASA funding from the Cosmochemistry and Mars Fundamental Research Programs.

References: (1) Abe, Y., Ohtani, E., Okuchi, T., Righter, K. and Drake, M.J. (2000) Water in the early Earth. in (R.M. Canup and K. Righter, eds.) *Origin of the Earth and Moon*, Univ. of Arizona Press, Tucson, 413-434; (2) Chou, C. L. (1978) Fractionation of siderophile elements in the Earth's upper mantle. *Proc. 9th. Lunar Planet. Sci. Conf.* 219–230; (3) Delsemme, A.H. (1991) Cometary Origin of nitrogen, carbon and water on the Earth. Origins of Life and Evolution of Biospheres 21, 279-289; (4) Righter, K., Humayun, M., Danielson, L.R. (2008) Partitioning of palladium at high pressures and temperatures during core formation/ Nature Geosciences 1, 321-324; (5) Leinenweber, K., Mosenfelder, J., Diedrich, T., Soignard, E., Sharp, T.G., Tyburczy, J.A., Wang, Y. (2006) High-pressure cells for in situ multi-anvil experiments. High Pressure Research 26, 283-292.

Phase transition in the mantles of large earth-like planets (Super-Earths)

Sang-Heon Dan Shim and Brent Grocholski, *Massachusetts Institute of Technology*
Vitali Prakapenka, *GSECARS, University of Chicago*

The last decade has witnessed remarkable developments in observing planets outside of our Solar system. Among those planets, some are believed to have similar composition as Earth (super-earths). Recent developments allow for the measurements of densities and masses of those planets. Therefore, equations of state and phase transitions in constituent materials can play important roles in modeling the structure and composition of the planets using the measured properties.

Recent computational mineral physics studies have proposed that $MgSiO_3$ breaks down to MgO and SiO_2 at the pressure-temperature conditions expected for the core-mantle boundary of super-earths. Although the pressure-temperature conditions exceed the capability of the diamond-anvil cell technique, the computational studies also predicted a similar breakdown in $NaMgF_3$ which is known as an excellent analog for $MgSiO_3$.

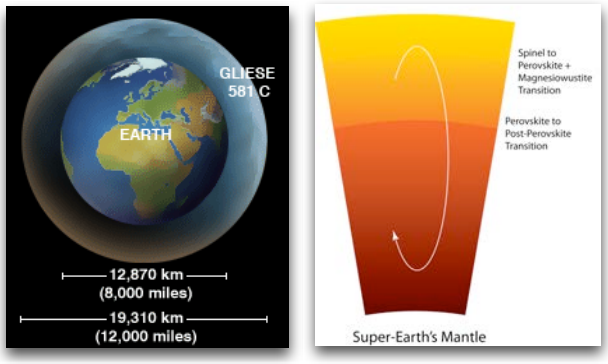

(Left) Size comparison between Earth and a super-earth. (Right) Schematic diagram of mantle convection in a super-earth.

We have conducted X-ray diffraction measurements on $NaMgF_3$ ($MgSiO_3$ analog) and MgF_2 (SiO_2 analog) at the GSECARS sector of the Advanced Photon Source. We found that the post-perovskite phase remains stable at pressure-temperature conditions much higher than those predicted for the breakdown in $NaMgF_3$. Our study on MgF_2 revealed a phase which is previously unknown. This new phase would make the breakdown products ($NaF + MgF_2$) less stable than the post-perovskite phase ($NaMgF_3$), expanding the stability field of the post-perovskite phase to much greater pressure-temperature than previously thought.

The possible breakdown of $MgSiO_3$ post-perovskite may have huge impact on the scale of mantle convection in super-earths. Our study suggests that there would be no major barrier for mantle convection in super-earths, opening the possibility of whole mantle convection in super-earths.

Publications

Grocholski, B., Shim, S.-H. and Prakapenka, V. B. Stability of the $MgSiO_3$ analog $NaMgF_3$ and its implication for mantle structure in super-Earths. Geophys. Res. Lett. 37, L14204, 2010.

Mineralogy, Crystal Chemistry, and Phase Transitions

Novel Disordered Materials at High Pressure

F.X. Zhang, M. Lang, R.C. Ewing *University of Michigan*
Z.X. Liu *Geophysical Laboratory, Carnegie Institution of Washington*

Pyrochlore, $A_2B_2X_6Y$, is an isometric structure with over 500 different compositions and a wide range of technological applications, from being radiation-resistant nuclear materials to fast ionic conductors. Properties change dramatically depending on composition and the degree of ordering in the cation sites and anion vacancies. A detailed quantitative study of pressure-induced disordering in $La_2Zr_2O_7$ pyrochlore was carried out by means of *in situ* synchrotron X-ray diffraction measurements using the COMPRES beamline X17C of the NSLS. The disordering in the cation and anion sites affects individual diffraction peaks, and the contribution of disordering to the diffraction intensities were quantitatively distinguished by Rietveld refinement analysis. With increasing pressure, anion disordering occurs below 5 GPa, whereas cation anti-site defects dominate the disordering process above 10 GPa. An anomalous lattice expansion was also confirmed in the lanthanum pyrochlore at 10 GPa by X-ray diffraction, Raman scattering, and infrared absorption measurements (COMPRES beamline U2A) in experiments utilizing a water-bearing pressure medium. Water intercalation in pyrochlore oxides may occur during pressurization or ion irradiation, and it is mainly caused by the cation antisite defects that result from disordering.

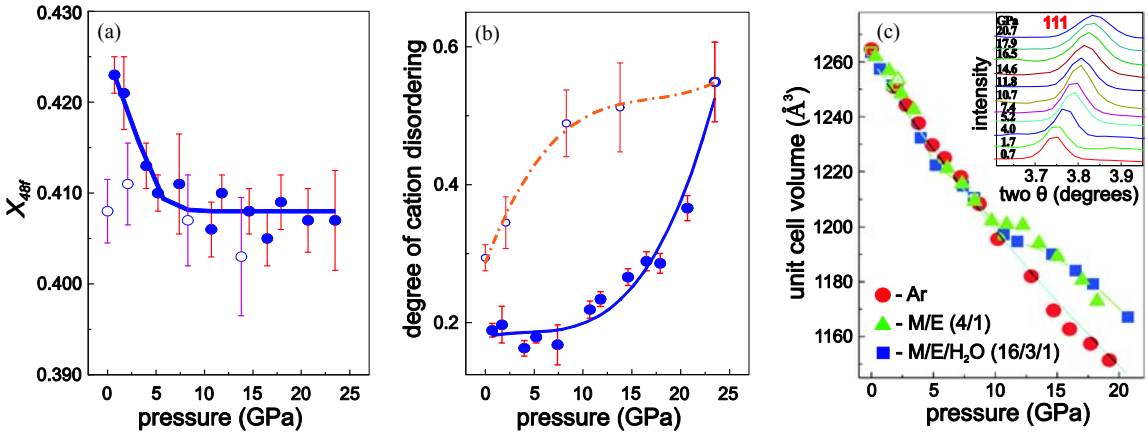

Figures: *Quantitative refinement analysis of $La_2Zr_2O_7$ XRD patterns at pressure yields the degree of (a) anion disordering, i.e., X_{48f} parameter, and (b) cation disordering. The open symbols were measured during pressure-quenching. The anion disordering precedes the formation of cation antisite defects. (c) Pressure (P)-volume (V) curves for $La_2Zr_2O_7$ pyrochlore measured with different pressure media. Only the P-V curve of the Ar pressure medium can be well fitted with the Birch-Murnaghan equation of state. An anomalous lattice expansion concurrent with the onset of cation disordering is evident at ~10 GPa due to water incorporation. The inset shows the normalized (111) diffraction maxima during pressurization with the M/E/H_2O pressure medium.*

Acknowledgements: This work was supported by the Office of Basic Energy Sciences of the U.S. Department of Energy, through Grant No. DE-FG02-97ER45656. The use of the X-ray beam line at X17C and infrared at the U2A station of NSLS is supported by NSF COMPRES EAR01-35554 and by USDOE contract DE-AC02-10886.

Reference: F.X. Zhang, M. Lang, Z.X. Liu, and R.C. Ewing, *Phys. Rev. Lett.* 105 (2010) 015503.

Highlights: This work was selected as 2010 science highlight at the Geophysical Laboratory at the Carnegie Institution.

Structural Transition and Electron Transfer in Coffinite, $USiO_4$, at High Pressure

F. Zhang, V. Pointeau, L. Shuller, M. Lang, U. Becker, R. Ewing *University of Michigan*
D.M. Reaman, W.R. Panero *Ohio State University*
Z.X. Liu *Geophysical Laboratory, Carnegie Institution of Washington*
J.Z. Hu *Stony Brook University*
C. Poinssot *Commissariat á l'Energie Atomique*

Coffinite, $USiO_4$, forms as an alteration product of uraninite (UO_2) under reducing conditions in the presence of silica-rich solutions occurring in nature as microscopic intergrowths with other minerals. Coffinite and thorite ($ThSiO_4$) are the only actinide minerals that have the zircon structure. The high-pressure behavior of synthetic coffinite was, for the first time, studied in a diamond-anvil cell up to 45 GPa. *In situ* synchrotron X-ray diffraction and infrared (IR) spectroscopy at the COMPRES beamlines X17C and U2A of the NSLS consistently evidenced a pressure-induced phase transition to a scheelite-structured polymorph at 14 – 17 GPa. This irreversible transformation, which occurs similarly in zircon ($ZrSiO_4$), was independently confirmed by quantum-mechanical calculations using density functional theory. Interestingly, the IR measurements suggest that water is partially covalently bonded within the coffinite structure in correlation with a possible pressure-induced increase in the oxidation state from U^{4+} to U^{5+}.

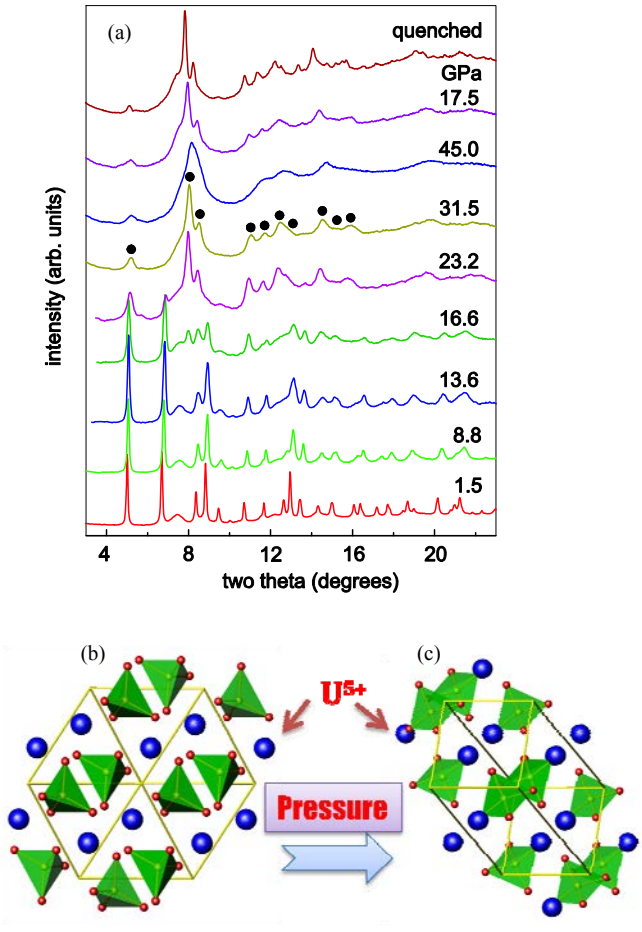

Figures: *(a) Selected XRD patterns show a pressure-induced phase transition in coffinite starting at ~16.6 GPa and a partial amorphization at significantly higher pressures. The dot symbols indicate the diffraction maxima from the scheelite-structured $USiO_4$ high-pressure phase. (b) Lattice of zircon-structured coffinite at ambient conditions and (c) scheelite-structured high-pressure phase. Blue spheres are U, green spheres are Si and red spheres are O.*

Reference: F.X. Zhang, V. Pointeau, L.C. Shuller, D.M. Reaman, M. Lang, Z.X. Liu, J. Hu, W.R. Panero, U. Becker, C. Poinssot, and R.C. Ewing, *Am. Mineral.* 94 (2009) 916-920.

Acknowledgements: This work was supported by the Office of Basic Energy Sciences of the U.S. Department of Energy, through grant no. DE-FG02-97ER45656 and the NSF NIRT program (EAR-0403732). Support for V.P. was provided by the Commissariat à L'Energie Atomique. M.L. acknowledges support from the German Research Foundation DFG. The use of the NSLS beamlines X17C and U2A are supported by NSF COMPRES EAR01-35554 and by US-DOE contract DE-AC02-10886.

Irradiation-Induced Stabilization of Zircon ($ZrSiO_4$) at High Pressure

M. Lang, F.X. Zhang, J. Lian, R.C. Ewing *University of Michigan*
C. Trautmann, R. Neumann *GSI Helmholtz Center for Heavy Ion Research*

Zircon, the most important accessory mineral of Earth's crust, transforms under high pressure to reidite, a scheelite-structured polymorph, which was recently found in association with meteorite impact structures. The influence of accumulated radiation damage on the zircon-to-reidite transition was studied by means of *in situ* synchrotron X-ray diffraction experiments at the COMPRES beamline X17C of the NSLS. It was evident that zircon, pre-irradiated with 1.47-GeV Xe ions to a fluence of $5x10^{12}$ ions/cm^2, formed only minor amounts of reidite up to 36 GPa, whereas an unirradiated zircon was almost completely transformed to reidite within the same pressure range. By means of Raman scattering and transmission electron microscopy, it was confirmed that the stability field of the irradiated zircon is expanded to higher pressures as a result of the interplay between pressure, ion beam-induced amorphization, and the formation of nanoscale damage domains. These results provide insight into the formation conditions of reidite in nature (e.g., during meteorite impact) and illustrate how pressure-induced phase transitions in minerals may be affected by pre-existing damage and microstructure of the starting material.

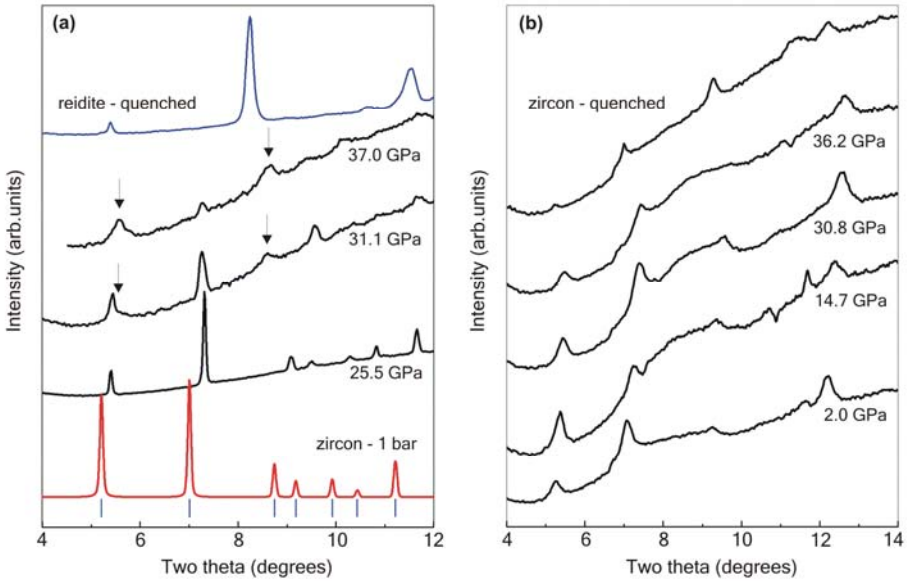

Figures: *XRD data of zircon pressurized in diamond anvil cells (a) unirradiated and (b) irradiated with 1.47-GeV Xe ions. (a) The unirradiated zircon gradually transformed to reidite above 25.5 GPa, as indicated by new peaks (arrows); the sample quenched from 37 GPa showed only reidite diffraction peaks. The vertical bars indicate the diffraction-peak positions of the zircon structure. (b) The irradiated specimen showed no noteworthy phase transition up to 36.2 GPa; the quenched sample exhibited only the typical diffraction peaks of heavily damaged zircon.*

Acknowledgements: This work was supported by the Office of Basic Energy Sciences, USDOE under DOE grant DE-FG02-97ER45656. The use of NSLS at X17C station is supported by NSF COMPRES EAR01-35554 and by US-DOE contract DE-AC02-10886. M. L. acknowledges support from German Science Foundation DFG.

Reference: M. Lang, F.X. Zhang, J. Lian, C. Trautmann, R. Neumann, R.C. Ewing, *Earth and Planetary Science Letters* 269 (2008) 291-295.

Response of Pyrochlore to Extreme Conditions

F.X. Zhang, J.W. Wang, J. Lian, M. Lang, U. Becker, R.C. Ewing *University of Michigan*

Pyrochlore has a flexible structure that can exist in more than 500 chemical compositions with a wide variety of chemical and electronic properties with many technological applications. Some pyrochlores can also incorporate actinides, such as plutonium, so there is great interest in their use as nuclear waste forms or as inert matrix fuels. In order to investigate the effects of high pressures and irradiation on pyrochlore, five closely related compositions from the gadolinium titanate oxide endmember, $Gd_2Ti_2O_7$, to the gadolinium zirconate oxide endmember, $Gd_2Zr_2O_7$, were compressed in diamond-anvil cells up to 45 GPa pressure. Synchrotron X-ray diffraction at the COMPRES beamline X17C of the NSLS was used to characterize structural details as a function of pressure. The structure of gadolinium titanate oxide remained relatively stable under the highest pressures tested (45 GPa), but the gadolinium zirconate oxide only maintained stability up to 23 GPa, above which it became structurally distorted. Upon pressure release, the zirconate pyrochlore disordered further to a very stable defect-fluorite structure, whereas the titanate pyrochlore transformed to the amorphous state. A surprisingly similar behavior is observed after ion-beam exposure. Quantum mechanical calculations show that subtle changes in structure significantly influence the response of pyrochlore to elevated pressure and irradiation fields. The performance of these materials in extreme environments is directly related to the energetics of the disordering process.

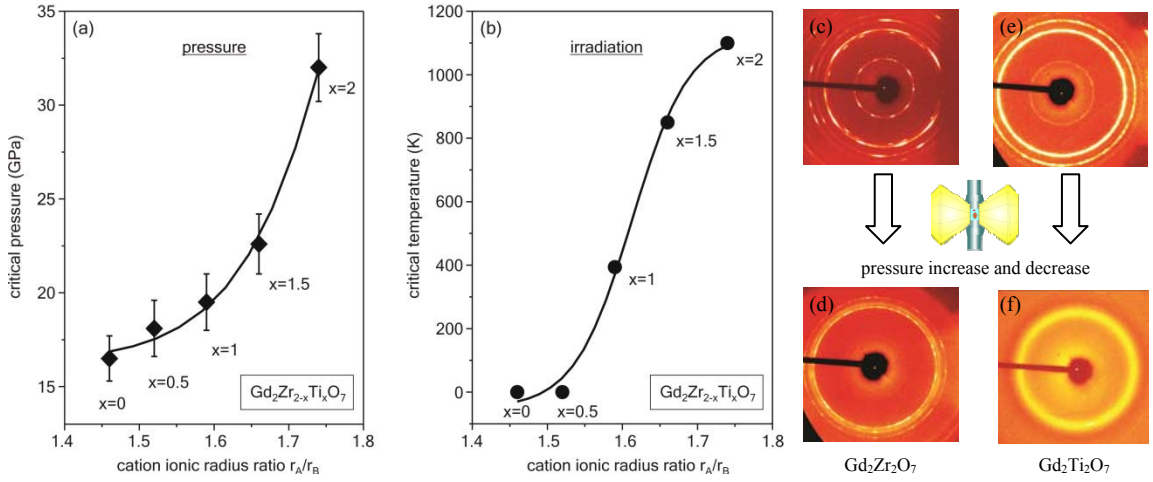

Figures: *(a) The replacement of Ti at the Zr site increases significantly the critical pressure of transition from the ordered pyrochlore structure to the distorted high-pressure phase in the binary system $Gd_2Zr_{2-x}Ti_xO_7$. (b) The same trend was found for the radiation damage-induced, crystalline-to-amorphous structural transformation expressed by the critical amorphization temperature, above which materials cannot be amorphized. Diffraction images after pressure increase to the maximum value and complete quenching show: (c,d) transformation of pyrochlore to defect-fluorite structure in $Gd_2Zr_2O_7$; (e,f) pressure-induced amorphization of $Gd_2Ti_2O_7$ pyrochlore.*

Acknowledgements: This work was supported by the Office of Basic Energy Sciences of the U.S. Department of Energy, through Grant No. DE-FG02-97ER45656 and the NSF NIRT program (EAR-0309772). The use of X-ray beamline at X17C station of NSLS is supported by NSF COMPRES EAR01-35554 and by US-DOE contract DE-AC02-10886.

Reference: F.X. Zhang, J.W. Wang, J. Lian, M.K. Lang, U. Becker, and R.C. Ewing, *Phys. Rev. Lett.* 100 (2008) 045503.

Highlights: This work was selected as 2008 COMPRES and 2009 NSLS science highlight.

High Pressure Synchrotron X-ray Diffraction Study of the Pyrochlores: $Ho_2Ti_2O_7$, $Y_2Ti_2O_7$ and $Tb_2Ti_2O_7$

Paul R. Scott[1] *, A. Midgley[1], O. Musaev[1], D.V.S. Muthu[2], S. Singh[3], R. Suryanarayanan[3], A. Revcolevschi[3], A.K. Sood[2], and M. B. Kruger[1]

[1] *Department of Physics, University of Missouri-Kansas City, MO 64110, USA*
[2] *Department of Physics, Indian Institute of Science, Bangalore 560012, India*
[3] *Laboratoire de Physico-Chimie de l'Etat Solide, ICMMO, CNRS, UMR8182, Bâtiment 414, Université Paris-Sud, 91405 Orsay, France*

Synchrotron based powder x-ray diffraction, at beamline X17C of the NSLS and at 12.2.2 at the ALS, was used to study the phase diagrams and determine the compressibilities of the pyrochlore rare earth titanates: $Ho_2Ti_2O_7$, $Y_2Ti_2O_7$ and $Tb_2Ti_2O_7$ to ~ 50 GPa. The bulk moduli of the cubic phase of these materials were calculated to be 213 ±2, 204 ±3 and 199 ±1 GPa, respectively. The onset of a structural phase change from cubic to monoclinic was observed near 37, 42 and 39 GPa, respectively. The bulk modulus for the high pressure monoclinic phase of $Y_2Ti_2O_7$ has been determined to be 185 ±3 GPa.

Recently, interest has grown in materials that crystallize in the rare earth titanate pyrochlore structure ($A_2Ti_2O_7$, where A is a rare earth trivalent ion) due to their magnetic properties. Materials that crystallize in this structure have been reported to exhibit Neel ordered ($Er_2Ti_2O_7$), spin-liquid ($Tb_2Ti_2O_7$) and spin-ice states ($Dy_2Ti_2O_7$ and $Ho_2Ti_2O_7$). The pyrochlore structure is also of interest due to its ability to immobilize actinides and thus it could aid in the disposal of radioactive waste and play a role in mitigating weapons proliferation.

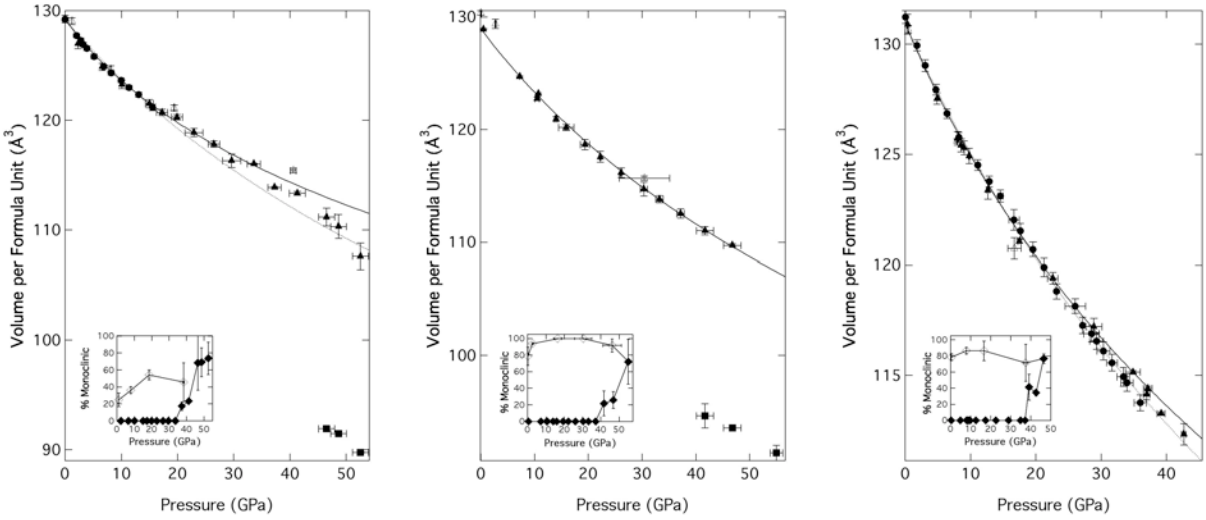

$Ho_2Ti_2O_7$ $Y_2Ti_2O_7$ $Tb_2Ti_2O_7$

Reference: P. R. Scott, A. Midgley, O. Musaev, D. V. S. Muthu, S. Singh, R. Suryanarayanan, A. Revcolevschi, A. K. Sood, and M. B. Kruger, 'High-pressure synchrotron X-ray diffraction study of the pyrochlores: $Ho_2Ti_2O_7$, $Y_2Ti_2O_7$ and $Tb_2Ti_2O_7$', High Pressure Research, **31**, 219-227 (2011)

This work was partially supported NSF Contract Number DMR-0605493 and DMR-0923166, NSF COMPRES EAR01-35554 and by US-DOE contract DE-AC02-10886 to NSLS. The Advanced Light Source is supported by the Director, Office of Science, Office of Basic Energy Sciences, of the U.S. Department of Energy under Contract No. DE-AC02-05CH11231.

Local structure variations observed in orthoenstatite at high-pressures

Dongzhou Zhang[1,*], Jennifer M. Jackson[1], Wolfgang Sturhahn[2], and Yuming Xiao[3]

[1] Seismological Laboratory, California Institute of Technology, Pasadena, CA 91125.
[2] Argonne National Laboratory, Argonne, IL 60439. Now at Jet Propulsion Laboratory.
[3] HP-CAT, Geophysical Laboratory, Carnegie Institution of Washington, Argonne, IL 60439.
*Email: dzzhang@caltech.edu

The site-specific behavior of iron in an orthoenstatite-structured ^{57}Fe-enriched (M1)(M2)Si_2O_6 powdered sample was explored using synchrotron Mössbauer spectroscopy (SMS) and diamond anvil cells in two independent experiments at ambient temperature (*Zhang et al.* Am. Min. 2011, *in press*). The SMS experiments were conducted at beamlines 3-ID-B and 16-ID-D of the Advanced Photon Source, Argonne National Laboratory. In one experiment, NaCl was used as the pressure-transmitting medium (ambient pressure to 36 GPa), and in another experiment, Ne surrounded the sample (4.1 to 26.8 GPa). The hyperfine parameters of the M1 and M2 sites at room pressure are in excellent agreement with previous literature values obtained using conventional Mössbauer spectroscopy and yield $(Mg_{0.98}Fe_{0.02})(Mg_{0.76}Fe_{0.24(1)})Si_2O_6$ as the chemical formula. Analyses of both data sets reveal a change in the trend or discontinuity in the hyperfine parameters, indicative of a transformation in orthopyroxene (Fig. 1) at around 10 GPa (~300 km depth). However, the detailed behaviors of the iron-sites with pressure appear to depend on the local stress conditions provided by the different pressure media. Our observations may help explain the reported variations in structural transition behavior for orthopyroxenes at high-pressures. In regions of the upper mantle, where lateral heterogeneity in stress conditions and temperature may exist, variations in structural transition behavior in orthopyroxene may occur.

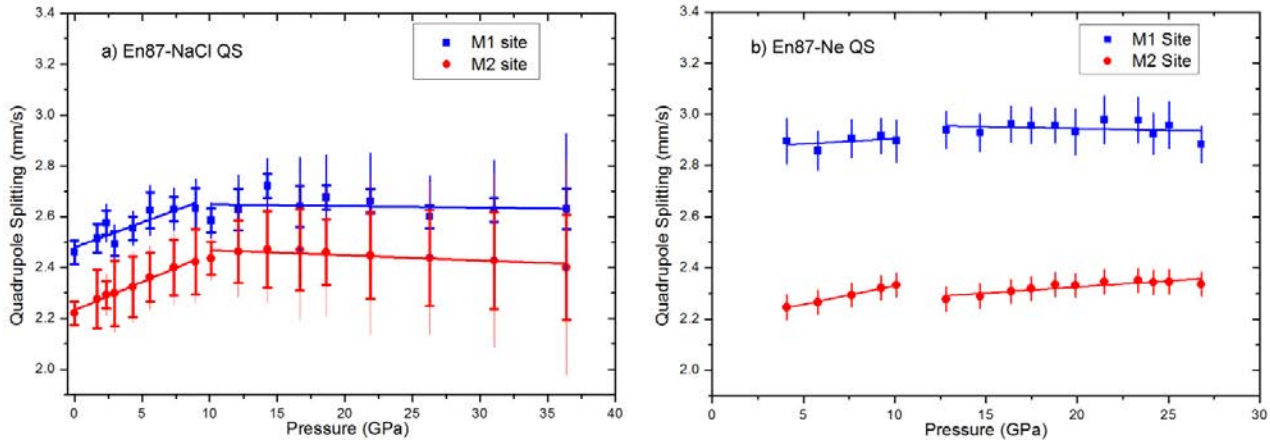

Figure 1: Quadrupole splittings for the two different iron sites in $(Mg_{0.98}Fe_{0.02})(Mg_{0.76}Fe_{0.24(1)})Si_2O_6$ enstatite (En87) as a function of pressure, determined from the best fit of the SMS spectra. Left panel: En87 in NaCl pressure medium; right panel: En87 in Ne pressure medium. The lines are linear fits to the data. In subfigure (a), the thicker vertical bars are the best-fit FWHM of QS, and the thin bars are the fitting errors.

Excess volume and exsolution in pyrope-grossular garnets at high P-T

Wei Du and Dave Walker [Lamont-Doherty Observatory, Columbia U.] and Simon Clark and Martin Kunz [ALS/COMPRES, Lawrence Berkeley Lab]

The study of halite-sylvite chlorides done during COMPRES I showed that excess volumes were strongly T and P dependent when measured *in situ* at P and T, but that those excesses were not quenchable. In contrast there are very large systematic differences in quenched excess volumes in the pyrope-grossular garnets prepared in piston/cylinder (PC), multianvil (MA), or diamond anvil (DAC) devices. The systematics of our quenched excess volumes from MA and DAC are much more positive and better behaved than in literature PC syntheses. These results suggest that disorder may be possible after all in this series even though previous attempts to identify it have met with limited success.

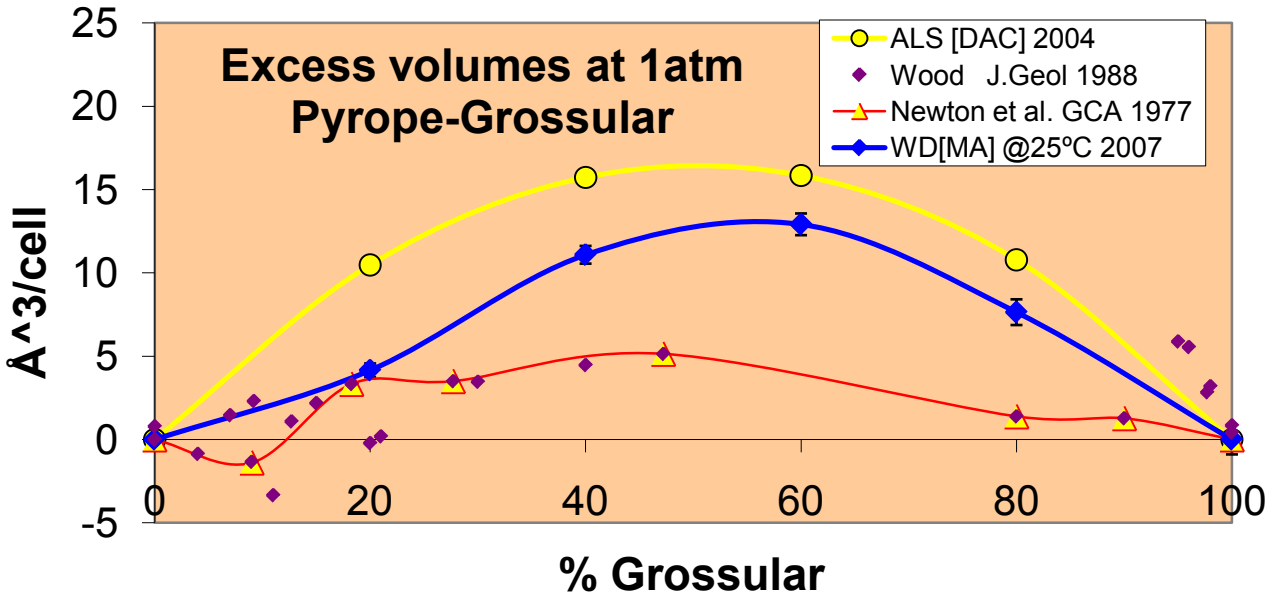

Large positive excess volumes were then measured on ALS beamline 12.2.2 at T to 600 °C and P to 10 GPa. The persistence of the large positive excess volumes at P-T suggested that immiscibility should be observable in this system in the laboratory. **Both convergent and divergent garnet pairs at Gr 14 and Gr 36 have been established at 1200 °C/8 GPa, confirming this proposition and constraining garnet mixing properties better than from H, S, and V measurements.** This forms the basis of Wei Du's PhD thesis at Columbia University. This work was supported by the COMPRES initiative, by the National Science Foundation under grant EAR02-07546 to DW, and by the Advanced Light Source, which is supported by the Director, Office of Science, Office of Basic Energy Sciences, Materials Sciences Division, of the U.S. Department of Energy under Contract No. DE-AC03-76SF00098 at Lawrence Berkeley National Laboratory.

Pressure induced phase transition of nanocrystalline and bulk maghemite (γ-Fe_2O_3) to hematite (a-Fe_2O_3)

Hongyang Zhu[1], Yanzhang Ma[1], Haibin Yang[1], Cheng Ji[1], Dongbin Hou[1], Lingyun Guo[1]
[1] Texas Tech University, [2]Jilin University

Maghemite (γ-Fe_2O_3) has a cubic inverse-spinel structure with a structural formula $Fe_{21.33}\square_{2.67}O_{32}$, (where $\square$ denotes vacancies) and can be considered as an oxidized magnetite. Maghemite is unstable at high pressure, converting to hematite. The previous reports found that the phase transition in γ-Fe_2O_3 was affected by the preparation method of the specimen, metal ion doping, particle size, etc. The unusual phase transition of γ-Fe_2O_3 is believed to be caused by its special structure, vacancies. The purpose of this work is to explore the effect of size on phase transition of γ-Fe_2O_3, as well as the role of vacancies in the phase transition process.

In this work, we did not observe the effect of size of particles on the phase transition pressure in nanocrystalline γ-Fe_2O_3, contrary to most other nanomaterials. The abnormal phase transition of bulk and nanocrystalline γ-Fe_2O_3 can be ascribed to its special structure, because of vacancies. Increasing pressure induces the stress concentration at vacancy sites. Thermodynamically, the new structure phase prefers to nucleate at a vacancy site. It can be considered the phase transition started from a certain vacancy site because of the stress concentration. Therefore, compared with the effect of vacancy, the effect of size is negligible.

The presence of vacancies in γ-Fe_2O_3 affects its compressibility, making compression even easier at low pressures and even harder at higher pressures. Therefore, the compression process can be molded as two compression steps, with the first being compression of crystal vacancies and the second being compression of crystal. This process leads to a larger K'_{OT} when volume-pressure data are fitted to third-order BM EoS.

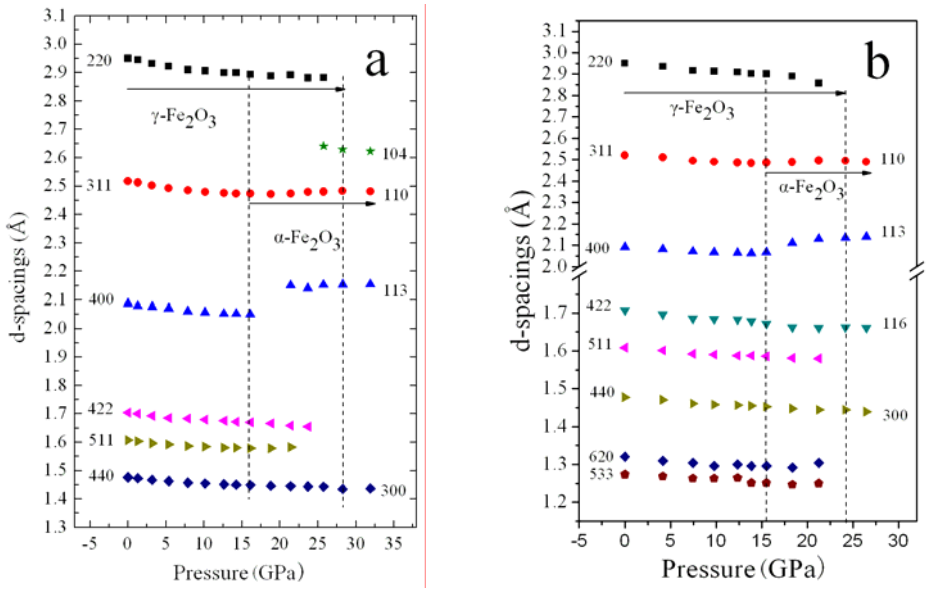

The pressure dependence of d-spacings of bulk (a) and nanocrystalline γ-Fe_2O_3 (b)

Synchrotron Infrared Studies of Synthetic $^{A}Na^{B}(Na_xLi_{1-x}Mg_1)^{C}Mg_5Si_8O_{22}(OH)_2$ (with x=1, 0.6, 0.2 and 0) $P2_1/m$ Amphiboles at High Pressure

Gianluca Iezzi [*Dipartimento di Scienze della Terra, Università G. D'Annunzio, I-66013 Chieti Scalo, Italy*], Zhenxian Liu [*Geophysical Laboratory, Carnegie Institution of Washington*], and Giancarlo Della Ventura [*Dipartimento di Scienze Geologiche, Università di Roma Tre, Largo S. Leonardo Murialdo 1, I-00146 Roma, Italy*]

The high-pressure behavior of three synthetic amphiboles crystallized with space group $P2_1/m$ at room conditions in the system Li_2O–Na_2O–MgO–SiO_2–H_2O has been studied by *in-situ* synchrotron infrared absorption spectroscopy. The amphiboles have compositions $^{A}Na^{B}(Na_xLi_{1-x}Mg_1)^{C}Mg_5Si_8O_{22}(OH)_2$ with x = 0.6, 0.2 and 0.0, respectively. The high-P experiments up to 32 GPa were carried out on the U2A beamline at Brookhaven National Laboratory using a diamond anvil cell. The two most intense absorption bands in the OH-stretching infrared spectra can be assigned to two non-equivalent O–H dipoles in the $P2_1/m$ structure, bonded to the same local environment $^{M1M3}Mg_3$–OH–^{A}Na, and pointing toward two differently kinked tetrahedral rings. In all samples these bands progressively merge to give a unique symmetrical absorption band with increasing pressure, suggesting a change in symmetry from $P2_1/m$ to $C2/m$. The pressure at which the transition occurs appears to be linearly correlated to the aggregate B-site dimension. The infrared spectra collected for amphibole B(Na0.2Li0.8Mg1) in the frequency range 50 to 1,400 cm^{-1} also show a series of changes with increasing pressure. The data reported here support the inference of previous results regarding a new high-pressure amphibole polymorph.

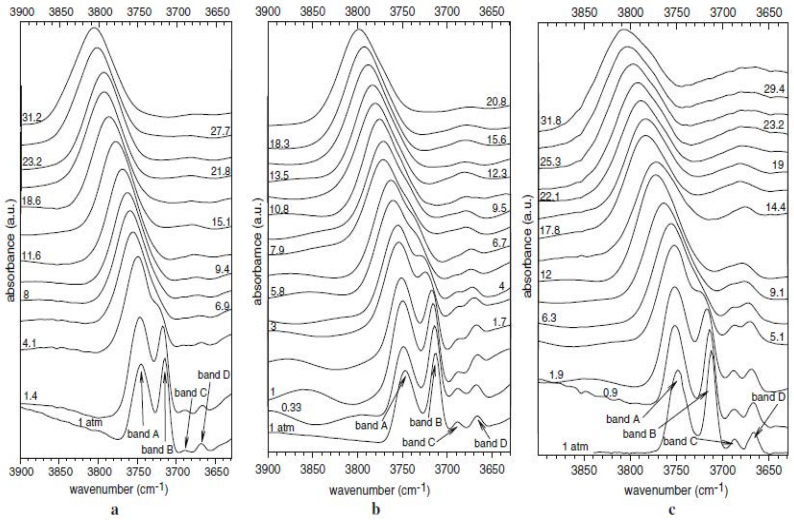

Figure 1a. FTIR absorption spectra of sample 405 (pure sample without pressure medium) on the OH-stretching modes as a function of pressure (in GPa).
b. FTIR OH-stretching vibrational modes of sample 406 (pure sample without pressure medium) as a function of pressure (in GPa).
c. FTIR OH-stretching vibrational modes of sample 407 (pure sample without pressure medium) as a function of pressure (in GPa)

Reference

Iezzi, G., Z. Liu, and G. Della Ventura, Synthetic $^{A}Na^{B}(Na_xLi_{1-x}Mg_1)^{C}Mg_5Si_8O_{22}(OH)_2$ (with x = 0.6, 0.2 and 0) $P2_1/m$ amphiboles at high pressure: A synchrotron infrared study, *Physics and Chemistry of Minerals*, *36*(6), 343-354, (2009).

Acknowledgments

Operation of beamline U2A at the NSLS is supported by COMPRES under NSF Cooperative Agreement Grant No. EAR 06-49658, and by the U.S. Department of Energy through the Carnegie/DOE Alliance Center (CDAC) contract DE-FC03-03N00144.

High-pressure behavior of otavite ($CdCO_3$)

R. Minch, L. Peters,W. Depmeier *Christian-Albrechts-Universität zu Kiel, Germany*
D.-H. Seoung, Y. Lee, *Yonsei University, Republic of Korea*
L. Ehm, L.A. Borkowski, J.B. Parise *Stony Brook University, USA*
L. Dubrovinsky *Bayerisches Geoinstitute, Germany*
B. Winkler *Johan-Wolfgang-Goethe Universität Frankfurt, Germany*
K. Knorr *BrukerAXS GmbH, Germany*

The high-pressure, room temperature behavior of otavite ($CdCO_3$) was investigated by angle-dispersive synchrotron radiation powder diffraction up to 40 GPa, Raman spectroscopy up to 23 GPa and quantum mechanical calculations based on density functional theory. The calcite-type structure of $CdCO_3$ is stable up to at least ~19 GPa as shown by Raman spectroscopy. The compression mechanism was obtained from structure refinements against the diffraction data. The quantum mechanical calculations propose a calcite–aragonite phase transition to occur at about 30 GPa. The existence of a pressure-induced phase transition is supported by the Raman and diffraction experiments. Evidence for the transformation is given by broadening of X-ray reflections and external Raman bands starting from about 19 GPa in both experiments.

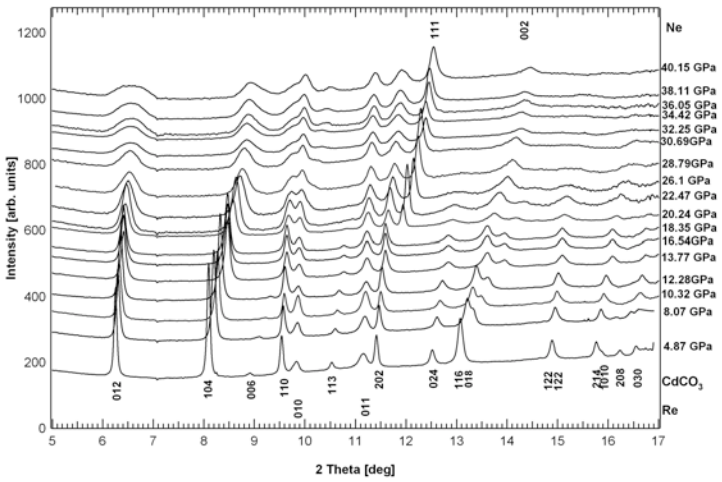

Top: Pressure dependence of diffraction patterns of $CdCO_3$ from 4.87(5) GPa to 40.15(9) GPa.

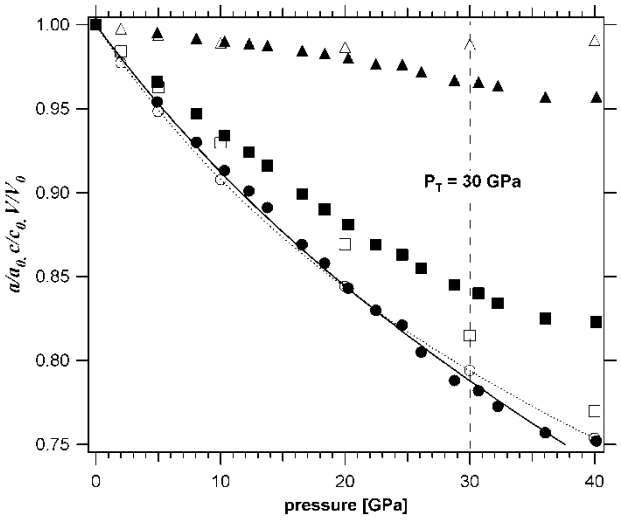

Right: Evolution of the normalized lattice parameters: a/a_0 (triangles), c/c_0 (squares), and the unit cell volume V/V_0 (circle) with pressure. Open symbols represent data from the *ab initio* calculations, closed symbols show experimental values.

Reference: Minch et al High-pressure behavior of otavite ($CdCO_3$). *Journal of Alloys and Compounds* 508, 251–257, 2010

This research was supported by the Deutsche Forschungsgemeinschaft under project number KN 507/5-1 in the framework of the priority program: "Synthesis, 'in situ' characterization and quantum mechanical modelling of Earth Materials, oxides, carbides, and nitrides at extremely high pressures and temperatures". The use of the beamline X17C was supported by COMPRES, the Consortium for Materials Properties Research in Earth Sciences under NSF Cooperative Agreement EAR 06-49658. Use of the National Synchrotron Light Source, Brookhaven National Laboratory, was supported by the U.S. Department of Energy, Office of Science, Office of Basic Energy Sciences, under Contract No. DE-AC02-98CH10886. Y. Lee and D.H. Seoung thank the support from the BK21 program to the Institute of Earth, Atmosphere, and Astronomy at Yonsei University and the Global Research Lab Program of the Ministry of Education, Science and Technology (MEST) of the Korean Government. Bjoern Winkler is grateful for funding from the BMBF in the framework of the Geotechnologienprogramm 03G0717B.

X-ray diffraction study of arsenopyrite at high pressure

D W Fan [1], M N Ma [2], W G Zhou [1], S Y Wei [1], Z Q Chen [3], H S Xie [1]

[1] Institute of Geochemistry of Chinese Academy of Science; [2] Graduate School of Chinese Academy of Science; [3] Stony Brook University

Arsenopyrite (FeAsS), the principal ore of the element arsenic, is considered as an economically unimportant mineral because it is usually in the form of the solid wastes of the mining operations (King 2002; Schaufuss et al. 2000). The connectivity of the atoms in arsenopyrite is somewhat similar to that in marcasite and pyrite (Vaughan and Craig 1978; Pang et al. 1993). There are no reports in the literature about the physical properties including the equation of state (EOS), and elasticity of arsenopyrite at high pressure. In this study we report the EOS of arsenopyrite under pressure conditions up to 28.2 GPa for the first time, and the isothermal bulk modulus has been derived based on our observed P-V data.

The *in situ* high-pressure X-ray angle dispersive diffraction experiments on arsenopyrite were carried out with a diamond anvil cell (DAC) at COMPRES beamline X17C, National Synchrotron Light Source, Brookhaven National Laboratory. No evidence for a phase transition in compression behavior was observed. The experimental P-V data are fitted to Birch-Murnaghan EOS. The results are K_0＝123(9) GPa, and K'_0=5.2(8), respectively. Furthermore, we confirm that the linear compressibilities (β) along *a*, *b* and *c* directions of arsenopyrite is elastically isotropic (β_a=6.82×10^{-4}, β_b=6.17×10^{-4} and β_c=6.57×10^{-4} GPa^{-1}).The bulk modulus of the arsenopyrite (123 GPa) in this study is smaller than those of pyrite (133.5-160 GPa) (Merkel et al. 2002; Drickamer et al. 1966; Page and Rodgers 2005; Fujii et al. 1986; Ahrens and Jeanloz 1987) and marcasite (146.5 GPa) (Chattopadhyay and Schnering 1982) in previous studies. Moreover, we infer that the differences in the elastic behavior of the arsenopyrite, pyrite and marcasite can be attributed to the different compositions and structures since the pyrite has a cubic structure belonging to the *Pa3* space group, the marcasite has an orthorhombic structure belonging to the *Pmnn*, and in contrast, the arsenopyrite has a monoclinic structure with space group $P2_1/c$ (Pang et al. 1993; Zhai and Wu 2010).

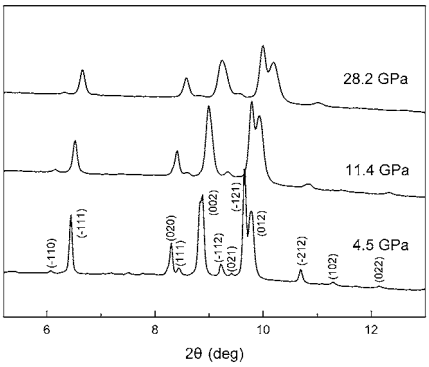

Fig.1 Representative X-ray diffraction patterns of arsenopyrite obtained in this study

Experiments were conducted at the X17C beamline of NSLS which is supported by COMPRES, the Consortium for Material Property Research in the Earth Sciences under NSF Cooperative Agreement EAR06-49658.

Pressure-induced phase transition in $BaCrO_4$

Tony Huang, National Cheng Kung University
Sean R. Shieh, **Arslan Akhmetov**, University of Western Ontario
Xi Liu, Peking University
Chih-Ming Lin, National Hsinchu University of Education
Jiann-Shing Lee, National Pingtung University of Education

$BaCrO_4$ was studied to 25 GPa in a diamond-anvil cell using both Raman spectroscopy and x-ray diffraction methods. *In situ* high-pressure x-ray diffraction was performed at beamline X17C, National Synchrotron Light Source at Brookhaven National Laboratory. Raman spectra were collected in a micro-Raman system (TRIAX 550) at National Hsinchu University of Education. Our results showed that $BaCrO_4$ exhibits a phase transition near 9 GPa from both Raman and x-ray diffraction measurements. The new high-pressure phase ($BaCrO_4$-II) is suggested as a monoclinic ($P2_1/m$) structure, different from other high-pressure forms of ABO_4-type compounds. Moreover, the high-pressure phase of $BaCrO_4$ is found to be reversible; the low-pressure phase is recovered at ~8 GPa upon decompression. The pressure-volume data of $BaCrO_4$ fitted to a third-order Birch-Murnaghan equation of state yield a bulk modulus of 53(1) GPa and a pressure derivative of 6.8(5), in agreement with the theoretical prediction. For the high-pressure phase $BaCrO_4$-II, the bulk modulus is 117(10) GPa and the pressure derivative is 3(1).

(A) (B) (C)

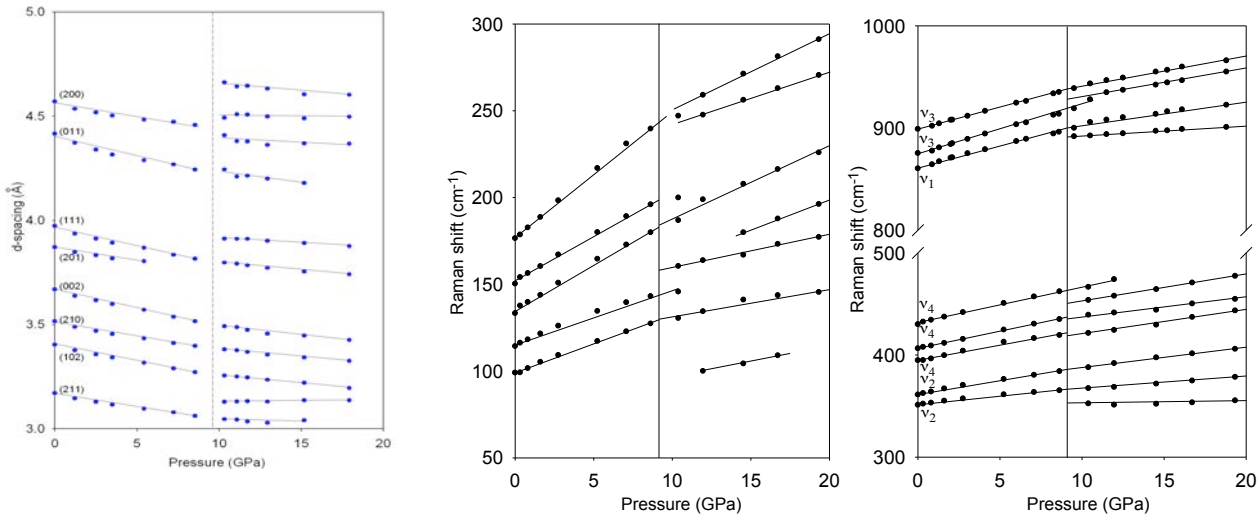

(A)Variations of *d*-spacings of $BaCrO_4$ at pressure to 18 GPa. The dashed line indicates the transition pressure. (B,C) Frequency shifts of Raman modes of $BaCrO_4$ as a function of pressure. (B) Lattice modes, (C) Internal modes.

Reference: Huang, T. S.R. Shieh, A. Akhmetov, X. Liu, C.M. Lin, and J.S. Lee, Pressure-Induced Phase Transition in $BaCrO_4$, *Phys. Rev. B* 81, 214117, 2010.

We thank to J. Hu for her assistance in synchrotron x-ray data collections. This work was supported by NSC, Taiwan, NSERC, Canada, and COMPRES, the Consortium for Materials Property Research in Earth Sciences.

Structure and Elasticity of Apatite and Kyanite at High Pressure

S. R. Shieh, M. Fleet, A. Akhmetov Department of Earth Sciences, University of Western Ontario
X. Liu, L. Zhang, Q. He School of Earth and Space Sciences, Peking University

Apatite is an important material in igneous and metamorphic rocks, biomineralization, environment and agriculture. Moreover, apatite is also an important component for bones and teeth. The high-pressure behavior of synthetic lead fluorapatite [$Pb_{9.35}(PO_4)_6F_2$], bioapatite (LM006) {[$Ca_{9.66}Na_{0.35}$][$(PO_4)_{5.56}(CO_3)_{0.44}$][$(OH)_{1.45}(CO_3)_{0.33}$]} (4.8 wt% CO_3) and bioapatite (LM005) {[$Ca_{9.13}Na_{0.87}$][$(PO_4)_{5.05}(CO_3)_{0.95}$][$(OH)_{0.36}(CO_3)_{0.86}$]} (11.2 wt% CO_3) and kyanite were investigated to ~20 GPa using diamond anvil cells. *In suit* high-pressure x-ray diffraction patterns of the apatites and kyanite were collected at beamline X17C, National Synchrotron Light Source. Our results show that lead fluorapatite is more compressible than those of $Ca_{10}(PO_4)_6X_2$ (X=F, Cl or OH) compounds and exhibits elastically isotropic structure in the investigated pressure range. For bioapatite, our results show that the hardness and strength of bioapatite decrease progressively with increasing carbonate contents. Compared to the bulk modulus of calcium hydroxylapatite, the bulk modulus of LM006 and LM005 is about 10% and 15% smaller, respectively.
The bulk modulus of iron-bearing kyanite, $(Al_{1.99}Fe_{0.01})SiO_5$ obtained from this study is 192±6 GPa when the pressure derivative is 6±1, in agreement with previous studies.

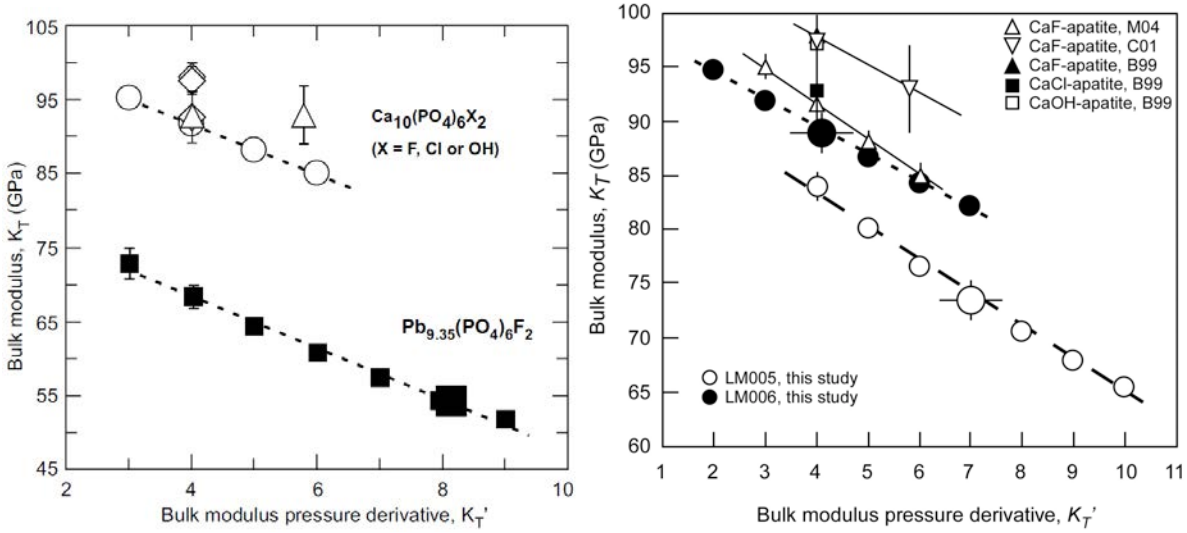

Note: LM006: [$Ca_{9.66}Na_{0.35}$][$(PO_4)_{5.56}(CO_3)_{0.44}$][$(OH)_{1.45}(CO_3)_{0.33}$] and LM005: [$Ca_{9.13}Na_{0.87}$][$(PO_4)_{5.05}(CO_3)_{0.95}$][$(OH)_{0.36}(CO_3)_{0.86}$]

References:

Liu, X., S. R. Shieh, M. E. Fleet, A. Akhmetov, *Am. Mineral.* **93**, 1581 (2008).
Liu, X., S.R. Shieh, M.E. Fleet and L. Zhang, The compressibility of a natural kyanite to 17.5 GPa, *Prog. Nat. Sci.* 19, 1281-1286, 2009.
Fleet, M.E., Liu, X., S.R. Shieh, Structural change in lead fluorapatite at high pressure, *Phys. Chem. Mineral.* 37, 1-9, 2010.
Liu, X., S.R. Shieh, M.E. Fleet L. Zhang and Q He, Equation of state of carbonated hydroxylapatite at ambient temperature to 10 GPa: Significance of carbonate, *Am. Mineral*. 96, 74-80, 2010.
Liu, X., M.E. Fleet, S.R. Shieh, and Q He, Synthetic lead bromapatite: X-ray structure at ambient pressure and compressibility up to about 20 GPa, *Phys. Chem. Mineral.* 2011.

This work was supported by NSERC to S. Shieh and M. Fleet, and also supported by COMPRES, the Consortium for Materials Property Research in Earth Sciences. We thank to S. Ghose and Z. Chen for their help at beamline X17C, NSLS.

Correlating cation coordination, stiffness, phase transition pressures, and smart materials behavior in metal phosphates

Dmitry Shakhvorostov , Martin H. Müser, **Yang Song and Peter R. Norton** *University of Western Ontario, London, Ontario, Canada*
Nicholas J. Mosey, *Queen's University, Kingston, Ontario, Canada*

In this study we present x-ray diffraction data on metal phosphates containing either high or low coordination number zinc or calcium. The experiments reveal that low-coordination zinc phosphate crystals are relatively soft at ambient conditions but stiffen dramatically with pressure, p, thereby exhibiting smart materials behavior. In comparison, high-coordination zinc and calcium phosphates have higher initial bulk moduli, K_0, and stiffen much less rapidly with increasing p. The investigated metal phosphate crystals all amorphize under compression when K reaches a value near 210±40 GPa: the precise value depending on the chemical details. Our interpretation of this result is that elastic properties and structural instabilities are related to the motion of rigid phosphate units, which becomes more hindered as the material density increases, and that stiffening can occur independent of a change of cation coordination. These ideas are supported by *ab initio* simulations of α zinc phosphate. The efficacy of low-coordination zinc phosphates as antiwear agents is discussed in the context of these results.

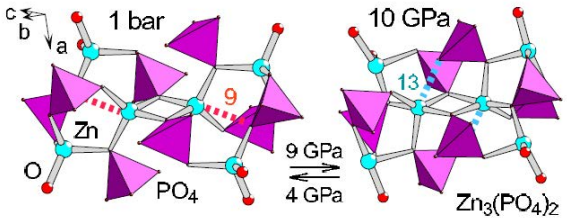

Pressure-induced transformation of α zinc phosphate.

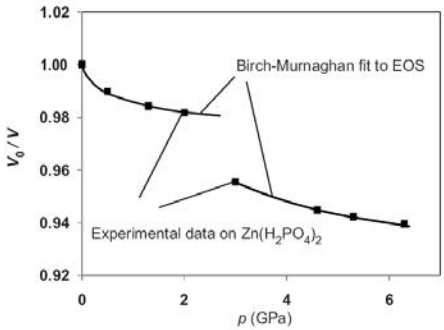

Equation of state of $Zn(H_2PO_4)_2$.

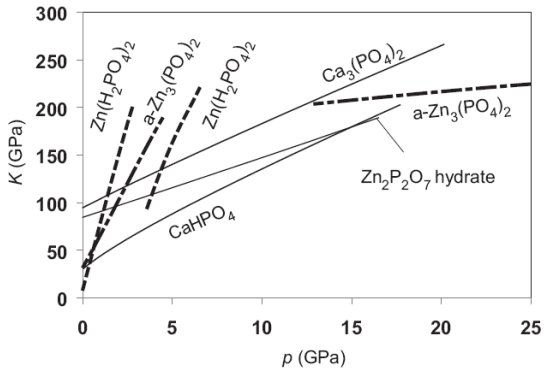

Bulk modules of several zinc phosphate as a function of pressure.

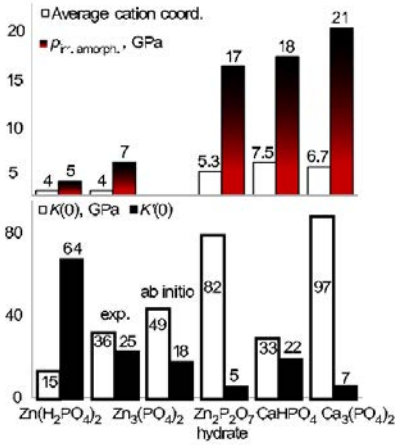

Summary of experimental and calculation results.

Reference: D Shakhvorostov, N Mosey, M Müser, Y Song, P Norton, Correlating Cation Coordination, Stiffness, Phase Transition Pressures, and Smart Materials Behavior in Metal Phosphates, *Phys. Rev. B: Condens. Matter*, **79**, 094107 (2009).

Acknowledgments: M.H.M., Y.S., and P.R.N. wish to acknowledge support from NSERC and General Motors of Canada Ltd., and M.H.M. from PREA. The research described in this paper was performed partially at the National Synchrotron Light Source at Brookhaven National Laboratory. We acknowledge J. Hu for useful discussions and technical support. D.S. would like to acknowledge O. Eisenbacher for meaningful and valuable discussion of the paper.

Polymorphism in TiO_2: laser radiation and a metastable phase transition.

Anastasia Kantor[1], Innokenty Kantor[2], Vitali Prakapenka, *GSECARS, University of Chicago*

[1]Present address: Bayerisches Geoinstitut, University of Bayreuth, Germany
[2]Present address: European Synchrotron Radiation Facility, Grenoble, France

It is known, that nanocrystalline anatase phase of TiO_2 became amorphous upon compression between 15 and 20 GPa. It was reported by Swamy et al. (PRL 96, 2006) that glassy TiO_2 undergoes amorphous-amorphous transition at about 20 GPa during decompression, based on X-ray diffraction study. Metastable amorphous-amorphous transitions attract a lot of attention due to their unusual physical nature and as an analogue to liquid-liquid phase transitions. In order to determine the effect of this transition on the sound velocities, we performed a high-pressure experiment in a DAC, combining Brillouin scattering and X-ray diffraction on GSECARS 13-BMD beamline at APS. The nanopowder sample was loaded along with a ruby-sphere and a piece of compressed Au-powder for pressure determination. The diffraction and Brillioun spectra (Fig. 1) were collected simultaneously during compression and decompression. We observed an amorphization around 18 GPa, however, no amorphous-amorphous transition was detected on decompression, neither in X-ray diffraction patterns, nor in sound velocities (Fig. 2).

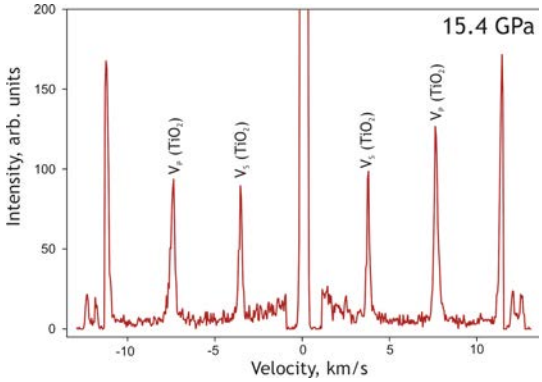

Fig. 1. Typical Brillouin scattering spectrum of TiO_2 at 15.4 GPa.

When the same measurements with the same sample were performed using X-ray diffraction only, we again observed amorphous-amorphous phase transition, similar to original report of Swamy et al. Therefore, we conclude that even a low-power (~100 mW) non-absorbing laser radiation can trigger metastable phase transition in amorphous TiO_2. We suppose that the laser scattering allows continuous relaxation of local structure in glass, contrary to step-like changes, observed when no laser radiation involved.

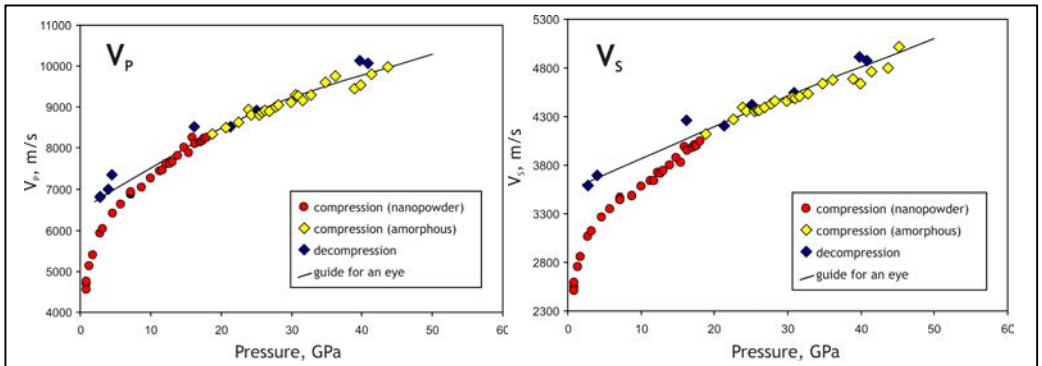

Fig. 2. Longitudinal (left) and transverse (right) sound velocities in TiO_2. Red circles – nanocrystalline TiO_2, yellow circles – amorphous TiO_2, blue diamonds – decompression. Lines are guides for the eye.

Pressure-and Heat-Induced Insertion of CO_2 into an Auxetic Small-Pore Zeolite

Yongjae Lee,* Dan Liu, Donghoon Seoung [Department of Earth System Sciences, Yonsei University, Seoul, Korea], Zhenxian Liu [Geophysical Laboratory, Carnegie Institution of Washington], Chi-Chang Kao [Stanford Synchrotron Radiation Lightsource, SLAC National Accelerator Laboratory], Thomas Vogt [NanoCenter and Department of Chemistry and Biochemistry, University of South Carolina]

We have recently succeeded in pressure-induced insertion of CO_2 into a small-pore zeolite natrolite. Mineral natrolite has been known to be a poor ion-exchanger and gas-absorber. When mineral natrolite is compressed to ca. 1.5 GPa and heated to ca. 110°C in the presence of CO_2, the unit cell volume of natrolite expands by 6.8% and ca. 12 wt% of CO_2 is contained in the expanded elliptical channels. This CO_2-insertion into natrolite is found to be reversible upon pressure release.

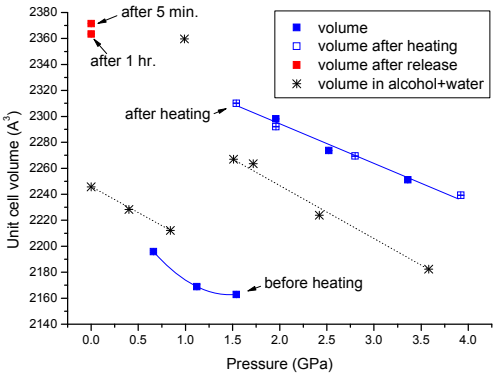

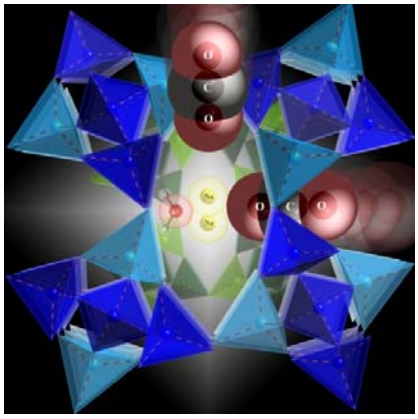

Figure (Left) Pressure-dependent changes in the refined unit cell volume of natrolite under CO_2 pressure medium (filled blue symbols upon pressure increase, open blue ones after heating, and filled red symbols after pressure release). The changes in the unit cell volume are also compared to the previous results (black asterisks) from the alcohol + water mixture medium run. (Right) A polyhedral representation of CO_2-inserted natrolite formed at 1.54(5) GPa after heating, viewed along [001], the chain/channel axis. Note that the CO_2 molecules lie on the plane perpendicular to the channel axis, tilted by φ=13˚. Dark (light) tetrahedra illustrate an ordered distribution of Si (Al) atoms in the framework.

References

Y. Lee, D. Liu, D. Seoung, Z. Liu, C-C Kao, T. Vogt, J. Am. Chem. Soc. 133, 1674-1677 (2011)

Acknowledgments

This work was supported by the Global Research Laboratory program of the National Research Foundation of the Korean Government. Y.L. acknowledges the support from the Nuclear R&D Program of the NRF to build the micro-Raman system used in this study. The authors thank Dr. Hyun-Hwi Lee for the operation of the 5A beamline at Pohang Accelerator Laboratory (PAL). Experiments at PAL were supported in part by the MEST and POSTECH. Operation of beamline U2A at the NSLS is supported by COMPRES under NSF Cooperative Agreement Grant No. EAR 06-49658, and by the U.S. Department of Energy through the Carnegie/DOE Alliance Center (CDAC) contract DE-FC03-03N00144. Accommodations for D. Liu and D. Seoung at NSLS were also supported by COMPRES.

Spectroscopic Study of the Effects of Pressure Media on High-Pressure Phase Transitions in Natrolite

Dan Liu[a], Wewei Lei[b], Zhenxian Liu[c], and Yongjae Lee[a]
[a]*Department of Earth System Sciences, Yonsei UniVersity, Seoul 120-749, Korea*
[b]*Max-Planck-Institute of Colloids and Interfaces, Department of Colloid Chemistry Research, Campus Golm, 14424 Potsdam, Germany, and* [c]*Geophysical Laboratory, Carnegie Institution of Washington, Washington, D.C. 20015, United States*

Zeolites are hydrated framework alumosilicates which comprise an important class of low-density materials. Their frameworks are composed of corner connecting of TO4 (Si, Al, Ge, Ga, ...) tetrahedra which yield cavities and channels of molecular dimensions. Exchangeable non-framework cations occupy the cavities and channels along with absorbed water molecules at ambient conditions. As such, a plethora of structural studies have been carried out as a function of framework type, composition, and/or temperature in order to understand their relationship to catalytic, molecular sieving, and ion-exchange properties. We have systematically studied the structural phase transitions in natrolite as a function of pressure and different hydrostatic media using micro-Raman scattering and synchrotron infrared spectroscopy. It was found that natrolite undergoes two reversible phase transitions at 0.86 and 1.53 GPa under pure water pressure medium. These phase transitions are characterized by the changes in the vibrational frequencies of four- and eight-membered rings related to the variations in the bridging T-O-T angles and the geometry of the elliptical eight-ring channels under pressure. Concomitant to the changes in the framework vibrational modes, the number of the O-H stretching vibrational modes of natrolite changes as a result of the rearrangements of the hydrogen bonds in the channels caused by a successive increase in the hydration level under hydrostatic pressure. Similar phase transitions were also observed at relatively higher pressures (1.13 and 1.59 GPa) under an alcohol-water pressure medium.

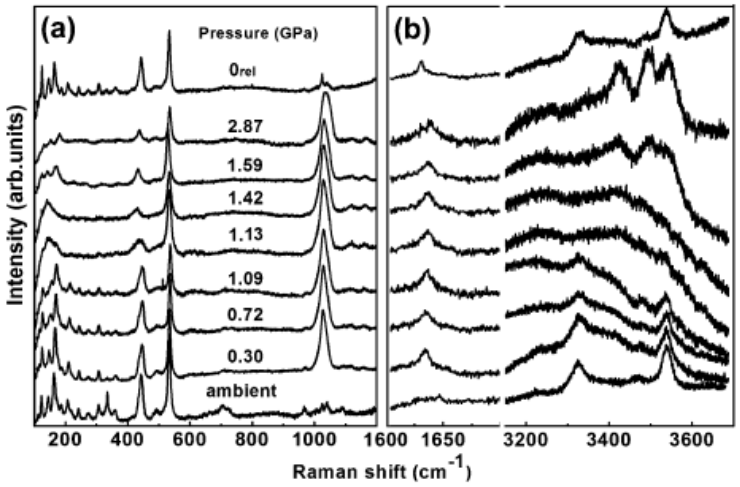

Figure 1. Raman spectra of natrolite at different pressures using more than 1:1 volume ratio between alcohol-water pressure transmitting medium and the powder sample. The top curve is the Raman spectrum at ambient pressure after decompression from 2.87 GPa.

References

Liu, D., W. Lei, Z. Liu, Y. Lee, *J. Phys. Chem. C,* 114(44), 18819–18824, (2010).

Acknowledgments

This work was supported by the Global Research Laboratory program of the National Research Foundation of the Korean Government. Operation of beamline U2A at the NSLS is supported by COMPRES under NSF Cooperative Agreement Grant No. EAR 06-49658, and by the U.S. Department of Energy through the Carnegie/DOE Alliance Center (CDAC) contract DE-FC03-03N00144. Accommodations for D. Liu at NSLS were also supported by COMPRES.

Equations of State and Elastic Properties

Thermal equation of state of $CaIrO_3$ post-perovskite

W. Liu[1], M. L. Whitaker[1], Q. Liu[1], L. Wang[1], N. Nishiyama[2], Y. B. Wang[2], A. Kubo[3]
T. S. Duffy[3], B. S. Li[1]

[1] *Mineral Physics Institute, State University of New York, Stony Brook, New York, USA*
[2] *Center for Advanced Radiation Sources, University of Chicago, Chicago, IL 60637, USA*
[3] *Department of Geosciences, Princeton University, Princeton, NJ 08544, USA*

The pressure–volume–temperature (P–V–T) relation of CaIrO3 post-perovskite (ppv) was measured at pressures and temperatures up to 8.6 GPa and 1,273 K, respectively, with energy-dispersive synchrotron X-ray diffraction using a DIA-type, cubic-anvil apparatus (SAM85). Unit-cell dimensions were derived from the LeBail full profile refinement technique, and the results were fitted using the third-order Birth-Murnaghan equation of state. The derived bulk modulus KT0 at ambient pressure and temperature is 168.3 ± 7.1 GPa with a pressure derivative K0T 0 = 5.4 ± 0.7. All of the high temperature data, combined with previous experimental data, are fitted using the high-temperature Birch-Murnaghan equation of state, the thermal pressure approach, and the Mie-Gruneisen-Debye formalism. The refined thermoelastic parameters for $CaIrO_3$ ppv are: temperature derivative of bulk modulus $(dK_T/dT)_P$ = -0.038 ± 0.011 GPa K^{-1}, αKT = 0.0039 ± 0.0001 GPa $K^{-1,}$ $(dKT/dT)_V$ = -0.012 ±0.002 GPa K^{-1}, and $(d^2P/dT^2)_V$ = 1.9 ± 0.3 9x10^{-6} GPa2 K^{-2}. Using the Mie-Gruneisen-Debye formalism, we obtain Gruneisen parameter γ_0 = 0.92 ± 0.01 and its volume dependence q = 3.4 ± 0.6. The systematic variation of bulk moduli for several oxide post-perovskites can be described approximately by the relationship K_{T0} = 5406.0/V(molar) + 5.9 GPa.

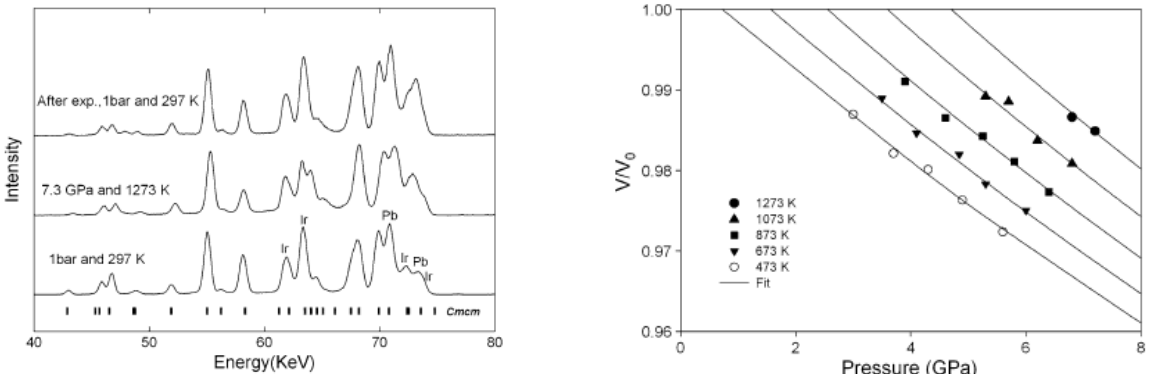

Figure. (Left) Synchrotron XRD patterns at selected pressure and temperatures, (Right) Compression of CaIrO3 post-perovskite along various isotherms and equation of state fit.

W. Liu, M. L. Whitaker, Q. Liu, L. Wang, N. Nishiyama, Y. B. Wang, A. Kubo, T. S. Duffy, B. S. Li, Thermal equation of state of $CaIrO_3$ post-perovskite, Phys Chem Minerals, DOI 10.1007/ s00269-010-0414-z.

Synchrotron experiments were conducted at the X17B2 beamline of NSLS which is supported by COMPRES under NSF Cooperative Agreement EAR06-49658.

Searching for Post-perovskite Transition in CaSnO3 at High Pressure: An Ultrasonic Velocity Study to 18 GPa

B. W. Schneider[1]; W. Liu[2]; B. S. Li[2]

[1]Brown University, Providence, RI, USA
[2]Mineral Physics Institute, Stony Brook University, New York, USA

Compressional (P) and shear (S)wave velocities of CaSnO3 perovskite were measured at room temperature using ultrasonic interferometry up to 18 GPa. Discontinuities of the magnitude suggested in previous theoretical calculations are not observed in derived velocities over the entire experimental pressure range explored here. A least squares fitting of the P and S wave velocities to third-order finite strain equations yielded zero pressure adiabatic bulk and shear moduli and their first pressure derivatives, K = 166(2) GPa, K' = 5.4(2), G = 88(1) GPa and G' = 1.2(1). These results are in agreement with previous experiments, within mutual uncertainties. Examinations of the current data as well as comparison with previous measurements at lower pressures conclude the presence of a post-perovskite phase transition in $CaSnO_3$ is not visible in the elasticity at ambient temperature within 0–18 GPa range.

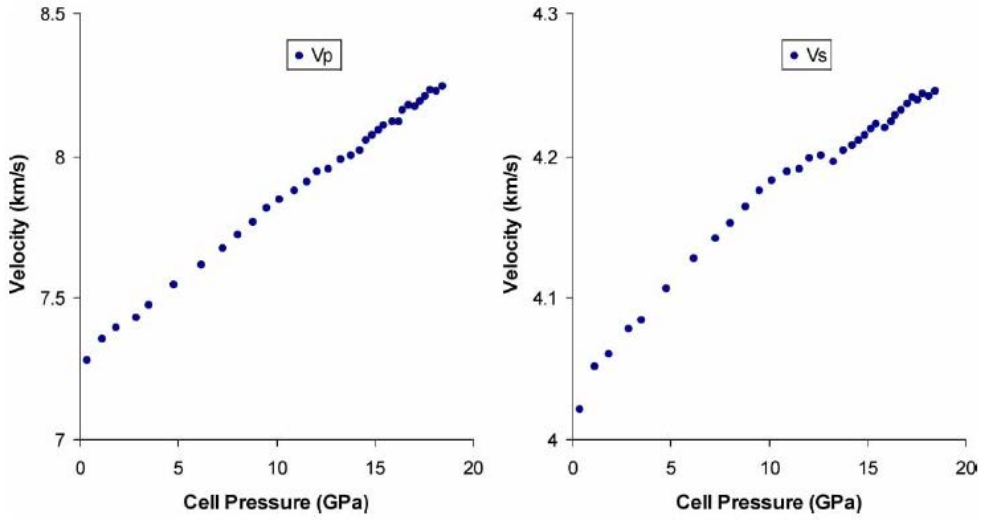

Figure. P(Left) and S (Right) wave velocities of $CaSnO_3$ perovskite as a function of pressure.

B. W. Schneider, W. Liu, B. S. Li, Searching for post-perovskite transition in $CaSnO_3$ at high pressure: an ultrasonic velocity study to 18 GPa, 28, 397-404, 2008.

Synchrotron experiments were conducted at the X17B2 beamline of NSLS which is supported by COMPRES under NSF Cooperative Agreement EAR06-49658.

Elastic properties of yttrium-doped $BaCeO_3$ perovskite

J. Zhang, Y. Zhao, H. Xu (Los Alamos National Laboratory), B. Li, D.J. Weidner (Stony Brook University), and A. Navrotsky (UC Davis)

The variation of elastic properties with oxygen vacancies, a fundamental problem in solid-state science as well as in materials design and application, has not been well understood by either experiments or theory. We studied the elasticity of the oxygen-deficient $BaCe_{1-x}Y_xO_{3-0.5x}$ perovskite with x = 0.00 and 0.15 using ultrasonic interferometry and synchrotron x-ray diffraction. Our results show that the presence of 2.5% oxygen vacancy has no measurable effect on the elastic bulk modulus. The shear modulus, however, decreases by approximately 5% in $BaCe_{0.85}Y_{0.15}O_{2.925}$ perovskite. The differences between Y^{3+} doped cerate and Al^{3+} doped silicate suggest that the effect of oxygen vacancy on the elastic properties could be system-dependent. In $BaCe_{1-x}Y_xO_{3-0.5x}$ perovskite, for example, the substitution of Y^{3+} for Ce^{4+} and formation of oxygen vacancies cause a decrease in the unit-cell volume, whereas an opposite trend is revealed by both experiments and theoretical calculations for the substitution of Al^{3+} into Mg-silicate perovskite.

Experiments were conducted at the X17C beamline of NSLS which is supported by COMPRES, the Consortium for Material Property Research in the Earth Sciences under NSF Cooperative Agreement EAR0649658.

Applied Physics Letters (Vol. 90, 161903-1-3, 2007).

Work performed on beamlines X17B2.

American Mineralogist, Volume 93, pages 745–750, 2008

Thermal equation of state of $CaGeO_3$ perovskite

WEI LIU,[1,*] JENNIFER KUNG,[2] LIPING WANG,[1] AND BAOSHENG LI[1]

[1]Mineral Physics Institute, Stony Brook University, Stony Brook, New York 11794, U.S.A.
[2]Department of Earth Sciences, National Cheng-Kung University, Tainan 70101, Taiwan

Pressure-volume-temperature data have been obtained for $CaGeO_3$ perovskite up to 9.6 GPa and 1100 K using a cubic anvil, DIA-type high-pressure apparatus in conjunction with synchrotron X-ray diffraction. The data were analyzed using Birch-Murnaghan equation of state and thermal pressure approach with the bulk modulus at ambient pressure, K_{T0}, and its pressure derivative, K'_{T0}, constrained by previous measurements. A fit of the unit-cell volume data to the high-temperature Birch-Murnaghan (HTBM) equation of state gives $(\partial K_T/\partial T)_P = -0.025 \pm 0.015$ GPa/K, $a = 1.047 \pm 0.356 \times 10^{-5}$/K, and $b = 3.282 \pm 0.735 \times 10^{-8}$/K^2 for the thermal expansion α expressed by $a + bT$. The thermal pressure approach yields $\alpha K_T = 4.04 \pm 0.37 \times 10^{-3}$ GPa/K and $(\partial^2 P/\partial T^2)_V = 6.17 \pm 1.28 \times 10^{-6}$ GPa/K^2. The energy dispersive X-ray diffraction data reveal no indication of a structural phase transition over the P-T range of the current experiment. A systematic relationship, $K_{S0} = 6720/V(\text{molar}) - 13.07$ GPa, has been established based on these isostructural analogues, which predicts $K_{S0} = 261(15)$ for $MgSiO_3$ perovskite and 225(8) for $CaSiO_3$ perovskite, respectively.

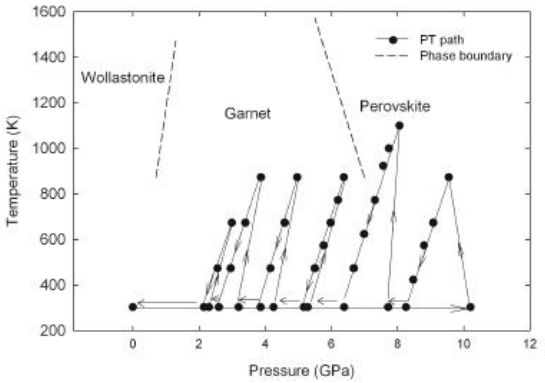

FIGURE 1. Pressure-temperature path of the experiment in this study. Each point represents a P-T condition where the X-ray diffraction of $CaGeO_3$ perovskite was taken. The dashed lines represent the phase boundaries of $CaGeO_3$ polymorphs after Ross et al. (1986).

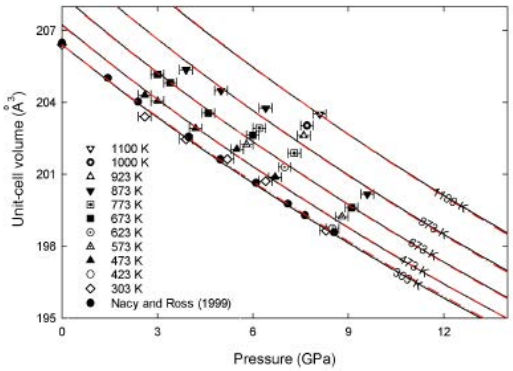

FIGURE 3. Unit-cell volumes as a function of pressures and temperatures. The error bars in pressures are estimated to be ±0.2 GPa. The solid and dashed lines are two fits with different constraints K_{T0} = 196 GPa, K'_{T0} = 6.1, and K_{T0} = 193 GPa, K'_{T0} = 6.4, respectively.

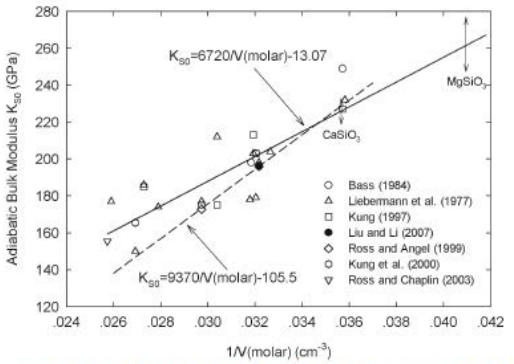

FIGURE 5. Variation of adiabatic bulk modulus K_{S0} with the molar volume V(molar) for oxide perovskites. The dashed line shows the trend proposed by Ross and Angel (1999) for Ca-oxide perovskites [converted from the linear trend $K_{T0} = 9277/V(\text{molar}) - 104.4$ GPa using $K_{S0}/K_{T0} = 1.01$]. The solid line represents the prediction for isostructural oxide perovskites from this study. The error bars represent the range of predicted values.

Acknowledgements

This work was supported by NSF grant (EAR00135550). JK thanks the support by NSF grant (EAR0229704 to RCL). The experiments were carried out at the National Synchrotron Light Source (NSLS), which is supported by the US Department of Energy, Division of Materials Sciences and Division of Chemical Sciences under Contract No. DE-AC02-76CH00016. The operation of X17B2 is supported by COMPRES, the Consortium for Materials Properties Research in Earth Sciences.

Compressional and shear-wave velocities of the polycrystalline $CaGeO_3$ perovskite to 10 GPa

Wei Liu and Baosheng Li
Mineral Physics Institute, Stony Brook University, Stony Brook, New York 11794, USA
(Received 17 August 2006; revised manuscript received 12 October 2006; published 10 January 2007)

Compressional and shear-wave velocities and unit-cell volumes of orthorhombic $CaGeO_3$ perovskite have been measured up to 10 GPa at ambient temperature using ultrasonic interferometry in conjunction with synchrotron x radiation. Fitting all velocity and unit-cell volume data to finite-strain equations yields the zero-pressure adiabatic bulk and shear moduli and their pressure derivatives K_{S0}=194.6 (11) GPa, G_0=109.5 (5) GPa, K_{S0}'=6.4 (2), G_0'=1.7 (1), with an rms misfit of 0.009 km s^{-1}. From the data in the current study, we have observed no discontinuities or elasticity softening for either the bulk or shear moduli up to the peak pressure of 10 GPa.

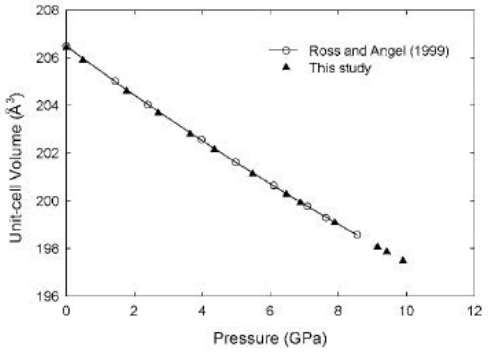

FIG. 1. Variation of unit-cell volumes of $CaGeO_3$ perovskite as a function of pressure. The solid line is the third-order equation of state generated using the K_{T0} and K_{T0}' measured in the study of Ross and Angel (Ref. 8).

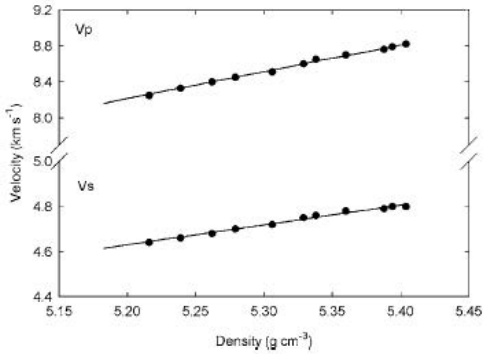

FIG. 2. Elastic compressional (V_P) and shear (V_S) wave velocities for $CaGeO_3$ perovskite as a function of density from ultrasonic and x-ray measurements to 10 GPa. The solid line is from the finite-strain fit to the observed elastic moduli data.

TABLE II. Elastic properties of $CaGeO_3$ perovskite. Values in parentheses are 1σ error in the last digits.

	This study	Ref. 1	Ref. 2	Ref. 3
Measurement	Ultrasonic & powder XRD	Ultrasonic	Single-crystal XRD[a]	EXAFS
Conditions	10 GPa	0.6 GPa	8.6 GPa	23 GPa
Fitting approach	3rd-order FS EoS[b]		BM EoS[c]	BMEoS
K_{T0} (GPa)			194.0(21)	220
K_{T0}'			6.1(5)	4 (fixed)
K_{S0} (GPa)	194.6(11)	198(15)		
G_0 (GPa)	109.5(5)	109(4)		
K_{S0}'	6.4(2)			
G_0'	1.7(1)			
rms misfit (km s^{-1})	0.009			

This work was supported by NSF grant (EAR00135550) to BL. The in-situ ultrasonic and X-ray experiments were carried out at the superconducting wiggler beamline (X17B2) of the National Synchrotron Light Source (NSLS), which is supported by the US Department of Energy, Division of Materials Sciences and Division of Chemical Sciences under Contract No. DE-AC02-76CH00016. The operation of X-17B2 is supported by COMPRES, the Consortium for Materials Properties Research in Earth Sciences under NSF Cooperative Agreement EAR 01-35554.

Raman and X-Ray Investigation of Pyrope Garnet $(Mg_{0.76}Fe_{0.14}Ca_{0.10})_3Al_2Si_3O_{12}$ under High Pressure

MA Yan-Mei(马艳梅), CHEN Hai-Yong(陈海勇), LI Xue-Fei(李雪飞),

GAO Ling-Ling(高玲玲), CUI Qi-Liang (崔启良), ZOU Guang-Tian(邹广田)

National Laboratory of Superhard Materials, Jilin University, Changchun 130012

Garnets are one of the most important constituents in Earth's upper mantle and transition zone, and pyrope is probably the most important member of the family. Most garnets are formed at high pressures and temperatures and also appear in eclogites or igneous rocks. The compressional behaviour of natural pyrope garnet is investigated by using angle-dispersive synchrotron radiation x-ray diffraction（COMPRES beamline X17C, NSLS） in a diamond anvil cell at room temperature. No changes in the diffraction pattern were observed in all the pressure range. The refinement module combined in the Materials Studio program has been employed to refine the parameters. The unit-cell volume was determined from the lattice parameters as a function of pressure in the range 0--25.3 GPa (Fig. 1). The unit-cell parameters decrease with the increasing pressure. They are then fitted to the Birch--Murnaghan equation of state

$$P = 3/2K_{T0}[(V_0/V)^{7/3} - (V_0/V)^{5/3}]\{1+3/4(K'_{T0} - 4)[(V_0/V)^{2/3} - 1]\},$$

where K_{T0} and K'_{T0} is the isothermal bulk modulus and its first pressure derivative, V_0 and V is the unit-cell volume at ambient pressure and at high pressure, respectively, and yielded a bulk modulus K_{T0}=199 GPa, with K'_{T0} fixed to 4.

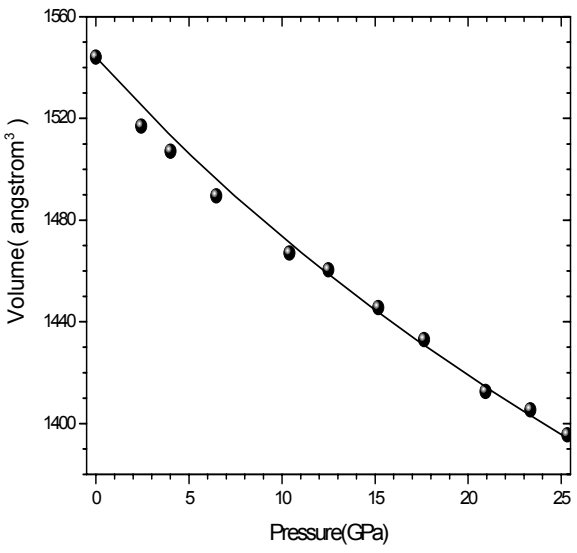

Fig. 1. Isothermal equation of state of pyrope

For the natural pyrope, Al^{3+} is easily substituted by other trivalent cations such as Fe^{3+},Cr^{3+}, $Ti^{3+}$and Zr^{3+}. In addition, from the electron microscopy data, Fe^{2+} and Ca^{2+} also substituted some Mg^{2+}. The atomic weights of these cations are larger than those of Al^{3+} and Mg^{2+}, so natural pyrope garnet becomes somewhat harder to compress than the synthetic pyrope crystal. Moreover, single-crystal hydrostatic compressions of synthetic pyrope, almandine ($Fe_3Al_2Si_3O_{12}$) and grossular ($Ca_3Al_2Si_3O_{12}$) also demonstrate that the bulk modulus of almandine and grossular are larger than that of pyrope.[

Experiments were conducted at the X17C beamline of NSLS which is supported by COMPRES, the Consortium for Material Property Research in the Earth Sciences under NSF Cooperative Agreement EAR06-49658.

High-temperature elasticity of magnesioeferrite spinel

S. M. Antao[1], I. Jackson[2], B. Li1, J. Kung[1], J. Chen[1], I. Hassan[3], R. C. Liebermann[1], J. B. Parise[1].
[1]Mineral Physics Institute & Department of Geosciences, Stony Brook University, [2]Research School of Earth Sciences, Australian National University, [3]Department of Chemistry, University of the West Indies

The elastic moduli of magnesioferrite spinel, MgFe2O4, and their temperature dependence have been determined for the first time by ultrasonic measurements on a polycrystalline specimen. The measurements were carried out at 300 MPa and to 550 ºC in a gas-medium high-pressure apparatus. On heating, both the elastic bulk (KS) and shear (G) moduli linearly to 350 C. By combining with extant thermal-expansion data, the values for the room-temperature KS and G and their temperature derivatives are as follows: K0 = 176.3 GPa, G0 = 80.1 GPa, (KS/ T)P = -0.032 GPa K^{-1} and (G/ T)P = -0.012 GPa K^{-1}. Between 350 and 400 ºC, there are abrupt increases of 1.4% in both of the elastic moduli; these closely coincide with the magnetic Curie transition that was observed by thermal analyses at about 360 ºC.

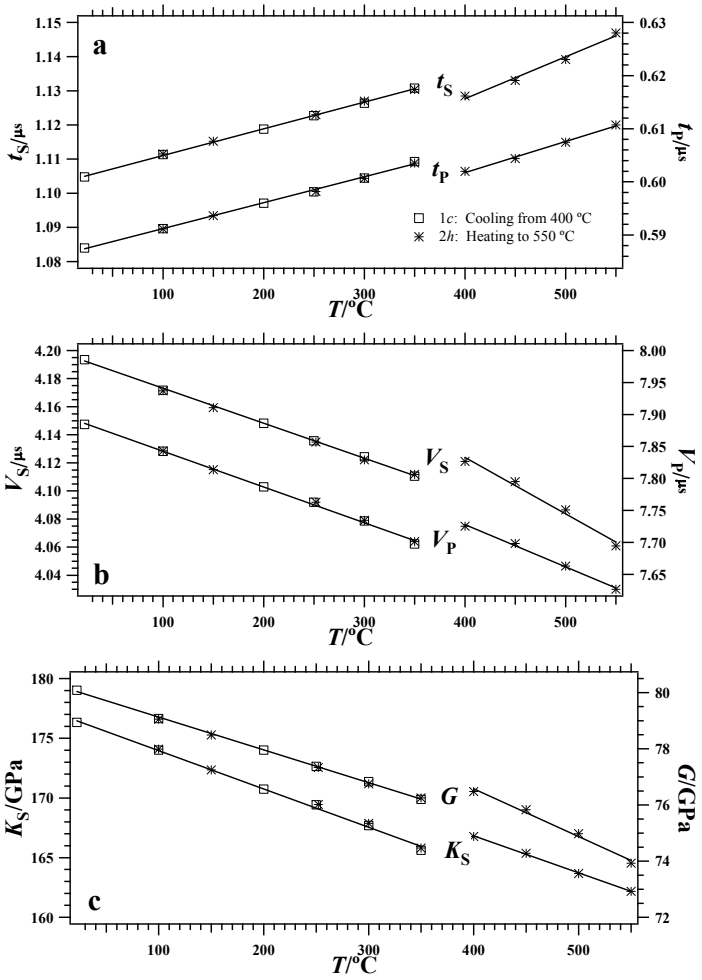

Figure 2. Variations in elastic data *vs*. temperature for magnesioferrite held at a constant pressure of 300 MPa. (a) travel-times for S waves (t_S) and P waves (t_P), (b) velocities for S waves (V_S) and P waves (V_P), and (c) bulk modulus (K_S), and shear modulus (G). Error bars are not seen if smaller than the symbols. A discontinuity is observed near the magnetic transition, $T_c \approx 360$ ºC. Linear trend lines are fitted to the data above and below T_c.

Publication: Antao, S. M., Ian Jackson, Baosheng Li, Jennifer Kung, Jiuhua Chen, Ishmael Hassan, Robert C. Liebermann, and John B. Parise, High-temperature elasticity of magnesioferrite spinel, Phys. Chem. Minerals, DOI 10.1007/s00269-007-0152-z, 2007

Acknowledgments The experimental work was performed in the high pressure laboratory at the Australian National University under funding from the Australian Research Council (LX0348106) This study was also partially supported by NSF grants EAR-0510501 to JBP and NSF-INT 0233849 to RCL for a collaborative research program with the Australian National University. RCL was supported by COMPRES, the NSF Consortium for Materials Properties in Earth Sciences under EAR01-35554 and 06-49658.

Polycrystalline ZnO: Brillouin scattering above 1.5 megabars.

Innokenty Kantor[1], Vitali Prakapenka, *GSECARS, University of Chicago*

[1]Present address: European Synchrotron Radiation Facility, Grenoble, France

Zinc oxide is a wide-bandgap semiconductor with a wide range of technological applications. At ambient conditions ZnO is hexagonal with the wurtzitic crystal structure and demonstrate extremely high piezoelectric effect. However, above ~15 GPa ZnO transforms to a cubic rocksalt structured phase. It is not possible to preserve single-crystal through this phase transitions, however, we were able to measured sound velocities in polycrystalline cubic ZnO up to 176 GPa using a diamond anvil cell. Unlike many other materials, in ZnO transverse phonons (corresponding to Vs) show much higher amplitude comparing with longitudinal phonons (Fig. 1), which makes it possible to observe both, Vp and Vs in polycrystalline ZnO up to the highest pressure reached (Fig. 2). To the best of our knowledge this is the highest pressure at which both, Vp and Vs were measured by mean of the Brillouin spectroscopy.

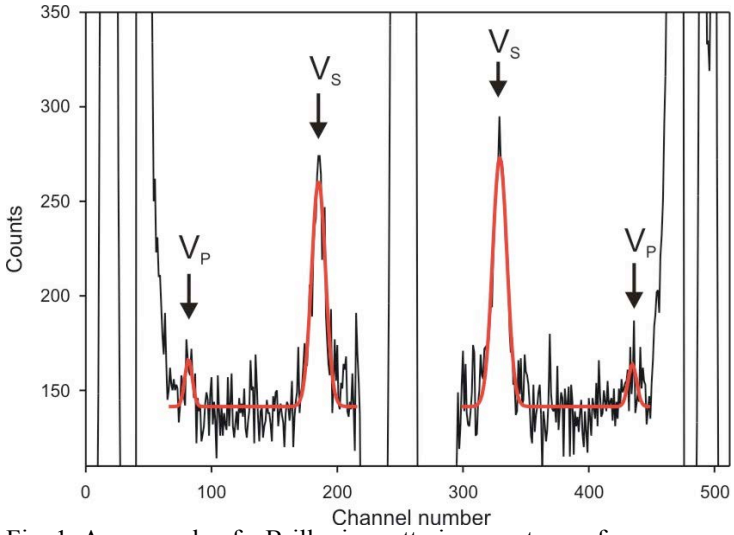

Fig. 1. An example of a Brillouin scattering spectrum of polycrystalline ZnO collected at 146 GPa. Central elastic peak and diamond Vs peaks (on the sides) are significantly stronger. Red line is a Gaussian fit.

The powdered sample together with a small piece of gold as a pressure calibrant was loaded in the DAC without pressure medium, so the stress conditions were strongly non-hydrostatic. However, no significant preferred orientation developed in the sample.

We found, that the measured sound velocities in a highly stressed material differ significantly from what can be expected based on bulk modulus, thus giving us better understanding of elastic phonons propagation under high non-hydrostatic stress.

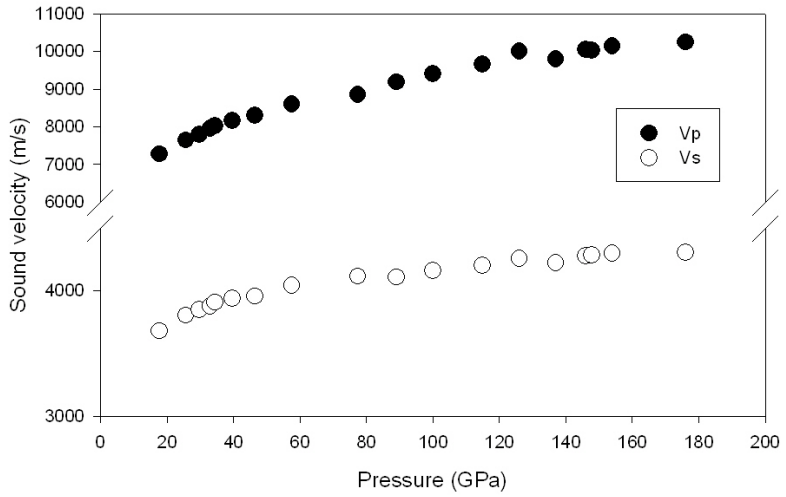

Fig.2. Elastic waves velocities in polycrystalline cubic ZnO. Open circles – Vs, solid circles – Vp.

Elasticity of amorphous zirconium tungstate at high pressure

Wei Liu[a] and Baosheng Li
Mineral Physics Institute, Stony Brook University, Stony Brook, New York 11794, USA

(Received 10 October 2008; accepted 22 October 2008; published online 11 November 2008)

Compressional (V_P) and shear wave (V_S) velocities of the amorphous phase of ZrW_2O_8 have been measured up to 10.4 GPa at room temperature using ultrasonic interferometry in conjunction with synchrotron x radiation. The pressure-density relation is determined using the measured velocities. Both V_P and V_S, as well as the adiabatic bulk and shear moduli, exhibit monotonic increase with increasing pressure. The pressure derivatives of the bulk and shear moduli are determined to be K'_{S0}=7.3(1) and G'_0=1.8(1), with bulk and shear moduli K_{S0}=61.7(5) GPa and G_0=35.0(2) GPa. Comparing with the α phase, V_P, V_S, K_{S0}, E, Θ_{ac}, and σ of the amorphous phase decrease by 14.8%, 10.0%, 17.2%, 2.9%, 1.2%, and 15.5%, along with 28% and 3.2% increase in density and shear modulus, respectively. © *2008 American Institute of Physics*. [DOI: 10.1063/1.3023049]

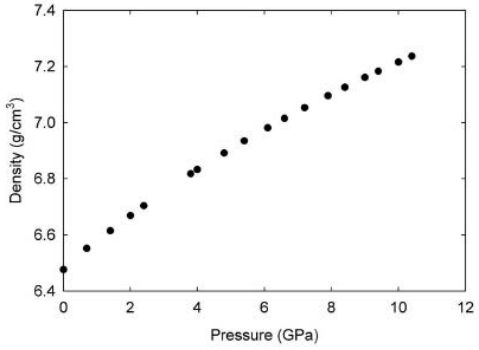

FIG. 2. Densities of amorphous ZrW_2O_8 in terms of pressure at room temperature.

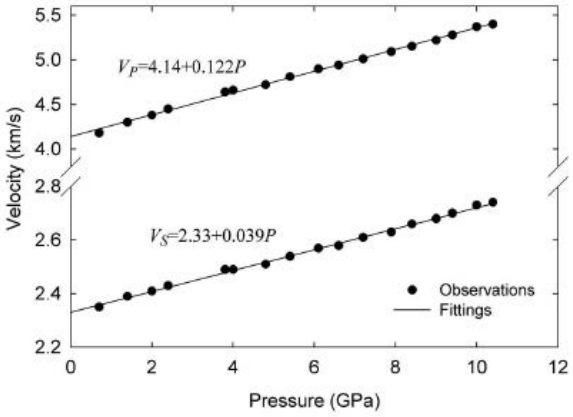

FIG. 1. P and S wave velocities of amorphous ZrW_2O_8 as a function of pressure at ambient temperature. The solid lines are linear fittings.

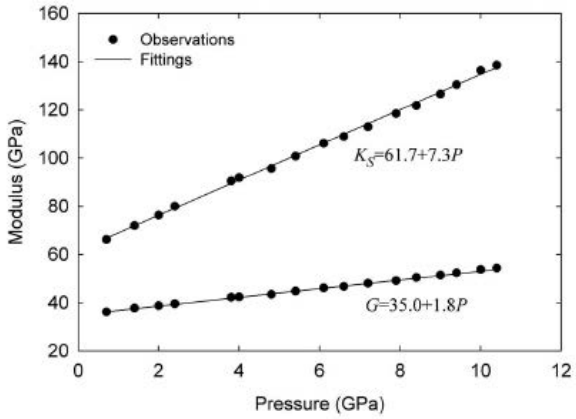

FIG. 3. Bulk and shear moduli of amorphous ZrW_2O_8 as a function of pressure at ambient temperature. The solid lines are linear fittings.

TABLE II. Ultrasonic wave velocities, elastic moduli, and selective elastic parameters of α and amorphous phase of ZrW_2O_8 at ambient conditions.

	V_P (km s^{-1})	V_S (km s^{-1})	ρ (g cm^{-3})	K_{S0} (GPa)	G_0 (GPa)	E (GPa)	Θ_{ac} (K)	σ
Amorphous (a)	4.14	2.33	6.477	61.7	35.0	85.7	317	0.256
α–ZrW_2O_8 [a]	4.86	2.59	5.059	74.5	33.9	88.3	321	0.303
$(a-\alpha)/\alpha$ (%)	−14.8	−10.0	28.0	−17.2	3.2	−2.9	−1.2	−15.5

Physica B 406 (2011) 52–55

Synchrotron X-ray study of filled skutterudites $CeFe_4Sb_{12}$ and $Ce_{0.8}Fe_3CoSb_{12}$

Wei Liu [a,*], Qing Jie [b], Qiang Li [b], Zhiqiang Chen [c], Baosheng Li [a]

[a] Mineral Physics Institute, Stony Brook University, Stony Brook, NY 11794, USA
[b] Condensed Matter Physics and Materials Science Department, Brookhaven National Laboratory, Upton, NY 11973, USA
[c] Department of Geosciences, Stony Brook University, Stony Brook, NY 11794, USA

A B S T R A C T

In situ synchrotron X-ray diffraction measurements are carried out on filled skutterudites $CeFe_4Sb_{12}$ and $Ce_{0.8}Fe_3CoSb_{12}$ up to 32 and 20 GPa, respectively, at room temperature. No phase transformation was observed for both samples in the pressure range. Fitting the pressure–volume data (up to 10 GPa) to the third-order Birch–Murnaghan equation of state, the bulk modulus B_0 is determined to be 74(4) GPa, with the pressure derivative $B'_0=7(2)$ for $CeFe_4Sb_{12}$, and $B_0=71(2)$ GPa and $B'_0=8(2)$ for $Ce_{0.8}Fe_3CoSb_{12}$. The bulk moduli of filled skutterudites $CeFe_4Sb_{12}$ and $Ce_{0.8}Fe_3CoSb_{12}$ in our study are smaller than those from previous studies on unfilled skutterudite $CoSb_3$. The P–V curves of the unfilled skutterudite $CoSb_3$ and filled skutterudites $Ce_yFe_{4-x}Co_xSb_{12}$ showed good agreement, indicating that the Ce filling fraction and the replacement of Fe with Co have little effect on their compression behaviors.

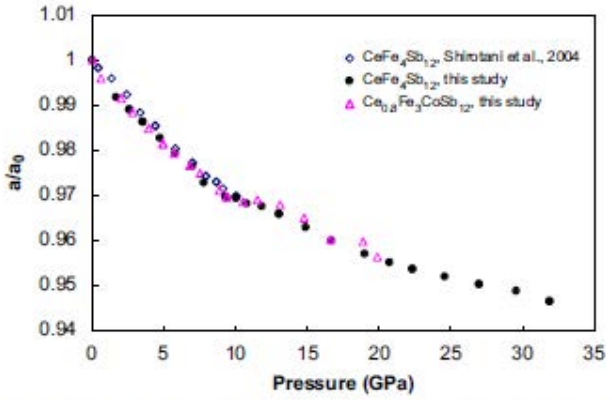

Fig. 3. Normalized lattice constants of $CeFe_4Sb_{12}$ and $Ce_{0.8}Fe_3CoSb_{12}$ at room temperature. The error bars are less than the symbols.

Table 1
Bulk moduli of $CeFe_4Sb_{12}$ and $Ce_{0.8}Fe_3CoSb_{12}$.

Samples	B_0 (GPa)	B'_0	V_0 (Å^3)	RMS misfit
$CeFe_4Sb_{12}$	74(4) [a]	7(2) [a]	762.066 [a]	0.17
	82(2)	4	762.066	0.22
	80(8)	6(2)	760.771(1677)	0.17
	88(4) [b]	4(1) [b]	763.326 [b]	
$Ce_{0.8}Fe_3CoSb_{12}$	71(2) [a]	8(2) [a]	753.884 [a]	0.10
	83(2)	4	753.884	0.22
	76(40)	7(1)	752.527(754)	0.09
$CoSb_3$	81(1) [b]	6(1) [b]	740.014 [b]	
	93.2(6) [c]	4 [c]	737.783 [c]	

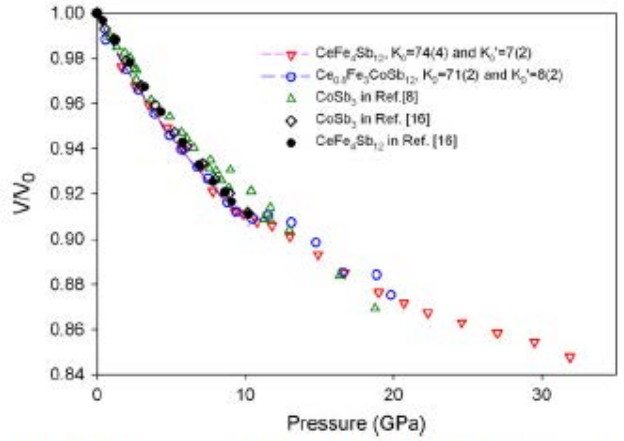

Fig. 4. Normalized pressure–volume data and the Birch–Murnaghan equation fitting results of $CeFe_4Sb_{12}$, $Ce_{0.8}Fe_3CoSb_{12}$, and $CoSb_3$.

Acknowledgements

We thank Dr. Sanjit Ghose for the support at the X17C beamline. This work was supported by DoE/NNSA (DEFG5209NA29458 to BL). QJ and QL are supported by the Office of Science, U.S. Department of Energy, under Contract No. DE-AC02-98CH10886. The experiments were carried out at the National Synchrotron Light Source (NSLS), which is supported by the US Department of Energy, Division of Materials Sciences and Division of Chemical Sciences under Contract No. DE-AC02-76CH00016. The operation of X17C is supported by COMPRES, the Consortium for Materials Properties Research in Earth Sciences.

Physics and Chemistry of Materials

Evidence of tetragonal nanodomains in the high-pressure polymorph of $BaTiO_3$

L. Ehm, L.A. Borkowski, J.B. Parise, Z. Chen *Stony Brook University*
S. Ghose *Brookhaven National Laboratory*

The pressure induced *P*4*mm*→*Pm*-3*m* phase transition in $BaTiO_3$ perovskite was investigated by x-ray total scattering. The evolution of the structure was analyzed by fitting pair distribution functions over a pressure range from ambient pressure up to 6.85(7) GPa. Evidence for the existence of tetragonal ferroelectric nanodomains at high pressure was found. The average size of the nanodomains in the high-pressure phase decreases with increasing pressure. Extrapolation of the domain size to pressures higher than studied experimentally suggests a disappearance of the ferroelectric domains at about 9.3(5) GPa and a cubic symmetry of $BaTiO_3$ high-pressure phase.

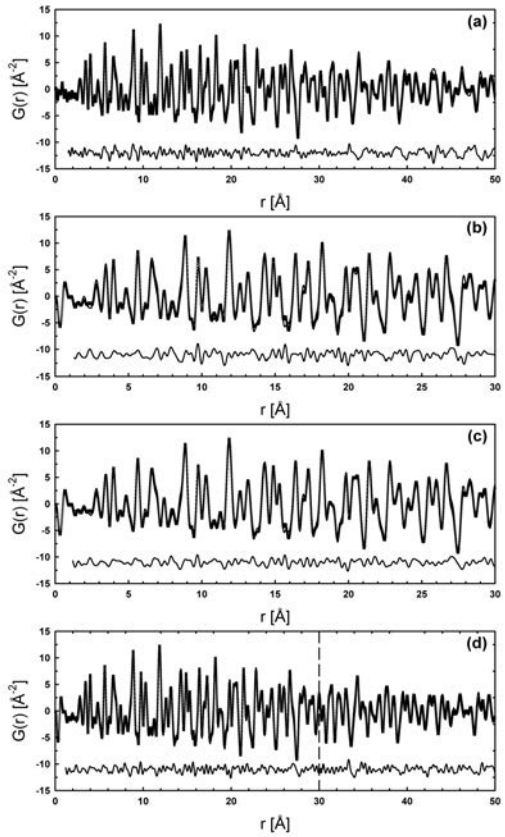

Left: Refinements of the pair distribution function (a) at ambient pressure in the diamond anvil cell using the tetragonal disordered structure model R_{wp} = 14.7%, (b) at 2.8(1) GPa refining the cubic model to r_{max} = 30 Å with R_{wp} = 18.9%, (c) at 2.8(1) GPa fitting the tetragonal disordered model to r_{max} = 30 Å with R_{wp} = 13.4%, (d) at pressure of 2.8(1) GPa as a combination of disordered tetrahedral phase up to r = 30 Å and the ordered cubic structure model in the r-range of 30–50 Å.

Bottom: Evolution of the Ti atom displacement (inset) and the average tetragonal domain size with pressure.

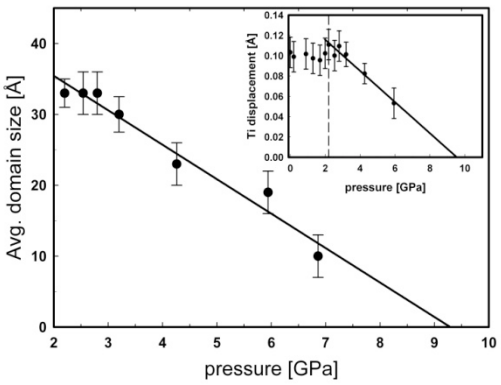

Reference: L. Ehm, L.A. Borkowski, J.B. Parise, S. Ghose and Z. Chen, Evidence of tetragonal nanodomains in the high-pressure polymorph of $BaTiO_3$. *Applied Physics Letters*, 98, 021901, 2011.

This research was partially supported by COMPRES, the Consortium for Materials Properties Research in Earth Sciences, under NSF Cooperative Agreement No. EAR 06-49658. Use of the National Synchrotron Light Source, Brookhaven National Laboratory, was supported by the U.S. Department of Energy, Office of Science, Office of Basic Energy Sciences, under Contract No. DE-AC02-98CH10886. J.B.P. is grateful for the support of the National Science Foundation through Grant No. DMR-0800415 and the Department of Energy through Grant No. DE-SC0002510.

Ionic high-pressure form of elemental boron

A. Oganov (Stony Brook), J. Chen (FIU), C Gatti (CNR), Y. Ma (TTU), Y. Ma (Jilin), C. Glass (ETH), Z. Liu (CIW), T. Yu (FIU), O. Kurakevych (Paris) and V. Solozhenko (Paris)

Boron is an element of fascinating chemical complexity. Although we now know of at least 16 polymorphs, the stable phase of boron is not yet experimentally established even at ambient conditions. Boron's complexities arise from frustration: situated between metals and insulators in the periodic table, boron has only three valence electrons, which would favour metallicity, but they are sufficiently localized that insulating states emerge. However, this subtle balance between metallic and insulating states is easily shifted by pressure, temperature and impurities.

The results of high-pressure experiments and *ab initio* evolutionary crystal structure predictions have found a new boron phase that we named γ-B_{28}. In situ high-pressure x-ray diffraction was performed at the x17C beamline of the NSLS.

The new phase is stable between 19 and 89 GPa, can be quenched to ambient conditions, and has a hitherto unknown structure (space group Pnnm, 28 atoms in the unit cell) consisting of icosahedral B-12 clusters and B-2 pairs in a NaCl- type arrangement. We find that the ionicity of the phase affects its electronic bandgap, infrared adsorption and dielectric constants, and that it arises from the different electronic properties of the B-2 pairs and B-12 clusters and the resultant charge transfer between them.

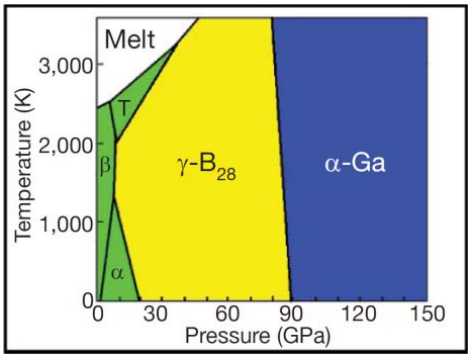

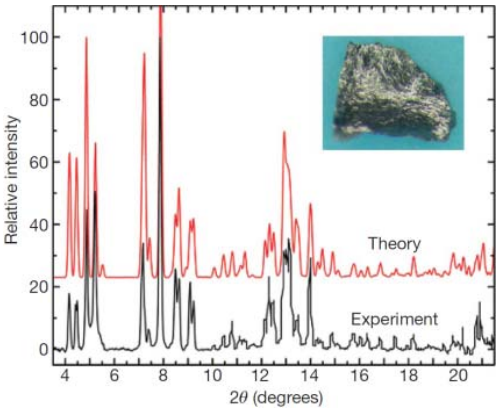

Upper: P-T phase diagram for elemental boron.

Lower: Comparison of x-ray diffraction pattern from X17C, NSLS with prediction of an *ab initio* evolutionary crystal structure prediction

Reference:

Artem R. Oganov, Jiuhua Chen, Carlo Gatti, Yanzhang Ma, Yanming Ma, Colin W. Glass, Zhenxian Liu, Tony Yu, Oleksandr , O. Kurakevych & Vladimir L. Solozhenko, Nature,457,863(2009)

Portions of the work were carried out at X17C and U2A beamlines of NSLS which are supported by COMPRES, the Consortium for Material Property Research in the Earth Sciences under NSF Cooperative Agreement EAR06-49658

The incompressibility of osmium metal at ultrahigh pressures and temperatures

Matt M. Armentrout and Abby Kavner, Earth & Space Science Department,
University of California, Los Angeles 90095

(Work performed at the ALS, HP-CAT, GSECARS, and also using the COMPRES gas-loading system at GSECARS)

Osmium is a third row transition metal in the iron group with a hexagonal close-packed structure, and is characterized by its high density, extremely low compressibility and high hardness. For these reasons it has been used to synthesize a number of ultra-hard materials of composed of a high valence transition metal covalently bonded to a lighter element. The behavior of ultra-hard materials is of significant interest for high temperature applications. We measured the thermal equation of state of osmium in the laser heated diamond anvil cell at pressures up to 50 GPa and temperatures up to 3000 K.

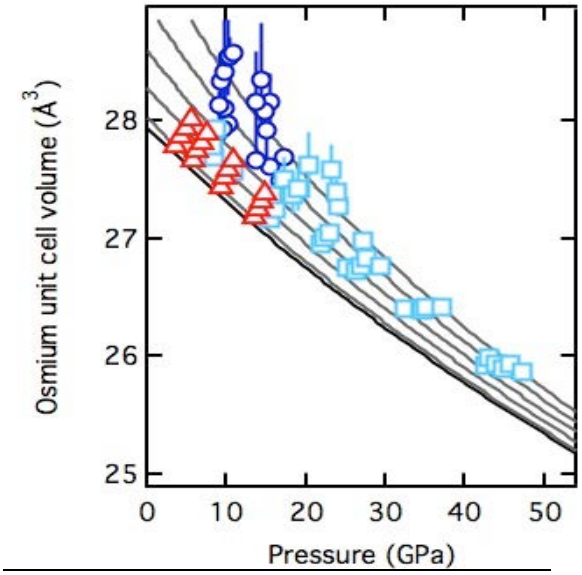

Figure 1. Measurements of osmium's unit cell volume as a function of pressure and temperature. High temperature measurements include those taken at COMPRES supported beamlines: 12.2.2 at the Advanced Light Source (circles), at HPCAT at the Advanced Photon Source (squares), and multianvil measurements by Voronin *et al* (2005). Isotherms at 300, 500, 1000, 1500, 2000, and 2500 K are plotted as a guide to the eye.

V_0 (Å^3)	K_0 (GPa)	K_0'	γ_0	q
27.941 (fixed)	421 (3)	4 (fixed)	2.32 (0.08)	7.2 (1.4)

Table 1. Fitted equation of state parameters for osmium metal. Data was fit to the isothermal third order Birch-Murnaghan equation with a Mie-Grüneisen-Debye thermal pressure correction.

The equation of state of osmium is notable both for its very high bulk modulus and for its very high q value. The later correlates to very small thermal expansions at elevated temperatures.

References

M. M. Armentrout* and A. Kavner, Incompressibility of osmium metal at high pressures and temperatures, *J. Appl. Phys*. Vol. 107 (9) 093528 (2010).
G. A. Voronin, C. Pantea, T. W. Zerda, L. Wang, and Y. Zhao, J. Phys. Chem. Sol. **66**, 706 (2005).

Pressure-Induced Invar Behavior in Pd_3Fe

M. L.Winterrose, M. S. Lucas, A. F. Yue, I. Halevy, L. Mauger, J. A. Munoz, Jingzhu Hu, M. Lerche, and B. Fultz (Caltech, Stony Brook, CIW)

Invar behavior, with its anomalously low thermal expansion, has been of interest for over a century. Alloys of Pd-Fe with compositions around 30% Pd have long been known for Invar behavior at ambient pressure, but the composition range is narrow, from approximately 25 to 35%Fe. Normal thermal expansion occurs for Fe concentrations above 35%.

With data from X17C at NSLS, we discovered that pressure can induce Invar behavior at the composition 75%Fe. Figure 1 shows results of measurements at 300 K at pressures up to 33 GPa. The anomaly around 10 GPa was shown to coincide with a loss of ferromagnetism in the material. A more impressive proof of Invar behavior is shown in Fig. 2, where diffraction data from X17C were acquired from a sample heated in a diamond anvil cell. The pressure was 7 GPa, near the onset of the transition at ambient temperature, and temperature was increased to 650 K. Heating the sample under a pressure of 7 GPa showed negligible thermal expansion from 300 to 523 K, demonstrating Invar behavior. Density functional theory calculations showed how pressure causes the energy of some majority-spin t_{2g} electronic states to increase past the Fermi level, causing a loss of magnetism and a change in mechanical properties.

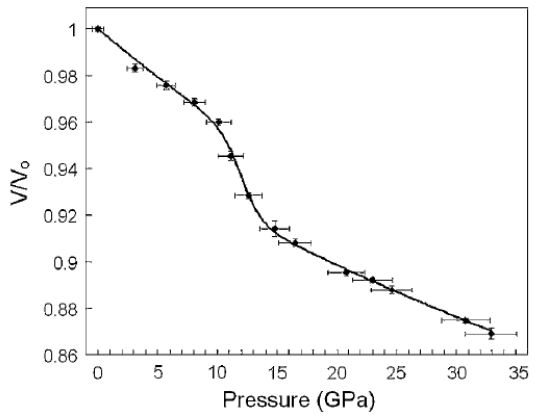

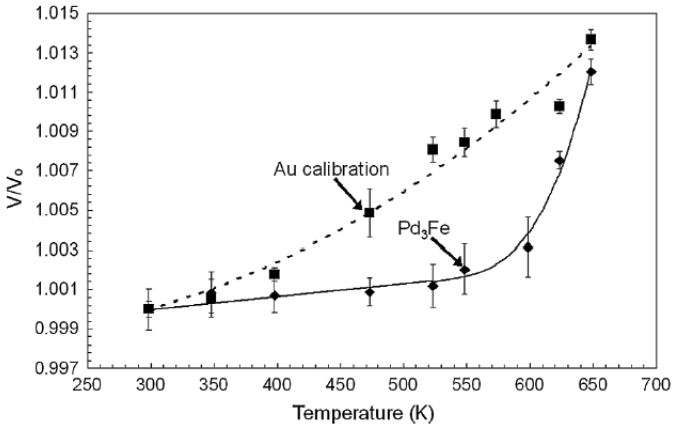

Fig. 1 (left). Volume-pressure data obtained from synchrotron x-ray diffraction measurements (symbols) and the fit of the data to the Weiss-like equation of state (line).

Fig. 2 (right). Volume-temperature data for Pd_3Fe (diamonds) and Au (squares), obtained from externally heating the diamond anvil cell at an approximately constant pressure of 7 GPa.

M.L. Winterrose, et al., Pressure-Induced Electronic Transition and Invar Behavior in Pd_3Fe, *Phys. Rev. Lett.*, 102, 237202 (2009).
M.L. Winterrose, et al., Dynamics of Fe atoms across the pressure-induced Invar transition in Pd_3Fe, *Phys. Rev. B*, in press.

Portions of this work were conducted at X17C, NSLS which is supported by COMPRES, the Consortium for Material Property Research in the Earth Sciences under NSF Cooperative Agreement EAR06-49658.

Network Rigidity in GeSe2 Glass at High Pressure

Sytle M. Antao,1,* Chris J. Benmore,1 Baosheng Li,2 Liping Wang,2 Evgeny Bychkov,3 and John B. Parise2

1*Advanced Photon Source, Argonne National Laboratory, Argonne, Illinois 60439, USA*
2*Mineral Physics Institute and Department of Geosciences, Stony Brook University, Stony Brook, New York 11794-2100, USA*
3*LPCA, UMR 8101 CNRS, Universite´ du Littoral, 59140 Dunkerque, France*

Acoustic measurements using synchrotron radiation have been performed on glassy GeSe2 up to pressures of 9.6 GPa. A minimum observed in the shear-wave velocity, associated anomalous behavior in Poisson's ratio, and discontinuities in elastic moduli at 4 GPa are indicative of a gradual structural transition in the glass. This is attributed to a network rigidity minimum originating from a competition between two densification mechanisms. At pressures up to 3 GPa, a conversion from edge- to cornersharing tetrahedra results in a more flexible network. This is contrasted by a gradual increase in coordination number with pressure, which leads to an overall stiffening of the glass.

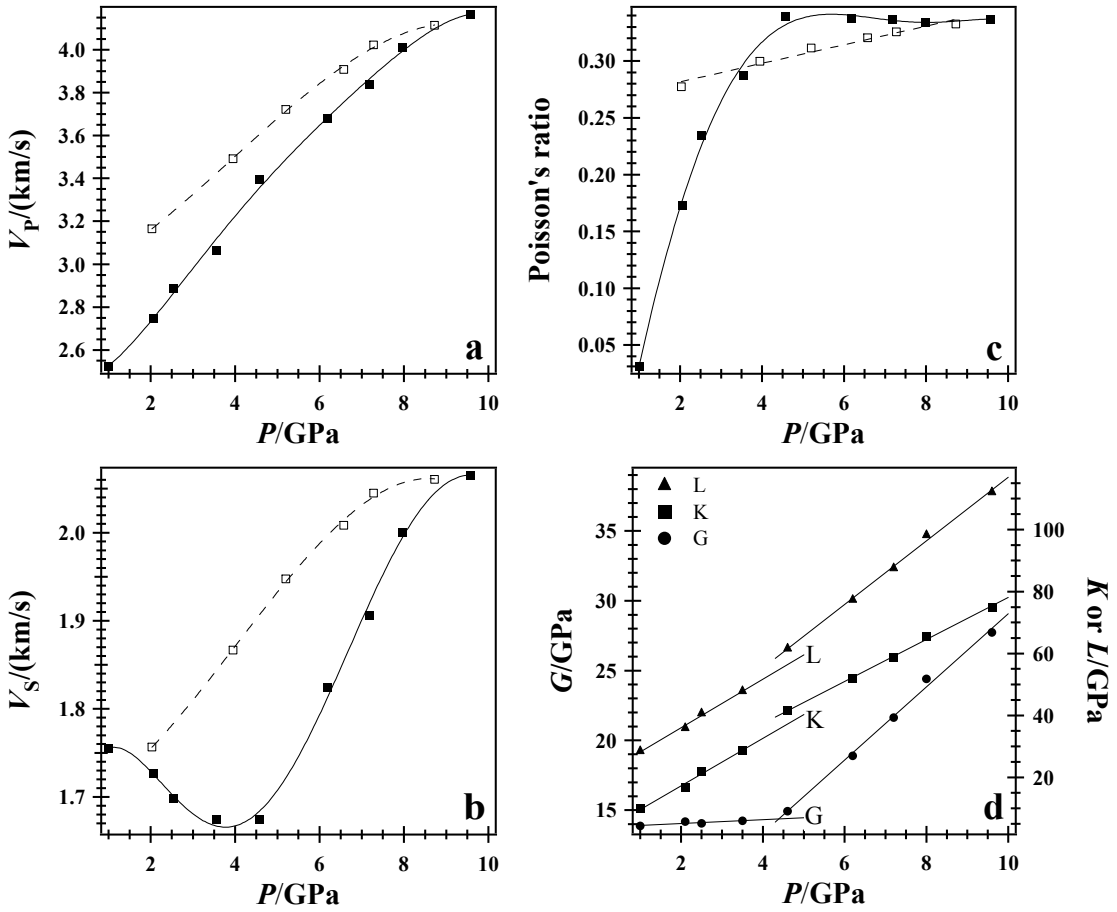

Fig. 3. Variations with pressure. (a) VP, (b) VS, (c) Poisson's ration, (d) elastic moduli.

Publication: Antao, S.M., Benmore, C.J., Li, B., Wang, L., Bychkov, E., and Parise, J.B. (2008): Network rigidity in $GeSe_2$ glass at high pressure. *Physical Review Letters*, 100, 115501.

Acknowledgements: This study was supported by NSF Grants No. EAR-0510501 and No. DMR-0800415 to J. B. P., and DoE/NNSA (No. DEFG5206NA26211) to B. L. The experimentalwork was performed at X17B2 of the National Synchrotron Light Source (NSLS), supported by the U.S.Department of Energy, Division of Materials Sciences and Division of Chemical Sciences, under Contract No. DEAC02-98CH10886. This research was partially supported by COMPRES, the Consortium for Materials PropertiesResearch in Earth Sciences under NSF Cooperative Agreement EAR 01-35554 and 06-49658.

Decomposition of $W(CO)_6$ at high pressures and temperatures

Nadine Rademacher, Björn Winkler *Goethe University Frankfurt, Los Alamos National Laboratory*
Lkhamsuren Bayarjargal, Alexandra Friedrich, Wolfgang Morgenroth *Goethe University Frankfurt*

The organometallic compound $W(CO)_6$ and its decomposition have been studied at high pressures and temperatures in heated autoclaves and laser-heated diamond anvil cells (DACs). The bulk modulus of $W(CO)_6$ has been determined to be around 13(1) GPa by fitting equations of state to pressure-volume data. A texture analysis has revealed that the application of pressure to $W(CO)_6$ results in lattice preffered orientation, which decreases after laser heating. The decomposition products were characterized by X-ray diffraction, Raman spectroscopy, scanning electron microscopy and pair distribution function analysis. At lower pressures a metastable tungsten carbide (W_2C) could be isolated and at higher pressures tungsten oxides (WO_2, W_3O_8) and graphite were obtained. All decomposition products were nanocrystalline and had disordered structures.

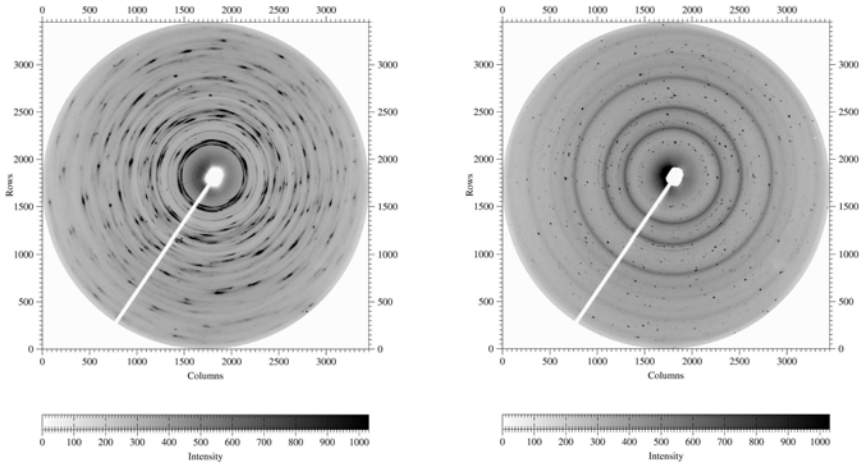

Figure 1: Typical 2D synchrotron X-ray diffraction images before (left) and after (right) laser heating W(CO)6. Note the texture present in the diffraction image before laser heating.

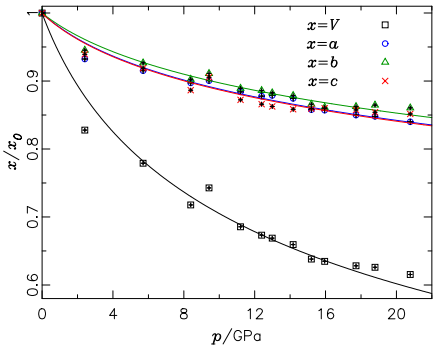

Figure 2: Least-squares fit of 2nd order Birch-Murnaghan equations of state to the lattice parameters and the unit cell volume of $W(CO)_6$ (solid line) as a function of pressure.

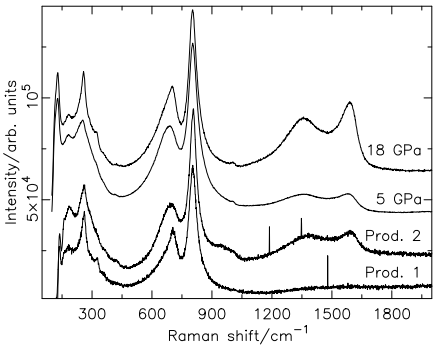

Figure 3: Raman spectra of the decomposition products of $W(CO)_6$ obtained in heated autoclaves and laser-heated DACs. Note the graphite modes around 1500 cm^{-1}.

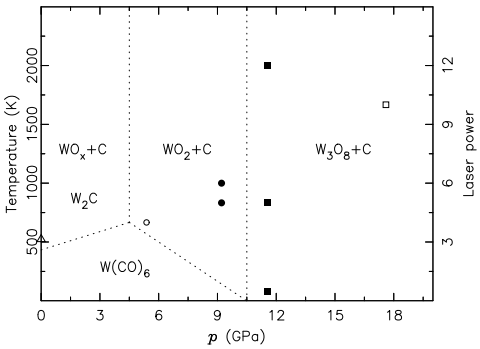

Figure 4: Schematic p,T-field of the decomposition products of $W(CO)_6$. The open triangle represents the experiment in the autoclave and the other symbols represent the experiments in the DACs.

Reference: N. Rademacher, L. Bayarjargal, A. Friedrich, W. Morgenroth, M. Avalos-Borja, S. C. Vogel, T. Proffen and B. Winkler, Decomposition of $W(CO)_6$ at high pressures and temperatures, *J. Appl. Cryst.*, 2011, submitted.

These high-pressure experiments were carried out at beamline 12.2.2 of the Advanced Light Source (ALS), which is supported by the Director, Office of Science, Office of Basic Energy Science, of the U.S. Department of Energy under contract DE-AC02-05CH11231 and by COMPRES, the Consortium for Materials Properties Research in Earth Science under NSF Cooperative Agreement EAR 06-49658. Financial support by the Goethe University Frankfurt and the "Vereinigung der Freunde und Förderer der Goethe-Universität" is gratefully acknowledged. We also thank the staff of the beamline for their support. NRs work at the Lujan Neutron Scattering Center and BWs Wheatley scholar stay have been funded by LANL.

Formation of TaB_2 from the elements in a laser heated diamond anvil cell

Björn Winkler, Alexandra Friedrich, Lkhamsuren Bayarjargal, Florian Schröder, Jasmin Biehler *Goethe University Frankfurt, Germany*
Erick A. Juarez-Arellano *Universidad del Papaloapan, Mexico*

In situ synchrotron X-ray diffraction was used to observe the reaction induced by laser heating of a mixture of tantalum and boron in a diamond anvil cell. Laser heating at pressures of 12 and 24 GPa resulted in the formation of TaB_2. No signs of the other five intermediate phases reported at room pressure (in increasing order of boron content Ta_2B, Ta_3B_2, TaB, Ta_5B_6, Ta_3B_4) were observed. The bulk modulus of TaB_2 (B_0 = 341(7) GPa) was determined from a fit of a second-order Birch-Murnaghan equation of state to the p–V data. Density functional theory based calculations complemented the experimental observations and were used to obtain the full tensor of elastic stiffness coefficients.

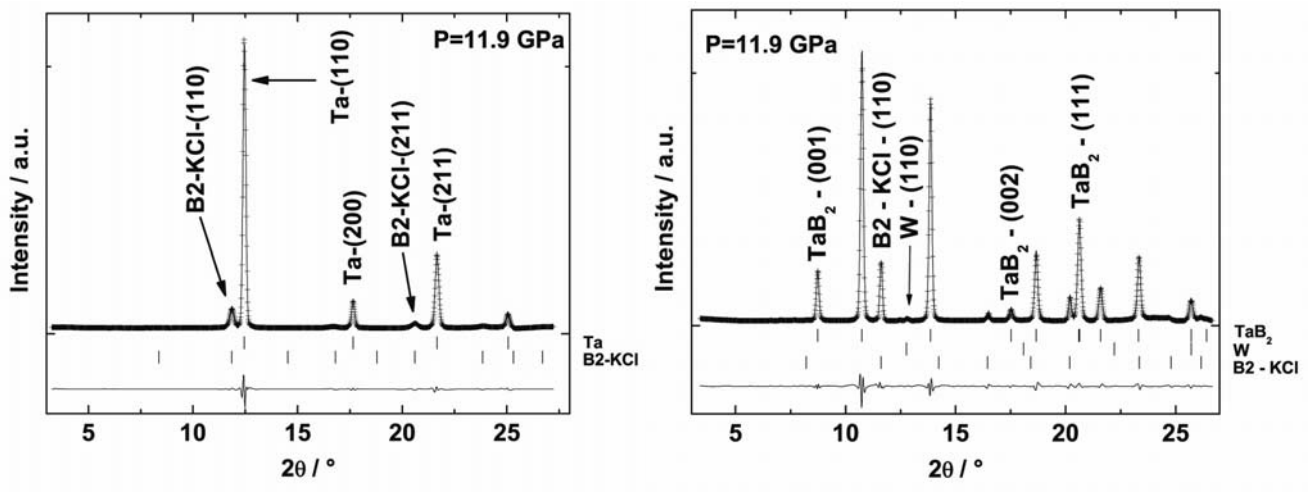

Diffraction pattern before (left) and after (right) laser heating a mixture of Ta and boron at 11.9 GPa, showing the formation of TaB_2 from the elements. Additional phases are B2-KCl (from the thermal insulation) and W (from the gasket).

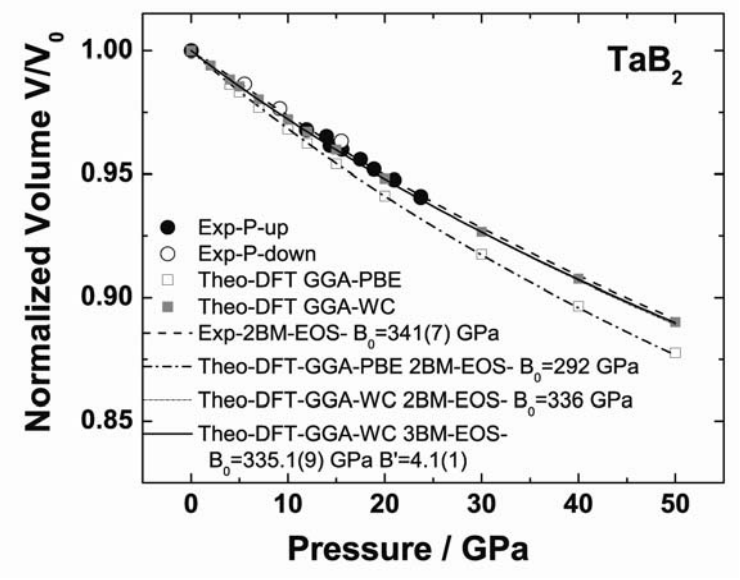

Variation of the experimental and theoretical unit cell volume versus pressure of TaB_2. Least-squares fits of 2nd and 3rd-order Birch-Murnaghan equations of state to the pressure-volume data are represented by lines.

Reference: B. Winkler, E.A. Juarez-Arellano, A. Friedrich, L. Bayarjargal, F. Schröder, J. Biehler, V. Milman, S.M. Clark, J. Yan, In situ synchrotron X-ray diffraction study of the formation of TaB_2 from the elements in a laser heated diamond anvil cell, *Solid State Sciences*, 12, 2059-2064, 2010.

This research was supported by Deutsche Forschungsgemeinschaft (Project Wi-1232), in the framework of the DFG-SPP 1236. These high-pressure experiments were carried out at beamline 12.2.2 of the Advanced Light Source (ALS), which is supported by the Director, Office of Science, Office of Basic Energy Science, of the U.S. Department of Energy under contract DE-AC02-05CH11231 and by COMPRES, the Consortium for Materials Properties Research in Earth Science under NSF Cooperative Agreement EAR 06-49658. We also thank the staff of the beamline, J. Yan and S.M. Clark, for their support, and the "Vereinigung der Freunde u. Förderer der Goethe-Universität Frankfurt" for financial support.

In situ observation of the reaction of tantalum with nitrogen in a laser heated diamond anvil cell

Alexandra Friedrich, Björn Winkler, Lkhamsuren Bayarjargal, Wolfgang Morgenroth, Jasmin Biehler, Florian Schröder *Goethe University Frankfurt, Germany*
Erick A. Juarez-Arellano *Universidad del Papaloapan, Mexico*

Tantalum nitrides were formed by reaction of the elements at pressures between 9(1) and 12.7(5) GPa and temperatures > 1600-2000 K in the laser-heated diamond anvil cell. The incorporation of small amount of nitrogen in the cubic tantalum structure was identified as the first reaction product on weak laser irradiation. Subsequent laser heating led to the formation of hexagonal β-Ta_2N and orthorhombic η-Ta_2N_3, which was the pure and stable phase at pressures up to 27 GPa and high temperatures. No evidence was found for the presence of ε-TaN, ϑ-TaN, δ-TaN, Ta_3N_5-I or Ta_3N_5-II, which was predicted to be the stable phase at $P > 17$ GPa and $T = 2800$ K, at the P,T-conditions of this experiment. η-Ta_2N_3 is very incompressible with a bulk modulus $B_0 = 319(6)$ GPa, which was determined from a 2nd-order Birch-Murnaghan equation of state fit to the experimental data. Quantum mechanical calculations using the density functional theory (DFT) gave a bulk modulus of $B_0 = 348.0(9)$ GPa for a 2nd-order fit or $B_0 = 339(1)$ GPa and $B' = 4.67(9)$ for a 3rd-order fit. From the DFT data the structural compression mechanism could be determined.

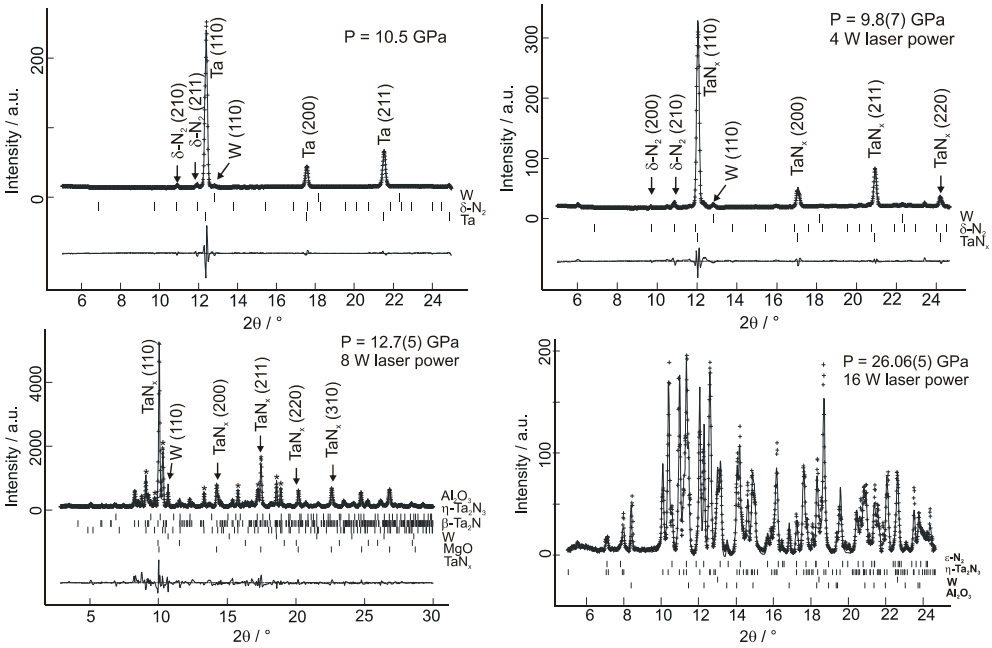

Powder x-ray diffraction patterns of the tantalum foil (top left), the TaN_x after short laser alignment (top right), the mixture of TaN_x, β-Ta_2N and η–Ta_2N_3 after subsequent heating (bottom left), and of the fully reacted η–Ta_2N_3 (bottom right) after strong laser heating and at maximum pressure.

Pressure dependencies of the normalized unit cell parameters of η–Ta_2N_3 (right). Dashed and solid lines represent least-squares fits of Birch-Murnaghan equations of state to the experimental and theoretical results, respectively. DFT data are plotted with open symbols.

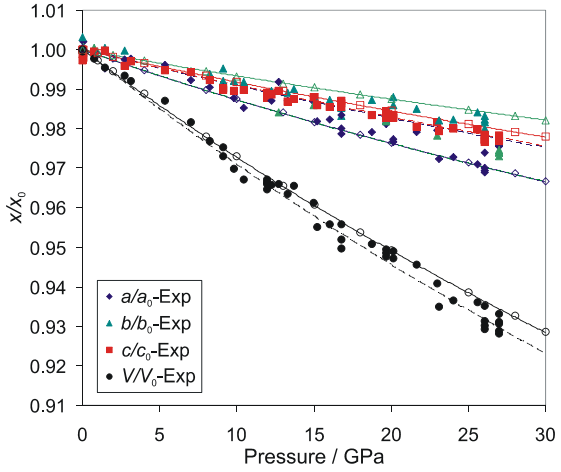

Reference: A. Friedrich, B. Winkler, L. Bayarjargal, E.A. Juarez-Arellano, W. Morgenroth, J. Biehler, F. Schröder, In situ observation of the reaction of tantalum with nitrogen in a laser heated diamond anvil cell, *Journal of Alloys and Compounds*, 502, 5-12, 2010.

This research was supported by Deutsche Forschungsgemeinschaft (grants WI-1232/25-1, WI-1232/26-1, FR-2491/2-1), in the framework of the DFG-SPP 1236. These high-pressure experiments were carried out at beamline 12.2.2 of the Advanced Light Source (ALS), which is supported by the Director, Office of Science, Office of Basic Energy Science, of the U.S. Department of Energy under contract DE-AC02-05CH11231 and by COMPRES, the Consortium for Materials Properties Research in Earth Science under NSF Cooperative Agreement EAR 06-49658. We also thank the staff of the beamline, J. Yan and S.M. Clark, for their support. Financial support from the Goethe university and the "Vereinigung der Freunde u. Förderer der Goethe-Universität Frankfurt" is gratefully acknowledged.

Novel ultra-incompressible rhenium nitrides: High-(p,T) synthesis in a laser heated diamond anvil cell and characterization

Alexandra Friedrich, Björn Winkler, Lkhamsuren Bayarjargal, Wolfgang Morgenroth *Goethe University Frankfurt, Germany*
Erick A. Juarez-Arellano *Universidad del Papaloapan, Mexico*

The formation of novel hexagonal rhenium nitrides from the elements was investigated by in situ synchrotron x-ray diffraction at $10 < p < 32$ GPa and $T > 1600$ K using the laser heated diamond anvil cell. At 13 GPa Re_3N (SG: $P\bar{6}m2$) was synthesised at about 1600 K and further heated up to 2300 K. Re_2N (SG: $P6_3/mmc$), which is isotypic to Re_2C, is formed when laser heating Re_3N at 20 GPa. Both phases are ultra-incompressible with bulk moduli of 395(7) GPa (Re_3N) and 401(10) GPa (Re_2N), similar to the most incompressible binary *TM*-carbides and -nitrides found to date. The recovered samples were further characterized by synchrotron x-ray Laue micro-diffraction at beamline 12.3.2 at the ALS and by micro-Raman spectroscopy.

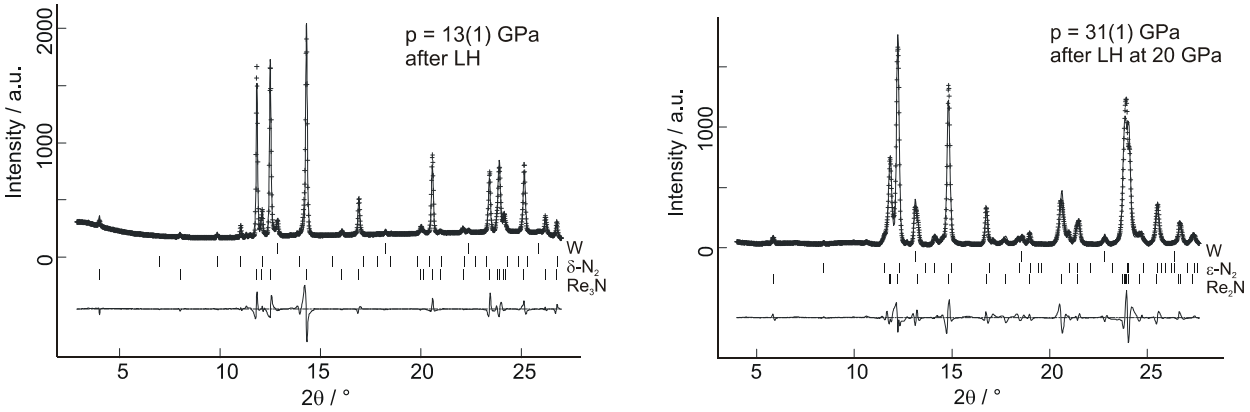

Powder x-ray diffraction patterns of (left) Re_3N after laser heating at 1700(200) K at 13(1) GPa and (right) Re_2N at 31(1) GPa after reaction during laser heating at 20(2) GPa and pressure increase.

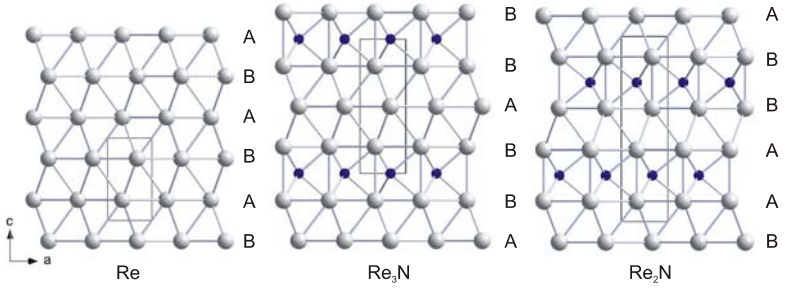

Structural considerations and DFT calculations resulted in a structural model for Re_3N, which shows an ABB stacking sequence of the rhenium atoms, and for Re_2N in an AABB stacking sequence. Nitrogen is located in the interstices between the AA and BB layers.

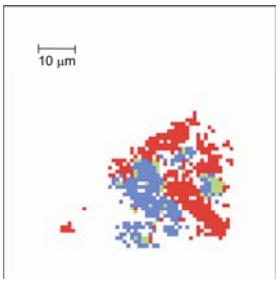

Left: Indexation of x-ray Laue diffraction patterns and monochromator scans confirmed the proposed unit-cell parameters for both rhenium nitrides and allowed the analysis of their phase distribution within the samples. Red: Re_3N, blue: Re_2N.

Right: All four Raman-active modes of Re_3N, which have been predicted by DFT using the proposed structural model, are observed experimentally.

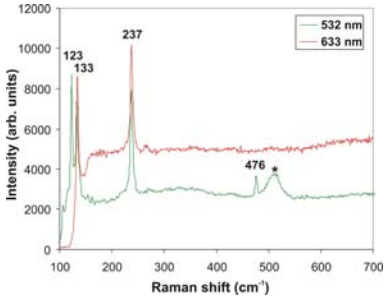

References: A. Friedrich, B. Winkler, L. Bayarjargal, W. Morgenroth, E.A. Juarez-Arellano, V. Milman, K. Refson, M. Kunz, K. Chen, Novel Rhenium Nitrides, *Phys. Rev. Lett*, 105, 085504, 2010. A. Friedrich, B. Winkler, K. Refson, V. Milman, Vibrational properties of Re_3N from experiment and theory, *Phys. Rev. B*, 82, 224106, 2010.

This research was supported by Deutsche Forschungsgemeinschaft (grants FR-2491/2-1, WI-1232/25-1), in the framework of the DFG-SPP 1236, and by the BMBF, Germany (grant 05KS7RF1). These high-pressure experiments were carried out at beamline 12.2.2 of the Advanced Light Source (ALS), which is supported by the Director, Office of Science, Office of Basic Energy Science, of the U.S. Department of Energy under contract DE-AC02-05CH11231 and by COMPRES, the Consortium for Materials Properties Research in Earth Science under NSF Cooperative Agreement EAR 06-49658. We also thank the staff of beamlines 12.2.2 and 12.3.2 for their support. Financial support from the FOKUS program of the Goethe university and the "Vereinigung der Freunde u. Förderer der Goethe-Universität Frankfurt" is gratefully acknowledged.

Ultra-incompressible Re_2C, synthesis and structural stability

Erick A. Juarez-Arellano *Universidad del Papaloapan, Mexico*
Björn Winkler, Alexandra Friedrich, Lkhamsuren Bayarjargal *Goethe University Frankfurt, Germany*

The formation of a hexagonal rhenium carbide phase, Re_2C, from the elements has been studied in a laser heated diamond anvil cell in a (p, V) range of 20–40 GPa and 1000–2000 K. No indication for the existence of cubic rhenium carbide, as suggested in the literature, or any other phase was found. Re_2C is the only phase formed in the Re–C system up to around 70 GPa and 4000 K. A fit of a 3rd-order Birch–Murnaghan equation of state to the experimental data results in a bulk modulus of $B_0 = 405(30)$ GPa ($B' = 4.6$). The linear compressibility of Re_2C along [0 0 1] (~500GPa) is significantly smaller than the compressibility in the (0 0 1) plane (~ 360 GPa ||[1 0 0]).

Overview of the pressure–temperature range in which Re_2C can be synthesized. The hexagonal rhenium carbide Re_2C is the only phase present up to around 70 GPa and 4000 K.

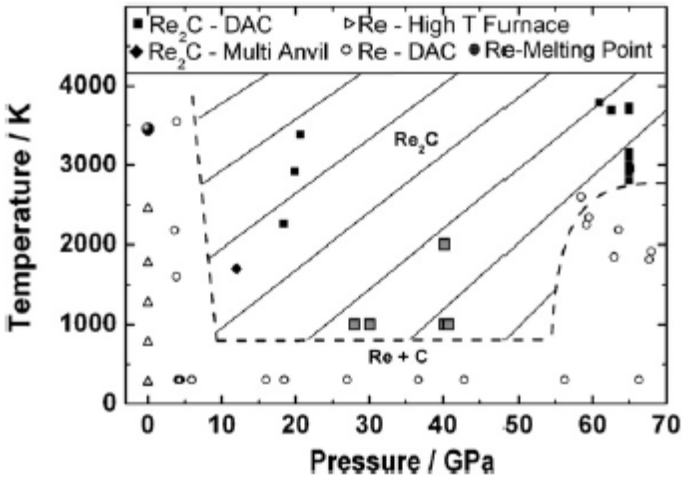

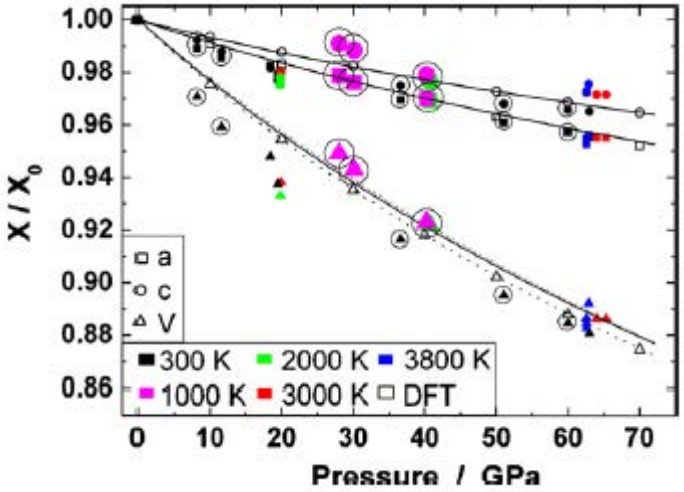

Pressure dependence of the Re_2C normalized unit cell parameters. Dashed and solid lines represent 2nd- (dashed line) and 3rd-order (solid line) BM-EOS fits, respectively, to the experimental results. The DFT results (open symbols) were not used for the fits. The dotted line represents a 3rd-order BM-EOS fit to the DFT results. Markers within a circle represent results from this study, while the rest were taken from [Zeitschrift für Kristallographie 223 (2008) 492-501]. Enlarged symbols represent data collected using NaCl (ALS) while the rest were collected using Ar (ESRF) as a pressure-transmitting medium.

Reference: E.A. Juarez-Arellano, B. Winkler, A. Friedrich, L. Bayarjargal, V. Milman, J. Yan, S.M. Clark, Stability field of the high-(P,T) Re_2C phase and properties of an analogous osmium carbide phase, *Journal of Alloys and Compounds*, 481, 577-581, 2009.

This research was supported by Deutsche Forschungsgemeinschaft (Project Wi-1232), in the framework of the DFG-SPP 1236. These high-pressure experiments were carried out at beamline 12.2.2 of the Advanced Light Source (ALS), which is supported by the Director, Office of Science, Office of Basic Energy Science, of the U.S. Department of Energy under contract DE-AC02-05CH11231 and by COMPRES, the Consortium for Materials Properties Research in Earth Science under NSF Cooperative Agreement EAR 06-49658. EAJA thanks the CONACyT and AF thanks the CNV-Foundation for financial support. Also, we are grateful to the staff of the beamline, J. Yan and S.M. Clark, for their support, and to the ESRF for beam time and financial support.

Reaction of titanium with carbon in a laser heated diamond anvil cell and reevaluation of a proposed pressure-induced structural phase transition of TiC

Björn Winkler, Alexandra Friedrich, Lkhamsuren Bayarjargal *Goethe University Frankfurt, Germany*
Erick A. Juarez-Arellano *Universidad del Papaloapan, Mexico*

The formation of cubic TiC_x from the elements was studied in a laser-heated diamond anvil cell at pressures up to 26 GPa. Annealed samples at these pressures show no splitting of the cubic (1 1 1) or (2 2 2) reflection. This is in contrast to an earlier study, in which a splitting of the (1 1 1) reflection was observed above 18 GPa. The recovered sample had a lattice parameter of 4.3238(6) Å, which implies that the synthesis gave fully stoichiometric TiC. Density functional theory-based model calculations were used to study the dependence of the total energy of a rhombohedral distortion. In these model calculations the total energy was minimal for the undistorted (cubic) lattice. Therefore, the results obtained here imply that at least for titanium carbides with a high carbon content no pressure-induced structural phase transition up to at least 26 GPa occurs. The appearance of a trigonal TiC_x polymorph during the synthesis is discussed in terms of its relative stability with respect to the cubic phase.

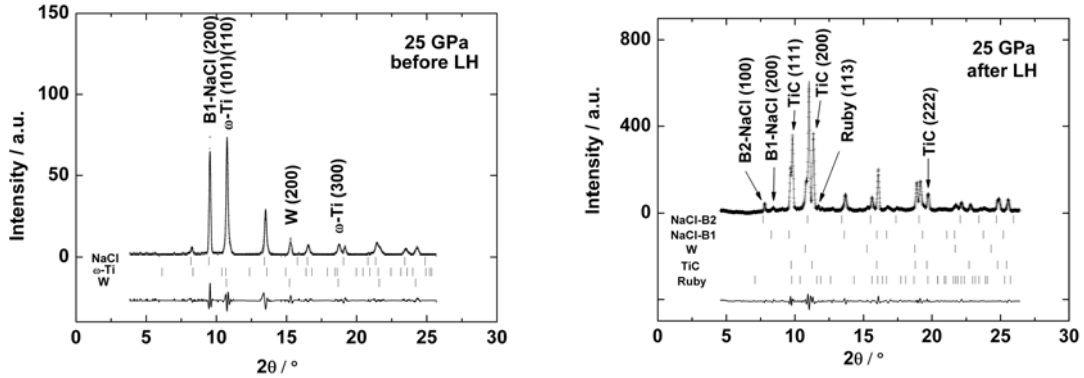

Powder x-ray diffraction patterns at 25 GPa before (left) and after (right) laser heating.

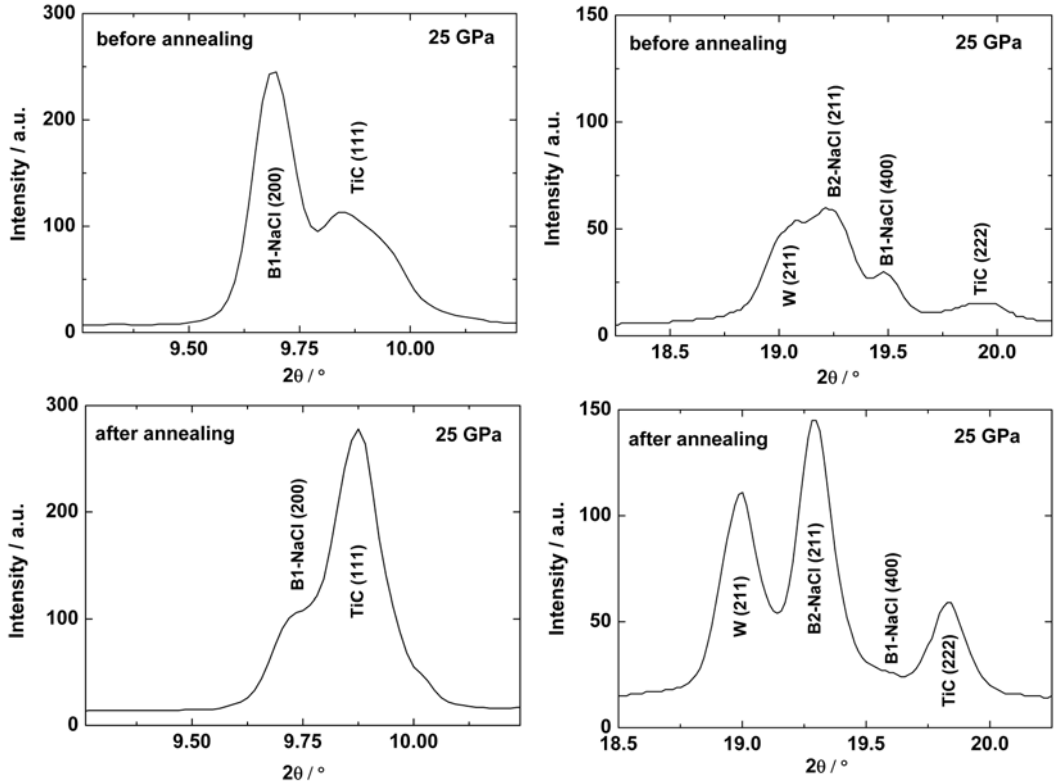

Powder x-ray diffraction patterns before and after annealing the sample at 25 GPa. The top row shows the cubic (1 1 1) reflection of TiC, the lower row shows the cubic (2 2 2) reflection.

Reference: B. Winkler, E.A. Juarez-Arellano, A. Friedrich, L. Bayarjargal, J. Yan, S.M. Clark, Reaction of titanium with carbon in a laser heated diamond anvil cell and reevaluation of a proposed pressure-induced structural phase transition of TiC, *Journal of Alloys and Compounds*, 478, 392-397, 2009.

This research was supported by Deutsche Forschungsgemeinschaft (project WI-1232), in the framework of the DFG-SPP 1236. These high-pressure experiments were carried out at beamline 12.2.2 of the Advanced Light Source (ALS), which is supported by the Director, Office of Science, Office of Basic Energy Science, of the U.S. Department of Energy under contract DE-AC02-05CH11231 and by COMPRES, the Consortium for Materials Properties Research in Earth Science under NSF Cooperative Agreement EAR 06-49658. We also thank the staff of the beamline, J. Yan and S.M. Clark, for their support.

Stabilization of the cubic ScC-B1 structure by oxygen incorporation at high-(p,T) conditions

Erick A. Juarez-Arellano *Universidad del Papaloapan, Mexico*
Björn Winkler, Lkhamsuren Bayarjargal, Alexandra Friedrich, Florian Schröder *Goethe University Frankfurt, Germany*
Monika Koch-Müller *GeoForschungsZentrum Potsdam, Germany*
Miguel Avalos-Borja *CNyN, UNAM, Mexico*

Synchrotron diffraction experiments with in situ laser heated diamond anvil cells and multi-anvil press synthesis experiments have been performed in order to investigate the reaction of scandium and carbon from the elements at high-(P,T) conditions. It was observed that the reaction is very sensitive to the presence of oxygen and that oxygen stabilizes the cubic ScC-B1 structure (ScO_xC_y). In an oxygen-rich environment the most stable phase is ScO_xC_y, where for these experiments x=0.39 and y=0.50–0.56. If only a small oxygen contamination is present, we have observed the formation of Sc_3C_4, Sc_4C_3 and a new orthorhombic ScC_x phase. All the phases formed at high pressures and temperatures are quenchable.

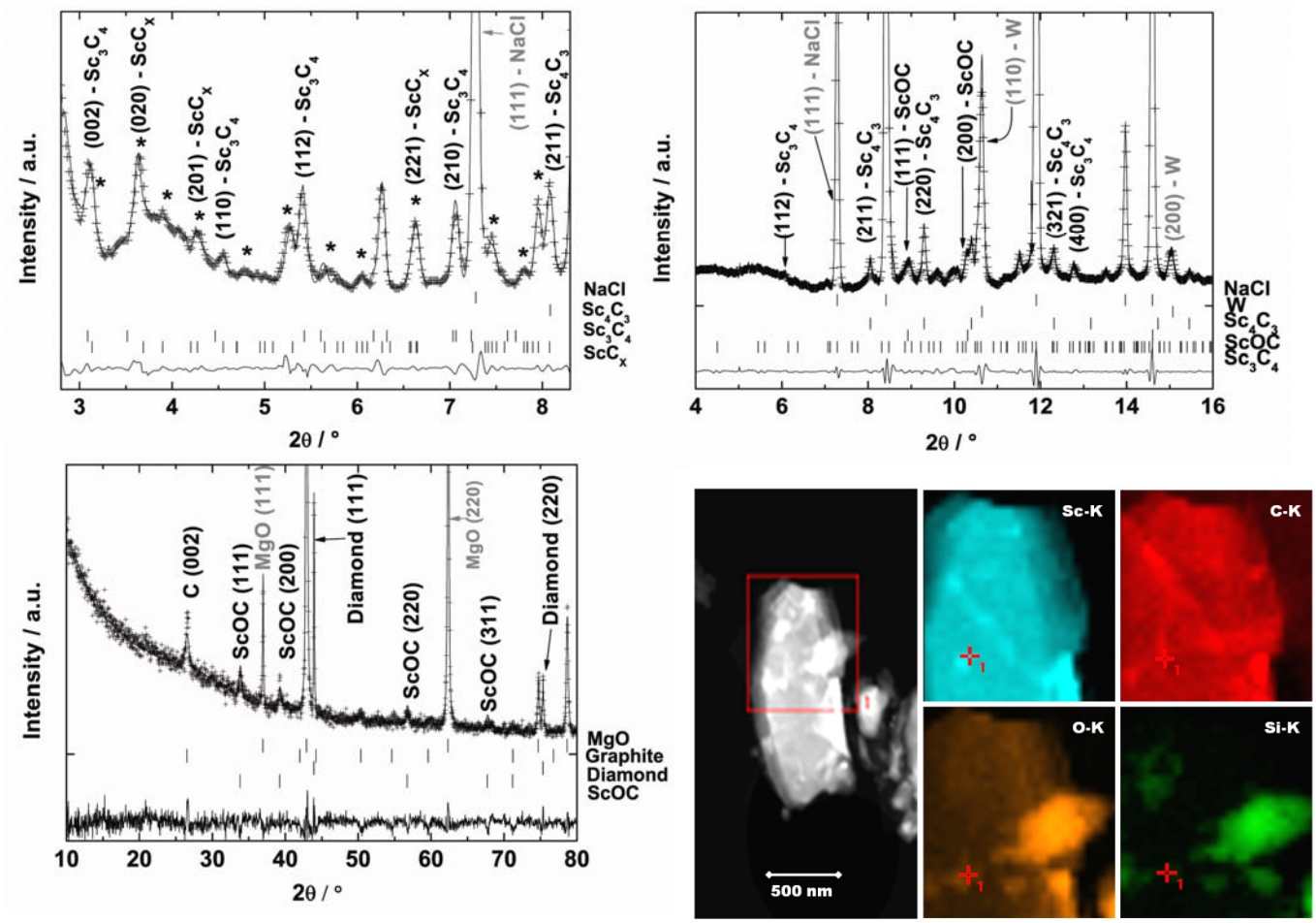

Diffraction pattern of (Top left) the recovered sample after
Laser Heating in a Diamond Anvil Cell (LH-DAC) α-Sc-foil and graphite at 9 GPa, (Top right) recovered sample after LH-DAC α-Sc-flakes and graphite at 13 GPa, and (Bottom left) recovered sample from a multi-anvil press at 10 GPa and 1673 K. (Bottom right) TEM-EDS mapping of the multi-anvil press recovered sample showing the homogeneous distribution of scandium, carbon and oxygen.

Reference: E.A. Juarez-Arellano, B. Winkler, L. Bayarjargal, A. Friedrich, V. Milman, D.R. Kammler, S.M. Clark, J. Yan, M. Koch-Müller, F. Schröder, and M. Avalos-Borja, Formation of scandium carbides and scandium oxycarbide from the elements at high-(*P*,*T*) conditions, *Journal of Solid State Chemistry*, 183, 975-983, 2010.

This research was supported by Deutsche Forschungsgemeinschaft (Project Wi-1232), in the framework of the DFG-SPP 1236, by DGAPA-UNAM grant IN-108908 and by CONACyT-DAAD PROALMEX grant. These high-pressure experiments were carried out at beamline 12.2.2 of the Advanced Light Source (ALS), which is supported by the Director, Office of Science, Office of Basic Energy Science, of the U.S. Department of Energy under contract DE-AC02-05CH11231 and by COMPRES, the Consortium for Materials Properties Research in Earth Science under NSF Cooperative Agreement EAR 06-49658. We also thank the staff of the beamline, J. Yan and S.M. Clark, for their support.

Axial ratio and electronic topological transitions in $Cd_{0.80}Hg_{0.20}$ at high pressures

S. Speziale[1], R. Jeanloz[1], S.M. Clark[2], S. Meenakshi[3], V. Vijayakumar[3], A.K. Verma[3], R.S. Rao[3], and B.K. Godwal[3]
[1]Univ. California, Berkeley, U.S.A.
[2]Lawrence Berkeley Natl. Laboratory, U.S.A.
[3]BARC, Mumbay, India

We performed high-pressure x-ray diffraction of $Cd_{0.8}Hg_{0.2}$. Our results show subtle discontinuities in the pressure dependence of the lattice parameters and of the bulk modulus at 8 and 22 GPa. By combining experimental results and quantum-mechanical computations we could attribute the observed anomalies to the effects of electronic topological transitions (ETT) caused by pressure-induced intersection of the Fermi surface and critical points in the electronic band structure of the alloy. Our study shows that high resolution x-ray diffraction measurements can identify very subtle elastic anomalies due to onset of ETTs in hcp metals.

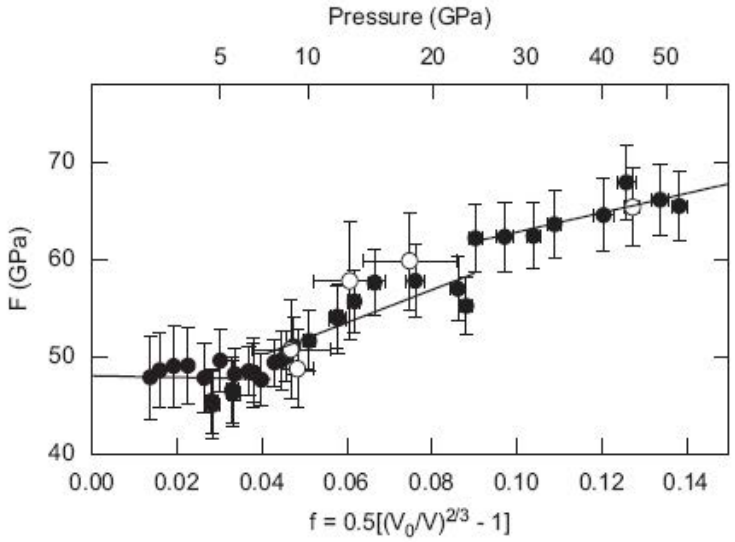

Figure 1. Normalized stress versus Eulerian strain plot for $Cd_{0.8}Hg_{0.2}$ compressed to 50 GPa. Two discontinuities at 8 and 22 GPa are related to ETTs.

Citation: Speziale S., R. Jeanloz, S.M. Clark, S. Meenakshi, V. Vijayakumar, A.K. Verma, R.S. Rao, and B.K. Godwal, Axial ratio and electronic topological transitions in $Cd_{0.80}Hg_{0.20}$ at high pressures, J. Phys. Chem. Solids, 69, 2325-2331, 2008.

Experimental work was performed at A.L.S. Beamline 12.2.2 supported by COMPRES, within the NSF cooperative agreement EAR 06-49658.

Thermomechanics of Nanocrystalline Nickel under High Pressure-Temperature conditions

Zhao Y, Zhang J, Clausen, B., Shen, T.D., Gray III, G.T., Wang, L.

Comparative *in-situ* deformation studies were conducted on nanocrystalline and bulk nickels using synchrotron x-rays at high pressures (*P*) and temperatures (*T*). We derived high-*P* triaxial compression yield strength as a function of temperature, which provides a new dimension to gain a thorough insight into the mechanical behaviors of materials. Contrary to tensile experiments of uniaxial loading, we observed significant work-hardening for the nano-Ni in high-pressure plastic deformation stage, whereas the micron-Ni experiences minor high-pressure work-softening and considerable energy dissipation into heat. The significantly reduced energy dissipation for the nano-Ni during the loading-unloading cycle indicates that the nanostructured materials can endure much greater mechanical fatigue in cyclic loadings. We also correlated the yielding with the nucleation, propagation, and storage of dislocations for plastically deforming nanocrystalline materials under triaxial loading and their variations with temperature. This is particularly important in research of nano-scale materials, as differences in specific defect concentration and/or distribution can greatly alter the point at which the material yields.

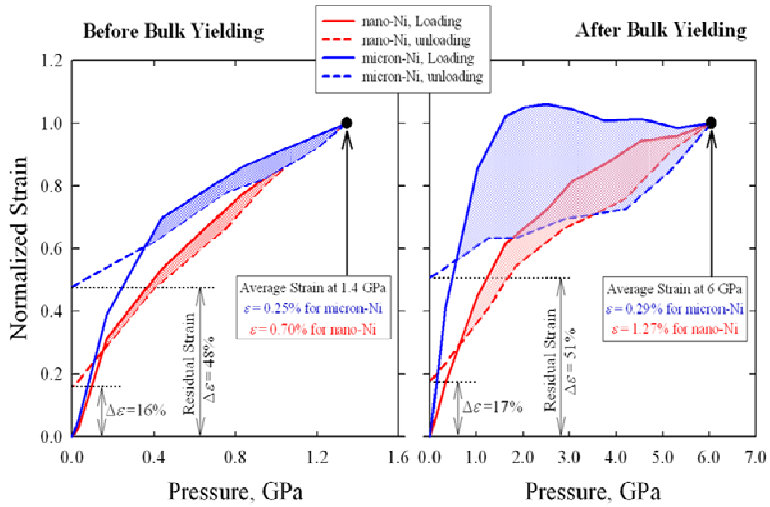

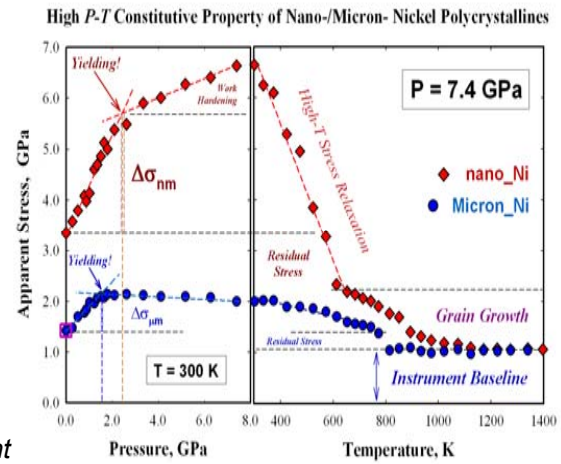

Experiments were conducted at the X17C beamline of NSLS which is supported by COMPRES, the Consortium for Material Property Research in the Earth Sciences under NSF Cooperative Agreement EAR0649658.

Nano Letters (Zhao Y, Zhang J, Clausen, B., Shen, T.D., Gray III, G.T., Wang, L. Vol. 7, 426-432, 2007).

Enhancement of Yield Strength in Zirconium Metal through High-Pressure Induced Structural Phase Transition

Y. Zhao and J. Zhang, Los Alamos National Laboratory

We conducted *in-situ* deformation studies on ultra-pure zirconium metal using synchrotron x-rays under high *P-T* conditions. With a well-known and also commonly used method of peak-profile analysis, we determined the differential strain and hence yield strength in polycrystalline zirconium samples under the applied stress. We observe a high-pressure phase-transition induced strengthening with more than 6-fold abrupt increase in yield strength at the transition pressure of *Pc* = 6 GPa, from 180 MPa in the low-pressure phase of a-Zr to 1180 MPa in the high-pressure phase of w-Zr (Figure 1). **T**he high-*P* phase transition induced enhancement in yield strength can be interpreted by: (1) soft metallic bonding in a-Zr *vs.* strong covalent bonding of w-Zr; (2) relatively easy sliding over smooth close-pack sheets in a-Zr *vs.* bumpy corrugation in slip plane for the open structure in w-Zr atomic layers; and (3) large population of (101)*hcp* twins and basal stacking faults in a-Zr *vs.* repulsive nature of the preferred grain orientations and related microscopic defects such as vacancies and dislocation loops in the w-Zr, which would present strong resistance to plastic flow in the high-pressure phase of zirconium. Our finding unveils a new route for the materials strengthening and is expects to provide new prospects for the understanding of the mechanisms underlying the phase-transition driving plasticity and ductility.

Y. Zhao and J. Zhang, *Applied Physics Letters*, Vol. 91, 201907-1-3, 2007.

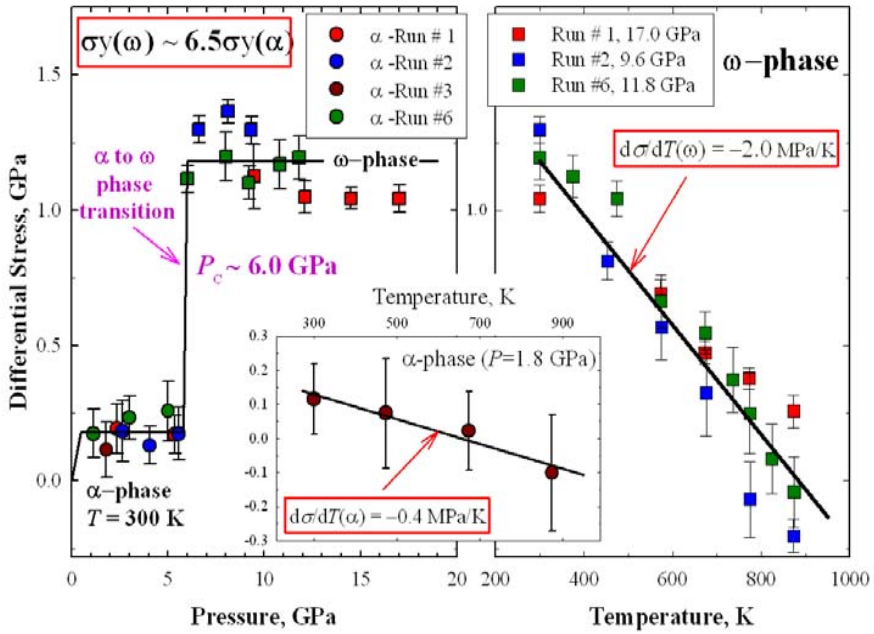

Strength of zirconium

Experiments were conducted at the X17C beamline of NSLS which is supported by COMPRES, the Consortium for Material Property Research in the Earth Sciences under NSF Cooperative Agreement EAR0649658.

Work performed on beamlines X17B2.

PHYSICAL REVIEW B 76, 144107 (2007)

Elasticity of ω-phase zirconium

Wei Liu,[1] Baosheng Li,[1] Liping Wang,[1] Jianzhong Zhang,[2] and Yusheng Zhao[2]
[1]*Mineral Physics Institute, Stony Brook University, Stony Brook, New York 11794, USA*
[2]*LANSCE Division, Los Alamos National Laboratory, Los Alamos, New Mexico 87545, USA*
(Received 4 September 2007; published 17 October 2007)

Compressional (V_P) and shear wave (V_S) velocities as well as unit-cell volumes of the ω phase of Zr have been measured at high pressure (6.9–10.9 GPa) at room temperature using ultrasonic interferometry in conjunction with synchrotron x radiation. Both V_P and V_S as well as the adiabatic bulk (K_S) and shear (G) moduli exhibit monotonic increase with increasing pressure. Using a finite strain equation of state approach, the elastic bulk and shear moduli and their pressure derivatives are derived from the directly measured velocities and densities, yielding K_{S0}=104.0 (16) GPa, G_0=45.1 (9) GPa, K'_{S0}=2.8 (2), and G'_0=0.6 (1) independent of pressure calibration. The low pressure dependence of K_{S0} and G_0 may be attributed to the pressure-induced progressive *s-d* electron transfer in the ω-Zr as suggested by previous Raman studies as well as static compressions at high pressure.

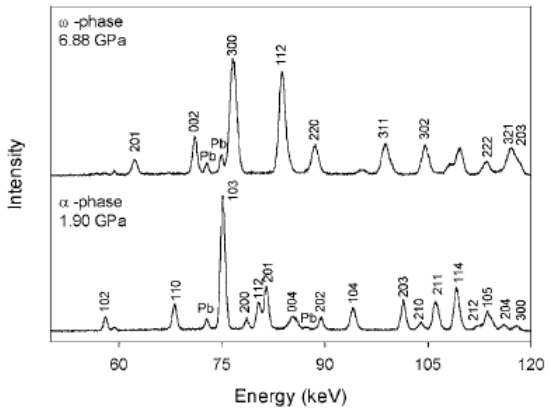

FIG. 1. Selected X-ray diffraction patterns.

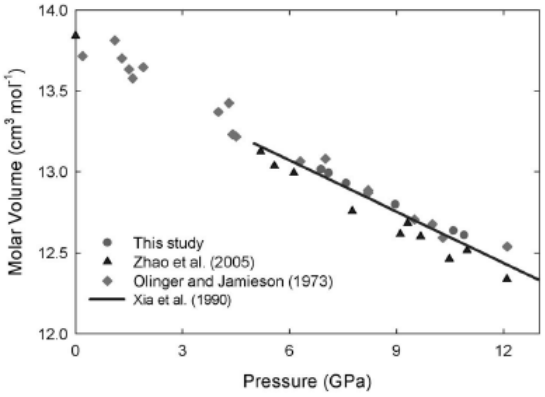

FIG.2. Variation of unit-cell volumes.

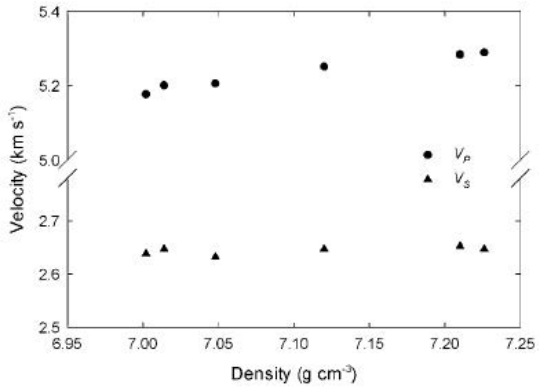

FIG. 3. *P* and *S* wave velocities of the ω-Zr as a function of density at ambient temperature.

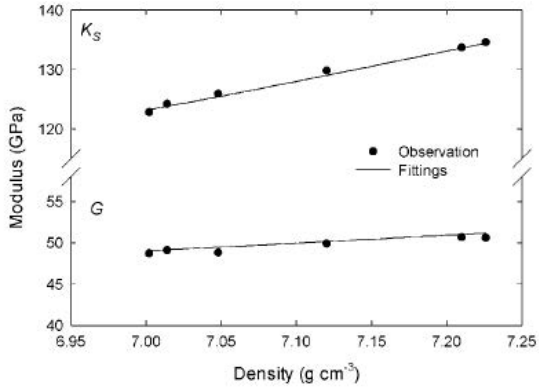

FIG. 4. Calculated moduli for the ω-Zr as a function of density. Third-order finite strain fit is shown as solid line.

This research is supported by DoE/NNSA (DEFG5206NA2621 to BL). We thank Michael Vaughan for technical support at the X17B2 beamline. These experiments were carried out at the National Synchrotron Light Source (NSLS), which is supported by the US Department of Energy, Division of Materials Sciences and Division of Chemical Sciences under Contract No. DE-AC02-76CH00016. X-17B2 is supported by COMPRES.

Simultaneous ultrasonic and synchrotron x-ray studies on pressure induced α-ω phase transition in zirconium

Wei Liu,[1,a)] Baosheng Li,[1] Liping Wang,[1] Jianzhong Zhang,[2] and Yusheng Zhao[2]
[1]*Mineral Physics Institute, Stony Brook University, Stony Brook, New York 11794, USA*
[2]*LANSCE-LC, Los Alamos National Laboratory, Los Alamos, New Mexico 87545, USA*

(Received 17 June 2008; accepted 6 August 2008; published online 1 October 2008)

Compressional and shear wave velocities as well as unit-cell volumes across the α-ω transition of Zr have been measured up to 10.5 GPa at room temperature using ultrasonic interferometry in conjunction with synchrotron x radiation. In the pressure range of 5.0 to 6.2 GPa, a mixture of α and ω phase is clearly identified and the α phase is completely transformed to ω phase at 6.8 GPa. The measured velocity jumps across the α-ω transition are 9.6% and 13.1% for P and S waves, respectively. Negative pressure dependence for the shear modulus of α-Zr has been found at pressures from 1.4 to 2.9 GPa, which may be ascribed to the shear instability of the α phase prior to transition. According to velocity data, the onset pressure of the α-ω transition is determined to be ~4.0 GPa. © *2008 American Institute of Physics*. [DOI: 10.1063/1.2987001]

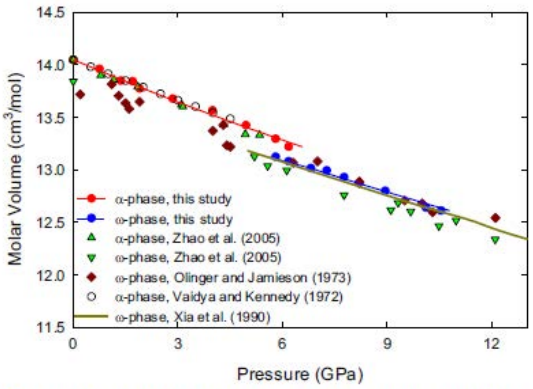

FIG. 1. (Color online) Variation in unit-cell volumes of the α and ω phases as a function of pressure and comparison with results obtained in previous studies. The solid lines are the third-order equations of state fitting to the present experimental data.

TABLE I. Elastic properties of α and ω phases of Zr at ambient conditions.

Phase	K_{S0} (GPa)	G_0 (GPa)	K'_{S0}	G'_0	K_{T0} (GPa)	K'_{T0}	Reference
α phase	95.3	36.3(5)	3.0 (10)	−0.1(2)	94.8	3.0(10)	[a]
	95.31	36.13	4.08	0.02	94.84	4.11	20
					92(3)	*4.0*	3
					94(3)	*3.1*	3
					102.841	3.142	22
					103.3		24
ω phase	104.0(16)	45.1(9)	2.8(2)	0.6(1)			14

[a]This study. Numbers in parentheses are standard deviation (1σ) in the last digit(s). Italic numbers indicate values being fixed.

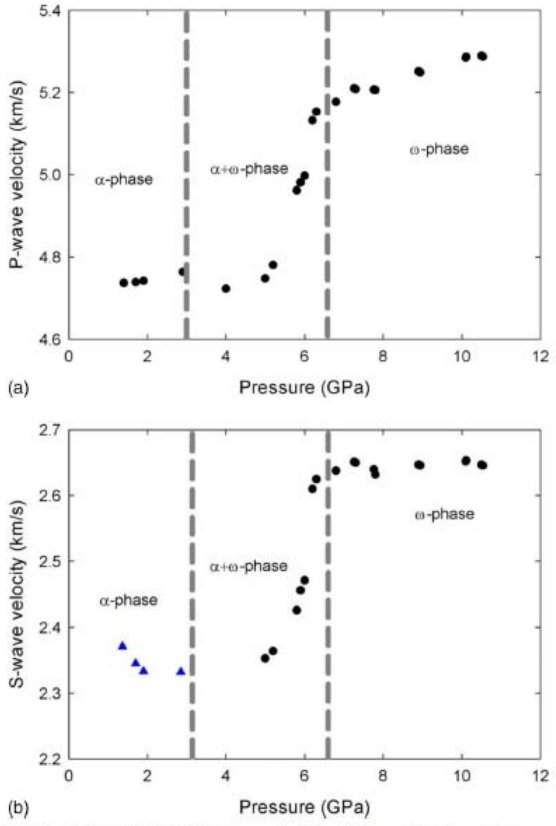

FIG. 2. (Color online) (a) P-wave velocities of Zr as a function of pressure at ambient temperature. (b) S-wave velocities of Zr as a function of pressure at room temperature. The calculated shear wave velocities of α-Zr are shown in solid triangle symbols.

TABLE II. Ultrasonic wave velocities, elastic moduli, and selective elastic parameters of α- and ω-Zr at ambient conditions.

	V_P (km s^{-1})	V_S (km s^{-1})	ρ(g cm^{-3})	K_{S0} (GPa)	G_0 (GPa)	E (GPa)	Θ_{ac} (K)	σ	λ
α	4.698	2.361	6.511	95.3	36.3	96.6	275.9	0.331	71.1
ω	4.996	2.616	6.589	104.0	45.1	118.3	306.1	0.311	74.2
$(\omega-\alpha)/\alpha$ (%)	6.3	10.8	1.2	9.4	24.2	22.4	11.0	−6.0	4.4

High Pressure Structural Stability of Multiferroic Hexagonal *RE*MnO_3

P. Gao, Z. Chen, T. A. Tyso, T. Wu and K. H. Ahn *New Jersey Institute of Technology*
Z. Liu *Carnegie Institution of Washington*
R. Tappero *National Synchrotron Light Source, Brookhaven National Laboratory*
S. B. Kim and S.-W. Cheong *Rutgers University, in New Brunswick*

Structural changes in *RE*MnO_3 (*RE*= Y, Ho, Lu) under high pressure were examined by synchrotron x-ray diffraction methods at room temperature. Compression occurs more readily in the *ab* plane than along the *c*-axis. With increased pressure, a pressure-induced hexagonal to orthorhombic phase transition was observed starting at ~22 GPa for Lu(Y)MnO_3. When the pressure is increased to 35 GPa, a small volume fraction of Lu(Y)MnO_3 is converted to the orthorhombic phase and the orthorhombic phase is maintained on pressure release. High pressure IR absorption spectroscopy and Mn K-edge near edge x-ray absorption spectroscopy confirm that the hexagonal $P6_3cm$ structure is stable below ~20 GPa and the environment around Mn ion is not changed. Shifts in the unoccupied p-band density of states with pressure are observed in the Mn K-Edge spectra. A schematic pressure-temperature phase diagram is given for the small ion *RE*MnO_3 system.

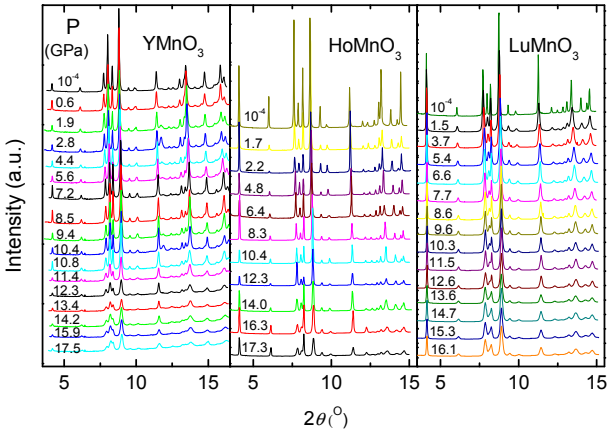

X-ray powder diffraction patterns of *RE*MnO_3 at various pressures (T = 298 K).

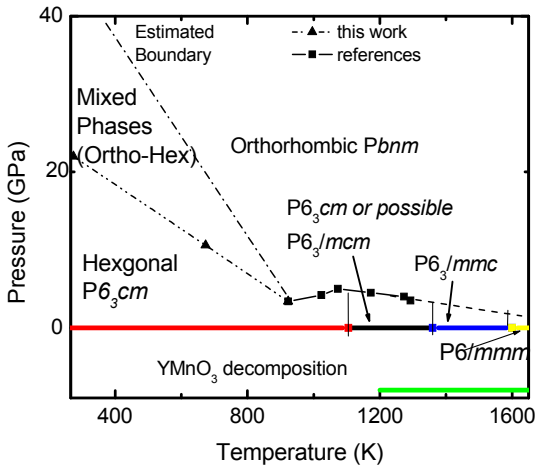

*RE*MnO3 system qualitative Pressure-Temperature phase diagram (based on the $YMnO_3$)

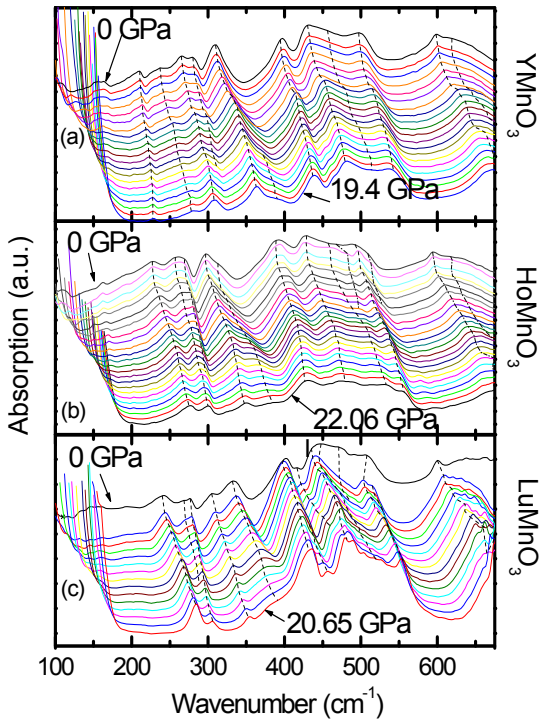

Pressure dependent IR optical density spectrum of Hex-*RE*MnO3 (T=298 K).

Reference: P. Gao, Z. Chen, T. A. Tyson, T. Wu, K. H. Ahn, Z. Liu, R. Tappero, S. B. Kim and S.-W. Cheong, High Pressure Structural Stability of Multiferroic Hexagonal *RE*MnO_3, **arXiv:1010.0653v1** (submitted to Phys. Rev. B.)**.**

This research was funded by DOE Grant DE-FG02-07ER46402 (NJIT) and DE-FG02-07ER46382 (Rutgers). The U2A beam line at the National Synchrotron Light Source is supported by COMPRES, the Consortium for Materials Properties Research in Earth Sciences under NSF Cooperative Agreement EAR01-35554, U.S. Department of Energy (DOE-BES and NNSA/CDAC). Use of NSLS at Brookhaven National Laboratory, was supported by the U.S. Department of Energy, Office of Science, Office of Basic Energy Sciences, under Contract No. DE-AC02-98CH10886. This research used resources of the National Energy Research Scientific Computing Center, which is supported by the Office of Science of the U.S. DOE under Contract No. DE-AC02-05CH11231.

Observation of Anomalous Phonons in Orthorhombic Rare-Rarth Manganites

P. Gao, H. Y. Chen and T. A. Tyson *New Jersey Institute of Technology*
Z. X. Liu *Carnegie Institution of Washington Geophysical Laboratory*
J. M. Bai *Oak Ridge National Laboratory*
L. P. Wang *Stony Brook University*
Y. J. Choi and S.-W. Cheong *Rutgers University, in New Brunswick*

Small rare-earth (*RE*) ion hexagonal *RE*MnO_3 (*RE* =Sc, Y, Ho-Lu) can be stabilized into the metastable orthorhombic (O) structure. These E-type antiferromagnetic metastable O-*RE*MnO_3 systems have been predicted to exhibit mainly electronic polarization (with no large structural distortions) with a large spontaneous polarization along the *a*-axis. We observe the appearance of a phonon near the lock-in temperature in orthorhombic *RE*MnO_3 (for *RE*= Lu and Ho) and anomalous phonon hardening in orthorhombic $LuMnO_3$. The anomalous phonon occurs at the onset of spontaneous polarization. No such changes were found in incommensurate orthorhombic $DyMnO_3$. These observations directly reveal different electric polarization mechanisms in the E-type and incommensurate-type orthorhombic *RE*MnO_3.

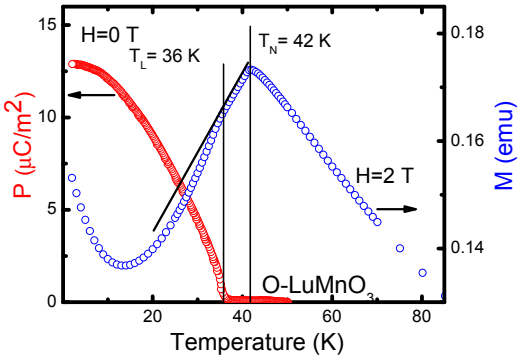

Electric polarization (H = 0 T) and magnetization (H = 2 T) of O-$LuMnO_3$

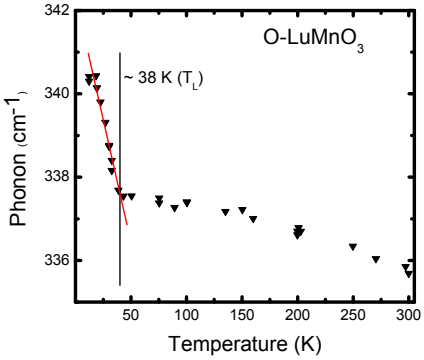

The anomalous phonon hardening of O-$LuMnO_3$ (335.7 cm^{-1}). The vertical line indicates the onset temperature near T_L.

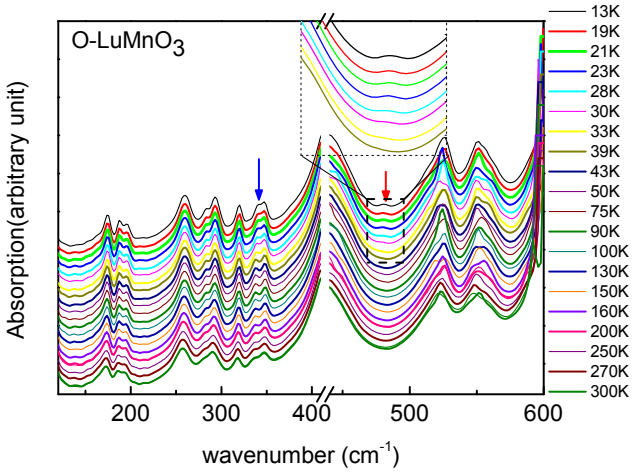

Temperature dependent infrared absorption spectra of O-$LuMnO_3$. Thin lines are for the cooling process and thick lines are for the warming process. Blue and red arrows indicate the anomalous phonon and the appearance of a phonon.

Reference: P. Gao, H. Y. Chen, T. A. Tyson, Z. X. Liu, J. M. Bai, L. P. Wang, Y. J. Choi, and S.-W. Cheong, Observation of anomalous phonons in orthorhombic rare-earth manganites *Appl. Phys. Lett.*, 97, 262905 (2010).

This study was funded by DOE Grants DE-FG02-07ER46402 (NJIT) and DE-FG02-07ER46382 (Rutgers). The U2A beam line at the National Synchrotron Light Source is supported by COMPRES, the Consortium for Materials Properties Research in Earth Sciences under NSF Cooperative Agreement EAR01-35554, U.S. Department of Energy (DOE-BES and NNSA/CDAC). Use of NSLS at Brookhaven National Laboratory, was supported by the U.S. Department of Energy, Office of Science, Office of Basic Energy Sciences, under Contract No. DE-AC02-98CH10886.

Optical Evidence of Mixed-Phase Behavior in Manganite Films

P. Gao, M. A. DeLeon and T. A. Tyson *New Jersey Institute of Technology*
Z. Liu *Carnegie Institution of Washington*
C. Dubourdieu *Laboratoire des Matériaux et du Génie Physique, CNRS*

A mixed valence configuration on Mn sites can be induced in the La-deficient $La_{1-x}MnO_{3-\delta}$ ($x>0$, $\delta>0$) manganite, which exhibit large magnetoresistance. Both ferromagnetic order and metallic conductivity can be obtained and the transition temperatures can be adjusted by both the oxygen content and the La deficiency. Synchrotron infrared measurements were conducted on a self-doped $La_xMnO_{3-\delta}$ ($x\sim0.8$) film. From these measurements we determined the conductivity and the temperature dependence of the effective number of carriers. While the metal-insulator transition temperature (T_{MI}) and the magnetic ordering temperature (T_C) approximately coincide, the onset of the change in the free carrier density occurs at a significantly lower temperature (K ~45 below). This suggests that local distortions exist below T_{MI} and T_C which trap the e_g conduction electrons. These regions with local distortions constitute an insulating phase which persists for temperatures significantly below T_{MI} and T_C.

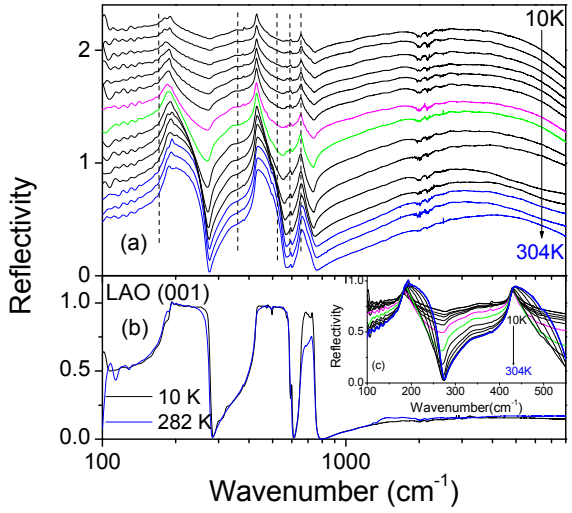

(a) $La_{0.8}MnO_{3-\delta}$ /LAO reflectivity spectra at 10, 20, 50, 80, 100, 125, 150 (purple), 200 (green), 225, 245, 255, 265, 275, 282, 304 K on a logarithmic energy scale. The vertical dashed lines indicate phonon positions. The y-scale corresponds to the 304 K spectrum, and the others are shifted up by 0.1 relative to the previous temperatures. (b) LAO substrate reflectivity spectra. The energy is given on a logarithmic scale in (a) and (b). (c) Insert is an expansion of curves in (a) over the range 100 to 550 cm^{-1} on a linear energy scale.

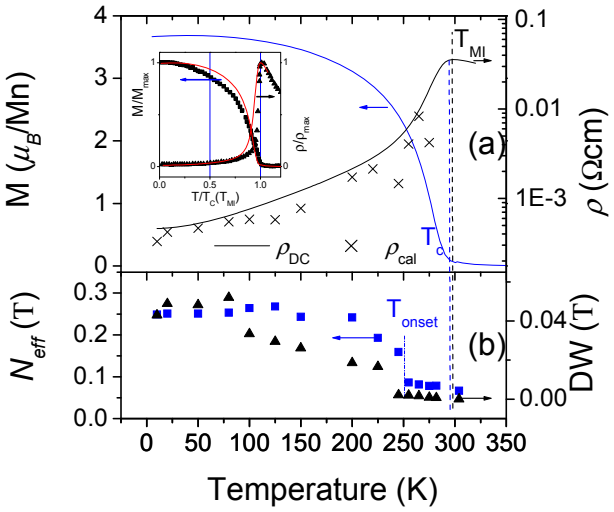

(a) Magnetization, calculated and measured DC resistivity of $La_{0.8}MnO_{3-\delta}$ /LAO film. Insert is the comparison for $La_{2/3}Ca_{1/3}MnO_3$ (symbols) and $La_{0.8}MnO_{3-\delta}$ line). (b) Effective carrier numbers (squares) and Drude Weight (free carriers, triangles).

Reference: [1] P. Gao, T. A. Tyson, M.A. Deleon, Z. X. Liu and C. Dubourdieu, Optical evidence of mixed-phase behavior in manganite films *Phys. Rev. B.*, 78, 220404(R) (2008).
[2] P. Gao,*Probing the Complex Magnetic, Electronic and Structural Properties in Correlated Manganese Oxides,* Ph. D. Thesis (NJIT).

This study was supported by NSF (Grants No. DMR-0512196 and No. INT-0233316) and CNRS/NSF (Project No. 14550). U2A beamline is supported by COMPRES, the Consortium for Materials Properties Research in Earth Sciences under NSF Cooperative Agreement No. EAR01-35554 and U.S. Department of Energy (DOE-BES and NNSA/CDAC). Use of the National Synchrotron Light Source, Brookhaven National Laboratory was supported by the Office of Science, Office of Basic Energy Sciences, U.S. Department of Energy under Contract No. DE-AC02-98CH10886.

Synchrotron X-ray diffraction and infrared spectroscopy studies of $C_{60}H_{18}$ under high pressure

Honglei Ma, Xuemei Zhang, Bingbing Liu, Quanjun Li, Qifeng Zeng, Shidan Yu, Bo Zou, Tian Cui, Gaungtian Zou [Jilin University, China], Zhenxian Liu [Geophysical Laboratory, Carnegie Institution of Washington], T. Wågberg and B. Sundqvist [Department of Physics, Umeå University, Sweden], Dag Noreus [Department of Structural Chemistry, Stockholm University, Sweden].

In situ high-pressure angle dispersive synchrotron X-ray diffraction and high-pressure mid-infrared (IR) spectrum measurements of $C_{60}H_{18}$ were carried out up to 32 GPa and 10.2 GPa, respectively. Our diffraction data indicated the fcc structure of $C_{60}H_{18}$ was stable up to 32GPa. The bulk modulus B_0 was determined to be 21±1.16 GPa, about 40 % higher than that of C_{60}. The C-H vibrations still existed up to 10.2 GPa and the vibrational frequencies decreased with increasing pressure. IR active vibrational frequencies and their corresponding eigenvectors of $C_{60}H_{18}$ were simulated by DMOL^3. The effects of hydrogen in the fullerene molecular cage on the stability of structure under high pressure were discussed.

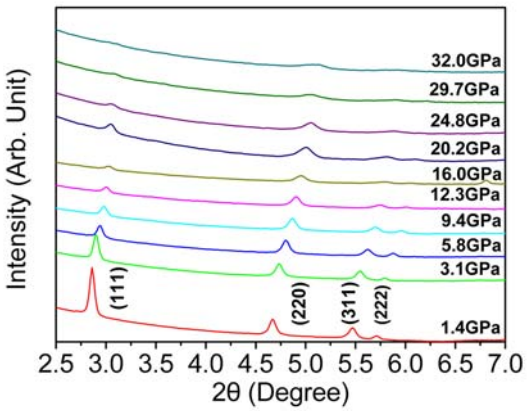

Synchrotron X-ray diffraction patterns of $C_{60}H_{18}$ under different pressures.

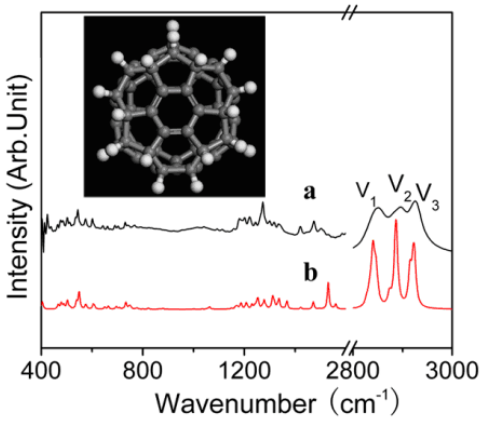

Experimental (a) and calculated (b) mid-IR absorption spectra of $C_{60}H_{18}$ at ambient pressure.

Reference: Honglei Ma, Xuemei Zhang, Bingbing Liu, Quanjun Li, Qifeng Zeng, Shidan Yu, Bo Zou, Tian Cui, Gaungtian Zou, Zhenxian Liu, T. Wågberg and B. Sundqvist, Dag Noreus. *Journal of Physical Chemistry Letters*, 2010, **1**, 714-719.

Acknowledgements: This work was supported financially by NSFC (10674053, 10979001, 20773043, 10574053), the National Basic Research Program of China (2005CB724400), an exchange grant from the Swedish Research Council through the SIDA-Swedish Research Links exchange program. The use of the National Synchrotron Light Source beamlines U2A and X17C are supported by NSF COMPRES EAR01-35554 and by US-DOE Contract DE-AC02-10886.

Pressure-Induced Interaction in Silane Hydrogen

T.A. Strobel, M. Somayazulu, and R.J. Hemley, *Geophysical Laboratory, Carnegie Institution of Washington*

Synchrotron infrared and Raman spectroscopies as well as synchrotron x-ray diffraction and optical microscopy were used to identify a novel molecular compound from silane-hydrogen mixtures with intermolecular interactions unprecedented for hydrogen-rich solids. A complex H_2 vibron spectrum with anti-correlated pressure-frequency dependencies and a striking H-D exchange below 10 GPa reveal strong and unusual attractive interactions between SiH_4 and H_2 and molecular bond destabilization at remarkably low pressure. The unique features of the observed $SiH_4(H_2)_2$ compound suggest a new range of accessible pressure-driven intermolecular interactions for hydrogen-bearing simple molecular systems, and a new approach to perturb the hydrogen covalent bond.

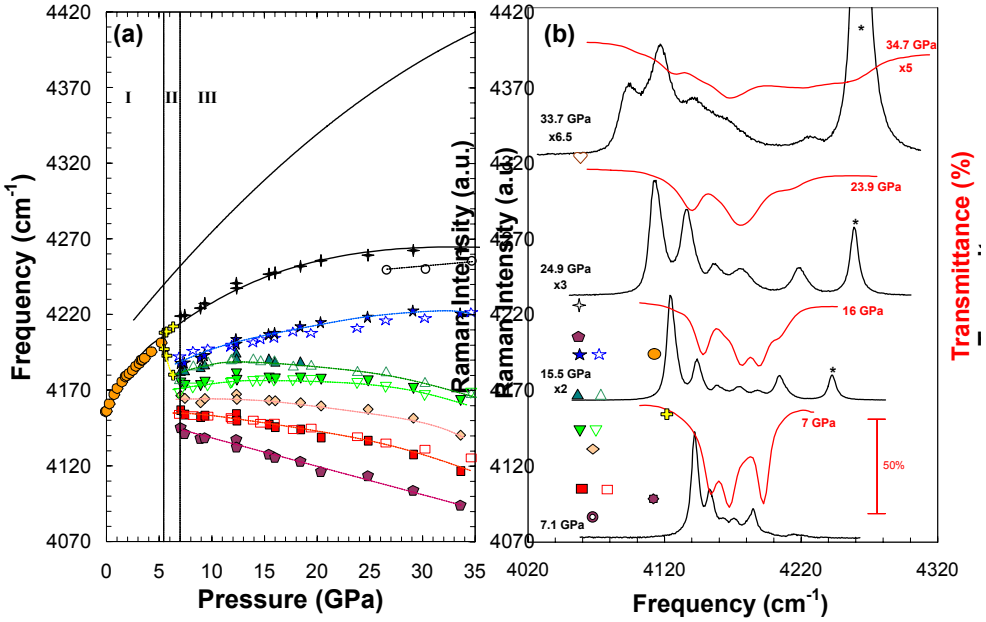

Figure 1. (a) Frequency of Raman (filled symbols) and IR (open symbols) H_2 vibrons as a function of pressure. Regions I, II and III indicate fluid, mixed fluid-solid, and solid phases (298 K). Dashed lines are drawn through the data to guide the eye. Solid lines represent Raman and IR data for bulk H_2. (b) Raman and transmission IR spectra for $SiH_4(H_2)_2$ as a function of pressure. Asterisks denote contributions from solid H_2.

Reference

T.A. Strobel, M. Somayazulu, R.J. Hemley *Phys. Rev. Lett.* **103**, 065701 (2009)

Acknowledgements

This work was supported by DOE-BES, DOE-NNSA (CDAC) and COMPRES, the Consortium for Materials Properties Research in Earth Sciences under NSF Cooperative Agreement EAR 10-43050. APS and NSLS are supported by DOE-BES under contract Nos. DE-AC02-06CH11357 and DE-AC02-98CH10886.

High Pressure Study of Silane to 150 GPa

T.A. Strobel, A.F. Goncharov, C.T. Seagle, Z. Liu, M. Somayazulu, V.V. Struzhkin, and R.J. Hemley, *Geophysical Laboratory, Carnegie Institution of Washington*

We present an extensive study on the optical, electronic and structural properties of silane (SiH_4) to 150 GPa through the use of Raman spectroscopy, optical microscopy, synchrotron infrared reflectivity, optical absorption and synchrotron x-ray diffraction measurements. Silane remains in the transparent and insulating $P2_1/c$ structure until ~40 GPa and shows a partial loss of crystallinity above ~50 GPa and appears to visibly darken. Above 100 GPa we observed crystallization into structures partially consistent with the previously reported non-molecular $I\text{-}42d$ and $I4_1/a$ types. In the absence of decomposition, silane remains partially transparent and non-metallic to at least 150 GPa with a band gap constrained between 0.6-1.8 eV. Under pressure, silane is sensitive to irradiation from x-rays and lasers, and may easily decompose into metallic silicon. We suggest previous reports of silane metallization are likely a consequence of decomposition and superconductivity may originate from silicon or hydrogen-doped silicon which is not silane. While silane may readily decompose, the inherent metastability provides access to a wide range of path and sample-history dependent states and suggests a unique range of physical properties for hydrogen-rich silicon alloys.

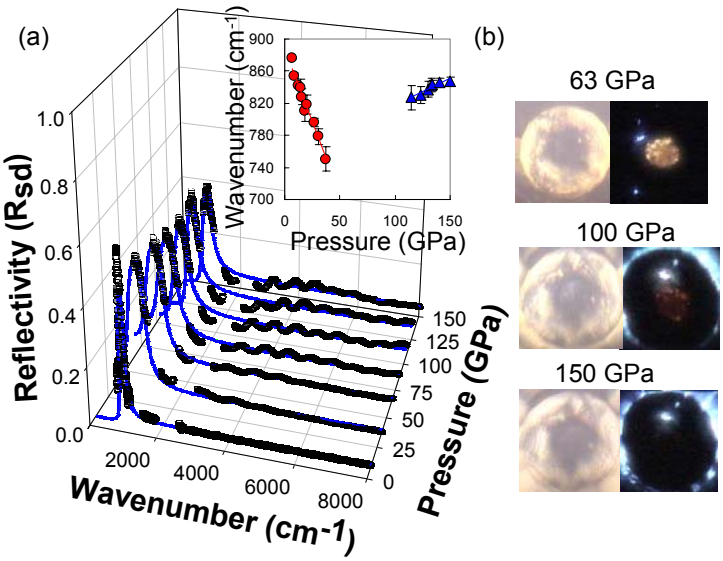

Figure 1. (a) Synchrotron IR Reflectivity at the diamond-silane interface as a function of pressure. (b) Photomicrographs obtained in reflection (left) and transmission (right). Integration time on the CCD camera was several seconds.

Reference

T.A. Strobel, A.F. Goncharov, C.T. Seagle, Z. Liu, M. Somayazulu, V.V. Struzhkin, R.J. Hemley *Phys. Rev. B.* in press (2011)

Acknowledgments

We acknowledge support from NSF-DMR (DMR-0805056). Portions of this work were performed at GeoSoilEnviroCARS (Sector 13), Advanced Photon Source (APS), Argonne National Laboratory. GeoSoilEnviroCARS is supported by the National Science Foundation - Earth Sciences (EAR-0622171) and Department of Energy - Geosciences (DE-FG02-94ER14466). Portions of this work were performed at HPCAT (Sector 16), Advanced Photon Source (APS), Argonne National Laboratory. HPCAT is supported by CIW, UNLV and LLNL through funding from ~DOE-NNSA, DOE-BES and NSF. APS is supported by DOE-BES, under Contract No. DE-AC02-06CH11357. The U2A beamline is supported by COMPRES, the Consortium for Materials Properties Research in Earth Sciences, under NSF Cooperative Agreement Grant No.~EAR06-49658 and the U.S. DOE (CDAC, Contract No.~DE-AC02-98CH10886).

Raman and infrared spectroscopy of pyridine under high pressure

Kirill K. Zhuravlev, Katrina Traikov, Zhaohui Dong, Shuntai Xie, and Yang Song, *University of Western Ontario, London, Ontario, Canada*
Zhenxian Liu, *Carnegie Institution of Washington, Washington, DC, USA*

We report the structural transitions of pyridine as a function of pressure up to 26 GPa using in situ Raman spectroscopy and infrared absorption spectroscopy. By monitoring changes of the Raman shifts in the lattice region as well as the band profiles in both Raman and IR spectra, a liquid-to-solid transition at 1 GPa followed by solid-to-solid transitions at 2 GPa, 8 GPa, 11 GPa and 16 GPa were observed upon compression. These transitions were found to be reversible upon decompression from 22 GPa. A further chemical transformation was observed when compressed beyond 22 GPa as evidenced by the substantial and irreversible changes of the Raman and infrared spectra, which could be attributed to the destruction of the ring structure. The observed transformations in pyridine were also compared to those for benzene. The similar transition sequence with well aligned transition pressures suggests that these isoelectronic aromtics may have similar structures and stabilities under high pressure.

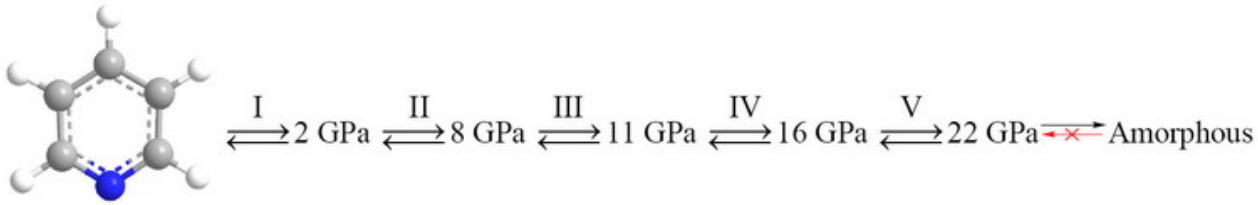

Pressure-induced transformation sequence observed in pyridine.

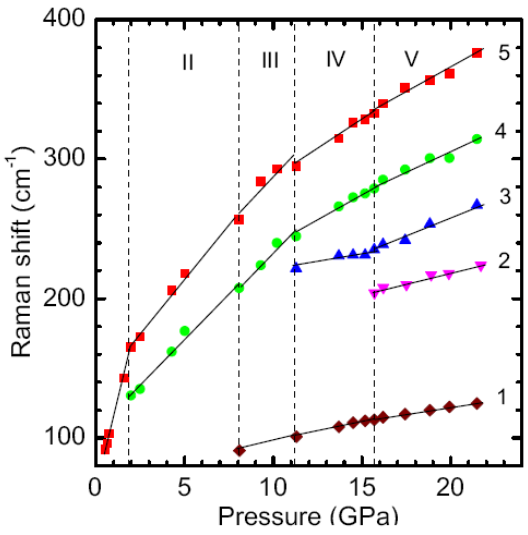

Proposed phase boundaries indicated by Raman lattice modes.

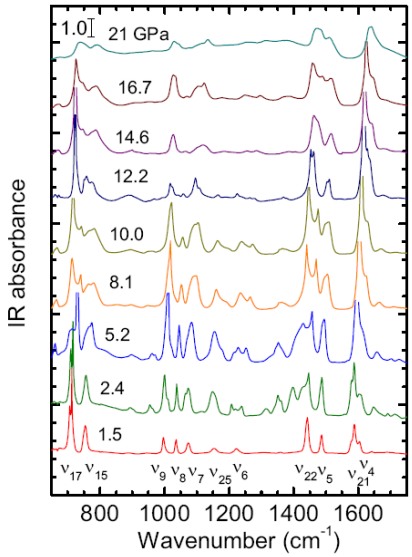

IR spectra of pyridine at selected pressures.

Reference: K Zhuravlev, K Traikov, Z Dong, S Xie, Y Song, Z Liu, Raman and Infrared Spectroscopy of Pyridine under High Pressure, *Phys. Rev. B: Condens. Matter*, **82**, 064116 (2010).

Acknowledgments: The authors acknowledge the support from a Discovery Grant and a Research Tools and Instruments Grant from the Natural Sciences and Engineering Council of Canada, a Leading Opportunity Fund from the Canadian Foundation for Innovation and an Early Researcher Award from the Ontario Ministry of Research and Innovation. IR measurements were performed at the U2A beamline at the NSLS at BNL. The U2A beamline is supported by COMPRES, the Consortium for Materials Properties Research in Earth Sciences under NSF Cooperative Agreement EAR06-49658, US Department of Energy (DOE), (CDAC), and NSF (DMR).

In situ High-pressure Study of Ammonia Borane by Raman and Infrared Spectroscopy

Shuntai Xie, and Yang Song, *University of Western Ontario, London, Ontario, Canada*
Zhenxian Liu, *Carnegie Institution of Washington, Washington, DC, USA*

Pressure-induced structural transformations of the ammonia borane complex (NH_3BH_3) were investigated in diamond anvil cells by Raman spectroscopy and synchrotron infrared (IR) spectroscopy up to 14 GPa at room temperature. Starting with a disordered tetragonal structure, NH_3BH_3 is found to undergo several transformations upon compression as monitored by *in situ* Raman measurements. These transformations are indicated by the sequential changes of characteristic Raman modes as well as by the pressure dependence of these modes. Synchrotron IR absorption spectroscopy provided supplementary and consistent information about the structural evolution of NH_3BH_3 under compression. Decompression measurements on NH_3BH_3 suggest the pressure-induced transformations are reversible in the entire pressure region. The combined Raman and IR data allowed analysis of possible high-pressure structures of NH_3BH_3. Our study significantly complements previous high-pressure Raman studies by providing new information on the structures and stabilities of NH_3BH_3.

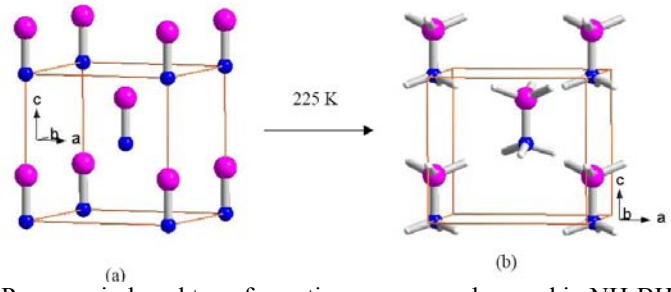

Pressure-induced transformation sequence observed in NH_3BH_3.

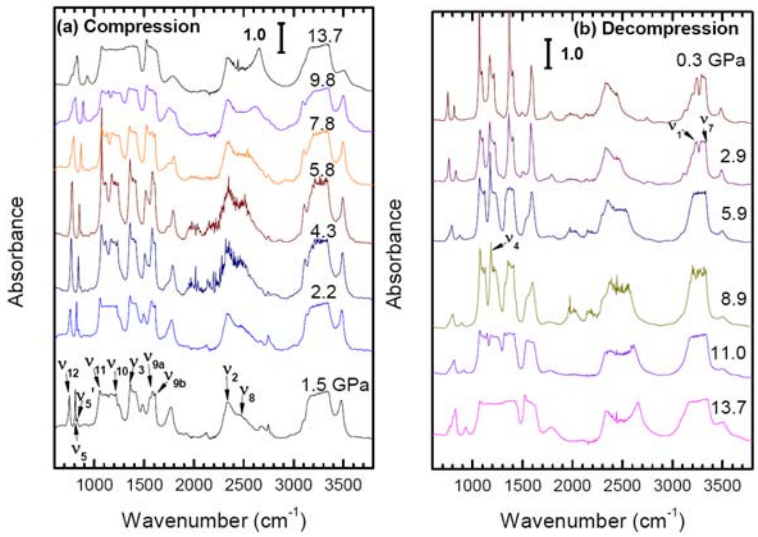

Mid-IR spectra of NH_3BH_3 upon compression and decompression.

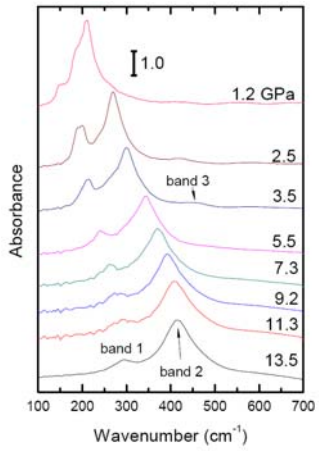

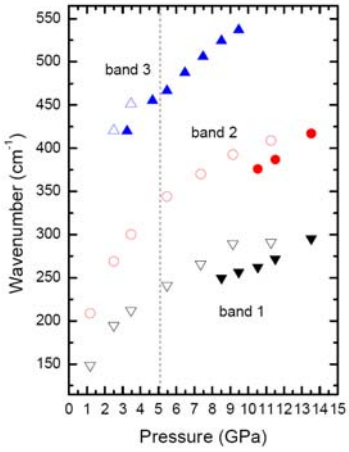

Far-IR region for NH_3BH_3.

Reference: S Xie, Y Song, Z Liu, In Situ High-Pressure Study of Ammonia Borane by Raman and IR Spectroscopy, *Can. J. Chem./Rev. Can. Chim.*, **87**(9), 1235-1247 (2009).

Acknowledgments: The authors acknowledge the support from a Discovery Grant and a Research Tools and Instruments Grant from the Natural Sciences and Engineering Council of Canada, a Leading Opportunity Fund from the Canadian Foundation for Innovation and an Early Researcher Award from the Ontario Ministry of Research and Innovation. IR measurements were performed at the U2A beamline at the NSLS at BNL. The U2A beamline is supported by COMPRES, the Consortium for Materials Properties Research in Earth Sciences under NSF Cooperative Agreement EAR06-49658, US Department of Energy (DOE), (CDAC), and NSF (DMR).

In situ High-pressure Study of Diborane by Infrared Spectroscopy

Yang Song and and Chitra Murli, *University of Western Ontario, London, Ontario, Canada*
Zhenxian Liu, *Carnegie Institution of Washington, Washington, DC, USA*

As the simplest stable boron hydride in its condensed phase, diborane exhibits an interesting structural chemistry with uniquely bridged hydrogen bonds. Here we report the first room-temperature infrared absorption spectra of solid diborane compressed to pressures as high as 50 GPa using a diamond anvil cell. At room temperature and 3.5 GPa, the infrared (IR) spectrum of diborane displays rich sharply resolved fundamentals and overtones of the IR active bands, consistent with the previous low-temperature IR measurements of condensed diborane at ambient pressure. When compressed stepwise to 50 GPa, several structural transformations can be identified at pressures ~ 3.5 to 5.4 GPa, ~ 6.9 to 9.9 GPa and ~ 14.7 to16.7 GPa as indicated by the change in the band profile as well as the pressure dependence of the characteristic IR modes and bandwidths. These transformations can be interpreted as being enhanced intermolecular interactions resulting from compression. The geometry of the four-member ring of B_2H_6, however, does not seem to be altered significantly during the transformations and the B_2H_6 molecule remains chemically stable up to 50 GPa.

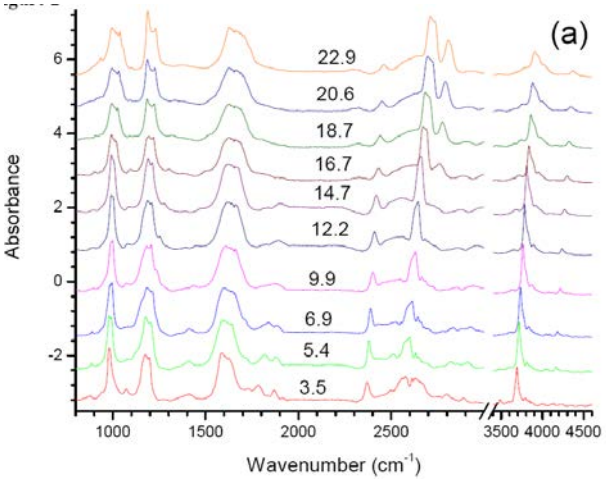

Mid-IR spectra of B_2H_6 on compression from 3.5 GPa to22.9 GPa.

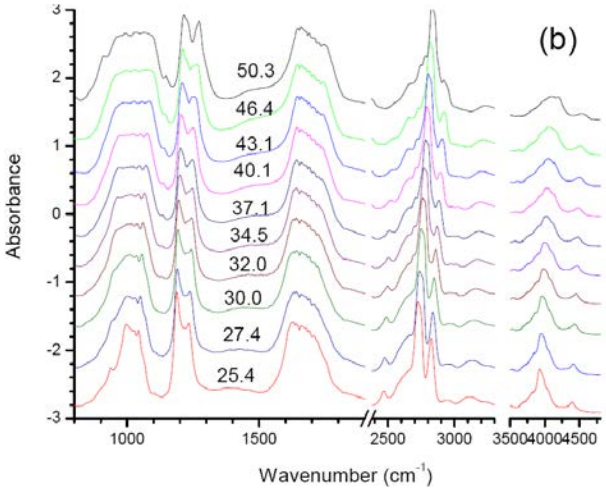

Mid-IR spectra of B_2H_6 on compression from 25.4 GPa to 50.3 GPa.

Reference: Y Song, C Murli, Z Liu, In situ High-pressure Study of Diborane by Infrared Spectroscopy, *J. Chem. Phys.*, **131**, 174506 (2009).

Acknowledgments: YS acknowledges the supports from the Discovery Grant and the RTI Grant from the NSERC of Canada, the Leaders Opportunity Fund from the Canadian Foundation for Innovation and the Early Researcher Award from the Ontario Ministry of Research and Innovation. CM acknowledges the CCP fellowship from UWO. IR measurements were performed at the U2A beamline at the NSLS at BNL. The U2A beamline is supported by COMPRES, the Consortium for Materials Properties Research in Earth Sciences under NSF Cooperative Agreement EAR06-49658, U.S. Department of Energy (DOE), (CDAC), and NSF (DMR).

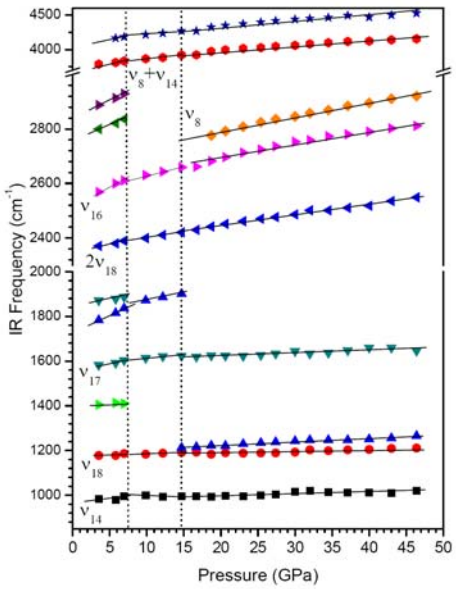

Pressure dependence of the IR frequencies of the fundamentals and selected combination modes of B_2H_6 on compression.

Studies of insensitive explosives at the U2A beamline.

Michael Pravica, Sergey Tkachev, Martin Galley, Brian Yulga, Edward Romano,
High Pressure Science and Engineering Center, Department of Physics & Astronomy, University of Nevada, Las Vegas

During the past reporting period, the Pravica group has engaged in a number of studies of insensitive energetic and other organic-based materials at the U2A beamline. Infrared spectroscopy is a complementary technique to Raman spectroscopy in developing a more complete vibrational picture of how molecules behave under extreme conditions. We have also found that whereas Raman spectroscopy can initiate molecular decomposition of the energetic materials that we studied, infrared is, by contrast, not damaging to the explosives and other organic molecules. Also, we have observed the Raman spectra of our samples often contaminated by fluorescence at higher pressures which we believe is due to structural damage via dislocations resulting in exciton formation. Infrared spectroscopy does not suffer from these effects. Thus, in our studies, infrared spectroscopy is a far superior method to Raman spectroscopy due to little or no damage inflicted on the samples by the IR beam and due to the lack of signal-contaminating fluorescence.

Among the energetic materials we examined, HMX, RDX, PETN, FOX7. All of these explosives are widely used in the DOE/DOD weapons facilities with the exception of newly-developed FOX7 (DADNE). Some highlights of our studies include the first reported far-IR studies of TATB, HMX, and FOX7 at high pressure, and the first mid-IR study at high pressure of FOX7. In HMX, we have found evidence for a new phase near 6 GPa and that HMX pressurizes reversibly up to at least 30 GPa with no damage contrary to prior reports.

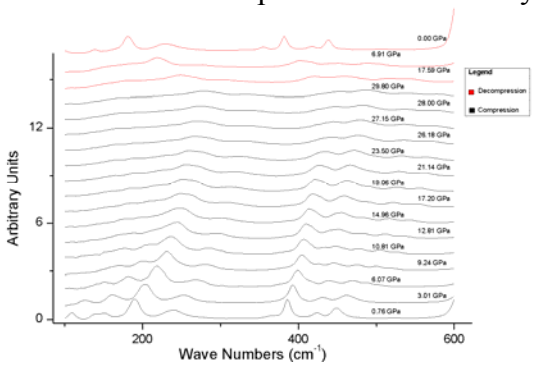

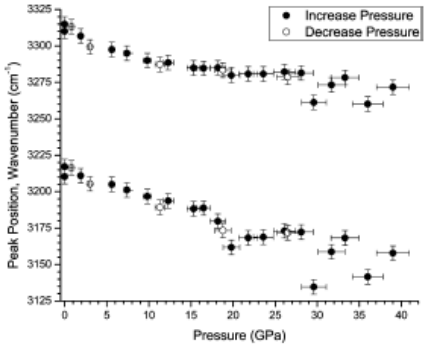

Left: The first reported far-IR data of HMX at high pressure. Right: Mid-IR results for the NH_2 symmetric & antisymmetric vibrations demonstrating the unusual negative shift of the frequencies due toto increasing hydrogen bonding with pressure.

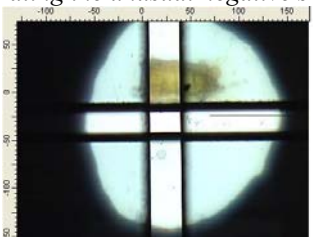

←*FOX7 sample at 28 GPa as observed through the IR microscope.*

References:

1. M Pravica, E Romano, S Tkachev, Z Liu, High Pressure Infrared Study of 1,3,5,7-cyclooctatetraene (COT), *J Phys.: Conf. Ser.*, 215, 012050 (2010).
2. M Pravica, M Galley, E Kim, P Weck, Z Liu, A far- and Mid-infrared Study of HMX (octahydro-1,3,5,7-tetranitro-1,3,5,7-terazocine) Under High Pressure, *Chem. Phys. Lett.*, 500, 28-34, (2010).
3. M Pravica, B Yulga, S Tkachev, Z Liu, High-Pressure Far- and Mid-Infrared Study of 1,3,5-Triamino-2,4,6-trinitrobenzene, *J. Phys. Chem. A*, 113(32), 9133-9137 (2009).
4. P Weck, C Gobin, E Kim, M Pravica, Organic Cyclic Difluoramino-Nitramines: Infrared and Raman Spectroscopy of 3,3,7,7-tetrakis(difluoramino)octahydro 1,5-dinitro-1,5-diazocine (HNFX), *J Raman Spectrosc.*, 40, 964-971 (2009).
5. M Pravica, B Yulga, Z Liu, O Tschauner, Infrared Study of 1,3,5-triamino-2,4,6-trinitrobenzene Under High Pressure, *Phys. Rev. B: Condens. Matter*, 76, 064102 (2007).

This work was supported by: We gratefully acknowledge support from US Army RDECOM ACQ CTR Contract W9011NF-05-1-0266, the UNLV/ARL SOldier FERST program, the Nevada/NASA space grant, and DOE DE-FC88-06NA27684 Cooperative Agreements with UNLV. Use of the National Synchrotron Light Source is supported by DOE Office of Science, Office of Basic Energy Sciences, under Contract No. DE-AC02-98CH10886. This research was partially supported by COMPRES, the Consortium for Materials Properties Research in Earth Sciences under NSF Cooperative Agreement EAR 10-43050.

The compressibility of the La-Mg-Ni alloy system.

Fangming [South China University of Technology, Guangdong Research Institute of Non-ferrous Metals], Cheng Ji, Yanzhang Ma, Hongyang Zhu, Dongbin Hou,[Texas Tech Univerisity],and Min Zhu[South China University of Technology]

We measured the compressibility of La, $La_2Mg_{16}Ni$, $LaMg_2Ni$, and $LaMg_3$ to 30.1 GPa by synchrotron X-ray diffraction (Figure 1). The bulk moduli are respectively determined to be 47.5, 54, 67, and 57 GPa (Figure 2). The strengthening of the compounds by the addition of nickel is insignificant. The compressibility is dominantly determined by that of La and Mg. The strength increase of the compounds compared to pure La and Mg elements is comparable to that caused by solid-solution strengthening. The axial compressibility differs for La and LaMg2Ni (Figure 3).

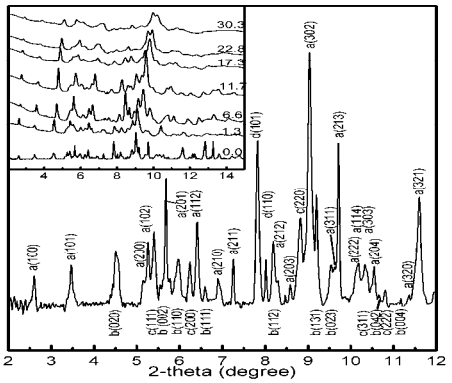

Figure 1. X-ray diffraction of the La-Mg-Ni sample. Letters a, b, c, and d respectively refer to the $La_2Mg_{16}Ni$, $LaMg_2Ni$, $LaMg_3$ and La phases, followed which are the Miller's Indexes of the corresponding diffraction peaks. Only two very weak peaks cannot be indexed which could be due to impurity or other phases. The inset displays the X-ray diffraction patterns at selected pressures of the compression experiments. The displayed patterns at ambient conditions are background corrected.

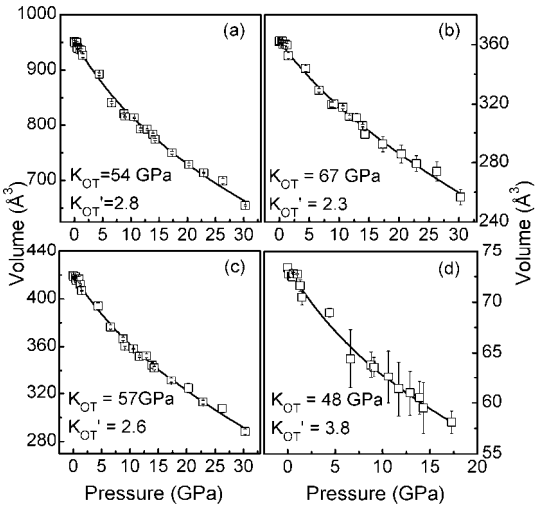

Figure 2. Unit cell volume compression of the $La_2Mg_{16}Ni$ (a), $LaMg_2Ni$ (b), $LaMg_3$ (c), and La (d) at high pressures.

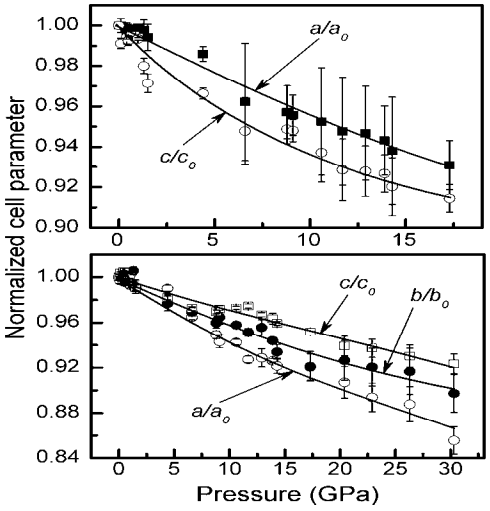

Figure 3. The axial compression of γ-La (top) and $LaMg_2Ni$ (bottom) at high pressures.

This study was supported by the National Science Foundation under grants DMR 0619215. The *in situ* X-ray experiments were carried out at the X-17C and X17B3 beamlines of the National Synchrotron Light Source (NSLS) which is supported by COMPRES, the Consortium for Materials Properties Research in Earth Sciences under contract number EAR 01-35554.

Structures of Cesium Azide: A Series of Phase Transitions under High Pressure

Dongbin Hou, Cheng Ji, Trevor Hannon, Hongyang Zhu, Jianzhe Wu, Yanzhang Ma [Texas Tech Univerisity],and Fuxiang Zhang [University of Michigan, Ann Arbor]

In situ X-ray diffraction measurements of cesium azide (CsN3) were performed at high pressures up to 55.4 GPa at room temperature. Three phase transitions were revealed as follows: tetragonal (Phase II) → monoclinic (Phase III) → monoclinic (Phase IV) → triclinic (Phase V), at 0.5 GPa, 4.4 GPa, and 15.4 GPa, respectively. The azide anions keep the chain structure but rotate obviously during the II-III phase transition, and then tend to orient more randomly and bond with each other during the III-IV transition. The compressibility of Phase II is dominated by the repulsions between azide anions. The deformation of unit cell is anisotropic in Phase II and III, and isotropic in Phase IV. With increasing pressures, the monoclinic angle increases in Phase III and then becomes stable in Phase IV. The bulk moduli of Phase II, III, IV, and V are determined to be 18 ± 4 GPa, 20 ± 1 GPa, 27 ± 1 GPa and 34 ± 1 GPa, respectively. *(Submitted)*

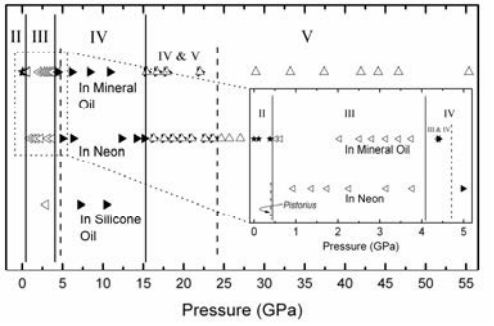

CsN_3 phase diagram.

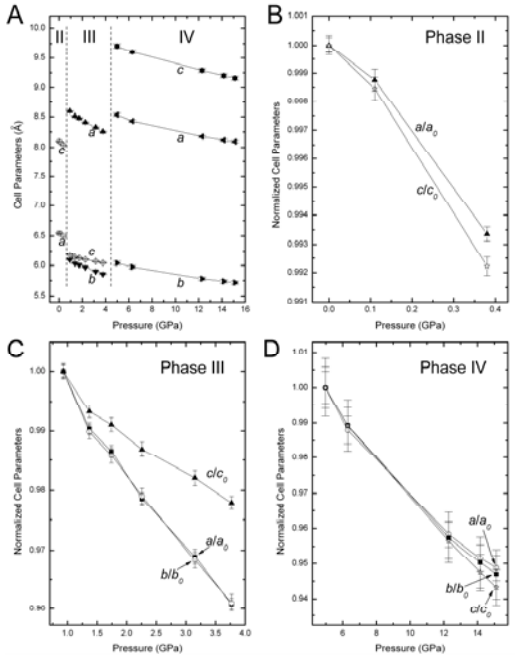

Pressure dependence of cell parameters.

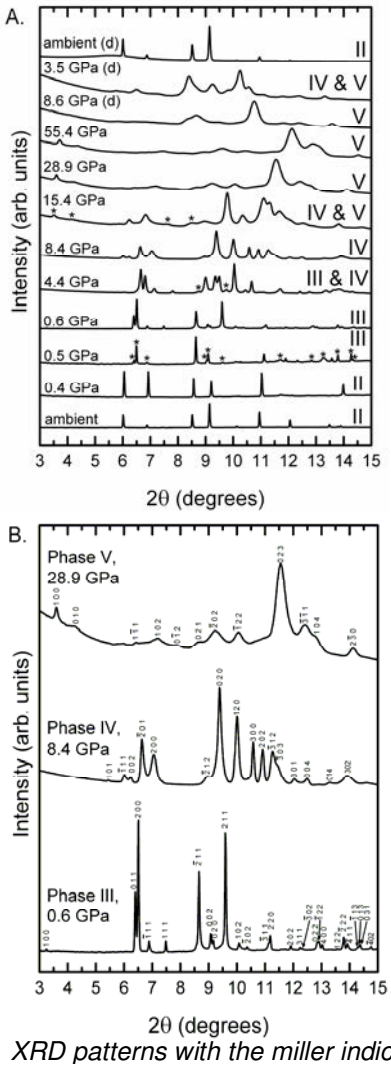

XRD patterns with the miller indices.

This study was supported by the National Science Foundation under grants DMR 0619215. The *in situ* X-ray experiments were carried out at the X-17C and X17B3 beamlines of the National Synchrotron Light Source (NSLS) which is supported by COMPRES, the Consortium for Materials Properties Research in Earth Sciences under contract number EAR 01-35554.

Class of tunable wide band gap semiconductors γ-$(Ge_xSi_{1-x})_3N_4$

PHYSICAL REVIEW B **81**, 155207 2010

T. D. Boyko,[1], E. Bailey,[2] A. Moewes,[1] and P. F. McMillan[2]
[1]*Department of Physics and Engineering Physics, University of Saskatchewan, 116 Science Place, Saskatoon, Saskatchewan, Canada S7N 5E2*
[2]*Department of Chemistry, University College London, 20 Gordon Street, London WC1H 0AJ, United Kingdom*

The solid solutions of γ-Si_3N_4 and γ-Ge_3N_4, γ-$(Ge_xSi_{1-x})_3N_4$ with x=0.000, 0.178, 0.347, 0.524, 0.875, and 1.000, are studied. The band gap values of the solid solutions measured with soft x-ray spectroscopy have a range of 3.50–5.00 0.20 eV. The hardness values of these solid solutions estimated using an empirical relationship have a range of 22.2–36.0 GPa. We use the generalized gradient approximation of Perdew-Ernzerhof-Burke GGA-PDE within density functional theory and obtained a calculated band gap value range of 2.20–3.56 eV. The simulated N absorption and emission spectra agree very well with our measurements and the compositional trend among the calculated band gap values corresponds well with the measured values. The agreement between experimental and theoretical spectra indicates that Ge prefers the site with tetrahedral bonding symmetry. The band gap and hardness estimates have two approximately linear regimes, when 0 x 1/3 and 1/3 x 1. The band gap decreases as Ge replaces Si on octahedral sites and this suggests that the type of cation in the octahedral sites is mainly responsible for decreasing the band gap in these spinel nitrides. Our results indicate that solid solutions of γ-$(Ge_xSi_{1-x})_3N_4$ provide a class of semiconductors with a tunable wide band gap suitable for UV laser or LED applications.

The materials studied here are solid solutions established between the end members γ-Si_3N_4 and γ-Ge_3N_4. Samples of γ-Si_3N_4 and γ-Si,Ge $_3N_4$ solid solutions were synthesized in a resistively heated multianvil press using COMPRES 8/3 MgO assemblies with a $LaCrO_3$ furnace at 1500 °C and P =23 GPa for 18–35 min. The pure γ-Ge_3N_4 end member was prepared at 12 GPa and 1200 °C for 2 h using a COMPRES 14/8 MgO assembly with a graphite furnace. All samples were fully characterized using x-ray diffraction, Raman spectroscopy and electron microprobe analysis in a previous study (E. Soignard, P. F. McMillan, and K. Leinenweber, Chem. Mater. **16**, 5344 2004).

.